# University of Alberta

Design and synthesis of inhibitors for the human neuraminidase 3 enzyme

by

Yao Zou

A thesis submitted to the Faculty of Graduate Studies and Research
in partial fulfillment of the requirements for the degree of

Master of Science

Department of Chemistry



Fall 2011
Edmonton, Alberta

# Abstract

Sialidase enzymes play an important role in regulation of cellular activities by hydrolyzing the terminal, non-reducing sialic acids attached to various glycolipids, glycoproteins, and gangliosides. The family of human sialidase enzymes, NEU1, NEU2, NEU3, and NEU4 contribute specifically to different cellular processes. In particular, the plasma membrane associated sialidase NEU3 was studied by our group due to its specificity for glycolipids and its proposed role in cell signaling. This thesis describes the design and synthesis of sialidase inhibitors based on the 2,3-didehydro-*N*-acetyl neuraminic acid scaffold. Specific inhibitors of these enzymes will allow us to explore their function *in vivo*. In Chapter 2 we describe a series of *C*9 and *N*5Ac modified analogs of DANA (2,3-Didehydro-2-deoxy-*N*-acetylneuraminic acid) which were designed, synthesized and biologically evaluated. Molecular docking experiments revealed NEU3 can tolerate large hydrophobic groups at the *C*9 position, however, *N*5Ac derivatives failed to inhibit NEU3. This result suggested that glycerol side-chain modified derivatives of DANA could prove to be potent inhibitors of the enzyme. In Chapter 3 we develop a synthetic route to generate a series of *C*7-modified DANA derivatives. We isolated several *C*7-hydrazone derivatives that will be tested against human neuraminidase enzymes as inhibitors. The results from these studies provided valuable insight regarding the interaction of small molecule inhibitors with the active site of the human NEU3 enzyme, and have improved

synthetic strategies towards DANA derivatives that may take advantage of the unique active site topology of NEU3.

# Acknowledgements

I would like to thank several people who have helped and supported me in completing this work. First of all, I would like to thank my supervisor, Dr. Christopher Cairo who has provided me with valuable guidance and continuous support throughout my graduate studies.

I would like to specifically thank Amgad Albohy for performing the assay and molecular docking studies undertaken in Chapter 2.

I would also like to thank Jessie Key for his generous help during my studies, and Mahendra Sandbhor, Li Xia, Yen-Ku Wu, Jack Lee, Mickey Richards, Zedu Huang, Akihiro Imamura, Cunsheng Zhu, Myles Poulin, and Lu Deng for their help advice during my time in graduate school. I would also like to thank all the Cairo group members for their help during three years.

Finally, I would like to thank my parents, my sister, and friends for their support.

# Table of Contents

# List of Schemes

# List of Tables

# List of Figures

## List of Abbreviations

| | |
|---|---|
| Boc | Butyloxy carbonyl |
| CAM | Ceric ammonium molybdate |
| CuAAC | Cu-catalyzed azide- alkyne cycloaddition |
| DANA | 2,3-Didehydro-2-deoxy-*N*-acetylneuraminic acid |
| DCM | Dichloromethane |
| DIPEA | *N*,*N*-Diisopropylethylaminie |
| EtOAc | Ethyl acetate |
| HA | Hemagglutinin |
| HPLC | High-performance liquid chromatography |
| HRMS | High-resolution mass spectrometry |
| KDN | 2-Keto-3-deoxy-D-glycero-D-galactononononic acid |
| LFA | Lymphocyte functional antigen |
| MBP | Maltose binding protein |
| MeOH | Methanol |
| 4MU-NA | 4-methylumbelliferyl-D-N-acetylneuraminic acid |
| NA | Neuraminidase |
| Neu | Neuraminic acid |
| Neu5Ac | 5-Acetamido-2-keto-3,5-dideoxy-D-glycero-D-galactononononic acid |
| Neu5Gc | *N*-glycolylneuraminic acid |
| NMR | Nuclear magnetic resonance |
| THF | Tetrahydrofuran |

| | |
|---|---|
| TLC | Thin layer chromatography |
| TMSOTf | Trimethylsilyl trifluoromethanesulfonate |
| Quant | Quantitative |
| SAR | Structure activity relationships |
| UV | Ultraviolet |

# Chapter 1

# Inhibitors of neuraminidase enzymes

### *1.1 Introduction to Neuraminidase*

Neuraminidase enzymes catalyze the hydrolysis of sialic acid residues from various glycoproteins, glycolipids, gangliosides, as well as oligo- and poly-saccharides. Due to their substrates (neuraminic acid, also known as sialic acid), these enzymes are interchangeably referred to as neuraminidase or sialidase enzymes. The two primary forms of sialidase are exo-α-sialidase (*N*-acylneuraminyl glycohydrolases) (Monti, E., Preti, A., et al. 2002) and endo-α-sialidase (endo-*N*-acylneuraminidase) (Cabezas, J.A. 1991). Sialidases are widely distributed in nature, and are found in viruses, fungi, protozoa, bacteria, and higher organisms such as avian and mammalian species (Achyuthan, K.E. and Achyuthan, A.M. 2001). However, neuraminidases are absent in plants, insects and yeast (Monti, E., Bonten, E., et al. 2010).

### *1.2 Sialic Acid*

Sialic acids are a family of nonulosonic ketosugars, which were first identified by Gunnar Blix and Ernst Klenk in 1940s (Ajit Varki, R.D.C., et al. 2009). Sialic acids are released as a cleavage product from hydrolysis of brain glycolipids or salivary mucins. Sialic acids are ubiquitous among higher animals, like mammalians, as well as in some microorganisms. The family of structures which make up sialic acids are composed of more than 50 members, all of which are *N*- or *O*-substituted derivatives of neuraminic acid (**1.1**, Neu) (Scheme **1.1**), which itself does not occur in nature. The two most typical representatives of sialic acids are 5-Acetamido-2-keto-3,5-dideoxy-D-glycero-D-galactonononic acid (**1.2**, *N*-acetylneuraminic acid, Neu5Ac) and 2-keto-3-deoxy-D-glycero-D-

galactononononic acid (**1.4**, 2-keto-3-deoxynononic acid, KDN) (Scheme **1.1**) (Ajit Varki, R.D.C., et al. 2009). The sialic acid backbone is a polyhydroxylated α-keto acid with a nine-carbon chain that includes a pyranose ring. The primary differences between Neu5Ac **1.2** and KDN **1.4** are found at the *C*5 position, which contains an *N*-acetyl group and a hydroxyl group in these two structures, respectively (Buschiazzo, A. and Alzari, P.M. 2008). Hydroxylation of the 5-*N*-acetyl group provides another frequently occurring member of sialic acids, *N*-glycolylneuraminic acid (**1.3**, Neu5Gc) (Scheme **1.1**).

Common modifications of sialic acids include modification of the hydroxyl groups at *C*4, *C*7, *C*8, and *C*9 positions. Substitutions include acylation, phosphorylation, sulfation, lactylation, and methylation (Schauer, R. 2004). Additionally, unsaturated and anhydro derivatives are known, the most common of these being 2,3-didehydro-2-deoxy-*N*-acetylneuraminic acid (**1.5**, Neu5Ac2en, DANA) (Scheme **1.1**) (Achyuthan, K.E. and Achyuthan, A.M. 2001), and the synthesis of DANA will be discussed in the second chapter. Formation of a lactone or lactam at the *C*1 position has also been identified (Ajit Varki, R.D.C., et al. 2009).

Sialic acids have been found to play crucial roles in biological processes including cell recognition, adhesion, differentiation, and disease states (Ajit Varki, R.D.C., et al. 2009). The importance of the sialic acid residue and its ubiquity in nature has resulted in significant research interest in the function of Neu5Ac in human biology. Hence there is great interest in the synthesis of Neu5Ac derivatives, either as enzyme inhibitors or biological probes (Miyagi, T., Wada,

T., et al. 2008; Sun, X.-L., Kai, T., et al. 1997; Morais, G.R., Oliveira, R.S., et al. 2009). Due to its key roles in influenza virus infection, a large amount of effort has been devoted to further understand the structure activity relationship of sialic acid interactions with the viral proteins, hemagglutinin and neuraminidase (von Itzstein, M. 2007). We will briefly discuss some of the approaches used to develop sialic acid-derived inhibitors of the viral neuraminidase enzyme below.

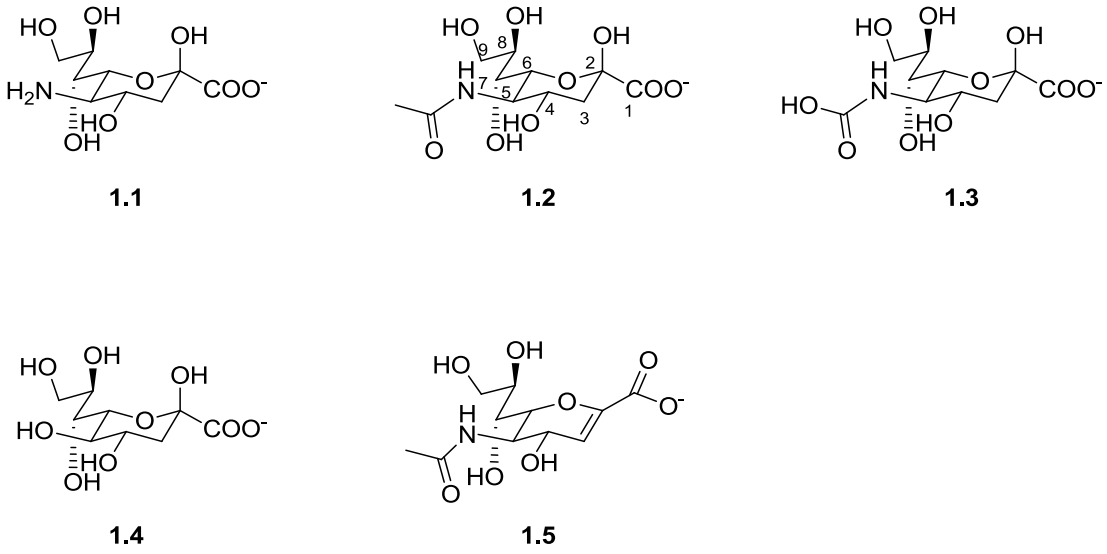


**Scheme 1.1. Structures of neuraminic acid 1.1 and four common Sialic acids, Neu5Ac 1.2, Neu5Gc 1.3, KDN1.4, and Neu5Ac2en 1.5 (DANA).** Structural diversity is due to modification at *C*5.

### *1.3 Inhibitors of viral sialidase*

Influenza virus infection is the cause of substantial fatigue and fatalities globally during the flu season. Influenza viruses consist of three classes: influenza virus A, influenza virus B and influenza virus C (We ̈wer, M., Chen, C.-C., et al. 2009), with influenza A and B responsible for clinical influenza (Dyason, J.C. and

von Itzstein, M. 2001). Influenza viruses are further classified based on the subtype of hemagglutinin and neuraminidase enzymes which they encode. For example, in 2007 a form of the virus emerged containing hemagglutinin 5, and neuraminidase 1 (H5N1). In 2007 and 2009, a form known as swine flu (influenza A/H1N1) resulted in a great number of deaths (Wen, W.-H., Wang, S.-Y., et al. 2010; Magesh, S., Sriwilaijaroen, N., et al. 2011). The viral hemagglutinin protein is responsible for binding of the virus particle to host cells through the ubiquitous sialic acid groups found at the termini of human glycoproteins and glycolipids. The neuraminidase enzyme of the virus acts to remove the sialic acid binding sites from host cells after virus particles depart from the cell. Since the viral neuraminidase is an enzyme, it provides a potential small molecule drug target. Due to the morbidity and mortality of influenza infection, the development of novel inhibitors against influenza virus has become an important area of research.

### *1.3.1 Viral sialidase*

The surface of the virus is composed of two major glycoproteins, hemagglutinin (HA) and sialidase (neuraminidase, NA). 16 hemagglutinin (H1 to H16) and 9 neuraminidase subtypes (N1 to N9) are known so far (Magesh, S., Sriwilaijaroen, N., et al. 2011). The viral hemagglutinin is a lectin, a carbohydrate binding protein which targets sialic acid, and is known to facilitate influenza adhesion to target cell-surface glycoconjugates by recognizing terminal *N*-acetylneuraminic acid residues on the host cell (Neu5Ac, **1.2**) (Kim, C.U., Lew, W., et al. 1997). Furthermore, it assists in the internalization of the virus during fusion of the viral envelope with the host cell membrane (Skehel, J.J. and Wiley,

D.C. 2000; von Itzstein, M. 2007; Matrosovich, M. and Klenk, H.-D. 2003). In contrast, the exoglycosyl hydrolase, sialidase, contributes to the removal of *N*-acetylneuraminic acid residues from both host cell and new viral progeny glycoproteins which promotes the movement of the viral particle and facilitates invasion of new cells (von Itzstein, M. 2007). Inhibition of neuraminidase will result in aggregation of virions and limit their infection to one round of replication (Moscona, A. 2005; Varghese, J.N. 1999). Thus, both viral hemagglutinin and neuraminidase are essential to the life cycle of the virus, and each of these proteins could be considered as drug design targets.

### *1.3.2 Influenza Inhibitors*

The M2 ion channel blockers Rimantadine (**1.6**) (Scheme **1.2**) and its derivative Amantadine (**1.7**) (Scheme **1.2**) were the first generation of anti-influenza inhibitors that were specifically targeted against influenza virus A (Govorkova, E.A., Fang, H.-B., et al. 2004). Unfortunately, their lack of efficacy against influenza virus B strains, sideeffects, and the rapid development of drug-resistant strains made design and discovery of a new generation of anti-influenza inhibitors inevitable and imperative (von Itzstein, M. 2007). Currently, two viral neuraminidase inhibitors are used clinically, zanamivir and oseltamivir. Zanamivir (**1.8**) was the first example of structure-based designed inhibitor of neuraminidase (von Itzstein, M., Wu, W.-Y., et al. 1993). A novel carbocyclic sialic acid analogue, called oseltamivir (**1.9**) (Scheme **1.2**) was later developed as

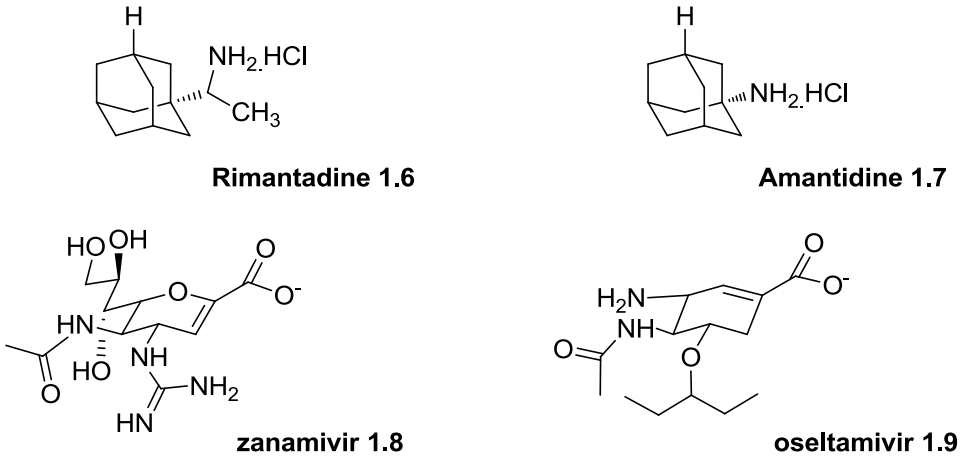


**Scheme 1.2. Structures of four influenza inhibitors.** Rimantadine **1.6** and Amantadine **1.7** block the ion channel of virus protein M2; zanamivir **1.8** and oseltamivir **1.9** are neuraminidase inhibitors.

a potent anti-influenza inhibitor with improved the oral bioavailability (Kim, C.U., Lew, W., et al. 1997; Kim, C.U., Lew, W., et al. 1998). The design of these important anti-viral compounds will be discussed below.

### *1.3.3 Discovery of influenza sialidase inhibitors, zanamivir and oseltamivir*

In the late 1960s DANA was identified as a micromolar inhibitor of influenza sialidase enzyme (Meindl, P., Bodo, G., et al. 1974). However, it had no selectivity against viral, bacterial, and mammalian sialidases (Dyason, J.C. and von Itzstein, M. 2001). DANA was considered an analogue of the transition-state sialosyl cation **1.10** and the difference between them is the position of the double bond, either between the ring oxygen and *C*2 in cation intermediate or *C*2 and *C*3 in DANA (Scheme **1.3**). Sialidase enzymes may generate small quantities of

DANA when incubated with sialic acid substrates, thus generating its own synthetic inhibitor (Burmeister, W.P., Henrissat, B., et al. 1993).

Based on an X-ray crystallographic study of DANA complexed with sialidase and computational calculations (Goodford, P.J. 1985), replacement of the *C*4 hydroxyl group of DANA (**1.5**) with a more basic amine **1.11** or bulkier guanidine group **1.8** (zanamivir), provided two more potent sialidase inhibitors (Scheme **1.4**). In addition, zanamivir has

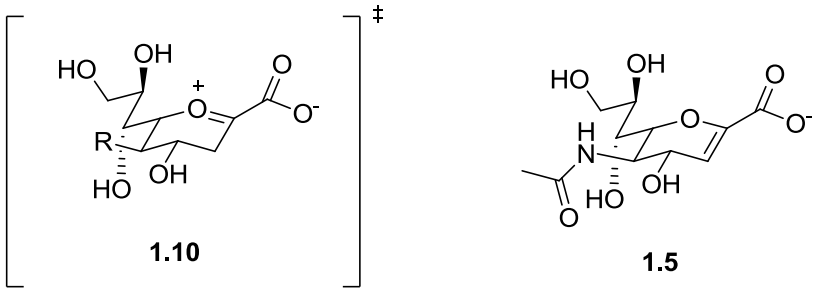


**Scheme 1.3. Structures of proposed transition state sialosyl cation 1.10 and DANA 1.5.**

higher selectivity for influenza sialidases than for other sialidases (Holzer, C.T., Itzstein, M., et al. 1993). Zanamivir was approved as an anti-influenza drug in 1999, known by the trade name relenza. However, poor oral absorption precluded use of relenza as an oral agent. In the next generation of sialidase inhibitors, oseltamivir was identified and shown to possess good oral bioavailabitiy against influenza infection.

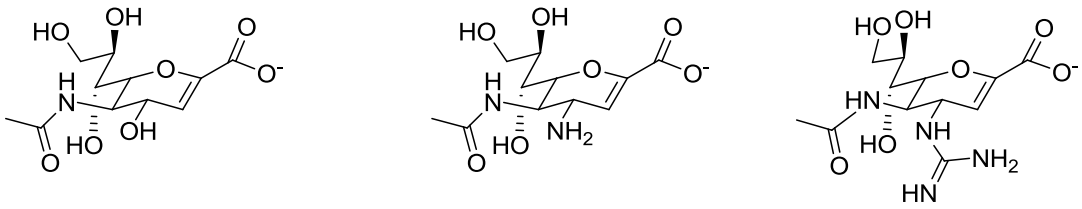


**Scheme 1.4. Structures of DANA 1.5, 4-amino-4-deoxy-Neu5Ac2en, and 4-deoxy-4-guanidino-Neu5Ac2en, zanamivir.** The *C*4 position consists of a hydroxyl, amine and guanidine group respectively.

In the design of oseltamivir, molecular modeling studies suggested that the ring oxygen did not play a key role in binding of the inhibitor (Taylor, N.R. and von Itzstein, M. 1994); therefore, replacement of the dihydropyran ring of DANA with a carbocyclic template should not change the binding affinity. A second major change in the structure was the position of the double bond. Two olefinic isomers were proposed as candidates: **1.12**, which resembles the oxonium cation intermediate **1.10**, and **1.13**, in which the position of the double bond is more similar to that found in DANA (**1.5**) (Scheme **1.5**). Experiments to measure the inhibitory potency of these derivatives showed that **1.12**, which is structurally closer to sialosyl-cation, had micromolar activity, while **1.13** did not inhibit the enzyme (Kim, C.U., Lew, W., et al. 1997).

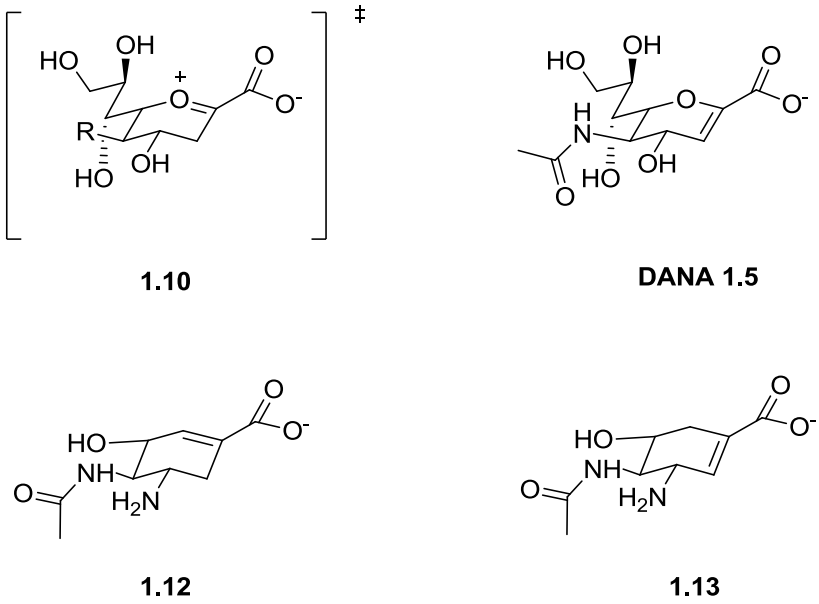


**Scheme 1.5. Comparison of the double bond position between 1.12 and 1.13.** Compound **1.12** mimics the transition state cation **1.10** and compound **1.13** resembles DANA (**1.5**).

To enhance the oral bioavailability of **1.12**, the glycerol chain was replaced with a lipophilic ethyl ester side chain. This more hydrophobic group improved bioavailability and did not reduce binding affinity to sialidase. Oseltamivir was approved in late 1999 for use in the clinic, and was given the trade name tamiflu (Kim, C.U., Lew, W., et al. 1997; Kim, C.U., Lew, W., et al. 1998; von Itzstein, M. 2007).

### *1.4 Inhibitors of mammalian sialidase*

While a great deal of research effort has been directed at developing inhibitors of the viral neuraminidase enzymes, little work has been directed at their mammalian counterparts. Mammals, including humans, express a family of neuraminidase enzymes which are responsible for cleavage and recycling of sialic

acid residues for glycoproteins and glycolipids (Miyagi, T. 2010). Deficiencies in some of these enzymes, particularly NEU1, result in lysosomal storage diseases (Seyrantepe, V., Poupetova, H., et al. 2003). As a result of their role in human health, it may seem counter-intuitive to design inhibitors of these enzymes. However, several forms of human sialidase are upregulated in diseases, such as cancer. Some evidence suggests that neuraminidase enzymes may be partly responsible for changes in the adhesion and metastasis of cancerous cells (Kakugawa, Y., Wada, T., et al. 2002; Miyagi, T., Wada, T., et al. 2004; Miyagi, T., Wada, T., et al. 2003). Additionally, if one considers that the human and viral sialidase enzymes likely share a similar transition state, antiviral drugs may have potentially serious off-target effects if they are potent inhibitors of the human enzymes (Albohy, A., Mohan, S., et al. 2011; Chavas, L.M.G., Kato, R., et al. 2010; Chavas, L.M.G., Tringali, C., et al. 2005).

### *1.4.1 Mammalian sialidase*

The mammalian sialidase enzymes are currently known to consist of four different genes: NEU1, NEU2, NEU3, and NEU4 (Monti, E., Bonten, E., et al. 2010). These enzymes were first cloned and identified between 1993 and 2004 (Monti, E., Bonten, E., et al. 2010). Structural data from X-ray crystallography is available for NEU2, including co-crystal structures with synthetic inhibitors (Chavas, L.M.G., Kato, R., et al. 2010; Chavas, L.M.G., Tringali, C., et al. 2005). Homology models of the other members of the family have been reported, suggesting that all have a similar six-bladed beta-propeller fold (Magesh, S., Suzuki, T., et al. 2006; Albohy, A., Li, M.D., et al. 2010). The enzymes are also

known to occur in different sub-cellular locations. The NEU1, NEU3, and NEU4 proteins are found at the plasma membrane of cells; while NEU2 is found in the cytoplasm (Monti, E., Bonten, E., et al. 2010). There is also a diversity in the substrates and function of the enzymes.

Only limited information is available on the substrate specificity of the human neuraminidase enzymes. Exo-sialidases may have (2,3), (2,6), or (2,8) linkage specificities; in general (2,8) linkages are found primarily in glycolipids and (2,6) linkages are found primarily in glycoproteins. The NEU1, NEU2, and NEU4 enzymes are known to act on glycoproteins, and NEU3 is specific to glycolipids (Miyagi, T. 2010; Miyagi, T., Wada, T., et al. 1999). Recent work has demonstrated that NEU2 cleaves both (2,3) and (2,6) linkages, with some preference for the latter (Li, Y., Cao, H., et al. 2011). A number of specific functions have been ascribed to the mammalian neuraminidase enzymes; however the identity of the responsible isoform is not always clear.

The proposed functions of the sialidase enzymes touch on a number of crucial aspects of human health and disease. Perhaps the first proposed role of human neuraminidases involves the "neuraminidase effect", a general observation that immune cells are pro-adhesive once treated with the enzyme (Bagriacik, E.U. and Miller, K.S. 1999; Weiss, L. 1963). In fact, neuraminidase treatment can disrupt the adhesion of cells in tissues (Kanwar, Y.S. and Farquhar, M.G. 1980). Even before cloning of the human enzymes, forms of neuraminidase activity had been partially purified from immune cells (Greffard, A., Pairon, J.C., et al. 1994). Neuraminidase activity in human cells has been implicated in the metastasis and

resistance to apoptosis of several cancers (Miyagi, T., Wada, T., et al. 2003). Neuraminidase activity has also been found to reveal specific cell surface epitopes that lead to important cell adhesion events (Quinn, M.T., Swain, S.D., et al. 2001; Gadhoum, S.Z. and Sackstein, R. 2008). For example, leukocyte adhesion is enhanced by a native sialidase activity (Cross, A.S., Sakarya, S., et al. 2003), one of whose targets has been recently shown to be the lymphocyte functional antigen-1 (LFA-1) (Feng, C., Zhang, L., et al. 2011). Thus, the human sialidases have crucial roles in human health; however specific small molecule inhibitors of these enzymes are unknown.

### *1.4.2 Inhibitors*

Known inhibitors of viral sialidase have unexpectedly weak potency against the human enzymes (Hata, K., Koseki, K., et al. 2008). This may be fortuitous, as these compounds may therefore have reduced off-target effects. It has been proposed that certain populations may be more susceptible to oseltamivir side effects due to mutations in sialidase genes (Li, C.-Y., Yu, Q., et al. 2007). Our group has examined the structure of the human NEU3 enzyme, and tested the activity of known antivirals against the protein. We observed that modifications of the oseltamivir *C*4 position (the equivalent of the glycerol side-chain of Neu5Ac) were detrimental to inhibitor potency, and that even modification of the *C*6 hydroxyl group to an amine did not recover activity (Albohy, A., Mohan, S., et al. 2011). Importantly, these studies indicate that our knowledge of human neuraminidase inhibitor design is lacking. Therefore, there is a need for studies of new synthetic inhibitors which help to define the structure-activity relationships

of these important enzymes – and which may ultimately generate specific and potent inhibitors of each isoform.

Only a handful of studies have sought to identify specific inhibitors of the human sialidase enzymes. The first of these was reported by Magesh et al., in which they tested a series of *C*9 modified forms of DANA (Magesh, S., Moriya, S., et al. 2008). The most potent of these showed specificity for NEU1, however the other family members were not targeted by this small library. Further studies by this group in 2009 tested benzoic acids as mimics of DANA, however very few compounds had significant activity against the human isoforms (Magesh, S., Savita, V., et al. 2009). Known anti-viral compounds have been tested against several of the human isoforms (Chavas, L.M.G., Kato, R., et al. 2010; Hata, K., Koseki, K., et al. 2008). Legionaminic acid derivatives have been tested against NEU2, and demonstrate some limited inhibitory effects (Watson, D.C., Leclerc, S., et al. 2010). Recently Li et al. have tested a series of DANA analogs against NEU2, and identified an *N*5-azidoacetyl derivative as having increased potency (Li, Y., Cao, H., et al. 2011). From all of these studies, it appears that zanamivir **1.8** is currently the best known inhibitor of the human enzymes while oseltamivir and its derivatives have little or no potency (Hata, K., Koseki, K., et al. 2008; Albohy, A., Mohan, S., et al. 2011).

### *1.5 Project objectives*

The human neuraminidase enzymes are an important biological target for human health and disease. There is a clear need for specific inhibitors of these enzyme isoforms both for research into the native function of these enzymes, and

as potential therapeutics. In this thesis we will describe studies of small molecule inhibitor design for the human enzyme, NEU3.

We considered the work of Magesh et al.in 2008, which demonstrated that some modifications of DANA resulted in a range of activity among the neuraminidase isoforms. In particular, modifications of *C*9 seemed to be tolerated by several isoforms. We hypothesized that modifications of the DANA core which were tolerated by the enzyme could be used to improve inhibitor potency for the isoform, NEU3. In Chapter 2 we will describe the synthesis of a series of DANA derivatives which feature modifications at the *C*9 and *N*5 positions (Scheme **1.6**). These compounds were designed to test the hypothesis that NEU3 has a larger binding pocket for the glycerol side-chain than is found in the viral enzymes. These compounds were tested for their potency against NEU3 using in vitro assays. We found that while *C*9 modifications are well tolerated, and may even improve potency, modifications at *N*5 were generally detrimental.

Based on these first results, we hypothesized that since the glycerol chain was able to accommodate modifications of *C*9 sterically, that alternative functional groups at this position could improve the specificity of binding. In Chapter 3 we describe a second generation of compounds which replace the linkage at *C*9 with a hydrazine (Scheme **1.6**). The synthetic route to these compounds will allow the generation of a library of compounds which will be tested against the human enzymes.

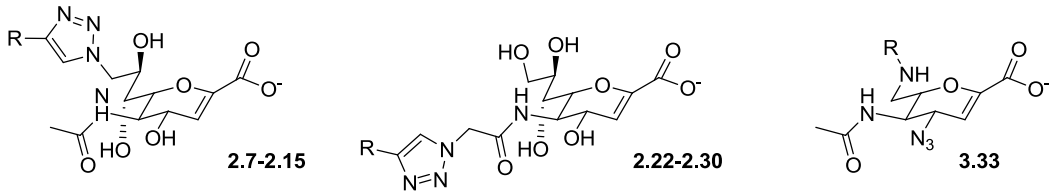


**Scheme 1.6. *C*9, *N*5 and *C*7 modification targets.** Synthesis of **2.7**-**2.15** and **2.22**-**2.30** is discussed in Chapter 2, and synthesis of **3.6** is studied in detail in Chapter 3.

### *1.6 References*


Achyuthan KE, Achyuthan AM. (2001). Comparative enzymology, biochemistry and pathophysiology of human exo-[alpha]-sialidases (neuraminidases). *Comparative Biochemistry and Physiology Part B: Biochemistry and Molecular Biology*, 129:29-64.

Ajit Varki RDC, Jeffrey D Esko, Hudson H Freeze, Pamela Stanley, Carolyn R Bertozzi, Gerald W Hart, and Marilynn E Etzler.2009.Essentials of Glycobiology, 2nd edition.

Albohy A, Li MD, Zheng RB, Zou C, Cairo CW. (2010). Insight into recognition and catalysis of the mammalian neuraminidase 3 (NEU3) through molecular modeling and site directed mutagenesis. *Glycobiology*, 20:1127-1138.

Albohy A, Mohan S, Pinto BM, Cairo CW. (2011). Inhibitor selectivity of a new class of oseltamivir analogs against viral neuraminidase over human neuraminidase enzymes. *Bioorg. Med. Chem.*, 19:2817-2822.

Bagriacik EU, Miller KS. (1999). Cell surface sialic acid and the regulation of immune cell interactions: the neuraminidase effect reconsidered. *Glycobiology*, 9:267-275.

Burmeister WP, Henrissat B, Bosso C, Cusack S, Ruigrok RWH. (1993). Influenza-B virus neuraminidase can synthesize its own inhibitor. *Structure*, 1:19-26.

Buschiazzo A, Alzari PM. (2008). Structural insights into sialic acid enzymology. *Curr. Opin. Chem. Biol.*, 12:565-572.

Cabezas JA. (1991). Some questions and suggestions on the type references of the official nomenclature (IUB) for sialidase(s) and endosialidase. *Biochem. J*, 278:311-310.

Chavas LMG, Tringali C, Fusi P, Venerando B, Tettamanti G, Kato R, Monti E, Wakatsuki S. (2005). Crystal structure of the human cytosolic sialidase Neu2 - Evidence for the dynamic nature of substrate recognition. *J. Biol. Chem.*, 280:469-475.

Chavas LMG, Kato R, Suzuki N, von Itzstein M, Mann MC, Thomson RJ, Dyason JC, McKimm-Breschkin J, Fusi P, Tringali C, Venerando B, *et al.* (2010). Complexity in Influenza Virus Targeted Drug Design: Interaction with Human Sialidases. *J. Med. Chem.*, 53:2998-3002.

Cross AS, Sakarya S, Rifat S, Held TK, Drysdale BE, Grange PA, Cassels FJ, Wang LX, Stamatos N, Farese A, Casey D, *et al.* (2003). Recruitment of murine neutrophils in vivo through endogenous sialidase activity. *J. Biol. Chem.*, 278:4112-4120.

Dyason JC, von Itzstein M. (2001). Anti-Influenza Virus Drug Design: Sialidase Inhibitors. *Aust. J. Chem.*, 54:663-670.

Feng C, Zhang L, Almulki L, Faez S, Whitford M, Hafezi-Moghadam A, Cross AS. (2011). Endogenous PMN sialidase activity exposes activation epitope on CD11b/CD18 which enhances its binding interaction with ICAM-1. *J. Leukocyte Biol.*, 90:313-321.

Gadhoum SZ, Sackstein R. (2008). CD15 expression in human myeloid cell differentiation is regulated by sialidase activity. *Nat. Chem. Biol.*, 4:751-757.

Goodford PJ. (1985). A computational procedure for determining energetically favorable binding sites on biologically important macromolecules. *J. Med. Chem.*, 28:849-857.

Govorkova EA, Fang H-B, Tan M, Webster RG. (2004). Neuraminidase Inhibitor-Rimantadine Combinations Exert Additive and Synergistic Anti-Influenza Virus Effects in MDCK Cells. *Antimicrob. Agents Chemother.*, 48:4855-4863.

Greffard A, Pairon JC, Terzidis-Trabelsi H, Heslan JM, Bignon J, Lambre CR, Pilatte Y. (1994). Initial characterization of human thymocyte sialidase activity: evidence that this enzymatic system is not altered during the course of T-cell maturation. *Int. J. Biochem.*, 26:769-776.

Hata K, Koseki K, Yamaguchi K, Moriya S, Suzuki Y, Yingsakmongkon S, Hirai G, Sodeoka M, Von Itzstein M, Miyagi T. (2008). Limited inhibitory effects of oseltamivir and zanamivir on human sialidases. *Antimicrob. Agents Chemother.*, 52:3484-3491.

Holzer CT, Itzstein M, Jin B, Pegg MS, Stewart WP, Wu W-Y. (1993). Inhibition of sialidases from viral, bacterial and mammalian sources by analogues of 2-deoxy-2,3-didehydro-<i>N</i>-acetylneuraminic acid modified at the C-4 position. *Glycoconjugate J.*, 10:40-44.

Kakugawa Y, Wada T, Yamaguchi K, Yamanami H, Ouchi K, Sato I, Miyagi T. (2002). Up-regulation of plasma membrane-associated ganglioside sialidase (Neu3) in human colon cancer and its involvement in apoptosis suppression. *Proc. Natl. Acad. Sci. U. S. A.*, 99:10718-10723.

Kanwar YS, Farquhar MG. (1980). Detachment of endothelium and epithelium from the glomerular basement membrane produced by kidney perfusion with neuraminidase. *Lab. Invest.*, 42:375-384.

Kim CU, Lew W, Williams MA, Liu H, Zhang L, Swaminathan S, Bischofberger N, Chen MS, Mendel DB, Tai CY, Laver WG, *et al.* (1997). Influenza Neuraminidase Inhibitors Possessing a Novel Hydrophobic Interaction in the Enzyme Active Site: Design, Synthesis, and Structural Analysis of Carbocyclic Sialic Acid Analogues with Potent Anti-Influenza Activity. *J. Am. Chem. Soc.*, 119:681-690.

Kim CU, Lew W, Williams MA, Wu H, Zhang L, Chen X, Escarpe PA, Mendel DB, Laver WG, Stevens RC. (1998). Structure−Activity Relationship Studies of Novel Carbocyclic Influenza Neuraminidase Inhibitors. *J. Med. Chem.*, 41:2451-2460.

Li C-Y, Yu Q, Ye Z-Q, Sun Y, He Q, Li X-M, Zhang W, Luo J, Gu X, Zheng X, Wei L. (2007). A nonsynonymous SNP in human cytosolic sialidase in a small Asian population results in reduced enzyme activity: potential link with severe adverse reactions to oseltamivir. *Cell Res.*, 17:357-362.

Li Y, Cao H, Yu H, Chen Y, Lau K, Qu J, Thon V, Sugiarto G, Chen X. (2011). Identifying selective inhibitors against the human cytosolic sialidase NEU2 by substrate specificity studies. *Mol. BioSyst.*, 7:1060-1072.

Magesh S, Suzuki T, Miyagi T, Ishida H, Kiso M. (2006). Homology modeling of human sialidase enzymes NEU1, NEU3 and NEU4 based on the crystal structure of NEU2: Hints for the design of selective NEU3 inhibitors. *Journal of Molecular Graphics and Modelling*, 25:196-207.

Magesh S, Moriya S, Suzuki T, Miyagi T, Ishida H, Kiso M. (2008). Design, synthesis, and biological evaluation of human sialidase inhibitors. Part 1: Selective inhibitors of lysosomal sialidase (NEU1). *Bioorg. Med. Chem. Lett.*, 18:532-537.

Magesh S, Savita V, Moriya S, Suzuki T, Miyagi T, Ishida H, Kiso M. (2009). Human sialidase inhibitors: Design, synthesis, and biological evaluation of 4-acetamido-5-acylamido-2-fluoro benzoic acids. *Bioorg. Med. Chem.*, 17:4595-4603.

Magesh S, Sriwilaijaroen N, Moriya S, Ando H, Miyagi T, Suzuki Y, Ishida H, Kiso M. (2011). Evaluation of a Set of C9 N-acyl Neu5Ac2en Mimetics as Viral Sialidase Selective Inhibitors. *International Journal of Medicinal Chemistry*, 2011.

Matrosovich M, Klenk H-D. (2003). Natural and synthetic sialic acid-containing inhibitors of influenza virus receptor binding. *Rev. Med. Virol.*, 13:85-97.

Meindl P, Bodo G, Palese P, Schulman J, Tuppy H. (1974). Inhibition of neuraminidase activity by derivatives of 2-deoxy-2,3-dehydro-N-acetylneuraminic acid. *Virology*, 58:457-463.

Miyagi T, Wada T, Iwamatsu A, Hata K, Yoshikawa Y, Tokuyama S, Sawada M. (1999). Molecular cloning and characterization of a plasma membrane-associated sialidase specific for gangliosides. *J. Biol. Chem.*, 274:5004-5011.

Miyagi T, Wada T, Yamaguchi K, Hata K. (2003). Sialidase and malignancy: A minireview. *Glycoconjugate J.*, 20:189-198.

Miyagi T, Wada T, Moriya S, Ueno S, Kato K, Yamaguchi K. (2004). A crucial role of plasma membrane-associated sialidase (NEU3) in the survival of human cancer cells. *Glycobiology*, 14:436.

Miyagi T, Wada T, Yamaguchi K, Hata K, Shiozaki K. (2008). Plasma Membrane-associated Sialidase as a Crucial Regulator of Transmembrane Signalling. *J. Biochem.*, 144:279-285.

Miyagi T. (2010). Mammalian sialidases and their functions. *Trends in Glycoscience and Glycotechnology*, 22:162-172.

Monti E, Preti A, Venerando B, Borsani G. (2002). Recent Development in Mammalian Sialidase Molecular Biology. *Neurochem. Res.*, 27:649-663.

Monti E, Bonten E, D'Azzo A, Bresciani R, Venerando B, Borsani G, Schauer R, Tettamanti G. 2010. Sialidases in Vertebrates: A Family Of Enzymes Tailored For Several Cell Functions. In: Derek H editor. Adv. Carbohydr. Chem. Biochem.: Academic Press. p. 403-479.

Monti E, Bonten E, D'Azzo A, Bresciani R, Venerando B, Borsani G, Schauer R, Tettamanti G, Derek H. 2010. Sialidases in Vertebrates: A Family Of Enzymes Tailored For Several Cell Functions*. Adv. Carbohydr. Chem. Biochem.: Academic Press. p. 403-479.

Morais GR, Oliveira RS, Falconer RA. (2009). Selective synthesis of Neu5Ac2en and its oxazoline derivative using BF3 Ŧt2O. *Tetrahedron Lett.*, 50:1642-1644.

Moscona A. (2005). Neuraminidase Inhibitors for Influenza. *New Engl. J. Med.*, 353:1363-1373.

Quinn MT, Swain SD, Parkos CA, Jutila KL, Siemsen DW, Kurk SL, Jesaitis AJ, Jutila MA. (2001). A carbohydrate neoepitope that is up-regulated on human

mononuclear leucocytes by neuraminidase treatment or by cellular activation. *Immunology*, 104:185-197.

Schauer R. (2004). Victor Ginsburg's influence on my research of the role of sialic acids in biological recognition. *Arch. Biochem. Biophys.*, 426:132-141.

Seyrantepe V, Poupetova H, Froissart R, Zabot MT, Maire I, Pshezhetsky AV. (2003). Molecular pathology of NEU1 gene in sialidosis. *Hum. Mutat.*, 22:343-352.

Skehel JJ, Wiley DC. (2000). Receptor binding and membrane fusion in virus entry: the influenza hemagglutinin *Annu. Rev. Biochem*, 69:531-569.

Sun X-L, Kai T, Takayanagi H, Furuhata K. (1997). Syntheses of sialic acid analogues with acylamino groups at C-4 (N-acyl regioisomers of sialic acids). *Carbohydr. Res.*, 298:181-189.

Taylor NR, von Itzstein M. (1994). Molecular Modeling Studies on Ligand Binding to Sialidase from Influenza Virus and the Mechanism of Catalysis. *J. Med. Chem.*, 37:616-624.

Varghese JN. (1999). Development of neuraminidase inhibitors as anti-influenza virus drugs. *Drug Dev. Res.*, 46:176-196.

von Itzstein M, Wu W-Y, Kok GB, Pegg MS, Dyason JC, Jin B, Phan TV, Smythe ML, White HF, Oliver SW, Colman PM, *et al.* (1993). Rational design of potent sialidase-based inhibitors of influenza virus replication. *Nature*, 363:418-423.

von Itzstein M. (2007). The war against influenza: discovery and development of sialidase inhibitors. *Nat. Rev. Drug Discov.*, 6:967-974.

Watson DC, Leclerc S, Wakarchuk WW, Young NM. (2010). Enzymatic synthesis and properties of glycoconjugates with legionaminic acid as a replacement for neuraminic acid. *Glycobiology*, 21:99-108.

Weiss L. (1963). Studies on cellular adhesion in tissue-culture. V. Some effects of enzymes on cell-detachment. *Exp. Cell Res.*, 30:509-520.

We ̈wer M, Chen C-C, Kemp MM, Linhardt RJ. (2009). Synthesis and Biological Evaluation of Non-Hydrolyzable 1,2,3-Triazole-Linked Sialic Acid Derivatives as Neuraminidase Inhibitors. *Eur. J. Org. Chem.*, 2009:2611-2620.

Wen W-H, Wang S-Y, Tsai K-C, Cheng Y-SE, Yang A-S, Fang J-M, Wong C-H. (2010). Analogs of zanamivir with modified C4-substituents as the inhibitors

against the group-1 neuraminidases of influenza viruses. *Biorg. Med. Chem.*, 18:4074-4084.

# Chapter 2

## Inhibition of human neuraminidase 3 (NEU3) by *C*9-triazole derivatives of 2,3-didehydro-*N*-acetylneuraminic acid[1,2,3]

[1] Portions of the work described in this chapter have been published in Zou Y, Albohy A, Sandbhor M, Cairo CW. (2010) "Inhibition of human neuraminidase 3 (NEU3) by C9-triazole derivatives of 2,3-didehydro-*N*-acetyl-neuraminic acid." *Bioorg. Med. Chem. Lett.*, 20:7529-7533.
[2] Assay studies (Table 2.3 and 2.4.6 $IC_{50}$ Curves) and molecular docking (Figure 2.1) were performed by Amgad Albohy (University of Alberta).
[3] Phenylpropargyl ether was synthesized by Mahendra Sandbhor (University of Alberta).

### *2.1 Introduction*

The mammalian sialidase enzymes are a family of glycosyl hydrolases which cleave the terminal sialic acid residue from glycoproteins and glycolipids (Monti, E., Preti, A., et al. 2002). Dysfunction of these enzymes can result in sialic acid storage disorders, such as type I and II sialidosis (Caciotti, A., Di Rocco, M., et al. 2009; Seyrantepe, V., Poupetova, H., et al. 2003). Mammalian sialidase enzymes also play essential roles in cellular function, with reported effects on diverse processes including neurite outgrowth (Varki, N.M. and Varki, A. 2007), immune cell activation (Chen, X.P., Enioutina, E.Y., et al. 1997), cellular communication (Papini, N., Anastasia, L., et al. 2004; Ueno, S., Saito, S., et al. 2006; Anastasia, L., Papini, N., et al. 2008), signalling (Sasaki, A., Hata, K., et al. 2003; Carubelli, I., Venerando, B., et al. 2006; Chen, X.P., Enioutina, E.Y., et al. 1997; Gadhoum, S.Z. and Sackstein, R. 2008), adhesion (Kato, K., Shiga, K., et al. 2006), as well as apoptosis (Azuma, Y., Sato, H., et al. 2007; Kakugawa, Y., Wada, T., et al. 2002) and metastasis of malignant cells (Uemura, T., Shiozaki, K., et al. 2009; Miyagi, T., Wada, T., et al. 2003). Selective, tight-binding inhibitors of sialidase isoforms could provide an essential tool for discerning the role of individual isozymes in cell biology. However, while nanomolar inhibitors are known for pathogenic neuraminidase enzymes, most notably the influenza viral neuraminidase, no inhibitors of similar potency are known for the human enzymes (Dyason, J.C. and von Itzstein, M. 2001).

Currently identified members of the sialidase enzyme family in humans consist of NEU1, NEU2, NEU3, and NEU4. All four enzymes are classified as

*exo*-sialidases (EC 3.2.1.18) and members of glycoside hydrolase family 33 in the CaZy database (Cantarel, B.L., Coutinho, P.M., et al. 2009). Among the mammalian enzymes, only the human NEU2 structure has been studied by crystallography, revealing that the enzyme adopts a 6-bladed β-propeller fold (Chavas, L.M.G., Tringali, C., et al. 2005; Chavas, L.M.G., Kato, R., et al. 2010). Homology models of all four human enzymes were first proposed by Magesh et al. in 2006; however, many of the specific features of the models remain to be experimentally tested (Magesh, S., Suzuki, T., et al. 2006). For example, the predicted catalytic residues have only been confirmed in NEU2 (Chavas, L.M.G., Tringali, C., et al. 2005) and NEU3 (Albohy, A., Li, M.D., et al. 2010). There are few reports of inhibitors tested against the family of human NEU enzymes. A panel of 9-amino-9-deoxy-2,3-didehydro-*N*-acetylneuraminic acid derivatives were tested against all four enzymes; the most potent of these inhibitors showed only low micromolar activity against NEU1 (Magesh, S., Moriya, S., et al. 2008). A library of benzoic acid derivatives have also been tested against all four isozymes (Magesh, S., Savita, V., et al. 2009). The viral neuraminidase inhibitors zanamivir and oseltamivir have limited potency against all of the human sialidases (Hata, K., Koseki, K., et al. 2008). However, tight binding (<1 μM) and selective inhibitors for individual isozymes remain to be identified.

Our group has studied the substrate recognition and catalysis of human NEU3, the plasma membrane-associated sialidase, which modifies glycolipid substrates (Albohy, A., Li, M.D., et al. 2010). This enzyme is particularly challenging to work with due to its hydrophobic character and propensity for

aggregation. We tested the predictions of a NEU3 homology model using site-directed mutagenesis, and validated both the catalytic residues and several residues which are essential for substrate recognition. As part of this study, we performed molecular docking of a well-known sialidase inhibitor, 2,3-didehydro-*N*-acetyl-neuraminic acid (DANA). Our molecular docking studies of DANA in the NEU3 binding site revealed a relatively large hydrophobic pocket adjacent to the *C*9 position of sialic acid. We hypothesized that this region of the binding site could be used to design improved inhibitors of NEU3 based on the DANA core structure.

Known substrates of NEU3 include α(2,3)-linked sialosides (Table **2.1**) found in glycolipid substrates, such as GM3 (Valaperta, R., Chigorno, V., et al. 2006). Additionally, α(2,8)-linked sialosides are known to be substrates for the enzyme, and there is evidence that the enyzme has a preference for this linkage.(Azuma, Y., Sato, H., et al. 2007) A common strategy for the design of sialidase inhibitors relies on the use of DANA as a transition state analog. The inhibition of NEU3 by DANA has been reported by several groups, and is usually found to be in the mid-micromolar range (Table **2.1**) (Albohy, A., Li, M.D., et al. 2010; Hata, K., Koseki, K., et al. 2008; Magesh, S., Moriya, S., et al. 2008). Interestingly, zanamivir, a potent viral NEU inhibitor has been reported to have low micromolar activity against NEU3, while oseltamivir is essentially inactive against the enzyme (Hata, K., Koseki, K., et al. 2008). Magesh et al. found that NEU3 could tolerate a relatively bulky phenyl-amide group at the *C*9-position of DANA, although these derivatives had relatively low potency (Table **2.1**)

(Magesh, S., Moriya, S., et al. 2008). We considered that a potential strategy for rapidly exploring the structure activity relationships (SAR) of DANA analogs for NEU3 could revolve around a modular synthetic strategy which introduced modifications at the *C*9- and *N*5Ac- positions from a common intermediate. Li et al. first reported the use of click chemistry to generate viral NEU inhibitors from a *C*4-azido-derivative of DANA (Li, J., Zheng, M., et al. 2006). Lu and Gervay-Hague expanded on this strategy by generating *C*4- and *C*7-azido DANA analogs, which could be elaborated to triazoles and multivalent derivatives of zanamivir (Lu, Y. and Gervay-Hague, J. 2007). In a related strategy, non-hydrolyzable sialoside derivatives have been generated by incorporating an azide at *C*2 of Neu5Ac (We ïwer, M., Chen, C.-C., et al. 2009).

We considered using a 1,2,3-triazole as an efficient way to introduce more diversity at the *C*9 and *N*5 positions. Triazoles are five-membered heterocycles containing one pyrrolic nitrogen atom, two pyridinic nitrogen atoms, and two carbon atoms (Theophil, E., Siegfried, H., et al. 2007; Schofield, K., M. R. Grimmett, 1976). The two common isomeric forms of the triazole, are named by the location of the N-atoms in the ring as the 1,2,3- and 1,2,4-triazole. The 1,2,3-triazole is aromatic because of the delocalization of six electrons in π-MOs. The 1,2,3-triazole is amphoteric (Shalini, K., Kumar, N., 2011), and a weak base, with a p*K*a value of 1.17. The unsubstituted pyrrolic nitrogen atom is NH-acidic with p*K*a a value of 9.3 (Theophil, E., Siegfried, H., et al. 2007). Triazole derivatives have attracted more and more attention because of their pharmacological properties including anti-bacterial, anti-HIV, anti-inflammatory, and anti-tumor

activates (Srividhya, D., Manjunathan, S., et al. 2009; Hotha, S., Anegundi, R. I., 2005). The 1,2,3-triazole heterocycle posses several advantages for small molecule inhibitors: (1) it has a high stability, and is inert to oxidation, reduction, and even high temperature conditions, (2) it has a high dipole moment, which could be favorable for water solubility, and (3) it acts as an acceptor of hydrogen bonds (Kaval, N., Ermolat'ev, D., 2005; Srividhya, D., Manjunathan, S., et al. 2009). Futhermore, the synthesis of the 1,2,3-trizole ring, using Cu-catalyzed azide-alkyne cycloaddition (CuAAC) (Meldal, M. and Tornøe, C.W. 2008), also known as a click reaction, is very efficient. Therefore we set out to generate a small library of DANA analogs introducing various 1,2,3-triazloe derivatives with modifications at the *C*9 and *N*5Ac as a means to explore the binding site topology of NEU3 and to identify new inhibitors of the enzyme.

### *2.2 Synthesis of C9-Azide, N5Ac-azido and –triazolyl derivatives*

The basis of our strategy relied on the generation of two derivatives, the *N*5-azidoacetyl- (**2.6**) and 9-azido-9-deoxy (**2.21**) DANA (**1.5**) derivatives (Scheme **2.1**). We began our synthesis from *N*5-acetyl-neuraminic acid (Neu5Ac), which could be converted to the peracetylated methyl ester, **2.1**, following reported methods (Marra, A. and Sinay, P. 1989; Martin, R., Witte, K.L., et al. 1998). We obtained moderate yields of the acetyl-protected 2,3-didehydro analog **2.2** using triphenylphosphine hydrobromide (Scheme **2.2**) (Bolitt, V., Mioskowski, C., et al. 1990; D. Burkart, M., P. Vincent, S., et al. 1999). To prepare compound **2.6** and the related triazole derivatives, **2.2** was deacetylated

(Bhaskar K. V., Duggan, P.J., et al. 2001) to give **2.3** and the *O*9 position was selectively converted to a sulfonate ester, **2.4** (Han, S., Collins, B.E., et al. 2005).

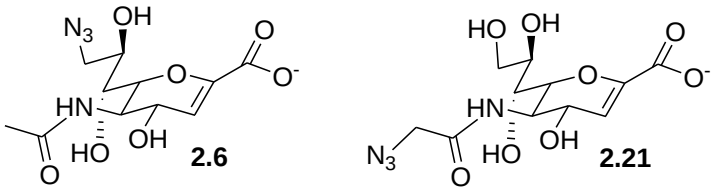


**Scheme 2.1. DANA analog synthetic targets.**

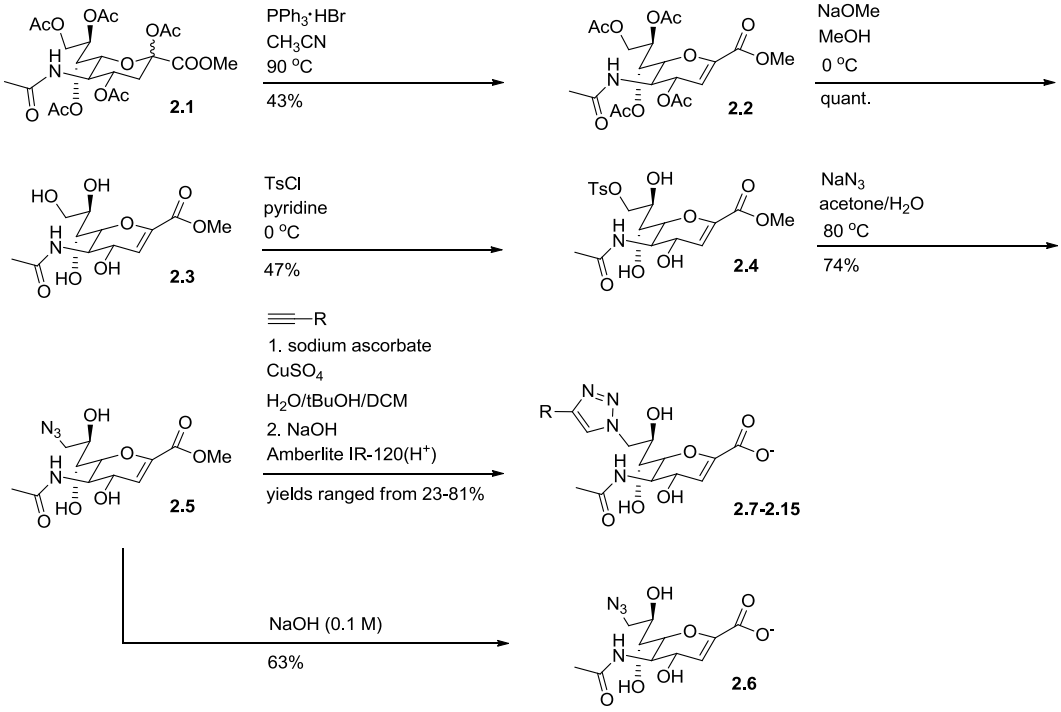


**Scheme 2.2. Synthesis of C9-azide derivatives.** Triazole-containing inhibitors **2.7-2.15** were generated in 23-81% yield, respectively, using the Cu-catalyzed azide-alkyne cycloaddition (CuAAC).

Compound **2.3** was hydrolyzed to afford Neu5Ac2en, DANA (**1.5**) in good yield (Scheme **2.3**). The sulfonate could then be displaced with sodium azide to give the methyl ester of **2.6**, compound **2.5** (Magesh, S., Moriya, S., et al. 2008; Han, S., Collins, B.E., et al. 2005). Hydrolysis of **2.5** under basic conditions provided the target compound **2.6**. Alternatively, **2.5** could be used to generate triazole derivatives using the copper-catalyzed 1,3-dipolar Huisgen cycloaddition of an

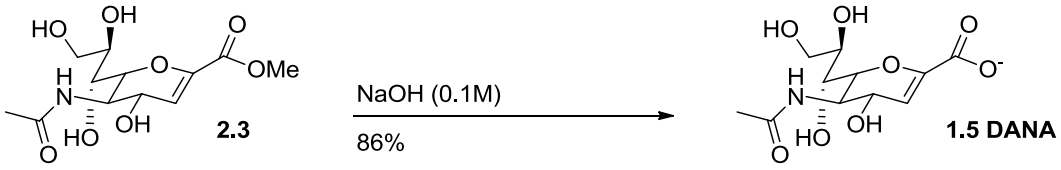


**Scheme 2.3. Synthesis of DANA.** DANA was provided by hydrolysis of **2.3** under basic conditions with 86% yield.

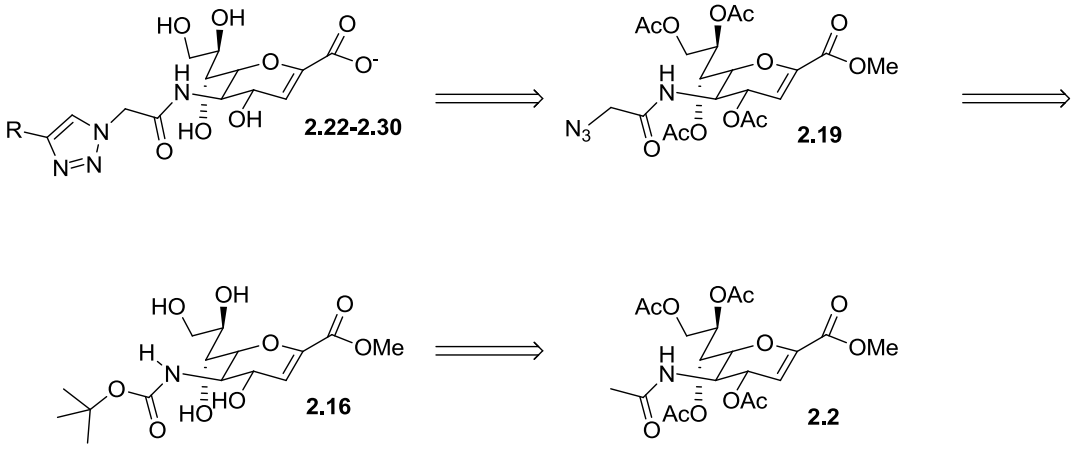


***Scheme 2.4. Retrosynthetic analysis of N5Ac–triazolyl derivatives.*** Triazole-containing inhibitors 2.22-2.30 can be generated from acetyl-protected 2,3-didehydro analog 2.2.

**Table 2.1. Previously reported inhibitors of NEU3.**

| Entry | Compound | Structure | NEU3 $IC_{50}$ μM |
|---|---|---|---|
| 1 | α -sialoside | 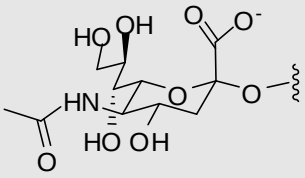 | na |
| | | | 70 ± 15 (Hata, K., Koseki, K., et al. 2008) [a] |
| 2 | DANA | 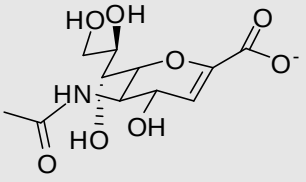 | 61 (Magesh, S., Moriya, S., et al. 2008)[b] |
| | | | 43± 7 (Albohy, A., Li, M.D., et al. 2010)[b] |
| 3 | zanamivir | 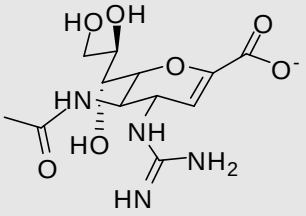 | 7± 3 (Hata, K., Koseki, K., et al. 2008)[a] |
| 4 | oseltavimir | 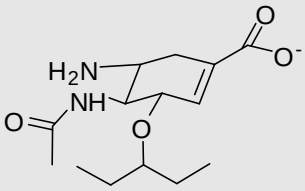 | >10000 (Hata, K., Koseki, K., et al. 2008)[a] |
| 5 | 10b [c] | 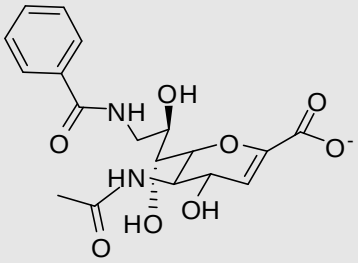 | 320 (Magesh, S., Moriya, S., et al. 2008)[b] |
| 6 | 10a [c] | 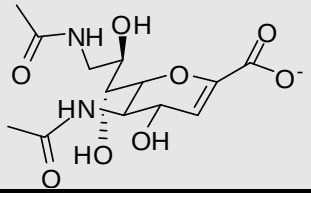 | >1000 (Magesh, S., Moriya, S., et al. 2008)[b] |

a. Determined by inhibition of GM3 hydrolysis.

b. Determined by inhibition of 4MU-NA hydrolysis.

c. Nomenclature as used in Magesh et al.(Magesh, S., Moriya, S., et al. 2008)

alkyne, also known as a Cu-catalyzed azide-alkyne cycloaddition (CuAAC) (Meldal, M. and Tornøe, C.W. 2008). We set out to generate a series of nine triazole derivatives of **2.6** which could be tested for potency against NEU3 (**2.7-2.15**, Table **2.3**) (Zou, Y., Albohy, A., et al. 2010).

We envisioned that the triazole-containing inhibitors **2.22-2.30** could be derived from the azide **2.19** in one step by CuAAC reaction as described before. To introduce the azide group at *N*5 position, removal of $Boc_2O$ group protected **2.16** is an essential step. The precursor **2.16** can be derived from acetyl-protected 2,3-didehydro analog **2.2** in two steps (Scheme **2.4**).

To prepare derivatives of compound **2.21**, we required selective deprotection of the *N*5 side chain. To achieve this, we first protected *N*5 with di-*tert*-butyldicarbonate, ($Boc_2O$) (Johansson, S., Nilsson, E., et al. 2009), followed by deacetylation to generate **2.16** (Scheme **2.5**). Subsequent *O*-acetylation provided compound **2.17**, which was selectively deprotected to reveal the free amine at *N*5 (**2.18**). With the free amine in hand, we introduced a modified *N*-acyl group that contained an azide handle. We employed an activated ester of azidoacetic acid (Yu, H., Huang, S., et al. 2006; Loka, R.S., Sadek, C.M., et al. 2010), which gave the azide **2.19** in excellent yield. Removal of the *O*-acetyl protecting groups provided the methyl ester **2.20**, which could be hydrolyzed to the target compound **2.21**. As before, we generated a series of triazole derivatives of **2.21** from **2.20** by CuAAC, followed by hydrolysis of the methylester (compounds **2.22-2.30**, Table **2.2, 2.3**).

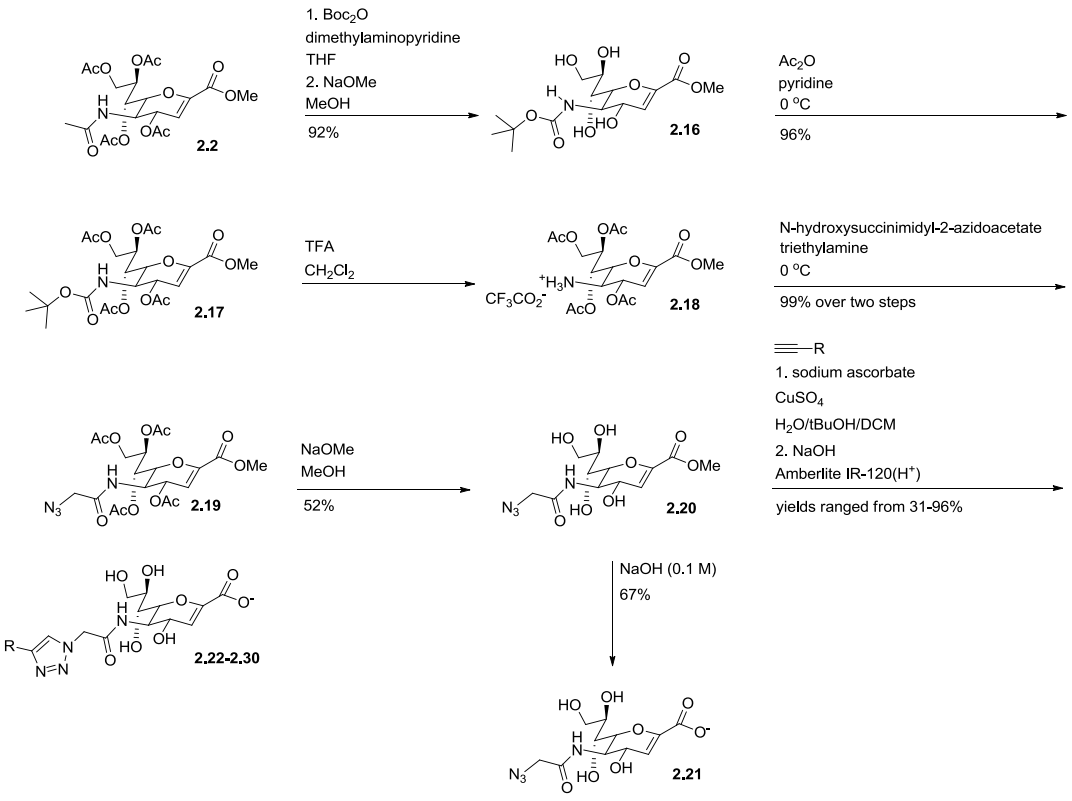


**Scheme 2.5. Synthesis of N5Ac–azido and –triazolyl derivatives.** The derivatives were generated in moderate yield (31-96%) from **2.20** by CuAAC, followed by hydrolysis of the methyl ester.

**Table 2.2. Alkynes used in CuAAC reactions of 2.19 and 2.5.**

| | | |
|---|---|---|
| 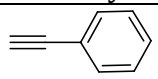 | 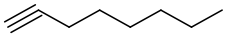 | 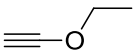 |
| 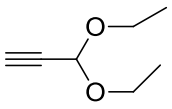 | 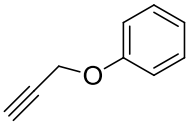 | 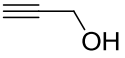 |
| 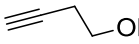 | 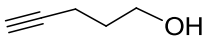 | 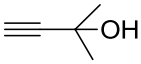 |

### *2.3 NEU3 inhibition assays*

We previously reported a bacterial expression system for NEU3 which could be exploited to test the potency of inhibitors (Albohy, A., Li, M.D., et al. 2010). Although there are previous reports of bacterial expression of this enzyme (Ha, K.T., Lee, Y.C., et al. 2004), we found that expression of the protein as an *N*-terminal fusion with the maltose binding protein (MBP) helped to stabilize the protein and prevent aggregation. Additionally, producing the protein in bacterial cells avoided background signal due to contaminating activity of other sialidase isoforms present in mammalian cells. Using purified MBP-NEU3, we tested the inhibitory potency of the *C*9 (**2.6**, **2.7**-**2.15**) and *N*5Ac (**2.21**, **2.22**-**2.30**) derivatives against NEU3 using a fluorescence assay based on the hydrolysis of 4-methylumbelliferyl α-D-*N*-acetylneuraminic acid (4MU-NA) (**2.33**) (Table **2.3**).

As expected, we observed that DANA was a good inhibitor of NEU3, with an $IC_{50}$ of approximately 40 μM (Hata, K., Koseki, K., et al. 2008; Magesh, S., Moriya, S., et al. 2008; Albohy, A., Li, M.D., et al. 2010). We found that modification of DANA at the *C*9 position by a triazole with a hydrophobic group which lacked a hydrogen bond donor lead to improved activity. The most potent compounds were the phenyl **2.7** (20 ± 10 μM), hexyl **2.8** (23 ± 4 μM), and phenoxymethyl **2.11** (45 ± 3 μM) derivatives. Importantly, the data suggest that the triazole portion of the inhibitor is partly responsible for the increased activity, as the azide derivative **2.6** has slightly reduced potency when compared to DANA (70 ± 20 μM). Bulky triazole substituents, such as **2.10**, had reduced potency (130 ± 20 μM). More polar groups, including ethoxy **2.9**, hydroxymethyl **2.12**, hydroxyethyl **2.13**, and hydroxypropyl **2.14** all showed significantly reduced

activity as compared to the parent DANA, or the azide **2.6**. Assays of compound **2.21** found a slightly improved potency over DANA (21 ± 8 μM), suggesting that the azide may provide some beneficial interactions. However, our data imply that the *N*5Ac pocket is relatively small, as all triazole derivatives of compound **2.21** tested (**2.22-2.30**) had potencies that were significantly reduced when compared to DANA (>500 μM ).

### *2.4 The active site topology of NEU3*

In order to understand the interactions responsible for the differences in potency among both series of compounds, we conducted molecular docking experiments using a previously reported homology model of NEU3 (Albohy, A., Li, M.D., et al. 2010). After docking, structures were subjected to molecular dynamics and minimized. Examination of the structures of DANA and compound **2.7** in the NEU3 active site suggest that a hydrophobic pocket adjacent to the glycerol-binding pocket (*C*7-*C9*) could contribute to the activity of compounds related to **2.7** (Figure **2.1**). The hydrophobic pocket is made up of residues V222, V224, P247, and H277. Additional interactions to the triazole are possible between Y181 and *N*3 of the triazole. We observed two changes to the active site residues upon binding of **2.7**, D50 became reoriented to interact with *HO*7, and an apparent edge-face interaction developed between the triazole and H277 (Figure **2.1**) (Bissantz, C., Kuhn, B., et al. 2010). The model of DANA binding is consistent with the limitations we observed for the *N*5Ac pocket, which would be predicted to be unable to accommodate the bulky triazole groups found in compounds **2.22-2.30**. Additionally, the *N*5Ac pocket is relatively hydrophobic,

although a carboxylate group from N88 is positioned close enough to contact *C*4 H-bond donors.

### *2.5 Conclusions*

These results support our previous study of the active site topology of NEU3 using site directed mutagenesis (Albohy, A., Li, M.D., et al. 2010). The compounds tested here suggest that the *N*5Ac pocket of NEU3 is sterically limited, and cannot accommodate large groups such as the triazole derivatives (**2.22-2.30**).

Importantly, we observed that modifications of the *C*9 position are well tolerated, and may have some specific requirements for potent inhibitors of the enzyme. Although previous studies have identified a tolerance for bulky groups at *C*9 (Table **2.1**) (Magesh, S., Moriya, S., et al. 2008), we observed that the addition of a triazole linker significantly improved activity (**2.7**, **2.8**, **2.11**). Based on our model of the active site, we propose that groups that bind in the *C*9 pocket should contain H-bond acceptors, to interact with Y181, and also hydrophobic side chains, to interact with V222 and V224 (Figure **2.1**). Additional H-bond acceptors distal from *C*9 may also take advantage of contacts with K195 or H277. Our results suggest that potent inhibitors of NEU3 may be developed by incorporation of a modified *C*9 side-chain of DANA analogs. Importantly, we identified compounds in this study with equivalent potency (**2.7**) to the best reported inhibitors of the enzyme (zanamivir) (Hata, K., Koseki, K., et al. 2008). This feature of NEU3 recognition may indicate that the enzyme can tolerate unusual sialic acid modifications found at *C*9 (Varki, N.M. and Varki, A. 2007).

In summary, based on structure activity relationships of DANA analogs for NEU3, we designed and synthesized a series of *C*9 and *N*5 modified DANA derivatives. Several of the *C*9-modified derivatives (**2.7**, **2.8**) demonstrated good inhibitory activity and may provide useful lead compounds for more potent inhibitors of human NEU3. Interestingly, compound **2.21** was found to be an inhibitor of NEU3 in our experiments, and this compound has been recently shown to also be an inhibitor of NEU2 (Li, Y., Cao, H., et al. 2011).

Our docking and inhibitor studies were consistent with a relatively large binding pocket for the glycerol side chain in the NEU3 active site. Further exploration of the *C*9 position and the glycerol side chain may help identify new, more potent lead compounds for the human neuraminidase enzymes. Therefore, in the following chapter we will discuss the design and synthesis of DANA-analogs that contain glycerol side chain modifications to test if replacement of this portion of the molecule can result in improved potency.

**Table 2.3. Inhibition of NEU3.**

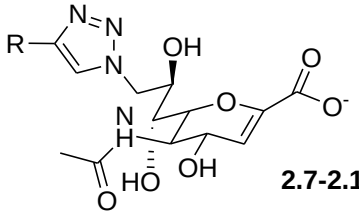

**2.7-2.15**

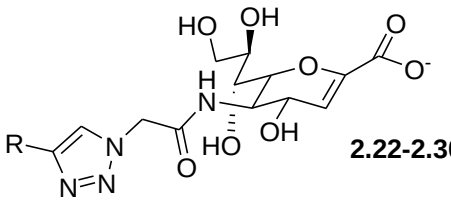

**2.22-2.30**

| Compound | R | $IC_{50}$ [μM] [a] | Compound | R | $IC_{50}$(μM) |
|---|---|---|---|---|---|
| **DANA** | na | 48 ± 5 | **DANA** | na | 48± 4 |
| **2.6** | na | 70 ± 20 | **2.21** | na | 21± 8 |
| **2.7** | 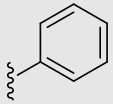 | 20 ± 10 | **2.22** | 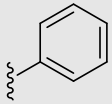 | > 500 |
| **2.8** | 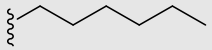 | 23 ± 4 | **2.23** | 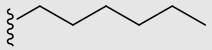 | > 500 |
| **2.9** | 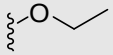 | 300 ± 200 | **2.24** | 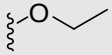 | > 500 |
| **2.10** | 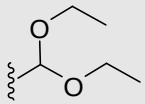 | 130 ± 20 | **2.25** | 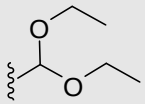 | > 500 |
| **2.11** | 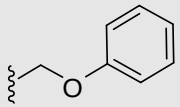 | 45 ± 3 | **2.26** | 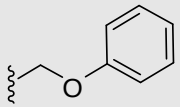 | > 500 |
| **2.12** | 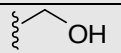 | 300 ± 400 | **2.27** | 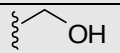 | > 500 |
| **2.13** | 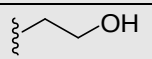 | 400 ± 600 | **2.28** | 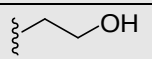 | > 500 |
| **2.14** |  | 500 ± 200 | **2.29** | 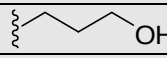 | > 500 |
| **2.15** | 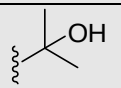 | 300 ± 500 | **2.30** | 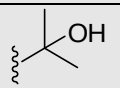 | > 500 |

*a.* Inhibitors which did not show significant change (> 50% decrease from control) were fit using the maximum inhibition value for DANA.

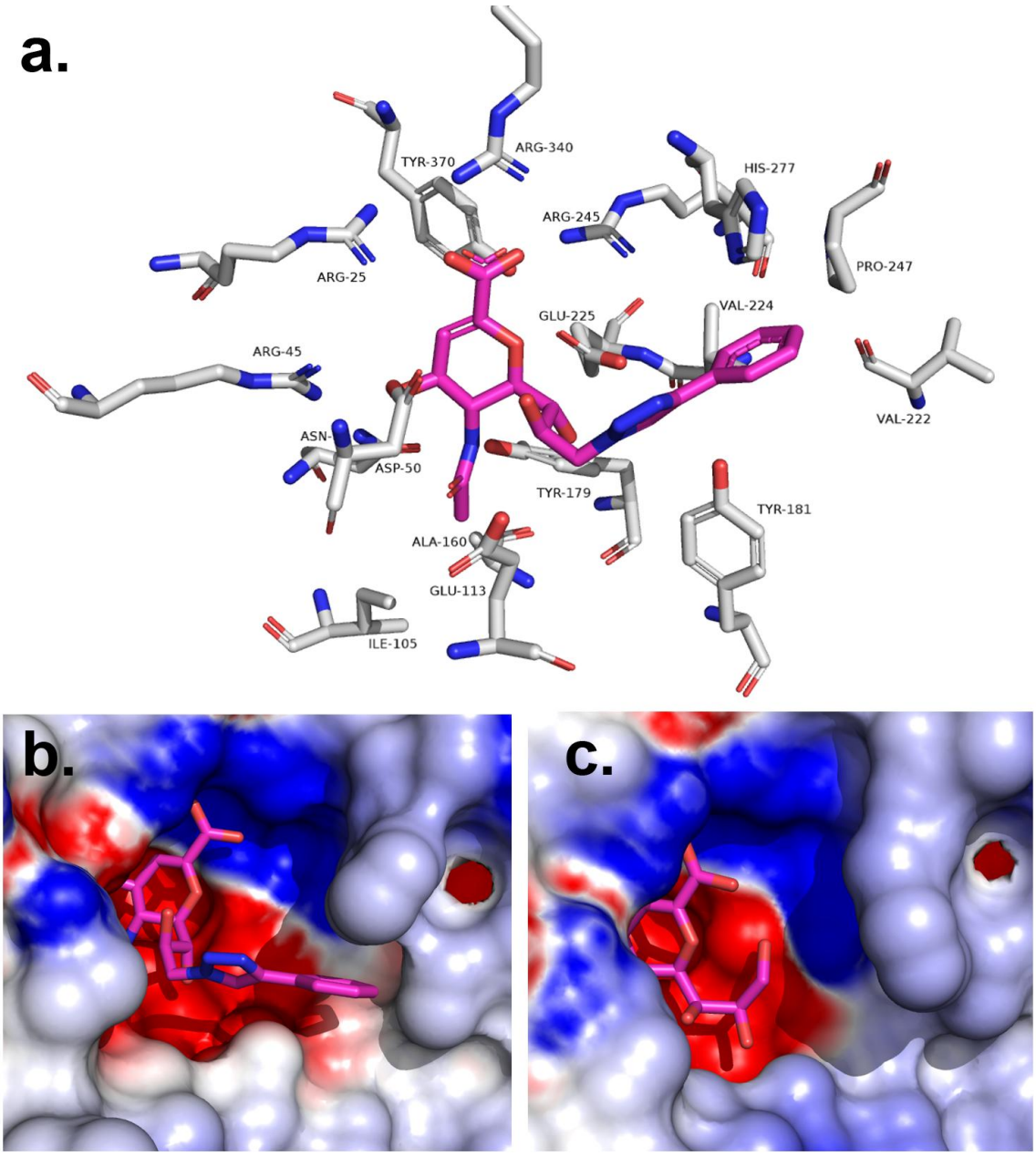


**Figure 2.1. Molecular docking of DANA and 2.7.**

Inhibitors were docked and subjected to molecular dynamics using a homology model of NEU3 to determine the binding mode of the triazole derivative **2.7** (Albohy, A., Li, M.D., et al. 2010). (**a.**) The binding site of NEU3 has a large hydrophobic pocket adjacent to the *C*9 position including V222, V224, P247 and

H277 which can accommodate hydrophobic groups. (**b.**) An electrostatic potential map is shown for the docked structure of **2.7** and (**c.**) DANA. Several residues have reoriented to accommodate **2.7**, notably H277 is rotated to engage in an edge-face interaction with the triazole linker of **2.7** (Bissantz, C., Kuhn, B., et al. 2010), and D50 has become more solvent exposed to engage in H-bond interactions with *O*7.

### *2.6 Experimental*

#### *2.6.1 General*

All reagents used were purchased from commercial sources and were used without further purification unless noted. All reactions were carried out under a positive pressure of Argon at room temperature unless indicated. The reactions were monitored by analytical TLC on silica get 60-$F_{254}$ (0.25 mm, Silicycle, Quebec, Canada) and the spots were visualized under UV light (254 nm) or stained by charring with Ceric Ammonium Molybdate (CAM). Organic solvents were evaporated under reduced pressure and the products were purified by column chromatography on silica gel (230-400 mesh, Silicycle, Quebec, Canada) or HPLC (Waters). $^{1}$H NMR spectra were performed on Varian 300, 400, or 500 MHz instruments at room temperature as noted. $^{13}$C NMR spectra were recorded at 100 or 125 MHz. Electrospray mass spectra were recorded on Agilent Technologies 6220 TOF.

### *2.6.2 Molecular docking of inhibitors to NEU3*

Compound **2.7** or **DANA** was docked to the active site of a NEU3 homology model (Albohy, A., Li, M.D., et al. 2010) using Autodock 4.0 with a grid box of 60 x 40 x 40 Å (Goodsell, D.S., Morris, G.M., et al. 1996). A representative structure of each inhibitor was obtained from the lowest energy cluster (-6.68 kcal $mol^{-1}$; cluster RMS 1.83). Clusters of higher energy (> 1 kcal $mol^{-1}$) were missing key interactions between the inhibitor and the arginine triad and the catalytic residues. The docked structures were minimized, and used for molecular dynamics simulations. Dynamics of **DANA** or compound **2.7** in the active site of NEU3 were calculated using Macromodel (30 ps, 300 K, *in vacuo*, OPLS2005 force field). The simulation was carried out with constraints on the distance between the carboxylate of the inhibitor and R340 (± 2.7 Å) to maintain the orientation of the inhibitor. The final structure was minimized without constraints to convergence. The electrostatic potential map was generated with the DelPhi software package (Gilson, M.K., Sharp, K.A., et al. 1988).

### *2.6.3 NEU3 inhibition assays*

NEU3 was expressed in *E. coli* as an MBP-NEU3 fusion (pMAL-c2x) and purified as described previously.(Albohy, A., Li, M.D., et al. 2010) Assays were conducted in 0.1 M sodium acetate buffer pH = 5.0, at a protein concentration of 0.1 mg/mL as determined by $A_{280}$. The neuraminidase solution was incubated with serial concentrations of 2-deoxy-2,3-didehydro-*N*-acetylneuraminic acid (DANA) (5, 10, 20, 50, 100, 200, 500 and 1000 μM) for 30 min at 37 °C. Fluorogenic substrate (4MU-NA, 500 μM final concentration) was added and

incubated for 1 h. The reaction was quenched and activity was determined by fluorescence (365 nm excitation; 445 nm emission). Assays were performed with five replicates for each point, error bars indicate the standard deviation. Reported $IC_{50}$ values were determined by non-linear regression. For curves which showed less than 50% decrease in signal, fits were conducted using the maximum inhibition of DANA (compounds **2.22-2.30**).

### *2.6.4 Synthetic methods*

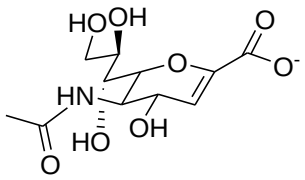


**2,3-didehydro-N-acetyl-neuraminic acid (Neu5Ac2en) (1.5)**

Compound **2.2** (23 mg, 0.05 mmol) was dissolved in methanol (5 mL), and sodium methoxide solution (0.2 mL, 0.2 mmol) was added dropwise to the reaction, followed by stirring for 1.5 h. Amberlite IR-120($H^+$) was then added to neutralize the reaction mixture (pH 7.0). The solution was filtered and concentrated in vacuo. Then the residue was treated with 0.1 M NaOH (1 mL) for 0.5 h at room temperature. The reaction was neutralized with Amberlite IR-120($H^+$), followed by filtration and evaporation of the solvent to provide **1.5** (86%). $^1$H NMR (498 MHz, $D_2O$) δ 5.92 (d, *J* = 2.4 Hz, 1H), 4.49 (dd, *J* = 8.8, 2.4 Hz, 1H), 4.25 (app d, *J* = 10.8 Hz, 1H), 4.06 (dd, *J* = 10.8, 8.8 Hz, 1H), 3.90 (ddd, *J* = 12.0, 6.0, 2.4 Hz, 1H), 3.86 (dd, *J* = 9.2, 2.8 Hz, 1H), 3.65 – 3.59 (m, 2H), 2.05 (s, 3H). $^{13}$C NMR (125 MHz, $D_2O$) δ 175.6, 167.4, 145.6, 112.1, 76.7, 70. 7,

68.9, 68.1, 63.9, 50.5, 22.9. HRMS (ESI) calculated for $C_{11}H_{16}NO_8$ $[M-H]^-$, 290.0881, found 290.0880.

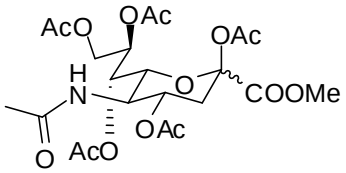


**Methyl-5-acetamido-2, 4, 7, 8, 9-penta-O-acetyl-3, 5-dideoxy-D-glycero-D-galacto-2-α/β-nonulopyranosonate (2.1)**

Methyl-5-acetamido-3,5-dideoxy-D-glycero-D-galactononulopyranosonate (3.349 g, 10.3 mmol) (Martin, R., Witte, K.L., et al. 1998) was stirred with anhydrous pyridine (40 mL) and acetic anhydride (48 mL) for 4 h at 0 ℃, then warmed to room temperature and stirred overnight. The solution was concentrated and the residue was purified by flash chromatography with 5:1 EtOAc-hexane as the mobile phase to give compound **2.1** as a white solid (93% yield, mixture of anomers). $^1$H NMR (400 MHz, $CDCl_3$) δ 5.37 (dd, *J* = 7.1, 2.4 Hz, 1H), 5.26 – 5.17 (m, 2H), 5.02 (ddd, *J* = 11.8, 10.2, 4.8 Hz, 1H), 4.69 (dd, *J* = 10.8, 2.4 Hz, 1H), 4.36 (dd, *J* = 12.5, 2.7 Hz, 1H), 4.21 – 4.02 (m, 2H), 3.76 (s, 3H), 2.56 (dd, *J* = 13.1, 4.8 Hz, 1H), 2.15 (d, *J* = 1.2 Hz, 1H), 2.13 (s, 3H), 2.11 (s, 3H), 2.10 (s, 3H), 2.04 (s, 3H), 2.03 (s, 3H), 1.90 (s, 3H). $^{13}$C NMR (101 MHz, $CDCl_3$) δ 170.8, 170.4(9), 170.4(7), 170.4(3), 170.2, 168.4, 166.5, 97.8, 73.1, 71.6, 68.5, 68.1, 62.4, 53.4, 49.6, 36.2, 23.4, 21.3, 21.1, 21.1, 21.0(1), 20.9(7). HRMS (ESI) calculated for $C_{22}H_{31}NNaO_{14}$ $[M+Na]^+$, 556.1637, found 556.1634.

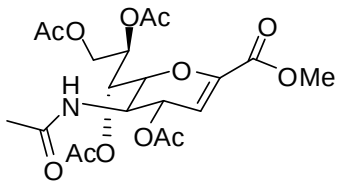

**Methyl 5-acetamido-4, 7, 8, 9-tetra-O-acetyl-2, 3, 5-trideoxy-D-glycero-D-galacto-2-nonulopyranosonate (2.2)**

Compound **2.1** (5.066 g, 9.5 mmol) was dissolved in $CH_3CN$ (60 mL) with a catalytic amount of $PPh_3HBr$. The solution was stirring at 90 ℃ under reflux. After 2 h, $NaHCO_3$ powder (1 g) was added. The reaction mixture was filtered and concentrated. The residue was purified by flash chromatography with 8:1 EtOAc-hexane to give **2.2** as a white solid (43% yield). $^1$H NMR (498 MHz, $CDCl_3$) δ 6.01 (d, *J* = 3.2 Hz, 1H), 5.57 – 5.52 (m, 1H), 5.52 – 5.48 (m, 2H), 5.37 (ddd, *J* = 7.0, 4.7, 3.3 Hz, 1H), 4.59 (dd, *J* = 12.3, 3.3 Hz, 1H), 4.39 (td, *J* = 4.9, 1.5 Hz, 2H), 4.20 (dd, *J* = 12.3, 6.9 Hz, 1H), 3.80 (s, 3H), 2.13 (s, 3H), 2.08 (s, 3H), 2.07 (s, 3H), 2.05 (s, 3H), 1.94 (s, 3H). $^{13}$C NMR (101 MHz, $CDCl_3$) δ 170.9, 170.8, 170.4, 170.3, 170.2, 161.8, 145.3, 108.1, 76.8, 70.8, 67.9, 67.9, 62.1, 52.8, 21.1, 21.0. HRMS (ESI) calculated for $C_{20}H_{27}NNaO_{12}$ $[M+Na]^+$, 496.1425, found 496.1415.

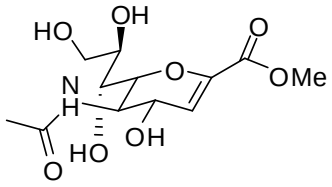


**Methyl 5-Acetamido-2, 3, 5 -trideoxy-D-glycero-D-galacto-2-nonulopyranosonate (2.3)**

Sodium metal (2.3 g) was dissolved in freshly distilled methanol (100 mL) under argon to generate sodium methoxide. Compound **2.2** (429 mg, 0.9 mmol) was dissolved in methanol (30 mL) under argon and cooled to 0 ℃. The sodium methoxide solution (0.4 mL) was then added dropwise, and the reaction mixture was stirred for 45 min. Amberlite IR-120(H+) was then added to neutralize the reaction mixture (pH 7.0). The solution was filtered, and evaporation of the

solvent under reduced pressure afforded **2.3** (quant.) as a white solid. $^{1}$H NMR (300 MHz, $CD_3OD$) δ 5.94 (d, *J* = 2.5 Hz, 1H), 4.43 (dd, *J* = 8.6, 2.5 Hz, 1H), 4.16 (dd, *J* = 10.8, 1.0 Hz, 1H), 3.98 (dd, *J* = 10.8, 8.7 Hz, 1H), 3.93 – 3.85 (m, 1H), 3.81 (dd, *J* = 11.4, 3.0 Hz, 1H), 3.77 (s, 3H), 3.66 (dd, *J* = 11.4, 5.2 Hz, 1H), 3.57 (dd, *J* = 9.2, 1.1 Hz, 1H), 2.04 (s, 3H). $^{13}$C NMR (125 MHz, $CD_3OD$) δ 164.4, 145.7, 145.2, 113.5, 78.2, 71.08, 70.1, 67.9, 64.9, 52.9, 52.0, 22.7. HRMS (ESI) calculated for $C_{12}H_{19}NNaO_8$ $[M+Na]^+$, 328.1003, found 328.0998.

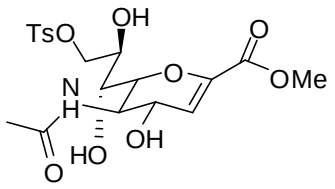


**Methyl 5-acetamido-2, 3, 5-trideoxy-9-p-toluenesulfonyl-D-glycero-D-galacto-2-nonulopyranosonate (2.4)**

*p*-Toluenesulfonyl chloride (262 mg, 1.4 mmol) and **2.3** (332 mg, 1.7 mmol) were dissolved in pyridine (20 mL) at 0 ℃. The mixture was stirred for 2 days at room temperature. After removal of the pyridine, the residue was purified by flash chromatography (15:1, $CH_2Cl_2$: MeOH) to give **2.4** (24% yield). $^{1}$H NMR (498 MHz, $CD_3OD$) δ 7.92 – 7.64 (m, 2H), 7.44 (d, *J* = 8.0 Hz, 2H), 5.92 (d, *J* = 2.5 Hz, 1H), 4.40 (dd, *J* = 8.7, 2.5 Hz, 1H), 4.29 (dd, *J* = 9.9, 2.1 Hz, 1H), 4.12 – 4.05 (m, 2H), 4.05 – 4.00 (m, 1H), 3.91 (dd, *J* = 10.8, 8.7 Hz, 1H), 3.76 (s, 3H), 3.49 (dd, *J* = 9.2, 1.1 Hz, 1H), 2.45 (s, 3H), 2.03 (s, 3H). $^{13}$C NMR (125 MHz, $CD_3OD$) δ 175.3, 164.2, 146.4, 145.1, 134.3, 131.0, 129.1, 113.6, 77.8, 73.8, 69.8, 68.7, 67.8, 52.8, 51.9, 22.6, 21.6. HRMS (ESI) calculated for $C_{19}H_{25}NNaO_{10}S$ $[M+Na]^+$, 482.1091, found 482.1087.

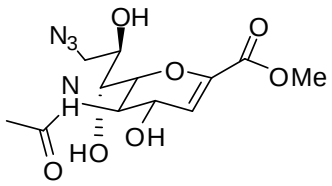

**Methyl 5-acetamido-9-azido-2, 3, 5, 9-tetradeoxy-D-glycero-D-galacto-2-nonulopyranosonate (2.5)**

Compound **2.4** (97 mg, 0.2 mmol) and sodium azide (57 mg, 0.9 mmol) was dissolved in acetone (5 mL), then water (0.3 mL) was added to the solution. The solution was heated at 67 ℃ under reflux for 48 h. The solvents were completely removed and the residue was purified by flash chromatography (10:1, $CH_2Cl_2$: MeOH) to give **2.5** (56% yield). $^1$H NMR (498 MHz, $CD_3OD$) δ 5.94 (d, *J* = 2.5 Hz, 1H), 4.42 (dd, *J* = 8.7, 2.5 Hz, 1H), 4.15 (dd, *J* = 10.8, 1.1 Hz, 1H), 4.03 (ddd, *J* = 9.0, 6.2, 2.6 Hz, 1H), 3.96 (dd, *J* = 10.8, 8.7 Hz, 1H), 3.78 (s, 3H), 3.59 – 3.48 (m, 1H), 3.39 (dd, *J* = 12.8, 6.2 Hz, 1H), 2.04 (s, 3H). $^{13}$C NMR (125 MHz, $CD_3OD$) δ 175.2, 164.3, 145.2, 113.6, 77.9, 70.8, 70.3, 67.9, 55.8, 52.9, 52.0, 22.7. HRMS (ESI) calculated for $C_{12}H_{18}N_4NaO_7$ $[M+Na]^+$, 353.1068, found 353.1063.

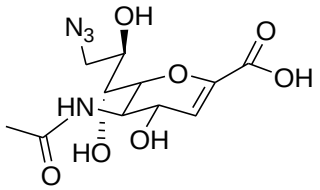

**5-Acetamido-9-azido-2, 3, 5, 9-tetradeoxy-D-glycero-D-galacto-2-nonulopyranosonic acid (2.6)**

Compound **2.5** was treated with 0.1 M NaOH (3 mL) for 0.5 h at room temperature. The solution was neutralized with Amberlite IR-120($H^+$ form), then filtered and reduced, to provide compound **2.6** (63% yield). $^1$H NMR (500 MHz, $D_2O$) δ 5.68 (d, *J* = 2.3 Hz, 1H), 4.46 (dd, *J* = 8.9, 2.3 Hz, 1H), 4.20 (dd, *J* = 11.0, 0.7 Hz,

1H), 4.09 (ddd, *J* = 8.9, 5.8, 2.7 Hz, 1H), 4.04 (dd, *J* = 10.9, 9.0 Hz, 1H), 3.64 (dd, *J* = 13.1, 2.7 Hz, 1H), 3.60 (d, *J* = 9.5 Hz, 1H), 3.51 (dd, *J* = 13.2, 5.8 Hz, 1H), 2.06 (s, 3H). $^{13}$C NMR (125 MHz, $D_2O$) δ 175.4, 170.3, 148.6, 108.4, 75.8, 69.4, 69.3, 68.2, 54.4, 50.6, 22.9. HRMS (ESI) calculated for $C_{11}H_{15}N_4O_7$ $[M-H]^-$, 315.0946, found 315.0949.

**General procedure for the click reaction of 2.7-2.15 and 2.22-2.30**

The reaction flask was charged with the azido-sugar (30 mg, 90 μmol, 1 equiv), the alkyne (2 equiv), $CuSO_4$ (3 mg, 18 μmol, 0.2 equiv), and sodium ascorbate (5.4 mg, 27 μmol, 0.3 equiv). A mixture of $H_2O$/*t*BuOH/DCM (1:2:1, 2 mL) was then added and the flask was covered with aluminum foil. After stirring overnight, the solution was reduced *in vacuo*. Triazole products were isolated by flash chromatography (EtOAc/2-propanol/$H_2O$, 2:2:1). The ester was then hydrolyzed by treatment with 0.1 M NaOH (3 mL) for 0.5 h at room temperature. The product was neutralized with Amberlite IR-120 ($H^+$ form) followed by filtration and evaporation of the solvents. Yields of **2.7-2.15** ranged from 23-81% and of **2.22-2.30** ranged from 31-96%.

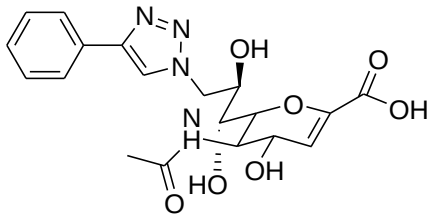


**5-Acetamido-9-(4-phenyl-[1,2,3]triazol-1-yl)-2, 3, 5, 9-tetradeoxy-D-glycero-D-galacto-2-nonulopyranosonic acid (2.7)**

Triazole **2.7** was generated by reaction of **2.5** with phenylacetylene (2 equiv), as described above (yield 42%). $^1$H NMR (700 MHz, $D_2O$) δ 8.36 (s, 1H), 7.90 –

7.79 (m, 2H), 7.54 (t, *J* = 7.8 Hz, 2H), 7.46 (t, *J* = 7.4 Hz, 1H), 5.69 (d, *J* = 2.2 Hz, 1H), 4.85 (dd, *J* = 14.4, 2.7 Hz, 1H), 4.66 (dd, *J* = 14.4, 6.8 Hz, 1H), 4.46 (dd, *J* = 8.9, 2.2 Hz, 1H), 4.38 (ddd, *J* = 9.5, 6.8, 2.7 Hz, 1H), 4.18 (d, *J* = 11.0 Hz, 1H), 4.04 (dd, *J* = 10.8, 9.0 Hz, 1H), 3.38 (d, *J* = 9.5 Hz, 1H), 1.96 (s, 3H). $^{13}$C NMR (126 MHz, $D_2O$) δ 175.7, 170.4, 148.8, 148.3, 130.4, 130.1, 129.7, 126.6, 124.0, 108.5, 75.9, 69.8, 68.9, 68.2, 54.4, 50.8, 22.8. HRMS (ESI) calculated for $C_{19}H_{21}N_4O_7$ $[M-H]^-$, 417.1416, found 417.1417.

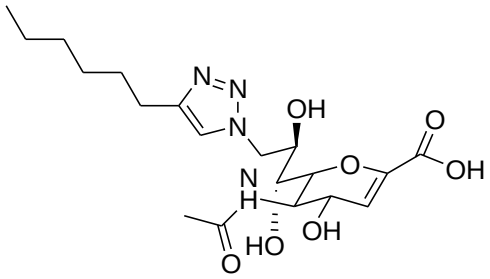


**5-Acetamido-9-(4-hexanyl-[1,2,3]triazol-1-yl)-2, 3, 5, 9-tetradeoxy-D-glycero-D-galacto-2-nonulopyranosonic acid (2.8)**

Triazole **2.8** was generated by reaction of **2.5** with 1-octyne (2 equiv), as described above (yield 27%). $^1$H NMR (700 MHz, $D_2O$) δ 7.80 (s, 1H), 5.69 (d, *J* = 1.6 Hz, 1H), 4.77 (dd, *J* = 3.5, 1.5 Hz, 1H), 4.55 (dd, *J* = 14.4, 6.9 Hz, 1H), 4.46 (dd, *J* = 8.9, 1.6 Hz, 1H), 4.30 (dd, *J* = 11.8, 4.8 Hz, 1H), 4.17 (d, *J* = 11.0 Hz, 1H), 4.10 – 3.89 (m, 1H), 3.36 (d, *J* = 9.1 Hz, 1H), 2.71 (t, *J* = 7.4 Hz, 2H), 2.04 (s, 3H), 1.75 – 1.60 (m, 2H), 1.41 – 1.22 (m, 6H), 0.85 (t, *J* = 6.8 Hz, 3H). $^{13}$C NMR (176 MHz, $D_2O$) δ 175.9, 170.6, 149.8, 149.0, 125.0, 108.6, 76.1, 70.0, 69.1, 68.4, 54.2, 51.0, 31.8, 29.6, 28.8, 25.4, 23.1, 22.9, 14.4. HRMS (ESI) calculated for $C_{19}H_{29}N_4O_7$ $[M-H]^-$, 425.2042, found 425.2038.

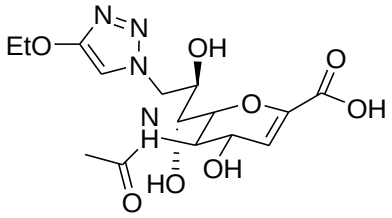

**5-Acetamido-9-(4-ethoxy-[1,2,3]triazol-1-yl)-2, 3, 5, 9-tetradeoxy-D-glycero-D-galacto-2-nonulopyranosonic acid (2.9)**

Triazole **2.9** was generated by reaction of **2.5** with ethylethynyl ether (2 equiv), as described above (yield 60%). $^{1}$H NMR (500 MHz, $D_2O$) δ 7.58 (s, 1H), 5.97 (d, *J* = 2.3 Hz, 1H), 4.72 (dd, *J* = 14.4, 2.6 Hz, 1H), 4.50 (dd, *J* = 8.9, 2.4 Hz, 1H), 4.45 (dd, *J* = 14.4, 7.4 Hz, 1H), 4.31 – 4.23 (m, 2H), 4.21 (dd, *J* = 14.2, 7.2 Hz, 2H), 4.06 (dd, *J* = 10.8, 9.0 Hz, 1H), 3.45 (d, *J* = 9.3 Hz, 1H), 2.04 (s, 3H), 1.37 (t, *J* = 7.1 Hz, 3H). $^{13}$C NMR (126 MHz, $D_2O$) δ 175.8, 167.1, 161.0, 145.3, 112.5, 110.2, 76.5, 69.8, 69.1, 68.8, 67.9, 55.1, 50.6, 22.9, 14.7. HRMS (ESI) calculated for $C_{15}H_{21}N_4O_8$ $[M-H]^-$, 385.1365, found 385.1364.

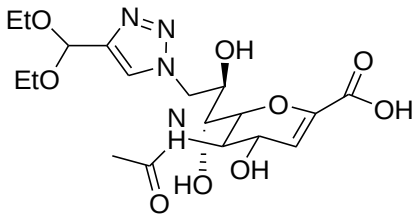

**5-Acetamido-9-(4-diethoxymethyl-[1,2,3]triazol-1-yl)-2, 3, 5, 9-tetradeoxy-D-glycero-D-galacto-2-nonulopyranosonic acid (2.10)**

Triazole **2.10** was generated by reaction of **2.5** with propargylaldehyde diethylacetal (2 equiv), as described above (yield 51%). $^{1}$H NMR (500 MHz, $D_2O$) δ 8.06 (s, 1H), 5.81 (s, 1H), 5.68 (d, *J* = 2.1 Hz, 1H), 4.81 (dd, *J* = 14.4, 2.7 Hz, 1H), 4.57 (dd, *J* = 14.4, 7.3 Hz, 1H), 4.45 (dd, *J* = 8.8, 2.2 Hz, 1H), 4.35 –

4.27 (m, 1H), 4.17 (d, *J* = 11.0 Hz, 1H), 4.03 (dd, *J* = 10.8, 9.0 Hz, 1H), 3.83 – 3.65 (m, 4H), 3.41 (d, *J* = 9.5 Hz, 1H), 2.03 (s, 3H), 1.22 (t, *J* = 7.1 Hz, 6H). $^{13}$C NMR (126 MHz, $D_2O$) δ 175.7, 170.4, 148.8, 146.6, 125.7, 108.5, 97.2, 75.9, 70.0, 68.9, 68.3, 64.0, 54.4, 50.8, 22.9, 15.1. HRMS (ESI) calculated for $C_{18}H_{27}N_4O_9$ $[M-H]^-$, 443.1784, found 443.1784.

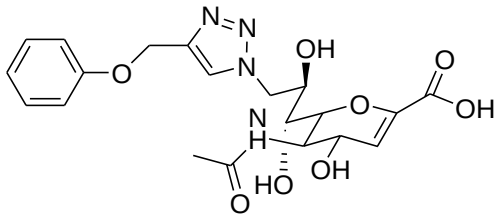

**5-Acetamido-9-[4-phenoxymethyl-[1,2,3]triazol-1-yl]-2, 3, 5, 9-tetradeoxy-D-glycero-D-galacto-2-nonulopyranosonic acid (2.11)**

Triazole **2.11** was generated by reaction of **2.5** with phenylpropargyl ether (2 equiv), as described above (yield 81%). $^1$H NMR (700 MHz, $D_2O$) δ 8.13 (s, 1H), 7.48 – 7.34 (m, 2H), 7.09 (ddt, *J* = 8.3, 7.2, 1.1 Hz, 3H), 5.69 (dd, *J* = 2.3, 1.1 Hz, 1H), 5.28 (s, 2H), 4.82 (dd, *J* = 14.4, 2.8 Hz, 1H), 4.58 (dd, *J* = 14.4, 7.2 Hz, 1H), 4.46 (ddd, *J* = 8.9, 2.3, 1.2 Hz, 1H), 4.38 – 4.29 (m, 1H), 4.17 (d, *J* = 11.0 Hz, 1H), 4.04 (dd, *J* = 10.4, 9.5 Hz, 1H), 3.41 (dd, *J* = 9.5, 1.1 Hz, 1H), 2.03 (s, 3H). $^{13}$C NMR (176 MHz, $D_2O$) δ 175.7, 170.3, 158.1, 148.7, 144.0, 130.7, 126.9, 122.9, 116.3, 108.5, 75.9, 69.9, 68.9, 68.2, 62.0, 54.3, 50.7, 22.9. HRMS (ESI) calculated for $C_{20}H_{23}N_4O_8$ $[M-H]^-$, 447.1521, found 447.1510.

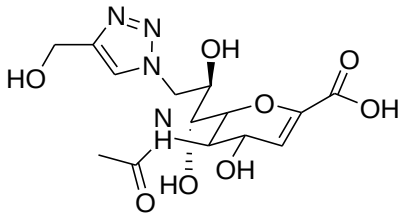

**5-Acetamido-9-[4-hydroxymethyl-[1,2,3]triazol-1-yl]-2, 3, 5, 9-tetradeoxy-D-glycero-D-galacto-2-nonulopyranosonic acid (2.12)**

Triazole **2.12** was generated by reaction of **2.5** with propargyl alcohol (2 equiv), as described above (yield 23%). $^{1}$H NMR (700 MHz, $D_2O$) δ 8.03 (s, 1H), 5.69 (d, *J* = 2.1 Hz, 1H), 4.82 (dd, *J* = 14.4, 2.7 Hz, 1H), 4.74 (s, 2H), 4.57 (dt, *J* = 17.1, 8.6 Hz, 1H), 4.47 (dd, *J* = 8.9, 2.2 Hz, 1H), 4.36 – 4.29 (m, 1H), 4.19 (d, *J* = 11.0 Hz, 1H), 4.05 (dd, *J* = 10.8, 9.1 Hz, 1H), 3.43 (d, *J* = 9.5 Hz, 1H), 2.05 (s, 3H). $^{13}$C NMR (176 MHz, $D_2O$) δ 177.3, 172.0, 150.4, 149.2, 125.9, 110.1, 77.5, 71.6, 70.6, 69.9, 57.1, 55.9, 52.4, 24.5. HRMS (ESI) calculated for $C_{14}H_{19}N_4O_8$ $[M-H]^-$, 371.1208, found 371.1208.

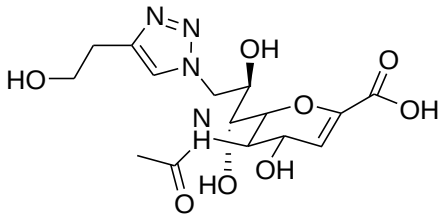


**5-Acetamido-9-[4-(2-hydroxy-ethyl)-[1,2,3]triazol-1-yl]-2, 3, 5, 9-tetradeoxy-D-glycero-D-galacto-2-nonulopyranosonic acid (2.13)**

Triazole **2.13** was generated by reaction of **2.5** with 3-butyn-1-ol (2 equiv), as described above (yield 33%). $^{1}$H NMR (500 MHz, $D_2O$) δ 7.88 (s, 1H), 5.69 (d, *J* = 1.1 Hz, 1H), 4.79 (dd, *J* = 1.5, 0.5 Hz, 1H), 4.55 (dd, *J* = 14.4, 7.1 Hz, 1H), 4.46 (dd, *J* = 8.8, 1.2 Hz, 1H), 4.35 – 4.23 (m, 1H), 4.17 (dd, *J* = 10.9, 0.8 Hz, 1H), 4.08 – 4.01 (m, 1H), 3.87 (t, *J* = 6.4 Hz, 2H), 3.41 (dd, *J* = 9.5, 0.8 Hz, 1H), 2.96 (t, *J* = 6.4 Hz, 2H), 2.04 (s, 3H). $^{13}$C NMR (126 MHz, $D_2O$) δ 175.7, 170.4, 149.0, 148.8, 125.6, 108.5, 75.9, 69.9, 69.0, 68.3, 61.6, 54.2, 50.8, 28.7, 22.9. HRMS (ESI) calculated for $C_{15}H_{21}N_4O_8$ $[M-H]^-$, 385.1365, found 385.1364.

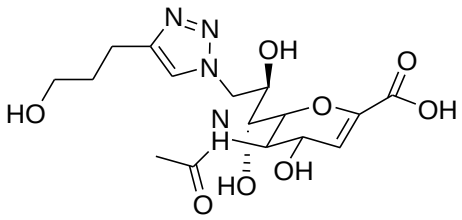

**5-Acetamido-9-[4-(3-hydroxy-propyl)-[1,2,3]triazol-1-yl]-2, 3, 5, 9-tetradeoxy-D-glycero-D-galacto-2-nonulopyranosonic acid (2.14)**

Triazole **2.14** was generated by reaction of **2.5** with 4-pentyn-1-ol (2 equiv), as described above (yield 48%). $^{1}$H NMR (500 MHz, $D_2O$) δ 7.84 (s, 1H), 5.69 (d, *J* = 2.3 Hz, 1H), 4.78 (d, *J* = 2.7 Hz, 1H), 4.55 (dd, *J* = 14.4, 7.0 Hz, 1H), 4.46 (dd, *J* = 8.8, 2.3 Hz, 1H), 4.30 (ddd, *J* = 8.4, 6.4, 2.2 Hz, 1H), 4.17 (d, *J* = 10.9 Hz, 1H), 4.03 (dd, *J* = 10.9, 8.9 Hz, 1H), 3.62 (t, *J* = 6.6 Hz, 2H), 3.37 (dd, *J* = 9.6, 0.9 Hz, 1H), 2.78 (t, *J* = 7.6 Hz, 2H), 2.04 (s, 3H), 1.96 – 1.84 (m, 2H). $^{13}$C NMR (125 MHz, $D_2O$) δ 175.7, 170.4, 148.7, 148.6, 125.0, 108.5, 75.9, 69.9, 68.9, 68.3, 61.7, 54.1, 31.9, 22.9, 21.9. HRMS (ESI) calculated for $C_{16}H_{23}N_4O_8$ $[M-H]^-$, 399.1521, found 399.1521.

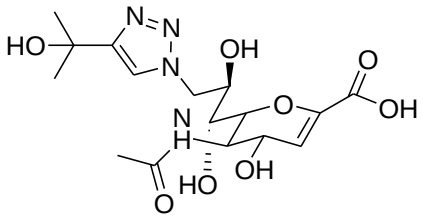

**5-Acetamido-9-[4-(1-hydroxy-1-methyl-ethyl)-[1,2,3]triazol-1-yl]-2, 3, 5, 9-tetradeoxy-D-glycero-D-galacto-2-nonulopyranosonic acid (2.15)**

Triazole **2.15** was generated by reaction of **2.5** with 2-methyl-3-butyn-2-ol (2 equiv), as described above (yield 58%). $^{1}$H NMR (400 MHz, $D_2O$) δ 7.96 (s, 1H), 5.68 (d, *J* = 2.3 Hz, 1H), 4.78 (dd, *J* = 14.5, 2.7 Hz, 1H), 4.55 (dd, *J* = 14.4, 7.1

Hz, 1H), 4.46 (dd, *J* = 8.8, 2.3 Hz, 1H), 4.31 (ddd, *J* = 9.7, 7.2, 2.7 Hz, 1H), 4.18 (d, *J* = 11.0 Hz, 1H), 4.03 (dd, *J* = 10.9, 8.9 Hz, 1H), 3.39 (d, *J* = 9.5 Hz, 1H), 2.03 (s, 3H), 1.61 (s, 6H). $^{13}$C NMR (101 MHz, $D_2O$) δ 175.6, 170.3, 155.6, 148.7, 123.4, 108.5, 75.9, 69.9, 69.0, 68.9, 68.2, 54.2, 50.7, 29.8, 22.9. HRMS (ESI) calculated for $C_{16}H_{23}N_4O_8$ [M-H]$^-$, 399.1521, found 399.1522.

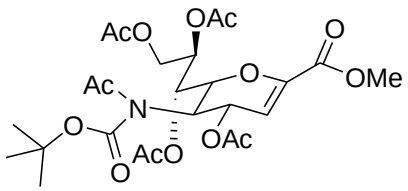


**Methyl 5-(N-tert-butoxycarbonylacetamido)-4, 7, 8, 9-tetra-O-acetyl-2, 3, 5-trideoxy-D-glycero-D-galacto-2-nonulopyranosonate**

A solution of **2.2** (288 mg, 0.61 mmol), di-*tert*-butyldicarbonate ($Boc_2O$) (371 mg, 1.7 mmol), and 4-dimethylaminopyridine (DMAP) (125 mg, 1.0 mmol) in dry THF (20 mL) was refluxed for 2 h under inert atmosphere. The reaction was monitored by TLC (toluene/ethanol, 10:1). After completion, the reaction mixture was cooled to room temperature, diluted with $CH_2Cl_2$, washed with 0.5 M aqueous HCl, water, and saturated $NaHCO_3$. The organic layer was dried and concentrated in vacuo. The product was purified by flash chromatography ($CH_2Cl_2$/MeOH, 20:1) to give methyl 5-(*N*-tert-butoxycarbonylacetamido)-4, 7, 8, 9-tetra-O-acetyl-2, 3, 5-trideoxy-D-glycero-D-galacto-2-nonulopyranosonate as a yellow oil (quant.). The product was used in subsequent steps without characterization.

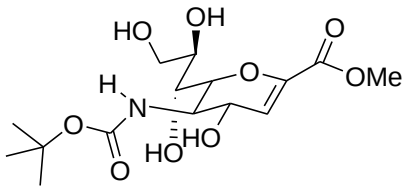


**Methyl 5-(N-tert-butoxycarbonyl)-2, 3, 5 -trideoxy-D-glycero-D-galacto-2-nonulopyranosonate (2.16)**

Sodium metal (0.46 g) was dissolved in freshly distilled methanol (10 mL) under inert atmosphere to generate sodium methoxide (2 M). Methyl 5-(*N-tert*-butoxycarbonylacetamido)-4, 7, 8, 9-tetra-O-acetyl-2, 3, 5-trideoxy-D-glycero-D-galacto-2-nonulopyranosonate (from last step) (349 mg, 0.61 mmol) was dissolved in methanol (24 mL), and 0.3 mL of the sodium methoxide solution was added dropwise to the reaction, followed by stirring for 2 h. Amberlite IR-120($H^+$) was then added to neutralize the reaction mixture (pH 7.0). The solution was filtered and concentrated *in vacuo*. The product was purified by flash chromatography ($CH_2Cl_2$/MeOH, 15:1) to afford 203 mg of **2.16** (92%) as a white powder. $^1$H NMR (498 MHz, $CD_3OD$) δ 5.91 (d, J = 2.5 Hz, 1H), 4.36 (dd, J = 8.7, 2.4 Hz, 1H), 4.12 (d, J = 10.8 Hz, 1H), 3.92 – 3.86 (m, 1H), 3.84 (dd, J = 11.3, 2.8 Hz, 1H), 3.77 (s, 3H), 3.66 (ddd, J = 16.8, 12.2, 7.2 Hz, 3H), 1.45 (s, 9H). $^{13}$C NMR (125 MHz, $CD_3OD$) δ 164.5, 159.4, 145.2, 113.7, 81.1, 78.7, 71.2, 70.3, 68.0, 65.1, 52.8, 52.6, 28.7. HRMS (ESI) calculated for $C_{15}H_{25}NnaO_9$ $[M+Na]^+$, 386.1429, found 386.1422.

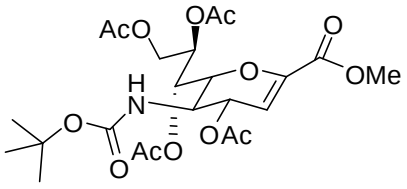

**Methyl 5-(N-tert-butoxycarbonyl)-4, 7, 8, 9-tetra-O-acetyl-2, 3, 5-trideoxy-D-glycero-D-galacto-2-nonulopyranosonate (2.17)**

A solution of methyl 5-(*N*-tert-butoxycarbonyl)-2, 3, 5 -trideoxy-D-glycero-D-galacto-2-nonulopyranosonate (258 mg, 0.71 mmol) in pyridine (12 mL) was stirred with acetic anhydride (6 mL) at 0 °C for 4 h. The reaction mixture was then warmed and stirred at room temperature overnight, concentrated, and coevaporated with toluene. The product was purified by flash chromatography (EtOAc/hexane, 3:1) to afford 362 mg of **2.17** (96%). $^{1}$H NMR (400 MHz, $CDCl_3$) δ 5.97 (d, *J* = 3.0 Hz, 1H), 5.54 (t, *J* = 4.1 Hz, 1H), 5.46 (dd, *J* = 7.5, 3.0 Hz, 1H), 5.35 (ddd, *J* = 7.0, 4.7, 3.6 Hz, 1H), 4.66 (d, *J* = 9.8 Hz, 1H), 4.59 (dd, *J* = 12.2, 3.2 Hz, 1H), 4.32 (dd, *J* = 9.0, 3.6 Hz, 1H), 4.17 (dd, *J* = 12.2, 6.9 Hz, 1H), 4.08 (dt, *J* = 17.1, 7.2 Hz, 1H), 3.78 (s, 3H), 2.15 – 2.03 (m, 12H), 1.40 (s, 9H). $^{13}$C NMR (101 MHz, $CDCl_3$) δ 170.6, 170.5, 169.9, 169.8, 161.6, 154.8, 145.0, 108.0, 80.4, 76.8, 70.5, 68.5, 67.8, 62.0, 52.5, 47.9, 28.1, 20.8, 20.8, 20.7, 20.6. HRMS (ESI) calculated for $C_{23}H_{33}NNaO_{13}$ $[M+Na]^+$, 554.1844, found 554.1851.

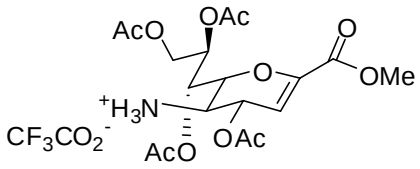


**Trifluoroacetate salt of methyl 5-amine-4, 7, 8, 9-tetra-O-acetyl-2, 3, 5-trideoxy-D-glycero-D-galacto-2-nonulopyranosonate (2.18)**

TFA (1.4 mL) was added to a solution of **2.17** (176 mg, 0.33 mmol) in $CH_2Cl_2$ (6 mL). The reaction mixture was stirred at room temperature for 1.5 h and the reaction was monitored by TLC (toluene/acetone, 1:1). The reaction mixture was concentrated, coevaporated with toluene, and dried to give the ammonium salt of

**2.18** as yellow syrup. The salt was carried forward without further characterization. HRMS (ESI) calculated for $C_{18}H_{26}NO_{11}$ $[M+H]^+$, 432.1500, found 432.1494.

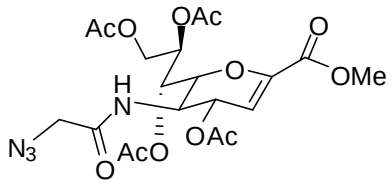

**Methyl 5-(N-2-azidoacetyl)-4, 7, 8, 9-tetra-O-acetyl-2, 3, 5-trideoxy-D-glycero-D-galacto-2-nonulopyranosonate (2.19)**

To a crude solution of **2.18** in dry $CH_2Cl_2$ (12 mL), *N*-hydroxysuccinimidyl-2-azidoacetate (112 mg, 0.56 mmol) (Johansson, S., Nilsson, E., et al. 2009) and $Et_3N$ (0.15 mL) were added at 0 °C. The mixture was stirred for 3 h at room temperature under inert atmosphere, and then concentrated. The compound was purified by flash chromatography (EtOAc/hexane, 8:1) to afford 169 mg of **2.19** (99%) as a white solid. $^1$H NMR (498 MHz, $CDCl_3$) δ 6.52 (d, *J* = 9.3 Hz, 1H), 5.98 (d, *J* = 2.9 Hz, 1H), 5.59 (dd, *J* = 7.7, 2.9 Hz, 1H), 5.49 (dd, *J* = 5.1, 3.1 Hz, 1H), 5.35 (ddd, *J* = 6.8, 5.1, 2.9 Hz, 1H), 4.61 (dd, *J* = 12.4, 2.9 Hz, 1H), 4.42 (ddd, *J* = 16.9, 9.4, 5.4 Hz, 2H), 4.18 (dd, *J* = 12.4, 6.8 Hz, 1H), 3.95 – 3.84 (m, 2H), 3.80 (s, 3H), 2.11 (s, 3H), 2.07 (s, 3H), 2.06 (s, 3H), 2.04 (s, 3H). $^{13}$C NMR (125 MHz, $CDCl_3$) δ 170.8, 170.6, 170.2, 170.1, 167.2, 161.5, 145.3, 108.1, 76.5, 70.7, 68.2, 67.4, 61.9, 52.6, 52.6, 46.7, 20.8, 20.8, 20.7, 20.7. HRMS (ESI) calculated for $C_{20}H_{26}N_4NaO_{12}$ $[M+Na]^+$, 537.1439, found 537.1431.

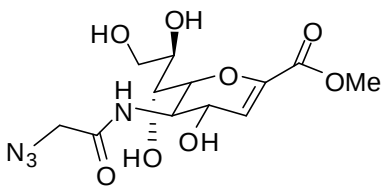

**Methyl 5-(N-2-azidoacetyl)-2, 3, 5 -trideoxy-D-glycero-D-galacto-2-nonulopyranosonate (2.20)**

Compound **2.19** (270 mg, 0.53 mmol) was dissolved in methanol (20 mL) under argon at room temperature. A solution of sodium methoxide (2.5 mL, 2M) was added dropwise to the solution and the reaction mixture was stirred for 1 h. Amberlite IR-120($H^+$) was then added to neutralize the reaction mixture (pH 7.0). The solution was filtered and concentrated. The product was purified by flash chromatography (EtOAc/MeOH/$H_2O$, 10:2:1) to afford 94 mg of **2.20** (52 %) as a white solid. $^1$H NMR (500 MHz, $CD_3OD$) δ 5.94 (d, *J* = 2.4 Hz, 1H), 4.48 (dd, *J* = 8.7, 2.4 Hz, 1H), 4.27 (d, *J* = 10.8 Hz, 1H), 4.07 (dd, *J* = 10.6, 8.9 Hz, 1H), 4.03 – 3.93 (m, 2H), 3.91 – 3.85 (m, 1H), 3.82 (dd, *J* = 11.4, 2.8 Hz, 1H), 3.78 (s, 3H), 3.66 (dd, *J* = 11.4, 5.4 Hz, 1H), 3.58 (d, *J* = 9.3 Hz, 1H). $^{13}$C NMR (126 MHz, $CD_3OD$) δ 171.7, 164.4, 145.2, 113.5, 77.9, 71.2, 70.0, 67.9, 64.9, 53.0, 52.9, 51.9. HRMS (ESI) calculated for $C_{12}H_{18}N_4NaO_8$ $[M+Na]^+$, 369.1071, found 369.1071.

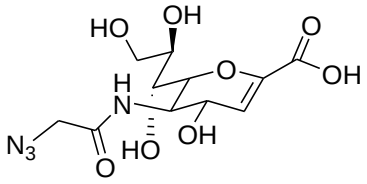


**Methyl 5-(N-2-azidoacetyl)-2, 3, 5 -trideoxy-D-glycero-D-galacto-2-nonulopyranosonic acid (2.21)**

Compound **2.20** was treated with 0.1 M NaOH (3 mL) for 0.5 h at room temperature. The reaction was neutralized with Amberlite IR-120($H^+$), followed by filtration and evaporation of the solvent (yield 67%). $^1$H NMR (400 MHz, $D_2O$) δ 5.93 (d, *J* = 2.4 Hz, 1H), 4.54 (dd, *J* = 8.9, 2.4 Hz, 1H), 4.34 (dd, *J* = 10.9, 0.9 Hz, 1H), 4.16 (dd, *J* = 10.9, 8.9 Hz, 1H), 4.10 (s, 2H), 3.96 – 3.88 (m, 1H), 3.85 (d, *J* = 2.7 Hz,

1H), 3.68 – 3.59 (m, 2H). $^{13}$C NMR (101 MHz, $D_2O$) δ 171.8, 167.6, 147.0, 111.8, 76.4, 70.7, 68.8, 68.0, 63.9, 52.8, 50.6. HRMS (ESI) calculated for $C_{11}H_{15}N_4O_8$ $[M-H]^-$, 331.0895, found 331.0895.

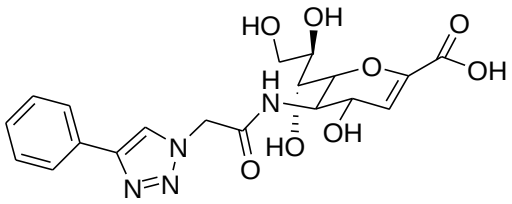


**Methyl 5-(N-2-(4-phenyl-[1,2,3]triazol-1-yl)acetyl)-2, 3, 5 -trideoxy-D-glycero-D-galacto-2-nonulopyranosonic acid (2.22)**

Triazole **2.22** was generated by reaction of **2.20** with phenylacetylene (2 equiv), as described above (yield 83%). $^1$H NMR (400 MHz, $D_2O$) δ 8.31 (s, 1H), 7.83 – 7.69 (m, 2H), 7.57 – 7.47 (m, 2H), 7.46 – 7.38 (m, 1H), 5.70 (d, *J* = 2.3 Hz, 1H), 5.41 – 5.27 (m, 2H), 4.52 (dd, *J* = 8.8, 2.4 Hz, 1H), 4.30 (dd, *J* = 10.9, 0.9 Hz, 1H), 4.15 (dd, *J* = 10.9, 8.8 Hz, 1H), 3.93 (ddd, *J* = 9.1, 6.1, 2.7 Hz, 1H), 3.86 (dd, *J* = 11.9, 2.7 Hz, 1H), 3.67 – 3.58 (m, 2H). $^{13}$C NMR (101 MHz, $D_2O$) δ 170.3, 169.1, 148.7, 148.5, 130.2, 130.1, 129.8, 126.6, 124.4, 108.5, 76.0, 70.7, 69.1, 68.3, 63.9, 53.1, 51.2. HRMS (ESI) calculated for $C_{19}H_{21}N_4O_8$ $[M-H]^-$, 433.1365, found 433.1361.

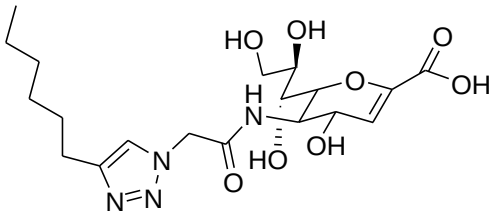


**Methyl 5-(N-2-(4-hexanyl-[1,2,3]triazol-1-yl)acetyl)-2, 3, 5 -trideoxy-D-glycero-D-galacto-2-nonulopyranosonic acid (2.23)**

Triazole **2.23** was generated by reaction of **2.20** with 1-octyne (2 equiv), as described above (yield 68%). $^{1}$H NMR (498 MHz, $D_2O$) δ 7.80 (s, 1H), 5.69 (d, *J* = 2.1 Hz, 1H), 5.31 – 5.22 (m, 2H), 4.51 (dd, *J* = 8.8, 2.1 Hz, 1H), 4.29 (d, *J* = 10.9 Hz, 1H), 4.12 (dd, *J* = 10.5, 9.2 Hz, 1H), 3.93 (ddd, *J* = 9.0, 6.3, 2.6 Hz, 1H), 3.87 (dd, *J* = 11.9, 2.5 Hz, 1H), 3.68 – 3.58 (m, 2H), 2.70 (t, *J* = 7.4 Hz, 2H), 1.69 – 1.59 (m, 2H), 1.35 – 1.22 (m, 6H), 0.83 (t, *J* = 6.8 Hz, 3H). $^{13}$C NMR (125 MHz, $D_2O$) δ 170.4, 169.3, 149.9, 148.8, 125.4, 108.4, 76.0, 70.8, 69.1, 68.3, 64.0, 52.9, 51.2, 31.6, 29.3, 28.6, 25.3, 22.8, 14.2. HRMS (ESI) calculated for $C_{19}H_{29}N_4O_8$ $[M-H]^-$, 441.1991, found 441.1985.

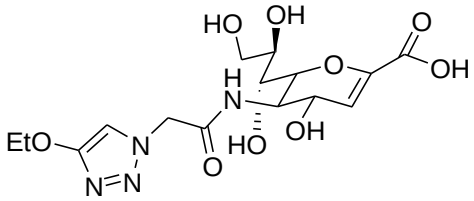


**Methyl 5-(N-2-(4-ethoxy-[1,2,3]triazol-1-yl)acetyl)-2, 3, 5-trideoxy-D-glycero-D-galacto-2-nonulopyranosonic acid (2.24)**

Triazole **2.24** was generated by reaction of **2.20** with ethylethynyl ether (2 equiv), as described above (yield 93%). $^{1}$H NMR (498 MHz, $D_2O$) δ 7.60 (s, 1H), 5.69 (d, *J* = 2.3 Hz, 1H), 5.29 – 5.14 (m, 2H), 4.51 (dd, *J* = 8.9, 2.4 Hz, 1H), 4.30 (dd, *J* = 10.9, 1.1 Hz, 1H), 4.22 (q, *J* = 7.1 Hz, 2H), 4.13 (dd, *J* = 10.9, 8.9 Hz, 1H), 3.94 (ddd, *J* = 9.1, 6.2, 2.8 Hz, 1H), 3.87 (dd, *J* = 11.9, 2.8 Hz, 1H), 3.65 (dd, *J* = 11.9, 6.2 Hz, 1H), 3.61 (dd, *J* = 9.3, 1.1 Hz, 1H), 1.37 (t, *J* = 7.1 Hz, 3H). $^{13}$C NMR (125 MHz, $D_2O$) δ 170.4, 169.1, 161.2, 148.7, 110.6, 108.4, 76.0, 70.8, 69.0, 68.9, 68.3, 63.9, 53.8, 51.1, 14.7. HRMS (ESI) calculated for $C_{15}H_{21}N_4O_9$ $[M-H]^-$, 401.1314, found 401.1310.

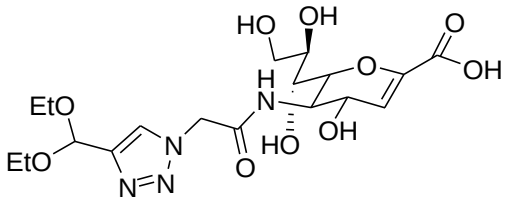

**Methyl 5-(N-2-(4-diethoxymethyl-[1,2,3]triazol-1-yl)acetyl)-2, 3, 5-trideoxy-D-glycero-D-galacto-2-nonulopyranosonic acid (2.25)**

Triazole **2.25** was generated by reaction of **2.20** with propargylaldehyde diethylacetal (2 equiv), as described above (yield 96%). $^{1}$H NMR (498 MHz, $D_2O$) δ 8.10 (s, 1H), 5.83 (s, 1H), 5.69 (d, *J* = 2.3 Hz, 1H), 5.42 – 5.20 (m, 2H), 4.51 (dd, *J* = 8.8, 2.4 Hz, 1H), 4.30 (dd, *J* = 10.9, 1.0 Hz, 1H), 4.13 (dd, *J* = 10.9, 8.9 Hz, 1H), 3.93 (ddd, *J* = 9.0, 6.2, 2.6 Hz, 1H), 3.87 (dd, *J* = 11.9, 2.7 Hz, 1H), 3.81 – 3.70 (m, 4H), 3.67 – 3.60 (m, 2H), 1.23 (t, *J* = 7.1 Hz, 6H). $^{13}$C NMR (101 MHz, $D_2O$) δ 170.0, 168.5, 148.4, 146.5, 125.9, 108.0, 96.8, 75.6, 70.3, 68.7, 67.9, 63.7, 63.6, 52.7, 50.7, 14.7. HRMS (ESI) calculated for $C_{18}H_{27}N_4O_{10}$ $[M-H]^-$, 459.1733, found 459.1732.

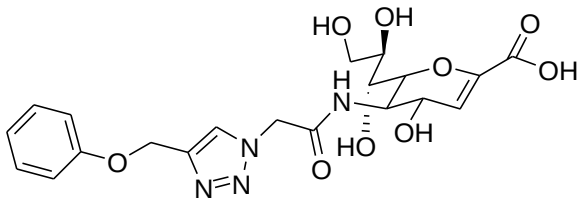

**Methyl 5-(N-2-(4-phenoxymethyl-[1,2,3]triazol-1-yl)acetyl)-2, 3, 5-trideoxy-D-glycero-D-galacto-2-nonulopyranosonic acid (2.26)**

Triazole **2.26** was generated by reaction of **2.20** with phenylpropargyl ether (2 equiv), as described above (yield 96%). $^{1}$H NMR (600 MHz, DMSO) δ 8.56 (d, *J* = 8.3 Hz, 1H), 8.17 (s, 1H), 7.29 (dd, *J* = 8.6, 7.4 Hz, 2H), 7.04 (d, *J* = 7.9 Hz, 2H), 6.94 (t, *J* = 7.3 Hz, 1H), 5.48 (s, 1H), 5.19 (s, 2H), 5.14 (s, 2H), 4.30 – 4.22

(m, 1H), 4.00 (d, *J* = 10.4 Hz, 1H), 3.79 (dd, *J* = 18.4, 8.5 Hz, 1H), 3.68 (d, *J* = 2.2 Hz, 1H), 3.61 (dd, *J* = 11.1, 3.4 Hz, 1H), 3.48 (d, *J* = 6.9 Hz, 1H), 3.36 (dd, *J* = 11.4, 5.9 Hz, 1H). $^{13}$C NMR (126 MHz, $D_2O$) δ 170.5, 169.1, 158.2, 148.8, 144.5, 130.8, 123.0, 116.3, 108.4, 76.0, 70.8, 69.1, 68.34, 64.0, 62.1, 53.1, 51.2. HRMS (ESI) calculated for $C_{20}H_{23}N_4O_9$ [M-H]$^-$, 463.1471, found 413.1471.

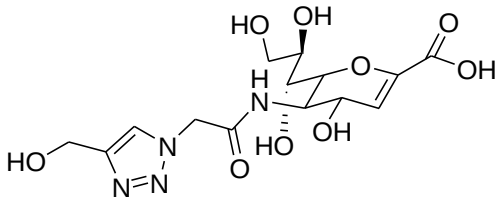


**Methyl 5-(N-2-(4-hydroxymethyl-[1,2,3]triazol-1-yl)acetyl)-2, 3, 5-trideoxy-D-glycero-D-galacto-2-nonulopyranosonic acid (2.27)**

Triazole **2.27** was generated by reaction of **2.20** with propargyl alcohol (2 equiv), as described above (yield 80%). $^1$H NMR (400 MHz, $D_2O$) δ 8.03 (s, 1H), 5.69 (d, *J* = 2.3 Hz, 1H), 5.41 – 5.25 (m, 2H), 4.74 (s, 1H), 4.51 (dd, *J* = 8.8, 2.3 Hz, 1H), 4.29 (dd, *J* = 10.9, 0.8 Hz, 1H), 4.13 (dd, *J* = 10.8, 8.9 Hz, 1H), 3.93 (ddd, *J* = 9.1, 6.1, 2.6 Hz, 1H), 3.87 (dd, *J* = 11.9, 2.7 Hz, 1H), 3.68 – 3.58 (m, 2H). $^{13}$C NMR (125 MHz, $D_2O$) δ 170.4, 169.2, 148.8, 147.9, 126.4, 108.4, 76.0, 70.7, 69.0, 68.3, 63.92, 55.5, 53.0, 51.2. HRMS (ESI) calculated for $C_{14}H_{19}N_4O_9$ [M-H]$^-$, 387.1158, found 387.1153.

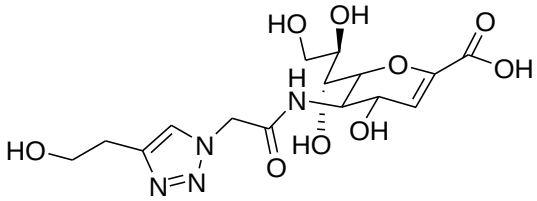


**Methyl 5-(N-2-(4-(2-hydroxy-ethyl)-[1,2,3]triazol-1-yl)acetyl)-2, 3, 5-trideoxy-D-glycero-D-galacto-2-nonulopyranosonic acid (2.28)**

Triazole **2.28** was generated by reaction of **2.20** with 3-butyn-1-ol (2 equiv), as described above (yield 31%). $^{1}$H NMR (498 MHz, $D_2O$) δ 7.90 (s, 1H), 5.69 (d, *J* = 2.4 Hz, 1H), 5.45 – 5.25 (m, 2H), 4.50 (dd, *J* = 8.9, 2.4 Hz, 1H), 4.29 (dd, *J* = 10.9, 1.2 Hz, 1H), 4.13 (dd, *J* = 10.9, 8.9 Hz, 1H), 3.93 (ddd, *J* = 6.2, 5.0, 2.7 Hz, 1H), 3.90 – 3.85 (m, 3H), 3.68 – 3.59 (m, 2H), 2.96 (t, *J* = 6.4 Hz, 2H). $^{13}$C NMR (126 MHz, $D_2O$) δ 170.5, 169.3, 148.8, 146.3, 126.2, 108.4, 76.0, 70.7, 69.1, 68.4, 64.0, 61.5, 52.9, 51.1, 28.6. HRMS (ESI) calculated for $C_{15}H_{21}N_4O_9$ $[M-H]^-$, 401.1314, found 401.1311.

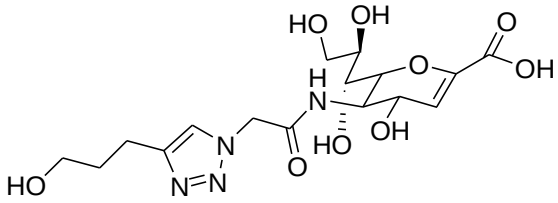


**Methyl 5-[N-2-(4-(3-hydroxy-propyl)-[1,2,3]triazol-1-yl)acetyl]-2, 3, 5-trideoxy-D-glycero-D-galacto-2-nonulopyranosonic acid (2.29)**

Triazole **2.29** was generated by reaction of **2.20** with 4-pentyn-1-ol (2 equiv), as described above (yield 54%). $^{1}$H NMR (498 MHz, $D_2O$) δ 7.84 (s, 1H), 5.69 (d, *J* = 2.3 Hz, 1H), 5.34 – 5.20 (m, 2H), 4.51 (dd, *J* = 8.8, 2.4 Hz, 1H), 4.29 (dd, *J* = 10.9, 0.9 Hz, 1H), 4.13 (dd, *J* = 10.8, 8.8 Hz, 1H), 3.97 – 3.90 (m, 1H), 3.87 (dd, *J* = 11.9, 2.7 Hz, 1H), 3.72 – 3.56 (m, 4H), 2.82 – 2.75 (m, 2H), 1.96 – 1.86 (m, 2H). $^{13}$C NMR (126 MHz, $D_2O$) δ 170.5, 169.3, 148.9, 148.8, 125.5, 108.4, 75.9, 70.7, 69.1, 68.4, 63.9, 61.6, 52.9, 51.1, 31.8, 21.9. HRMS (ESI) calculated for $C_{16}H_{23}N_4O_9$ $[M-H]^-$, 415.1471, found 415.1474.

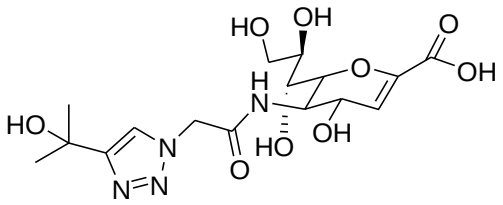

**Methyl 5-(N-2-(4-(1-hydroxy-1-methyl-ethyl)-[1,2,3]triazol-1-yl)acetyl)-2, 3, 5-trideoxy-D-glycero-D-galacto-2-nonulopyranosonic acid (2.30)**

Triazole **2.30** was generated by reaction of **2.20** with 2-methyl-3-butyn-2-ol (2 equiv), as described above (yield 90%). $^{1}$H NMR (400 MHz, $D_2O$) δ 7.97 (s, 1H), 5.69 (d, *J* = 2.3 Hz, 1H), 5.44 – 5.19 (m, 2H), 4.51 (dd, *J* = 8.8, 2.3 Hz, 1H), 4.30 (dd, *J* = 10.9, 0.9 Hz, 1H), 4.13 (dd, *J* = 10.9, 8.9 Hz, 1H), 3.93 (ddd, *J* = 9.1, 6.2, 2.7 Hz, 1H), 3.87 (dd, *J* = 11.9, 2.7 Hz, 1H), 3.68 – 3.58 (m, 2H), 1.61 (s, 6H). $^{13}$C NMR (101 MHz, $D_2O$) δ 170.4, 169.1, 155.9, 148.8, 124.1, 108.4, 75.9, 70.7, 69.1, 69.0, 68.3, 63.9, 53.0, 51.1, 29.8. HRMS (ESI) calculated for $C_{16}H_{23}N_4O_9$ $[M-H]^-$, 415.1471, found 415.1464.

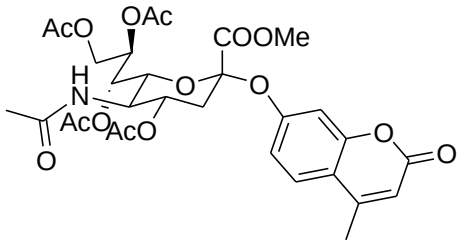

**Methyl (4-methylcoumarin-7-yl 5-acetamido-4, 7, 8, 9-tetra-O-acetyl-3, 5-dideoxy-α-D-glycero-D-galacto-2-nonulopyranosid)onate (2.31)**

**2.2** was converted to 4,7,8,9-penta-O-acetyl-2-chloro-β-Neu5Ac in 33% yield by treatment with dichloromethyl ether (DCMME) and $SnCl_4$ in $CH_2Cl_2$. **2.2** (457 mg, 0.97 mmol) (Helm, R.F., Ralph, J., et al. 1991) was dissolved in $CH_2Cl_2$ (24 mL) under an atmosphere of argon, and dichloromethyl methyl ether (1.6 mL,

4.42 mmol) and $SnCl_4$ (0.7 mL, 1M in $CH_2Cl_2$) were added with stirring. A white precipitate formed immediately upon the addition of the $SnCl_4$, which dissolved over the course of 2 h. The resulting solution was washed by cold saturated, aqueous $NaHCO_3$. The $CH_2Cl_2$ layers were combined and evaporated. The product was purified by flash chromatography (EtOAc/Hexane, 6:1) to afford 143 mg of 4,7,8,9-penta-O-acetyl-2-chloro-β-Neu5Ac. 4,7,8,9-penta-O-acetyl-2-chloro-β-Neu5Ac (471 mg, 0.92 mmol) (Kuboki, A., Sekiguchi, T., et al. 1998) was added to a solution of 4-methylumbelliferone (325 mg, 2 mmol) and diisopropylethylamine (1 mL, 7.74 mmol ) in acetonitrile (20 mL) at room temperature overnight with stirring under argon. The mixture was concentrated *in vacuo* and diluted with toluene for three times. Purification was performed by flash chromatography with 4:1 EtOAc-hexane to give 191 mg of **2.31** (32%). $^1$H NMR (300 MHz, $CDCl_3$) δ 7.52 (d, *J* = 8.7 Hz, 1H), 7.07 (dd, *J* = 9.0, 2.4 Hz, 1H), 7.01 (d, *J* = 2.4 Hz, 1H), 6.20 (d, *J* = 1.2 Hz, 1H), 5.40 – 5.37 (m, *J* = 4.0 Hz, 3H), 5.00 (ddd, *J* = 15.0, 10.2, 4.5 Hz, 1H), 4.52 (app d, *J* = 10.2 Hz, 1H), 4.34 – 4.27 (m, 1H), 4.18 – 4.08 (m, 2H), 3.70 (s, 3H), 2.73 (dd, *J* = 12.9, 4.5 Hz, 1H), 2.42 (d, *J* = 1.2 Hz, 3H), 2.26 (app t, *J* = 12.6 Hz, 1H), 2.17 (s, 3H), 2.14 (s, 3H), 2.05 (s, 6H), 1.93 (s, 3H).

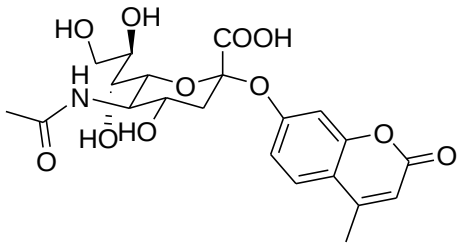


**4-Methylumbelliferyl -D-N-acetylneuraminic acid (2.32)**

Compound **2.32** (70 mg, 0.11 mmol) was dissolved in methanol (12 mL), and sodium methoxide solution (0.3 mL, 0.3 mmol) was added dropwise to the reaction, followed by stirring for 2 h. Amberlite IR-120($H^+$) was then added to neutralize the reaction mixture (pH 7.0). The solution was filtered and concentrated in vacuo. Then the residue was treated with 0.1 M NaOH (3 mL) for 0.5 h at room temperature. The reaction was neutralized with Amberlite IR-120($H^+$), followed by filtration and evaporation of the solvent. Purification was performed by flash chromatography with 2:2:1 2-propanol-EtOAc-$H_2O$ (65%). $^1$H NMR (498 MHz, $D_2O$) δ 7.65 (d, *J* = 9.0 Hz, 1H), 7.17 – 7.12 (m, 2H), 6.20 (d, *J* = 1.5 Hz, 1H), 4.07 (dd, *J* = 10.5, 2.0 Hz, 1H), 3.95 (app t, J = 10.0 Hz, 1H), 3.91 – 3.85 (m, 2H), 3.79 (ddd, *J* = 14.4, 10.0, 5.0 Hz, 1H), 3.64 (dd, *J* = 12.5, 6.5 Hz, 1H), 3.60 (dd, *J* = 9.0, 1.5 Hz, 1H), 2.87 (dd, *J* = 12.5, 4.5 Hz, 1H), 2.38 (d, *J* = 1.0 Hz, 3H), 2.05 (s, 3H), 2.02 – 1.96 (m, 1H). $^{13}$C NMR (125 MHz, $D_2O$) δ 175.9, 173.5, 165.4, 158.1, 157.0, 154.2, 127.0, 118.4, 117.0, 112.5, 108.8, 103.5, 74.5, 72.5, 69.2, 68.7, 63.6, 52.6, 41.8, 22.9, 18.8. HRMS (ESI) calculated for $C_{21}H_{24}NO_{11}$ $[M-H]^-$, 466.1355, found 466.1351.

### *2.6.5 $IC_{50}$ curves for C9-derivatives (2.6, 2.7-2.15) and N5-derivatives (2.21, 2.22-2.30)*

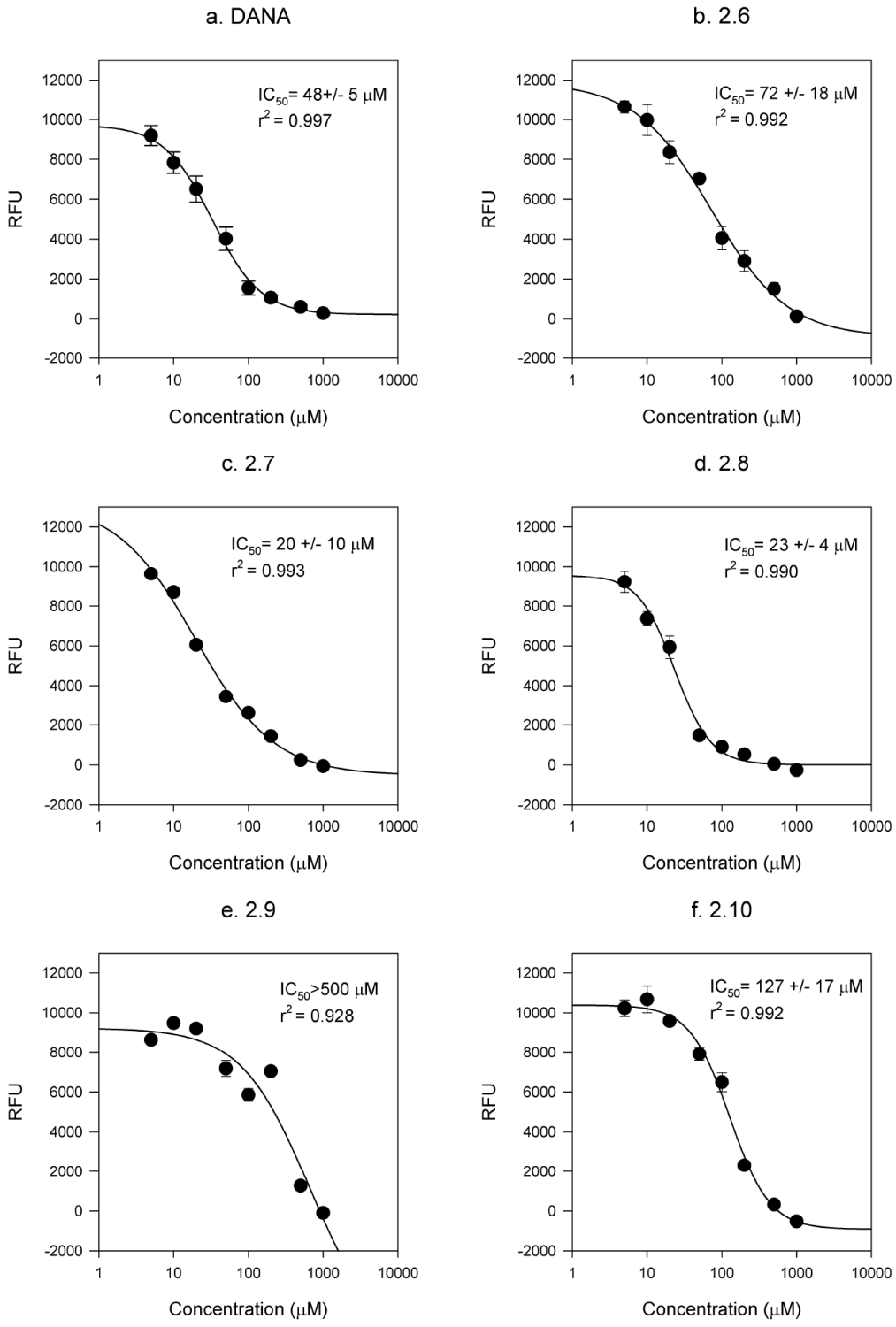

g. 2.11

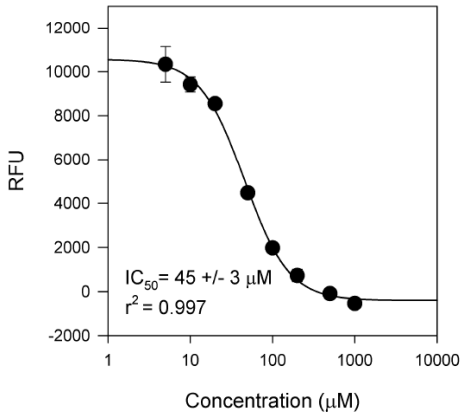


h. 2.12

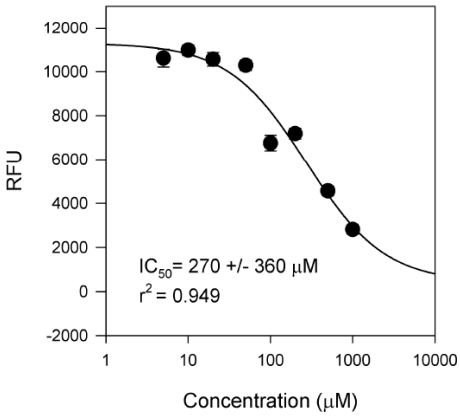


i. 2.13

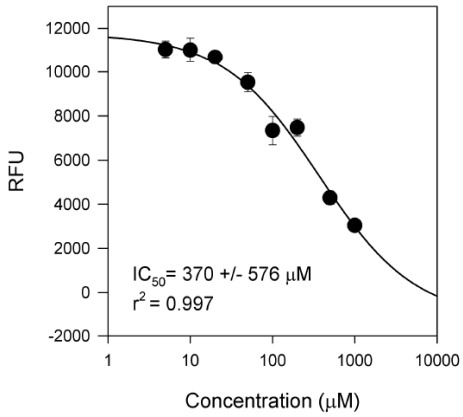


j. 2.14

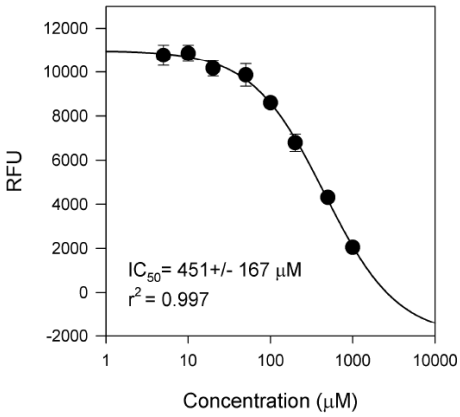


k. 2.15

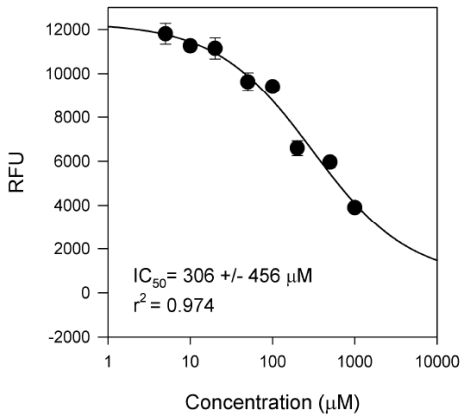

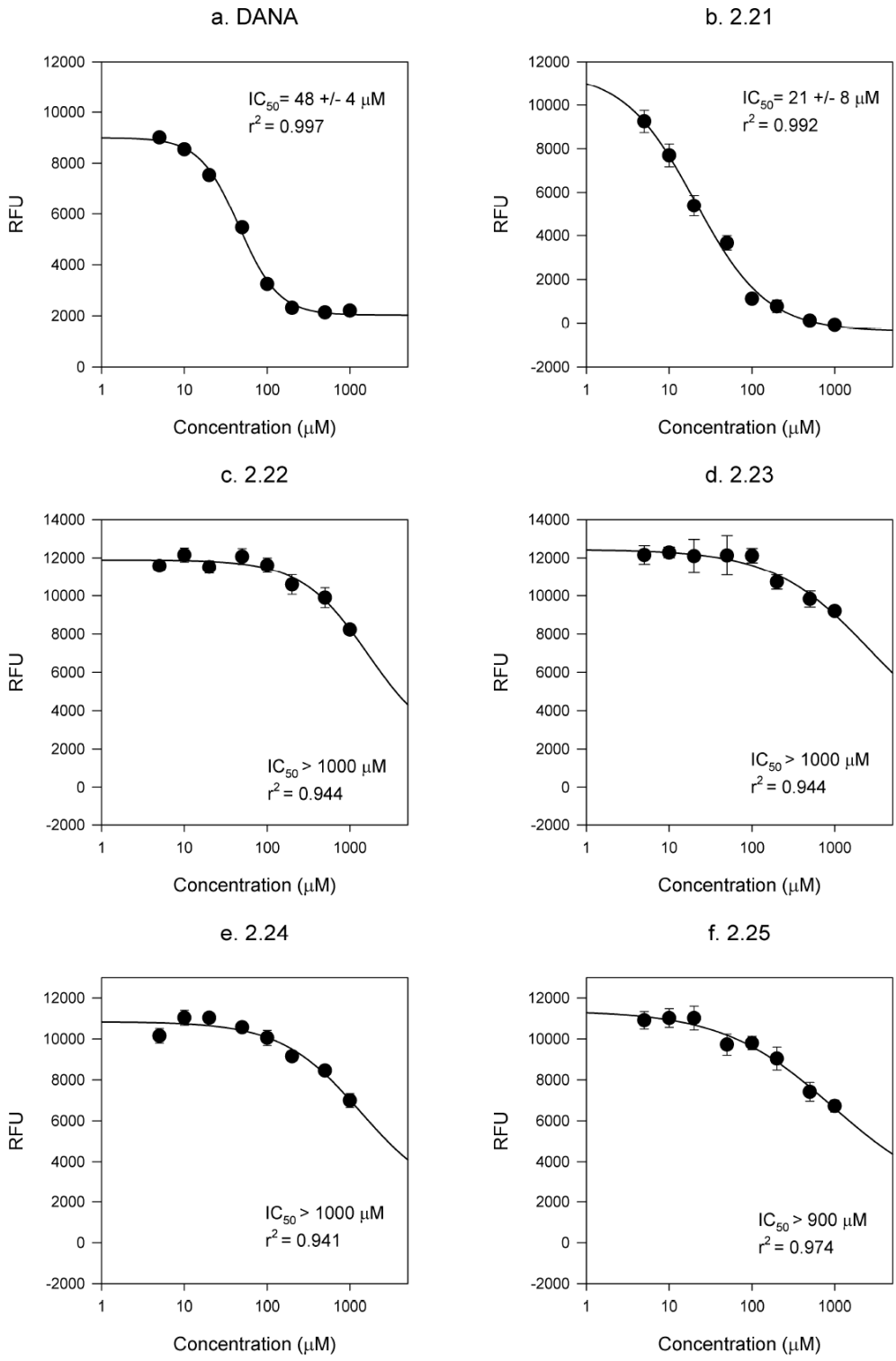
a. DANA
IC50= 48 +/- 4 μM
r2 = 0.997
RFU
Concentration (μM)
b. 2.21
IC50= 21 +/- 8 μM
r2 = 0.992
RFU
Concentration (μM)
c. 2.22
IC50 > 1000 μM
r2 = 0.944
RFU
Concentration (μM)
d. 2.23
IC50 > 1000 μM
r2 = 0.944
RFU
Concentration (μM)
e. 2.24
IC50 > 1000 μM
r2 = 0.941
RFU
Concentration (μM)
f. 2.25
IC50 > 900 μM
r2 = 0.974
RFU
Concentration (μM)

g. 2.26

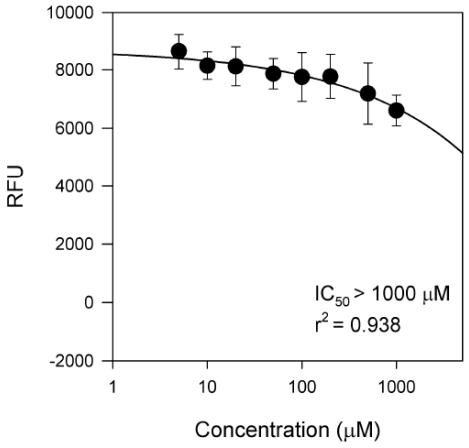


h. 2.27

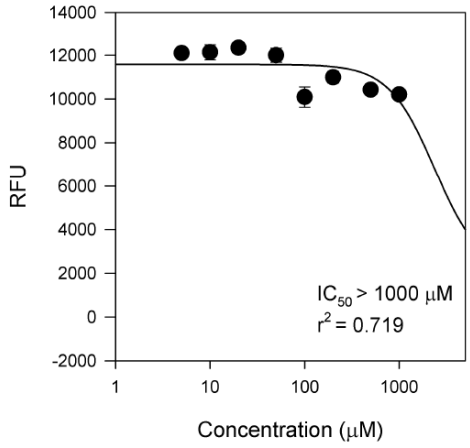


i. 2.28

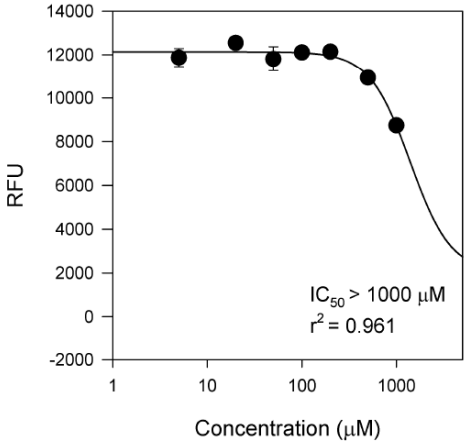


j. 2.29

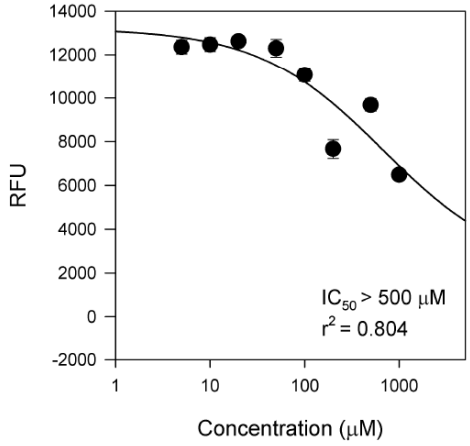


k. 2.30

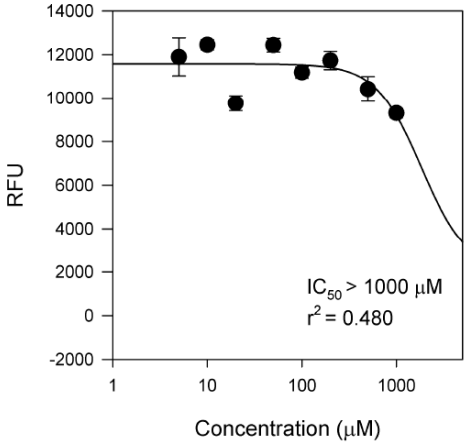

### *2.7 References*


Albohy, A., Li, M.D., Zheng, R.B., Zou, C. and Cairo, C.W. (2010) Insight into substrate recognition and catalysis by the human neuraminidase 3 (NEU3) through molecular modeling and site-directed mutagenesis. *Glycobiology*, 20, 1127-1138.

Anastasia, L., Papini, N., Colazzo, F., Palazzolo, G., Tringali, C., Dileo, L., Piccoli, M., Conforti, E., Sitzia, C., Monti, E., Sampaolesi, M., Tettamanti, G. and Venerando, B. (2008) NEU3 sialidase strictly modulates GM3 levels in skeletal myoblasts C2C12 thus favoring their differentiation and protecting them from apoptosis. *Journal of Biological Chemistry*, 283, 36265-36271.

Azuma, Y., Sato, H., Higai, K. and Matsumoto, K. (2007) Enhanced Expression of Membrane-Associated Sialidase Neu3 decreases GD3 and increases GM3 on the surface of Jurkat cells during etoposide-induced apoptosis. *Biological & Pharmaceutical Bulletin*, 30, 1680-1684.

Bhaskar K, V., Duggan, P.J., Humphrey, D.G., Krippner, G.Y., McCarl, V. and Offermann, D.A. (2001) Phenylboronic acid as a labile protective agent: the selective derivatisation of 1,2,3-triols. *Journal of the Chemical Society, Perkin Transactions 1*, 1098-1102.

Bissantz, C., Kuhn, B. and Stahl, M. (2010) A medicinal chemist's guide to molecular interactions. *Journal of Medicinal Chemistry*, 53, 5061-5084.

Bolitt, V., Mioskowski, C., Lee, S.G. and Falck, J.R. (1990) Direct preparation of 2-deoxy-D-glucopyranosides from glucals without Ferrier rearrangement. *The Journal of Organic Chemistry*, 55, 5812-5813.

Caciotti, A., Di Rocco, M., Filocamo, M., Grossi, S., Traverso, F., d'Azzo, A., Cavicchi, C., Messeri, A., Guerrini, R., Zammarchi, E., Donati, M. and Morrone, A. (2009) Type II sialidosis: review of the clinical spectrum and identification of a new splicing defect with chitotriosidase assessment in two patients. *Journal of Neurology*, 256, 1911-1915.

Cantarel, B.L., Coutinho, P.M., Rancurel, C., Bernard, T., Lombard, V. and Henrissat, B. (2009) The Carbohydrate-Active EnZymes database (CAZy): an expert resource for Glycogenomics. *Nucleic Acids Research*, 37, D233-D238.

Carubelli, I., Venerando, B. and Stamatos, N.M. (2006) Sialidases Neu1 and Neu3 on the surface of human monocyte-derived dendritic cells may influence cell activity by desialylating GM3 ganglioside. *Glycobiology*, 16, 285.

Chavas, L.M.G., Kato, R., Suzuki, N., Von Itzstein, M., Mann, M.C., Thomson, R.J., Dyason, J.C., McKimm-Breschkin, J., Fusi, P., Tringali, C., Venerando, B., Tettamanti, G., Monti, E. and Wakatsuki, S. (2010) Complexity in influenza virus targeted drug design: Interaction with human sialidases. *Journal of Medicinal Chemistry*, 53, 2998-3002.

Chavas, L.M.G., Tringali, C., Fusi, P., Venerando, B., Tettamanti, G., Kato, R., Monti, E. and Wakatsuki, S. (2005) Crystal structure of the human cytosolic sialidase Neu2: Evidence for the dynamic nature of substrate recognition. *Journal of Biological Chemistry*, 280, 469-475.

Chen, X.P., Enioutina, E.Y. and Daynes, R.A. (1997) The control of IL-4 gene expression in activated murine T lymphocytes - A novel role for neu-1 sialidase. *Journal of Immunology*, 158, 3070-3080.

D. Burkart, M., P. Vincent, S. and Wong, C.-H. (1999) An efficient synthesis of CMP-3-fluoroneuraminic acid. *Chemical Communications*, 1525-1526.

Dyason, J.C. and von Itzstein, M. (2001) Anti-Influenza Virus Drug Design: Sialidase Inhibitors. *Australian Journal of Chemistry*, 54, 663-670.

Gadhoum, S.Z. and Sackstein, R. (2008) CD15 expression in human myeloid cell differentiation is regulated by sialidase activity. *Nature Chemical Biology*, 4, 751-757.

Gilson, M.K., Sharp, K.A. and Honig, B.H. (1988) Calculating the electrostatic potential of molecules in solution: Method and error assessment. *Journal of Computational Chemistry*, 9, 327-335.

Goodsell, D.S., Morris, G.M. and Olson, A.J. (1996) Automated docking of flexible ligands: Applications of autodock. *Journal of Molecular Recognition*, 9, 1-5.

Ha, K.T., Lee, Y.C., Cho, S.H., Kim, J.K. and Kim, C.H. (2004) Molecular characterization of membrane type and ganglioside-specific sialidase (Neu3) expressed in E. coli. *Molecules and Cells*, 17, 267-273.

Han, S., Collins, B.E., Bengtson, P. and Paulson, J.C. (2005) Homomultimeric complexes of CD22 in B cells revealed by protein-glycan cross-linking. *Nature Chemical Biology*, 1, 93-97.

Hata, K., Koseki, K., Yamaguchi, K., Moriya, S., Suzuki, Y., Yingsakmongkon, S., Hirai, G., Sodeoka, M., von Itzstein, M. and Miyagi, T. (2008) Limited

inhibitory effects of oseltamivir and zanamivir on human sialidases. *Antimicrobial Agents and Chemotherapy*, 52, 3484-3491.

Helm, R.F., Ralph, J. and Anderson, L. (1991) Regioselective protection strategies for D-xylopyranosides. *The Journal of Organic Chemistry*, 56, 7015-7021.

Hotha, S., Anegundi, R. I., and Natu, A. A. (2005) Expedient synthesis of 1,2,3-triazole-fused tetracyclic compounds by intramolecular Huisgen ('click') reactions on carbohydrate-derived azido-alkynes. *Tetrahedron Letters*, 46, 4584-4588.

Johansson, S., Nilsson, E., Qian, W., Guilligay, D., Crepin, T., Cusack, S., Arnberg, N. and Elofsson, M. (2009) Design, synthesis, and evaluation of *N*-Acyl modified sialic acids as inhibitors of adenoviruses causing epidemic keratoconjunctivitis. *Journal of Medicinal Chemistry*, 52, 3666-3678.

Kakugawa, Y., Wada, T., Yamaguchi, K., Yamanami, H., Ouchi, K., Sato, I. and Miyagi, T. (2002) Up-regulation of plasma membrane-associated ganglioside sialidase (Neu3) in human colon cancer and its involvement in apoptosis suppression. *Proceedings of the National Academy of Sciences*, 99, 10718-10723.

Kato, K., Shiga, K., Yamaguchi, K., Hata, K., Kobayashi, T., Miyazaki, K., Saijo, S. and Miyagi, T. (2006) Plasma-membrane-associated sialidase (NEU3) differentially regulates integrin-mediated cell proliferation through laminin- and fibronectin-derived signalling. *Biochemical Journal*, 394, 647-656.

Kaval, N., Ermolat'ev, D., Appukkuttan, P., Dehaen, W., Kappe, C. O., and der Eycken, E. V. (2005) The aapication of "click chemistry" for the decoration of 2(1*H*)-pyrazinone scalffold:generation of templates. *J. Comb. Chem*, 7, 490-502.

Kuboki, A., Sekiguchi, T., Sugai, T. and Ohta, H. (1998) A facile access to Aryl α-sialosides: the combination of a volatile amine base and acetonitrile in glycosidation of sialosyl chlorides. *Synlett*, 1998, 479,482.

Li, J., Zheng, M., Tang, W., He, P.-L., Zhu, W., Li, T., Zuo, J.-P., Liu, H. and Jiang, H. (2006) Syntheses of triazole-modified zanamivir analogues via click chemistry and anti-AIV activities. *Bioorganic & Medicinal Chemistry Letters*, 16, 5009-5013.

Li, Y., Cao, H., Yu, H., Chen, Y., Lau, K., Qu, J., Thon, V., Sugiarto, G. and Chen, X. (2011) Identifying selective inhibitors against the human cytosolic sialidase NEU2 by substrate specificity studies. *Molecular BioSystems*, 7, 1060-1072.

Loka, R.S., Sadek, C.M., Romaniuk, N.A. and Cairo, C.W. (2010) Conjugation of Synthetic N-Acetyl-Lactosamine to Azide-Containing Proteins Using the Staudinger Ligation. *Bioconjugate Chemistry*, 21, 1842-1849.

Lu, Y. and Gervay-Hague, J. (2007) Synthesis of C-4 and C-7 triazole analogs of zanamivir as multivalent sialic acid containing scaffolds. *Carbohydrate Research*, 342, 1636-1650.

Magesh, S., Moriya, S., Suzuki, T., Miyagi, T., Ishida, H. and Kiso, M. (2008) Design, synthesis, and biological evaluation of human sialidase inhibitors. Part 1: Selective inhibitors of lysosomal sialidase (NEU1). *Bioorganic & Medicinal Chemistry Letters*, 18, 532-537.

Magesh, S., Savita, V., Moriya, S., Suzuki, T., Miyagi, T., Ishida, H. and Kiso, M. (2009) Human sialidase inhibitors: Design, synthesis, and biological evaluation of 4-acetamido-5-acylamido-2-fluoro benzoic acids. *Bioorganic & Medicinal Chemistry*, 17, 4595-4603.

Magesh, S., Suzuki, T., Miyagi, T., Ishida, H. and Kiso, M. (2006) Homology modeling of human sialidase enzymes NEU1, NEU3 and NEU4 based on the crystal structure of NEU2: Hints for the design of selective NEU3 inhibitors. *Journal of Molecular Graphics and Modelling*, 25, 196-207.

Marra, A. and Sinay, P. (1989) Acetylation of N-acetylneuraminic acid and its methyl ester. *Carbohydrate Research*, 190, 317-322.

Martin, R., Witte, K.L. and Wong, C.-H. (1998) The synthesis and enzymatic incorporation of sialic acid derivatives for use as tools to study the structure, activity, and inhibition of glycoproteins and other glycoconjugates. *Bioorganic & Medicinal Chemistry*, 6, 1283-1292.

Meldal, M. and Tornøe, C.W. (2008) Cu-Catalyzed Azide−Alkyne Cycloaddition. *Chemical Reviews*, 108, 2952-3015.

Miyagi, T., Wada, T., Yamaguchi, K. and Hata, K. (2003) Sialidase and malignancy: A minireview. *Glycoconjugate Journal*, 20, 189-198.

Monti, E., Preti, A., Venerando, B. and Borsani, G. (2002) Recent Development in Mammalian Sialidase Molecular Biology. *Neurochemical Research*, 27, 649-663.

Papini, N., Anastasia, L., Tringali, C., Croci, G., Bresciani, R., Yamaguchi, K., Miyagi, T., Preti, A., Prinetti, A., Prioni, S., Sonnino, S., Tettamanti, G.,

Venerando, B. and Monti, E. (2004) The Plasma Membrane-associated Sialidase MmNEU3 Modifies the Ganglioside Pattern of Adjacent Cells Supporting Its Involvement in Cell-to-Cell Interactions. *Journal of Biological Chemistry*, 279, 16989-16995.

Sasaki, A., Hata, K., Suzuki, S., Sawada, M., Wada, T., Yamaguchi, K., Obinata, M., Tateno, H., Suzuki, H. and Miyagi, T. (2003) Overexpression of plasma membrane-associated sialidase attenuates insulin signaling in transgenic mice. *Journal of Biological Chemistry*, 278, 27896-27902.

Seyrantepe, V., Poupetova, H., Froissart, R., Zabot, M.-T., Maire, I. and Pshezhetsky, A.V. (2003) Molecular pathology of NEU1 gene in sialidosis. *Human Mutation*, 22, 343-352.

Schofield,K., M. R. Grimmett, Thornton Keene, B., R.(1976) Syndics of the Cambridge University Press. ISBN:0521205190. 1-25

Shalini, K., Kumar, N., Drabu, S., and Sharma, P. K. (2011) Advances in synthetic approach to and antifungal activity of triazoles. *Beilstein Journal of Organic Chemistry*. 7, 668-677.

Srividhya, D., Manjunathan, S., Thirumaran, S., Saravanan, C., Senthil, S. (2009) Synthesis and characterization of [1,2,3]-triazole containing liquid crystals through click reaction.*Journal of Molecular structure*, 927, 7-13.

Theophil, E., Siegfried H., (2003) The Chemistry of Heterocycles. Wiley-VCH, ISBN: 3527307206 , 200-202.

Uemura, T., Shiozaki, K., Yamaguchi, K., Miyazaki, S., Satomi, S., Kato, K., Sakuraba, H. and Miyagi, T. (2009) Contribution of sialidase NEU1 to suppression of metastasis of human colon cancer cells through desialylation of integrin [beta]4. *Oncogene*, 28, 1218-1229.

Ueno, S., Saito, S., Wada, T., Yamaguchi, K., Satoh, M., Arai, Y. and Miyagi, T. (2006) Plasma Membrane-associated Sialidase Is Up-regulated in Renal Cell Carcinoma and Promotes Interleukin-6-induced Apoptosis Suppression and Cell Motility. *Journal of Biological Chemistry*, 281, 7756-7764.

Valaperta, R., Chigorno, V., Basso, L., Prinetti, A., Bresciani, R., Preti, A., Miyagi, T. and Sonnino, S. (2006) Plasma membrane production of ceramide from ganglioside GM3 in human fibroblasts. *The FASEB Journal*, 20, 1227-1229.

Varki, N.M. and Varki, A. (2007) Diversity in cell surface sialic acid presentations: implications for biology and disease. *Laboratory Investigation*, 87, 851-857.

We ïwer, M., Chen, C.-C., Kemp, M.M. and Linhardt, R.J. (2009) Synthesis and Biological Evaluation of Non-Hydrolyzable 1,2,3-Triazole-Linked Sialic Acid Derivatives as Neuraminidase Inhibitors. *European Journal of Organic Chemistry*, 2009, 2611-2620.

Yu, H., Huang, S., Chokhawala, H., Sun, M., Zheng, H. and Chen, X. (2006) Highly Efficient Chemoenzymatic Synthesis of Naturally Occurring and Non-Natural α-2,6-Linked Sialosides: A P. damsela α-2,6-Sialyltransferase with Extremely Flexible Donor–Substrate Specificity. *Angewandte Chemie International Edition*, 45, 3938-3944.

Zou, Y., Albohy, A., Sandbhor, M. and Cairo, C.W. (2010) Inhibition of human neuraminidase 3 (NEU3) by C9-triazole derivatives of 2,3-didehydro-N-acetyl-neuraminic acid. *Bioorganic & Medicinal Chemistry Letters*, 20, 7529-7533.

# Chapter 3

## Design and synthesis of inhibitors of NEU3 featuring a modified *C*7 side-chain[1]

[1] 2, 4-hydrazino-7-nitro-benzofurazan hydrazine was synthesized by Jessie A. Key (University of Alberta).

### *3.1 Introduction*

We have previously generated a series of *C*9 and *N*5Ac modified analogs of 2,3-didehydro-*N*-acetyl-neuraminic acid (DANA), which were elaborated using Cu-catalyzed azide-alkyne cycloaddition (CuAAC) to generate triazole-containing inhibitors (**Chapter 2**) (Zou, Y., Albohy, A., et al. 2010). Our results suggested that the *N*5 binding pocket cannot accommodate large groups, while the *C*9 binding pocket can tolerate large hydrophobic groups. We set out to develop a route to a new series of DANA analogs with a modified glycerol side chain to further examine the *N*5 and *C*9 binding pocket tolerances.

Examination of the structure-activity relationships (SAR) for the glycerol side-chain of zanamivir with viral neuraminidase has been previously reported. Replacement of the glycerol chain with a series of hydrophobic groups was used to explore inhibitor potency (Taylor, N.R., Cleasby, A., et al. 1998). Smith et al. (Smith, P.W., Sollis, S.L., et al. 1996; Smith, P.W., Sollis, S.L., et al. 1998) reported the synthesis of a series of 4*H*-pyran carboxamide influenza sialidase inhibitors, including the dipropylamide **3.1** (Scheme **3.1**). Later in 1999, Smith et al. (Smith, P.W., Robinson, J.E., et al. 1999) synthesized the dihydropyran analogues **3.2** and **3.3** (Scheme **3.1**) to further test their biological activities against influenza virus A and B. Analogues of zanamivir, such as **3.4** (Scheme **3.1**), have also been prepared with carbamate substituents at the *C*7 position (Andrews, D.M., Cherry, P.C., et al. 1999).

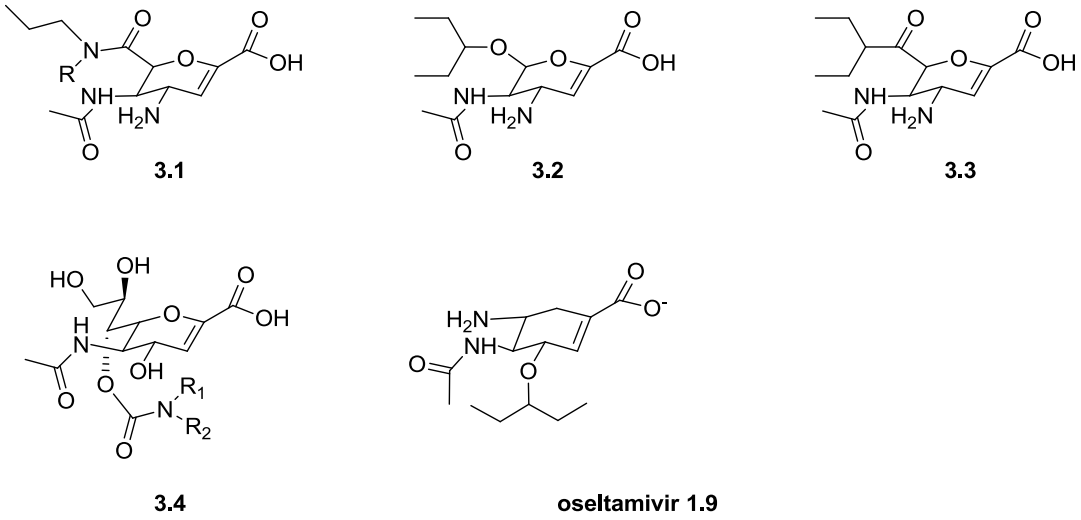


**Scheme 3.1. Previously reported DANA derivatives and carbocyclic analogues of sialic acid featuring modified glycerol side chains.**

An analog of oseltamivir **1.9** (Scheme **3.1**) which contains a modification of the *C*7 side chain, is a potent inhibitor against influenza virus. Having a lipophilic moiety in place of glycerol side chain improved the oral bioavailability of oseltamivir, and also resulted in significant increases in potency (Kim, C.U., Lew, W., et al. 1997; Kim, C.U., Lew, W., et al. 1998). Structural studies have demonstrated that a residue in the viral active site, Glu276, alters its orientation to allow packing of the hydrophobic side chain (Kim, C.U., Lew, W., et al. 1997). Although only limited studies of the human neuraminidase enzymes are available, it has been proposed that the *C*7-*C*9 binding pocket of the human enzymes may play a key role in the selectivity of inhibitors between viral and human neuraminidase enzymes (Albohy, A., Mohan, S., et al. 2011). The best current data to support this hypothesis is work by Albohy et al. who found that derivatives

of oseltamivir containing the same *C*4 side chain as zanamivir had no activity against the human enzymes (Albohy, A., Mohan, S., et al. 2011). Previously, oseltamivir and zanamivir had been tested directly against the human enzymes and only zanamivir had significant potency (Hata, K., Koseki, K., et al. 2008). Thus, Albohy et al. concluded that the hydrophobic side chain of oseltamivir is a significant contributor to this loss in activity.

Examination of the glycerol binding pocket of NEU3 in our homology model suggests that the key differences in the binding interaction are due to additional tyrosine residues. These residues form a relatively open and acidic binding pocket. To explore the tolerance of this binding site to alternative functionality we considered synthetic strategies to introduce new chemical functionality that could be complimentary to the binding site.

### *3.2 Synthesis of modified C7 side chain derivatives*

A variety of methods could be envisioned for generating *C*7-modified DANA analogs. A convenient method of functionalizing the glycerol sidechain of sialic acid is the oxidative cleavage of the *C*7-*C*8 bond using sodium periodate (Sollis, S.L., Smith, P.W., et al. 1996). This generates an aldehyde at *C*7, which can then be coupled using reductive amination (Lane, C.F. 1975), or allylic stannane addition (Smith, P.W., Robinson, J.E., et al. 1999). A common coupling method is initial oxidation of the aldehyde and subsequent introduction of a carboxamide sidechain via pentafluorophenyl ester (Sollis, S.L., Smith, P.W., et al. 1996; Smith, P.W., Sollis, S.L., et al. 1998) (Scheme **3.2**) Roy et al. and Kajihara et al. have each reported the derivatization of sialic acids in this way

using aldehyde-amine coupling (Roy, R. and Laferrière, C.A. 1990; Kajihara, Y., Kamiyama, D., et al. 2004). Compared to other coupling methods, reductive amination requires fewer steps and the reaction conditions are mild. We first examined the utility of reductive amination with a protected DANA derivative. Previous reports suggest that a basic functional group at the *C*4 position may increase inhibitory activity (Li, J., Zheng, M., et al. 2006). Therefore, we planned to include in our scheme a method to introduce an azide handle at *C*4 position which could be converted into amine or guanidine group when needed.

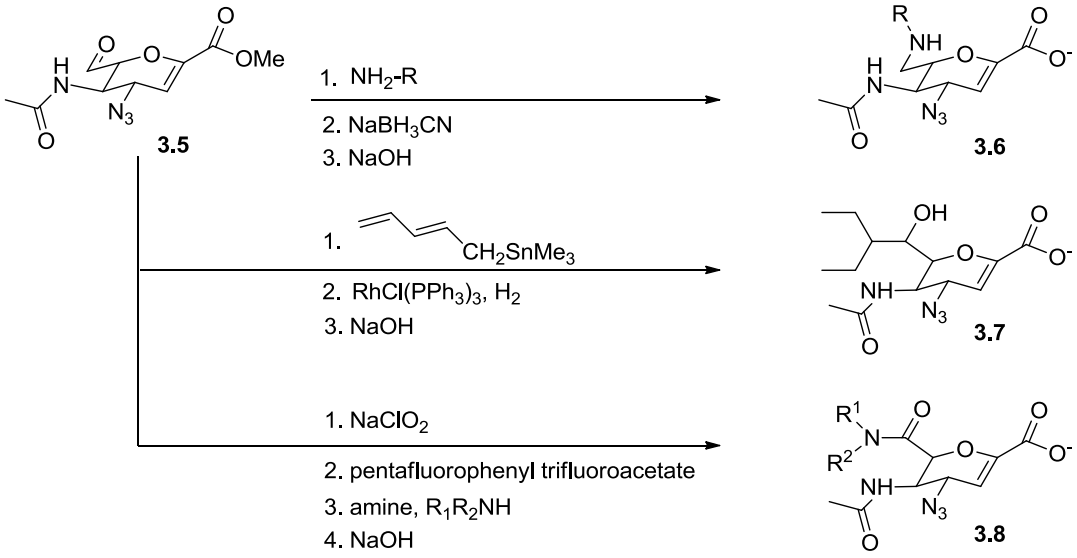


**Scheme 3.2. Potential coupling methods to modify the glycerol side-chain.** The intermediate aldehyde, **3.5**, could be coupled with amines, allylic stannane or converted into a carboxylic acid which can be coupled with an amine.

We first explored reductive amination of **3.5**. The strategy utilizes oxidative cleavage of the glycerol chain and subsequent replacement with a series of amine derivatives. First we coupled the intermediate aldehyde **3.5** with various

amines to form an imine intermediate. These compounds could then be reduced using sodium cyanoborohydride to generate a library of amine derivatives. Treatment of aldehyde **3.5** with propylamine generated an imine, which was then reduced to amine **3.9**. However, coupling between the aldehyde and the amine proved challenging and only one of the amine targets (**3.9**) was detected by High-Resolution Mass Spectroscopy (HRMS) (Scheme **3.3**). Therefore, we considered changing our strategy to use more reactive hydrazine nucleophiles as the coupling partner of aldehyde **3.5**, to form hydrazone derivatives.

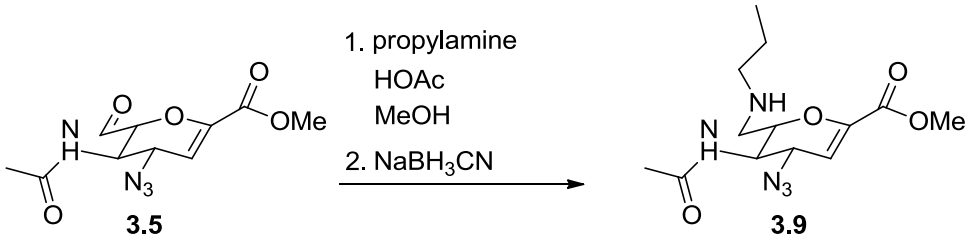


**Scheme 3.3. Coupling of aldehyde 3.5 with propylamine.** The aldehyde was treated with propylamine forming an imine, which was then reduced by $NaBH_3CN$ to generate propylamino derivative **3.9**. Product formation was observed by mass spectrometry due to low isolated yields.

We started the synthesis of **3.9** from peracetylated methyl ester of *N*-acetylneuraminic acid **2.1**. Peracetylated methyl ester **2.1** was converted to oxazoline **3.10** in moderate yield by using trimethylsilyl trifluoromethanesulfonate in dry ethyl acetate (Chandler, M., Bamford, M.J., et al. 1995). The preparation of the reactive intermediate oxazoline **3.10** was also

achieved by treatment of acetyl-protected 2,3-didehydro analog **2.2** with boron trifluoride diethyl etherate. Treatment of oxazoline **3.10**

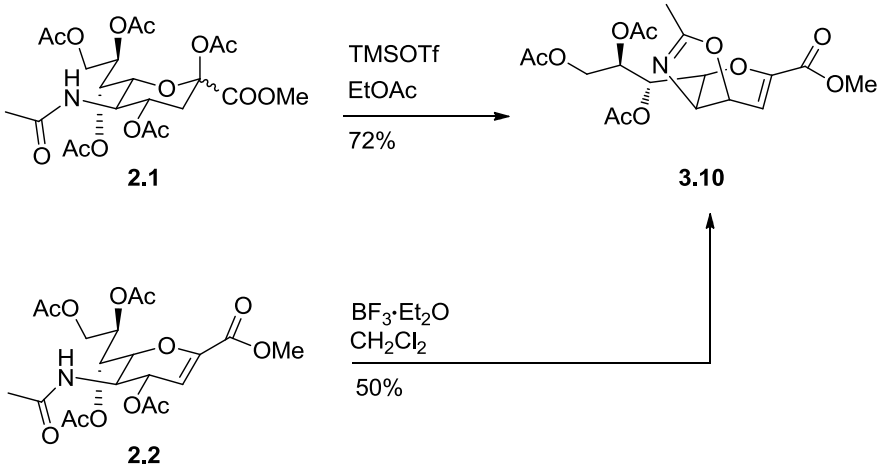


**Scheme 3.4. Generation of oxazoline 3.10.** Oxazoline **3.10** was generated by two methods, in moderate yields, from different starting materials. The reaction of **2.1** with trimethylsilyl trifluoromethanesulfonate was higher yielding and required fewer synthetic steps.

with azidotrimethylsilane provided peracetylated 4-azido-2-deoxy-2,3-dehydro-*N*-acetylneuraminic acid methyl ester **3.11** (Scheme **3.5**) (Lu, Y. and Gervay-Hague, J. 2007). It was reported that the methyl ester protected 4-azido-4-deoxy-Neu5Ac2en **3.11** could be prepared via a Mitsunobu reaction on the protected precursor **3.12** (Schreiner, E., Zbiral, E., et al. 1991). The azide group was reduced to an amine group using triphenylphosphine to give **3.13** in moderate yield (Scheme **3.5**). Removal of the *O*-acetyl protecting groups of **3.11** provided methyl ester **3.14**, which could be hydrolyzed to the target compound **3.15**. Reaction of **3.14** with triphenylphosphine gave the stable P-N ylides **3.16**, which

could hydrolyze when heated or in the aqueous triethylamine conditions (Schreiner, E., Zbiral, E., et al. 1991; Kajihara, Y., Kamiyama, D., et al. 2004).

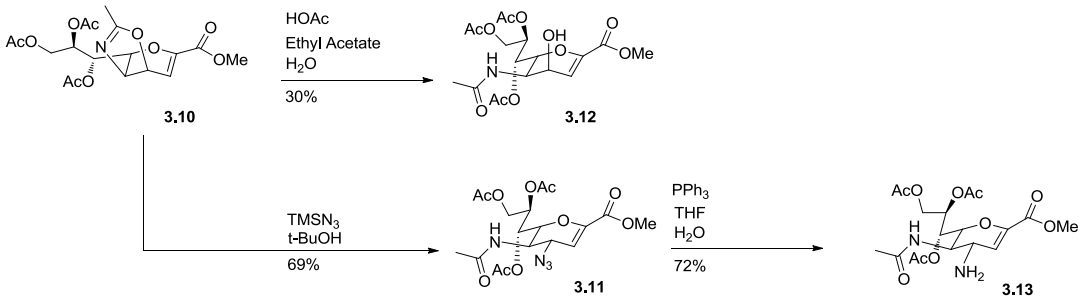


**Scheme 3.5. Reaction of 3.10 to form C4-azido derivatives of DANA.** After generation of azide **3.11** from **3.10**, the *C*4 position is easily reduced to an amine **3.13**.

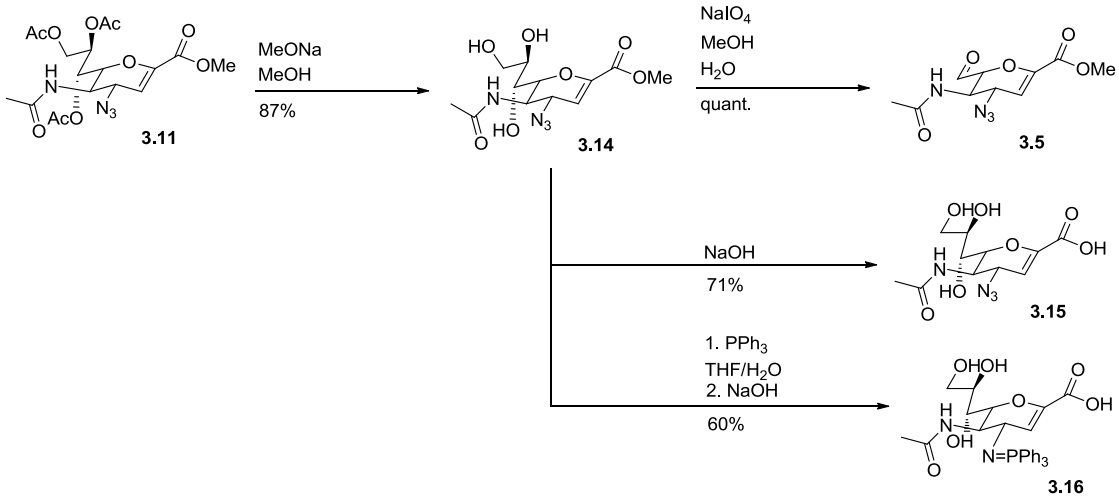


**Scheme 3.6. Synthesis of intermediate 3.5.** Azide **3.14** was generated by nucleophilic substitution. Oxidative cleavage gave **3.5** quntitaviely. The azide group at the *C*4 position could then be reduced to an imino phosphorane group **3.16**.

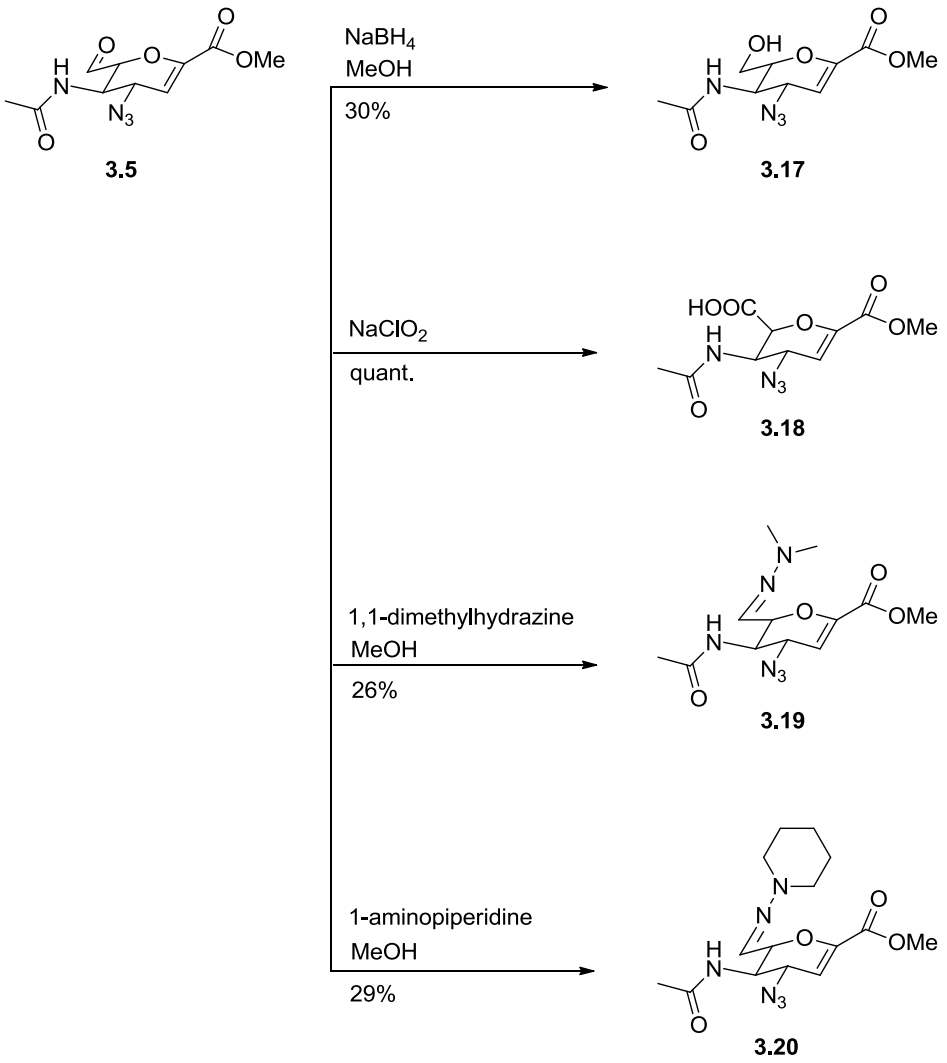


**Scheme 3.7. Reactions of aldehyde 3.5 to form hydrazone derivatives.** The aldehyde could be converted into either alcohol **3.17** or acid **3.18**. Coupling of **3.5** with hydrazines provided hydrazone derivatives **3.19** and **3.20**.

The key intermediate aldehyde **3.5** was prepared from **3.14** using sodium periodate without further purification (Scheme **3.6**) (Smith, P.W., Sollis, S.L., et al. 1996). The *C*7 aldehyde could also be reduced to an alcohol, **3.17**, or oxidized to the corresponding acid, **3.18**. Acid **3.18** can be further elaborated with other

functional groups through amide bond formation (Scheme **3.7**) (Smith, P.W., Sollis, S.L., et al. 1998).

With the key intermediate aldehyde **3.5** in hand, we attempted to introduce the hydrazone side chain. Formation of the hydrazone linker, **3.19**, was by reaction of **3.5** with 1,1-dimethylhydrazine (Scheme **3.7**) (Kajihara, Y., Kamiyama, D., et al. 2004). Similarly, we generated the hydrazone derivatives **3.20, 3.21, 3.22, 3.23, 3.24**, and **3.25** by treatment of **3.5** with 1-aminopiperidine, phenyl hydrazine, 2, 4-hydrazino-7-nitro-benzofurazan hydrazine, 2, 4-dinitrophenylhydrazine, 3-hydroxybenzylhydrazine, and 3-benzyloxyphenylhydrazine respectively. Yields of the hydrazine condensation reaction were generally low, with compounds **3.19**, **3.20**, **3.21**, **3.22**, **3.23** giving 25-36% yields. The TLC appeared several spots of **3.24** and **3.25** which were separated by column chromatography, but unfortunately, none of them were clean as showed by NMR spectra. Compounds **3.24** and **3.25** were observed by HRMS (Table **3.1**).

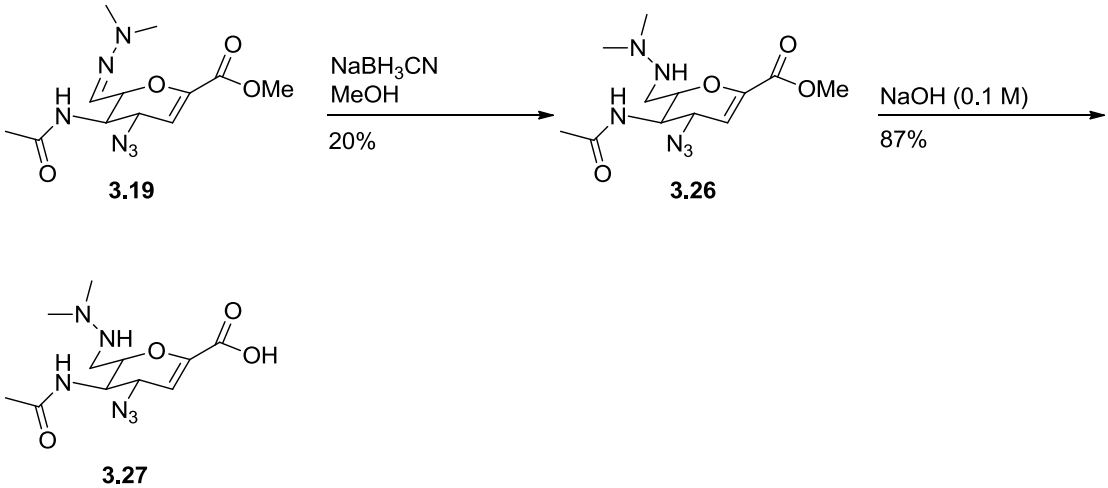


**Scheme 3.8. Generation of acid 3.27.** The aldehyde **3.5** was treated with 1,1-dimethylhydrazine, followed by the reduction of imino group by $NaBH_3CN$.

After hydrazone formation between the aldehyde and the 1,1-dimethylhydrazine, the hydrazone group was reduced by $NaBH_3CN$ to give hydrazine **3.26**. Hydrolysis of the ester of **3.26** was performed under basic conditions giving the target acid **3.27** (Scheme **3.8**). Treatment of hydrazone **3.20** with $NaBH_3CN$ generated hydrazine **3.28** by the previous method. Surprisingly, the C-N bond was cleaved by hydrolysis of **3.28** using sodium hydroxide to provide carboxylic acid **3.29**. Alternatively, **3.29** could be used to couple with 1-aminopiperidine to afford the target compound **3.30** (Scheme **3.9**).

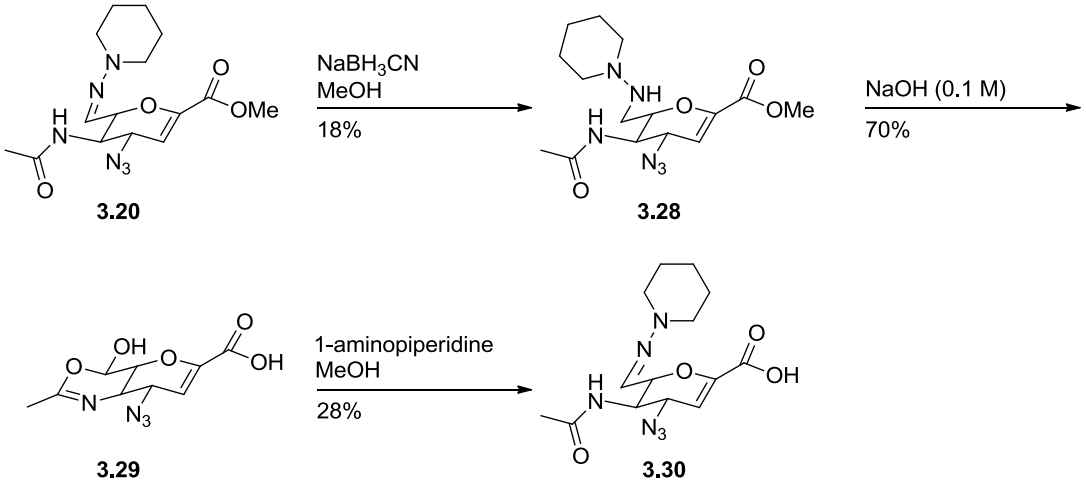


**Scheme 3.9. Synthetic scheme for generation of carboxylic acid 3.30.** The aldehyde **3.5** was treated with 1-aminopiperidine, followed by the reduction of imino group by $NaBH_3CN$. Although the C-N bond was cleaved under basic condition, repeat of the hydrazine coupling gave the desired product **3.30**.

To avoid C-N bond cleavage under hydrolysis conditions, we decided to hydrolyze the methyl ester first, and then perform the hydrazine coupling reaction at the end of the route. Compounds **3.31**, **3.32**, and **3.33** were produced by the

coupling of **3.29** with 2, 4-hydrazino-7-nitro-benzofurazan hydrazine, 4-phenoxybenzohydrazide, and 2-cyanoethylhydrazine, respectively. Compounds **3.32** and **3.33** could only be confirmed by HRMS (Table **3.1**) due to the low yields observed. As before, we attempted to purify those products by column chromatography; however, all the fractions collected showed unclean NMR spectra. It may be due to the instability of the products in acidic conditions. And the use of HPLC also failed to give pure compounds.

We also attempted to couple **3.29** with phenyl hydrazine. Unfortunately, the formation of the product without the $N_3$ group ($C_{15}H_{15}N_3O_4$) was observed by HSMS. Further analysis will need to be performed after isolation of quantities of product that will allow for more extensive NMR analysis by 13C.

### *3.3 Conclusion and future directions*

In this chapter, we describe a synthetic route to a new generation of DANA derivatives with modification of the *C*7 glycerol side-chain. Oxidative cleavage of the side-chain successfully provided the key intermediate, aldehyde **3.5**. Reductive amination of **3.5** with various amines did not give reliable yields of the desired products. The reason may be that the aldehyde **3.5** was not a good electrophile and the steric hindrance as well. However, the more nucleophilic hydrazines gave improved yields of the corresponding hydrazones after coupling. The hydrazine derivatives are likely more reactive due the alpha effect (Edwards, J.O. and Pearson, R.G. 1962).

Although the hydrazone coupling was successful for modification of the glycerol side-chain, the reductive amination was slow and the products of the

reaction were more difficult to isolate. Additionally, we found that the basic conditions used in the cleavage of the *C*1 methylester can cleave the *C*7-N bond of some hydrazone products, forming **3.29**. This observation led us to modify the route to deprotect the methyl group first, followed by the hydrazine coupling. However, this modification raised a new potential problem in the route. Under the conditions used for the hydrazone coupling, we observed a lose of azide group in the product. More analytical method, like X-ray crystallography may help identify the structure. One alternative way to solve this problem is using another protecting group, like 2-(*p*-Methoxyphenyl)ethyl ester, for carboxylic acid (Yoo, S.-E., Hye, R.K., et al. 1990).

One of the greatest obstacles to generating the final hydrazone products in significant quantities is the purification of the compounds. The high nitrogen content renders these compounds highly polar, making flash chromatography difficult. Further optimization of purifucation using HPLC will likely facilitate using this strategy for the synthesis of a final panel of inhibitors. The *C*7 side-chain modified derivatives isolated here (**3.27**, **3.30**) will be useful in future in inhibitor studies of NEU3 and other human neuraminidase enzymes.

Smith and colleagues (Smith, P.W., Sollis, S.L., et al. 1998) have reported replacement of the glycerol side-chain of DANA with carboxamide derivatives via carboxylic acid **3.18**, and we have developed here a feasible strategy to replace it instead with hydrazone or hydrazine derivatives via aldehyde **3.5**. Future studies may explore the modification of alcohol **3.17**, or alternative hydrazone or hydrazine side-chains.

### *3.4 Experimental*

#### *3.4.1 General*

All reagents including hydrazines and amines used were purchased from commercial sources such as Sigma-Aldrich (Oakville, Ont) and Acros Organics. They were used without further purification unless noted. All reactions were carried out under a positive pressure of Argon at room temperature unless indicated. The reactions were monitored by analytical TLC on silica get 60-$F_{254}$ (0.25mm, Silicycle, Quebec, Canada) and the spots were visualized under UV light (254 nm) or stained by charring with Ceric Ammonium Molybdate (CAM). Organic solvents were evaporated under reduced pressure and the products were purified by column chromatography on silica gel (230-400 mesh, Silicycle, Quebec, Canada) or HPLC (Waters). $^{1}$H NMR spectra were performed on Varian 300, 400, or 500 MHz instruments at room temperature as noted. $^{13}$C NMR spectra were recorded at 100 or 125 MHz. Electrospray mass spectra were recorded on Agilent Technologies 6220 TOF.

#### *3.4.2 Synthetic methods*

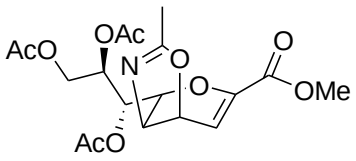


**2-Methyl-(methyl-7,8,9-tri-O-acetyl-2,6-anhydro-3,5-dideoxy-O-glycero-D-talo-non-2-enonate)-[4,5-d]-2-oxazoline** (**3.10**)

To a solution of **2.1** (100 mg, 0.195 mmol) (Chandler, M., Bamford, M.J., et al. 1995) in ethyl acetate at 30 °C was added TMSOTf (0.1 mL, 0.55 mol) dropwise

with stirring under Argon. After the addition was completed the temperature was raised to 52 °C. After 4 h at this temperature the reaction mixture was allowed to cool and solid sodium hydrogen carbonate was added (pH > 7.5). After *ca.* 5 min the solution was filtered and the filtrate was then evaporated to leave an amber gum (72%). Purification was performed by column chromatography (EtOAc/hexanes). Alternative method(von Itzstein, M., Jin, B., et al. 1993): To a solution of Neu4Ac2en **2.2** (90 mg, 0.19 mmol) in $CH_2Cl_2$ (2 mL) were added MeOH (7 µL) and $BF_3$ ·$Et_2O$ (225 µL, 1.82 mmol). This mixture was stirred at room temperature under argon overnight. This mixture was then added solid sodium hydrogen carbonate. The solid was filtered, and evaporation of the solvent under reduced pressure. The residue was purified by flash chromatography with 8:1 EtOAc-hexane to afford **3.10** in a moderate yield (50%). $^1$H NMR (500 MHz, $CDCl_3$) δ 6.36 (d, *J* = 4.0 Hz, 1H), 5.61 (dd, *J* = 6.0, 2.5 Hz, 1H), 5.42 (td, *J* = 6.6, 3.0 Hz, 1H), 4.80 (dd, *J* = 9.0, 4.0 Hz, 1H), 4.57 (dd, *J* = 12.5, 2.5 Hz, 1H), 4.20 (dd, *J* = 12.5, 6.5 Hz, 1H), 3.95 – 3.91 (m, 1H), 3.79 (s, 3H), 3.41 (dd, *J* = 10.0, 2.5 Hz, 1H), 2.13 (s, 3H), 2.04 (s, 3H), 2.03 – 2.03 (s, 3H), 1.98 (d, *J* = 0.9 Hz, 3H). $^{13}$C NMR (126 MHz, $CDCl_3$) δ 170.6, 169.8, 169.6, 167.1, 161.9, 147.2, 107.6, 76.8, 72.2, 70.3, 68.9, 62.1, 62.0, 52.5, 20.8, 20.8, 20.6, 14.1. HRMS (ESI) calculated for $C_{18}H_{24}NO_{10}$ $[M+H]^+$, 414.1395, found 414.1393, calculated for $C_{18}H_{23}NNaO_{10}$ $[M+Na]^+$, 436.1214, found 436.1214.

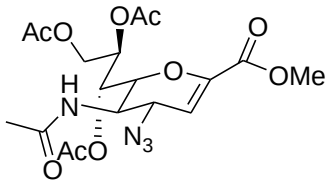

**5-Acetamido-7,8,9-tri-O-acetyl-2,6-anhydro-4-azido-3,4,5-trideoxy-D-glycero-D-galacto-non-2-enonic acid methyl ester** (**3.11**)

Oxazoline **3.11** (189 mg, 0.458 mmol) (Chandler, M., Bamford, M.J., et al. 1995)was dissolved in tert-butyl alcohol (4mL) and azidotrimethylsilane (300 µL, 2.3mmol) was added dropwise with stirring under argon, and the solution was heated at 80°C. After overnight the reaction mixture was allowed to cool and solid sodium hydrogen carbonate was added. After *ca.* 5 min the solution was filtered and the filtrate was evaporated. Then ethyl acetate and water were added, and then the organic extracts were washed by brine, following by drying over $MgSO_4$, and concentrated *in vacuo*. Purification was performed by column chromatography (EtOAc/hexanes). The product was obtained in as a yellow oil (69%).$^{1}$H NMR (400 MHz, $CDCl_3$) δ 6.12 (d, *J* = 9.2 Hz, 1H), 6.00 (d, *J* = 2.8 Hz, 1H), 5.45 (dd, *J* = 4.8, 2.4 Hz, 1H), 5.31 (ddd, *J* = 8.0, 5.2, 2.8 Hz, 1H), 4.63 (dd, *J* = 12.4, 2.8 Hz, 1H), 4.48 (dd, *J* = 10.0, 2.4 Hz, 1H), 4.42 (dd, *J* = 8.8, 2.8 Hz, 1H), 4.18 (dd, *J* = 12.4, 6.8 Hz, 1H), 3.90 (q, *J* = 8.8 Hz, 1H), 3.80 (s, 3H), 2.12 (s, 3H), 2.05 (s, 3H), 2.04 (s, 3H), 1.98 (s, 3H). $^{13}$C NMR (101 MHz, $CDCl_3$) δ 170.3, 170.3, 170.0, 169.8, 161.1, 144.7, 107.2, 75.47, 70.5, 67.3, 61.6, 57.4, 52.2, 48.0, 22.9, 20.5, 20.4 HRMS (ESI) calculated for $C_{18}H_{24}N_4NaO_{10}$ $[M+Na]^+$, 479.1385, found 479.1388.

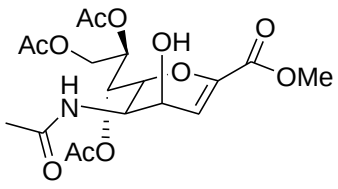

**Methyl 5-Acetamido-7,8,9-tri-*O*-acetyl-2,3-didehydro-2,3,5-tri-deoxy-D-glycero-D-galacto-2-nonulopyranosidonate** (**3.12**)

To a stirred solution of oxazoline **3.10** (146m g, 0.35 mmol) in ethyl acetate (7 mL) under argon was added acetic acid (0.2 mL) and water (0.2 mL). The resulting mixture was stirred for two days at room temperature before being diluted with ethyl acetate. The solution was washed with 5% $NaHCO_3$ solution and water, then concentrated *in vacuo*. Purification was performed by column chromatography (EtOAc/hexanes) (30%). (Laurence M. von Izstein, N.F.W.-Y.W., Mount Waverley; Tho V. Phan, Carnegie; Basil Danylec, Box Hill; Betty Jin, Mount Waverley, all of Australia. 1994) $^1$H NMR (500 MHz, $CDCl_3$) δ 6.15 (d, *J* = 5.5 Hz, 1H), 6.02 (d, *J* = 9.5 Hz, 1H), 5.45 (dd, *J* = 4.5, 2.5 Hz, 1H), 5.31 (ddd, *J* = 7.5, 4.0, 2.5 Hz, 1H), 4.77 (dd, *J* = 12.0, 2.5 Hz, 1H), 4.36 (dd, *J* = 11.0, 4.0 Hz, 1H), 4.25 – 4.22 (m, 2H), 4.12 (dd, *J* = 12.0, 7.5 Hz, 1H), 3.81 (s, 3H), 2.11 (s, 3H), 2.07 (s, 3H), 2.06 (s, 3H), 1.96 (s, 3H). $^{13}$C NMR (126 MHz, $CDCl_3$) δ 170.7, 170.6, 170.2, 170.2, 162.1, 145.5, 109.1, 73.2, 71.9, 67.9, 62.3, 61.6, 52.6, 46.3, 23.3, 21.0, 20.8, 20.8. MS (ESI) calculated for $C_{18}H_{26}NO_{11}$ $[M+H]^+$, 432.2, found 432.2, calculated for $C_{18}H_{25}NnaO_{11}$ $[M+Na]^+$, 454.1, found 454.1.

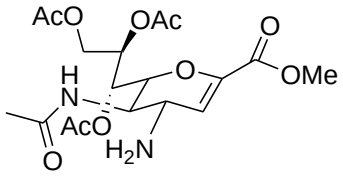


**5-Acetylamino-4-amino-6-(1,2,3-triacetoxy-propyl)-5,6-dihydro-4*H*-pyran-2-carboxylic acid methyl ester** (**3.13**)

Azide **3.11** (22 mg, 0.048 mmol) and triphenylphosphine (12.6 mg, 0.048 mmol) were dissolved in THF (2 mL) and the mixture was stirred overnight under argon

at room temperature. After evaporation of the solvent, the resulting residue was dissolved in methanol/water (1:1, 2mL) with stirring for 2 days. The solvent was removed *in vacuo*. Purification was performed by column chromatography (Iatrobeads) (72%). $^{1}$H NMR (500 MHz, $D_2O$) δ 6.14 (d, *J* = 2.6 Hz, 1H), 5.55 (d, *J* = 7.0 Hz, 1H), 5.48 – 5.45 (m, 1H), 4.60 (dd, *J* = 12.5, 2.5 Hz, 1H), 4.41 (app d, *J* = 10.5 Hz, 1H), 4.33 (dd, *J* = 12.5, 5.0 Hz, 1H), 3.96 (app t, *J* = 9.5 Hz, 1H), 3.89 (s, 3H), 3.69 – 3.61 (m, 1H), 2.22 (s, 3H), 2.18 (s, 3H), 2.17 (s, 3H), 2.07 (s, 3H). $^{13}$C NMR (126 MHz, $D_2O$) δ 175.3, 174.8, 173.7, 173.7, 164.8, 143.8, 116.0, 77.1, 71.0, 68.6, 63.3, 53.8, 51.1, 50.3, 23.1, 21.2, 21.2, 21.1. HRMS (ESI) calculated for $C_{18}H_{27}N_2O_{10}$ $[M+H]^+$, 431.1660, found

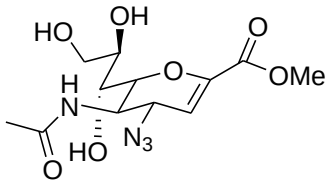


**5-Acetamido-2,6-anhydro-4-azido-3,4,5-trideoxy-D-glycero-D-galacto-non-2-enonic acid methyl ester** (**3.14**)

To a stirred solution of triacetate **3.11** (1.14 g, 2.499 mmol) in anhydrous methanol (24 mL) under argon was added sodium methoxide (1.4 mL, 1.4 mmol) and the resulting mixture was stirred for 0.5 h at 0 °C. Amberlite resin was then added to adjust the pH to 7 and indicated by universal indicator paper and the mixture was filtered. The resin was further washed with methanol and the combined filtrates were concentrated *in vacuo* (87%). $^{1}$H NMR (500 MHz, $CD_3OD$) δ 5.91 (d, *J* = 2.5 Hz, 1H), 4.34 (dd, *J* = 9.5, 2.5 Hz, 1H), 4.26 (dd, *J*=11.0, 1.0 Hz, 1H) 4.12 (dd, *J* = 11.0, 9.5 Hz, 1H), 3.86 (ddd, *J* = 9.5, 5.5, 3.0 Hz, 1H), 3.80 (dd, *J* = 11.5, 3.0 Hz, 1H), 3.78 (s, 3H), 3.65 (dd, *J* = 11.5, 5.5 Hz,

1H), 3.59 (dd, *J*=9.5, 1.0 Hz, 1H), 2.01 (s, 3H). $^{13}$C NMR (126 MHz, $CD_3OD$) δ 174.5, 163.8, 146.9, 108.4, 78.1, 71.1, 69.7, 64.8, 59.8, 53.0, 49.9, 22.7. HRMS (ESI) calculated for $C_{12}H_{18}N_4NaO_7$ $[M+Na]^+$, 353.1068, found 353.1068.

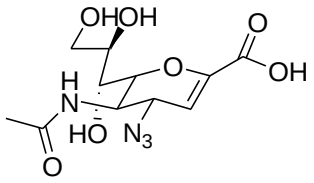

**5-acetamido-4-azido-5,6-dihydro-6-((1R,2R)-1,2,3-trihydroxypropyl)-4H-pyran-2-carboxylic acid (3.15)**

Compound **3.14** (10.5 mg, 0.032 mmol) was treated with 0.1 M NaOH (0.4 mL) for 0.5 h at room temperature. The mixture was neutralized with Amberlite IR-120($H^+$), followed by filtration and evaporation of the solvent to provide **3.15** (71%). $^1$H NMR (500 MHz, $D_2O$) δ 5.90 (d, *J* = 2.5 Hz, 1H), 4.43 – 4.38 (m, 2H), 4.29 (app t, *J*=9.5, 1H), 4.01 (ddd, *J* = 9.0, 6.0, 2.5 Hz, 1H), 3.95 (dd, *J* = 12.0, 2.5 Hz, 1H), 3.74 – 3.70 (m, 2H), 2.14 (s, 3H). $^{13}$C NMR (126 MHz, $D_2O$) δ 175.6, 168.8, 148.9, 106.0, 76.4, 70.8, 68.9, 64.0, 60.1, 48.7, 23.1. HRMS (ESI) calculated for $C_{11}H_{15}N_4O_7$ $[M-H]^-$, 315.0946, found 315.0944.

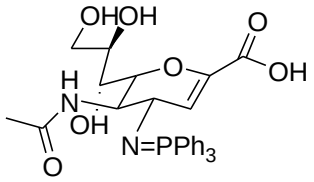

**5-Acetamido-2,3-didehydro-2,3,4,5-tetradeoxy-4 (triphenylphosphoranylidenamino)-D-glycero-D-galacto-2 nonulopyranosidonate** (**3.16**)

Compound **3.14** (13.9 mg, 0.042 mmol) and triphenylphosphine (11 mg, 0.042 mmol) were dissolved in tetrahydrofuran/water (1:1, 2 mL) and stirred at room

temperature for 2 days. The solvent was removed *in vacuo*. Then the residue was treated with 0.1 M NaOH (0.3 mL) for 0.5 h at room temperature. The reaction was neutralized with Amberlite IR-120($H^+$), followed by filtration and evaporation of the solvent to provide **3.16**. Purification was performed by column chromatography (Iatrobeads) (60%). $^1$H NMR (500 MHz, $D_2O$) δ 7.90 (app t, *J* = 7.4 Hz, 3H), 7.89 – 7.85 (m, 6H), 7.82 – 7.79 (m, 6H), 5.79 (d, *J* = 2.0 Hz, 1H), 4.31 (app t, *J* = 10.0 Hz, 1H), 4.22 – 4.16 (m, 1H), 4.08 (app t, *J*= 10.0 Hz, 1H), 3.98 – 3.91 (m, 2H), 3.68 (dd, *J* = 12.0, 6.0 Hz, 1H), 3.57 (app d, *J* = 10.0 Hz, 1H), 1.76 (s, 3H). $^{13}$C NMR (126 MHz, $D_2O$) δ 174.7, 170.1, 150.0, 136.3, 136.3, 134.9, 134.8, 130.9, 130.8, 122.0, 121.2, 107.3, 76.5, 70.6, 69.1, 64.0, 52.6, 49.9, 23.1. MS (ESI) calculated for $C_{29}H_{32}N_2O_7P$ $[M+H]^+$, 551.2, found 551.2, calculated for $C_{29}H_{31}N_2NaO_7$ $[M+Na]^+$, 573.2, found 573.2.

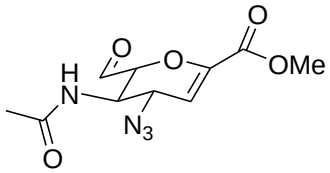


**Methyl 5-acetamido-4-azido-6-formyl-5, 6-dihydro-4H-pyran-2-carboxylate (3.5)**

To a solution of **3.14** (119 mg, 0.36 mmol) (Smith, P.W., Sollis, S.L., et al. 1998) in methanol/water (3:1, v/v, 4 mL) was added sodium periodate (156 mg, 0.729 mmol), and the reaction mixture was stirred at room temperature for 30 min. The solid was removed by filtration, and the filtrate was evaporated *in vacuo* to give a white solid. The aldehyde intermediate was carried forward without further characterization. HRMS (ESI) calculated for $C_{10}H_{12}N_4NaO_5$ $[M+Na]^+$, 291.0700, found 291.0702.

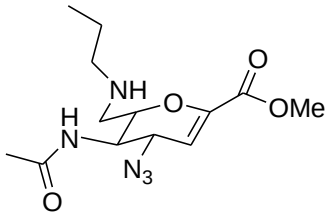


**Methyl 5-acetamido-4-azido-5,6-dihydro-6-((propylamino)methyl)-4H-pyran-2-carboxylate** (**3.9**)

To a solution of aldehyde **3.5** (54 mg, 0.20 mmol) in MeOH (3 mL) was added propylamine (82 µL, 1mmol) and HOAc (40 µL), and the mixture was stirred at room temperature overnight. To this solution was added $NaBH_3CN$ (25 mg, 0.4 mmol), and the mixture was stirred for 24 h at room temperature under argon. The solvent was concentrated *in vacuo*. Purification was performed by column chromatography. HRMS (ESI) calculated for $C_{13}H_{22}N_5O_4$ $[M+H]^+$, 312.1666, found 312.1671.

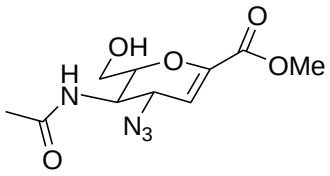


**Methyl 5-acetamido-4-azido-5, 6-dihydro-6-(hydroxymethyl)-4H-pyran-2-carboxylate** (**3.17**)

To a stirred solution of aldehyde **3.5** (81 mg, 0.30 mmol) in anhydrous methanol (24 mL) under argon was added sodium borohydride (30 mg, 0.79 mmol). The resulting mixture was stirred for 2 h at room temperature before being neutralized by adding acetic acid dropwise. Purification was performed by column chromatography (2-propanol/ethyl acetate/water) (30%). $^1$H NMR (500 MHz, $CD_3OD$) δ 5.94 (d, *J* = 2.5 Hz, 1H), 4.31 (dd, *J* = 9.0, 2.5 Hz, 1H), 4.04 – 3.96 (m,

1H), 3.80 (s, 3H), 3.77 (dd, *J* = 12.5, 2.0 Hz, 1H), 3.70 (dd, J = 12.5, 4.5 Hz, 1H), 1.99 (s, 3H). $^{13}$C NMR (126 MHz, $CDCl_3$) δ 176.5, 166.4, 149.0, 111.0, 83.0, 64.4, 55.7, 52.0, 25.3. HRMS (ESI) calculated for $C_{10}H_{14}N_4NaO_5$ $[M+Na]^+$, 293.0856, found 291.0851.

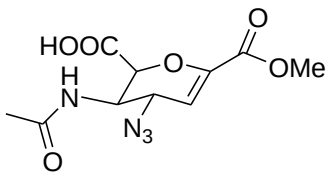


**6-(methoxycarbonyl)-3-acetamido-4-azido-3,4-dihydro-2H-pyran-2-carboxylic acid** (**3.18**)

To a rapidly stirred solution of **3.5** (53.6 mg, 0.2 mmol) in *tert*-butyl alcohol (3 mL) and cyclohexene (0.3 mL) was added sodium chlorite (133 mg, 1.46 mmol) and potassium dihydrogen orthophosphate (132 mg, 0.96 mmol) in water (2 mL). The resulting mixture was stirred for 3 h at room temperature. Then ethyl acetate and water were added, and the organic extracts were washed by brine, followed by drying over magnesium sulfate. The solvent was removed *in vacuo* to give the acid as white foam **3.18**. (quant.) $^1$H NMR (500 MHz, DMSO) δ 8.27 (d, *J* = 8.0 Hz, 1H), 6.02 (dd, *J* = 5.5, 1.5 Hz, 1H), 4.79 (dd, *J* = 3.0, 1.5 Hz, 1H), 4.40 – 4.36 (m, 1H), 4.12 (ddd, *J* = 5.5, 3.0, 1.5 Hz, 1H), 3.77 (s, 3H), 1.83 (s, 3H). $^{13}$C NMR (126 MHz, DMSO) δ 169.3, 168.1, 161.5, 144.4, 104.1, 73.6, 53.0, 52.3, 46.7, 22.3. HRMS (ESI) calculated for $C_{10}H_{11}N_4O_6$ $[M-H]^-$, 283.0684, found 283.0680.

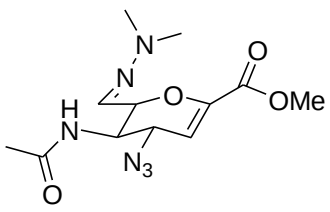

**(2S,3R,4S)-methyl 3-acetamido-4-azido-2-((2,2-dimethylhydrazono)methyl)-3,4-dihydro-2H-pyran-6-carboxylate** (**3.19**)

**General procedure for coupling reaction of 3.19, 3.20, 3.21, 3.22, 3.23, 3.24, and 3.25.**

To a solution of aldehyde **3.5** (54 mg, 0.20 mmol) in MeOH (3 mL) was added 1,1-dimethylhydrazine (100 μL, 1.32mmol) and HOAc (40 μL), and the mixture was stirred at room temperature overnight. The mixture was diluted with ethyl acetate and washed with brine. The organic layer was dried on $MgSO_4$, and concentrated *in vacuo*. Purification was performed by column chromatography (EtOAc/hexanes) (26%). (Kajihara, Y., Kamiyama, D., et al. 2004) $^1$H NMR (400 MHz, $CD_3OD$) δ 6.44 (d, *J* = 6.8 Hz, 1H), 5.95 (d, *J* = 2.8 Hz, 1H), 4.39 (dd, *J* = 10.0, 6.8 Hz, 1H), 4.28 (dd, *J* = 8.8, 2.8 Hz, 1H), 4.15 (dd, *J* = 8.8, 9.6 Hz, 1H), 3.79 (s, 3H), 2.80 (s, 6H), 1.92 (s, 3H). $^{13}$C NMR (101 MHz, $CD_3OD$) δ 173.0, 163.2, 146.1, 129.8, 108.2, 80.4, 58.6, 52.6, 50.8, 42.2, 22.4. HRMS (ESI) calculated for $C_{12}H_{18}N_6NaO_4$ $[M+Na]^+$, 333.1282, found 333.1285.

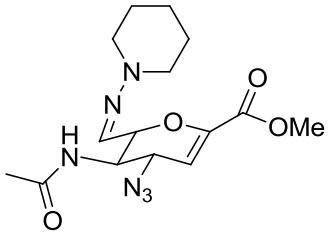


**methyl 5-acetamido-4-azido-5,6-dihydro-6-((piperidin-1-ylimino)methyl)-4*H*-pyran-2-carboxylate** (**3.20**)

Hydrazone **3.20** was generated by reaction of **3.5** with 1-aminopiperidine (5 equiv.), as described above (yield 29%). $^1$H NMR (498 MHz, $CD_3OD$) δ 6.74 (d, *J* = 6.5 Hz, 1H), 5.95 (d, *J* = 2.5 Hz, 1H), 4.39 (dd, *J* = 10.0, 6.5 Hz, 1H), 4.28

(dd, *J* = 9.0, 2.5 Hz, 1H), 4.15 (dd, *J* = 10.0, 9.0 Hz, 1H), 3.78 (s, 3H), 2.99 – 2.95 (m, 4H), 1.92 (s, 3H), 1.69 – 1.63 (m, 4H), 1.53 – 1.49 (m, 2H). $^{13}$C NMR (125 MHz, $CD_3OD$) δ 171.7, 161.8, 144.7, 131.1, 106.9, 79.1, 57.2, 51.3, 51.1, 49.3, 24.2, 23.3, 21.1. MS (ESI) calculated for $C_{15}H_{23}N_6O_4$ $[M+H]^+$, 351.2, found 351.2, calculated for $C_{15}H_{22}N_6NaO_4$ $[M+Na]^+$, 373.2, found 373.2.

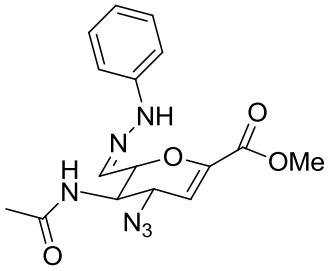


**(3R,4S)-methyl 3-acetamido-4-azido-2-((Z)-(2-phenylhydrazono)methyl)-3,4-dihydro-2H-pyran-6-carboxylate** (**3.21**)

Methyl ester protected hydrazone **3.21** was generated by reaction of **3.5** with phenyl hydrazine (5 equiv.), as described above (yield 36%). $^1$H NMR (400 MHz, $CDCl_3$) δ 7.87 (s, 1H), 7.21 (dd, *J* = 10.5, 9.5 Hz, 2H), 7.02 (dd, *J* = 8.0, 0.5 Hz, 1H), 6.94 (dd, *J* = 10.5, 1.0 Hz, 2H), 6.87 – 6.83 (m, 1H), 6.04 (d, *J* = 3.5 Hz, 1H), 6.02 (d, *J* = 11.0 Hz, 1H), 4.68 (dd, *J* = 8.5, 11.0 Hz, 1H), 4.35 – 4.28 (m, 1H), 4.22 (dd, *J* = 9.5, 4.0 Hz, 1H), 3.83 (s, 3H), 1.94 (s, 3H). $^{13}$C NMR (101 MHz, $CDCl_3$) δ 171.1, 162.4, 145.5, 144.5, 132.8, 129.7, 121.0, 113.2, 107.7, 79.0, 57.4, 53.3, 50.0, 23.7. HRMS (ESI) calculated for $C_{16}H_{18}N_6NaO_4$ $[M+Na]^+$, 381.1281, found 381.1294.

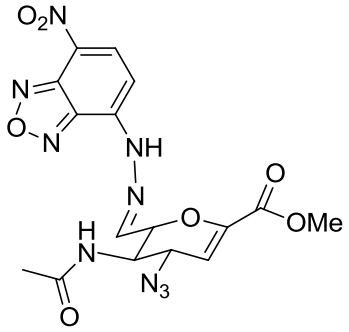

**(3R,4S)-methyl 3-acetamido-4-azido-2-((E)-(2-(7-nitrobenzo[c][1,2,5]oxadiazol-4-yl)hydrazono)methyl)-3,4-dihydro-2H-pyran-6-carboxylate** (**3.22**)

Compound **3.22** was generated by reaction of **3.5** with 2, 4-hydrazino-7-nitro-benzofurazan hydrazine (5 equiv.), as described above (yield 25 %). $^{1}$H NMR (500 MHz, $CD_3OD$) δ 8.57 (d, *J* = 8.5 Hz, 1H), 7.70 (d, *J* = 6.5 Hz, 1H), 7.06 (d, *J* = 8.5 Hz, 1H), 6.07 (d, *J* = 3.0 Hz, 1H), 4.72 (dd, *J* = 8.5, 6.0 Hz, 1H), 4.35 (dd, *J* = 8.0, 3.5 Hz, 1H), 4.28 (app t, *J*=9.0 Hz, 1H), 3.83 (s, 3H), 1.92 (s, 3H). $^{13}$C NMR (126 MHz, $CD_3OD$) δ 173.6, 163.4, 146.8, 146.0, 145.4, 144.4, 141.8, 137.1, 126.8, 108.7, 103.0, 79.1, 58.0, 53.2, 50.6, 22.7. HRMS (ESI) calculated for $C_{16}H_{15}N_9NaO_7$ $[M+Na]^+$, 468.0987, found 468.0988.

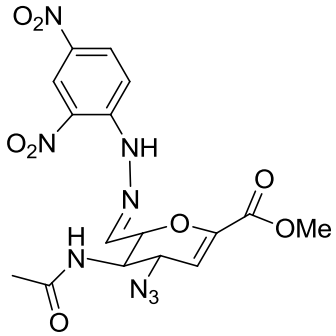

**(3R,4S)-methyl 3-acetamido-4-azido-2-((E)-(2-(2,4-dinitrophenyl)hydrazono)methyl)-3,4-dihydro-2H-pyran-6-carboxylate** (**3.23**)

Compound **3.23** was generated by reaction of **3.5** with 2,4-dinitrophenylhydrazine (5 equiv.), as described above (yield 22%). $^1$H NMR (400 MHz, $CDCl_3$) δ 9.44 (s, 1H), 9.11 (d, *J* = 2.8 Hz, 1H), 8.34 – 8.31 (m, 1H), 7.88 (d, *J* = 9.2 Hz, 1H), 7.55 (d, *J* = 5.6 Hz, 1H), 6.16 (d, *J* = 4.0 Hz, 1H), 5.93 – 5.91 (m, 1H), 4.97 (app t, *J* = 6.0 Hz, 1H), 4.44 – 4.36 (m, 1H), 4.27 (app t, *J*=4.8 Hz 1H), 3.88 (s, 3H), 2.04 (s, 3H). HRMS (ESI) calculated for $C_{16}H_{15}N_8O_8$ $[M-H]^-$, 447.1018, found 447.1035, calculated for $C_{16}H_{16}ClN_8O_8$ $[M+Cl]^-$, 484.0785, found 483.0804, calculated for $C_{18}H_{16}F_3N_8O_{10}$ $[M+CF_3COO]^-$, 561.0947, found 561.0968,

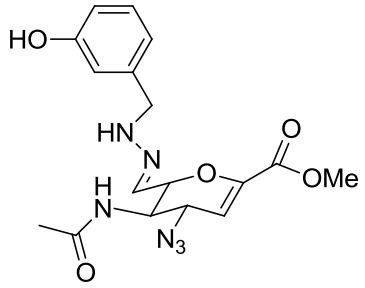


**(3R,4S)-methyl 3-acetamido-4-azido-2-((E)-(2-(3-hydroxybenzyl)hydrazono)methyl)-3,4-dihydro-2H-pyran-6-carboxylate** (**3.24**)

Compound **3.24** was generated by reaction of **3.5** with 3-Hydroxybenzylhydrazine (5 equiv.), as described above. HRMS (ESI) calculated for $C_{17}H_{20}N_6NaO_5$ $[M+Na]^+$, 411.1387, found 411.1396.

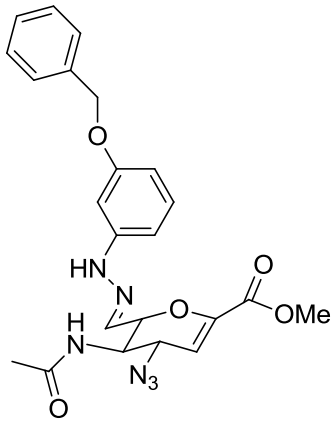

**(3R,4S)-methyl 3-acetamido-4-azido-2-((E)-(2-(3-(benzyloxy)phenyl)hydrazono)methyl)-3,4-dihydro-2H-pyran-6-carboxylate** (**3.25**)

Compound **3.25** was generated by reaction of **3.5** with 3-Benzyloxyphenylhydrazine (5 equiv.), as described above. HRMS (ESI) calculated for $C_{23}H_{25}N_6O_5$ $[M+H]^+$, 465.1881, found 465.1890, calculated for $C_{23}H_{24}N_6NaO_5$ $[M+Na]^+$, 487.1700, found 487.1699.

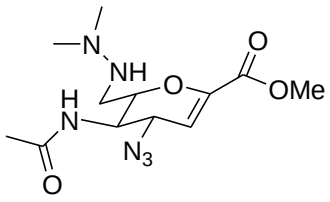

**(2R,3R,4S)-methyl 3-acetamido-4-azido-2-((2,2-dimethylhydrazinyl)methyl)-3,4-dihydro-2H-pyran-6-carboxylate** (**3.26**)

To a solution **3.19** (6 mg, 0.019 mmol) in MeOH (2 mL) was added $NaBH_3CN$ (10 mg, 0.161 mmol), and the mixture was stirred for 18 h at room temperature under argon. The solvent was concentrated *in vacuo*. Purification was first performed by column followed by purification by HPLC (20%). $^1$H NMR (500 MHz, $CD_3OD$) δ 5.98 (d, *J* = 3.0 Hz, 1H), 4.30 (dd, *J* = 9.0, 2.5 Hz, 1H), 4.18 –

4.15 (m, 1H), 4.04 – 4.00 (m, 1H), 3.82 (s, 3H), 3.34 – 3.31 (m, 1H), 3.20 (dd, *J* = 12.0, 6.5 Hz, 1H), 2.89 (d, *J* = 8.5 Hz, 6H), 2.03 (s, 3H). $^{13}$C NMR (126 MHz, $CD_3OD$) δ 172.1, 162.1, 144.1, 107.4, 76.4, 57.3, 51.5, 50.8, 50.0, 48.7, 47.8, 21.1. HRMS (ESI) calculated for $C_{12}H_{21}N_6O_4$ $[M+H]^+$, 313.1619, found 313.1622, calculated for $C_{12}H_{20}N_6NaO_4$ $[M+Na]^+$, 335.1438, found 335.1441.

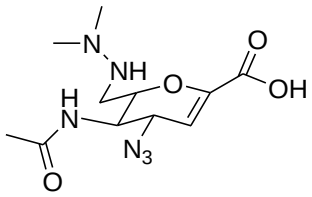


**(3R,4S)-3-acetamido-4-azido-2-((2,2-dimethylhydrazinyl)methyl)-3,4-dihydro-2H-pyran-6-carboxylic acid** (**3.27**)

Hydrazine **3.26** (1.2 mg, 0.004 mmol) was dissolved in methanol (0.5 mL). To this mixture was added 0.1 M NaOH (0.1 mL) and the reaction was stirred for 0.5 h at room temperature. Amberlite IR-120($H^+$) was then added to neutralize the reaction mixture (pH 7.0). The solution was filtered and concentrated *in vacuo* (87%). $^1$H NMR (500 MHz, $CD_3OD$) δ 5.98 (d, *J* = 2.5 Hz, 1H), 4.30 (dd, *J* = 9.0, 2.5 Hz, 1H), 4.15 (ddd, *J* = 10.0, 7.0, 2.5 Hz, 1H), 4.04 – 4.00 (m, 1H), 3.33 – 3.31 (m, 1H), 3.19 (dd, *J* = 12.0, 7.0 Hz, 1H), 2.90 (s, 3H), 2.88 (s, 3H), 2.03 (s, 3H). $^{13}$C NMR (126 MHz, $CD_3OD$) δ 173.9, 165.1, 146.4, 108.9, 78.1, 59.2, 52.7, 51.6, 50.5, 49.5, 22.8. HRMS (ESI) calculated for $C_{11}H_{17}N_6O_4$ $[M-H]^-$, 297.1317, found 297.1322.

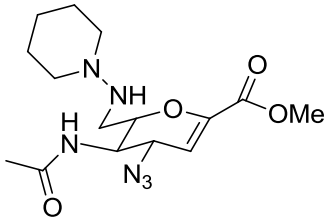

**methyl 5-acetamido-4-azido-5,6-dihydro-6-((piperidin-1-ylamino)methyl)-4H-pyran-2-carboxylate** (**3.28**)

To a solution **3.20** (12 mg, 0.034 mmol) in MeOH (2 mL) was added $NaBH_3CN$ (19 mg, 0.301 mmol), and the mixture was stirred for 2 days at room temperature under argon. The solvent was concentrated *in vacuo*. Purification was first performed by column chromatography but the NMR was not clean, then the material was purified by HPLC (18%). $^1$H NMR (400 MHz, $CD_3OD$) δ 5.96 (d, *J* = 2.8 Hz, 1H), 4.25 (dd, *J* = 8.4, 2.8 Hz, 1H), 4.14 (ddd, *J* = 10.0, 7.2, 3.2 Hz, 1H), 3.98 (dd, *J* = 10.0, 8.8 Hz, 1H), 3.80 (s, 3H), 3.12 – 3.02 (m, 2H), 2.74 – 2.61 (m, 4H), 2.00 (s, 3H), 1.66 – 1.59 (m, 4H), 1.43 – 1.40 (m, 2H). $^{13}$C NMR (101 MHz, $CD_3OD$) δ 173.6, 163.3, 145.4, 109.0, 97.2, 77.9, 58.6, 56.7, 52.9, 49.9, 47.1, 24.6, 22.8, 22.6. HRMS (ESI) calculated for $C_{15}H_{25}N_6O_4$ $[M+H]^+$, 353.1932, found 353.1932, calculated for $C_{15}H_{24}N_6NaO_4$ $[M+Na]^+$, 375.1751, found 375.1751.

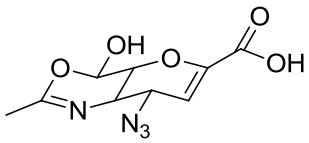


**(4R,8S,8aR)-8-azido-4-hydroxy-2-methyl-4,4a,8,8a-tetrahydropyrano[3,2-d][1,3]oxazine-6-carboxylic acid (3.29)**

Compound **3.5** (73 mg, 0.272 mmol) was treated with 0.1 M NaOH (1 mL) for 0.5 h at room temperature. The mixture solution was neutralized with Amberlite IR-120($H^+$), followed by filtration and evaporation of the solvent to provide **3.29** (65%). $^1$H NMR (500 MHz, $D_2O$) δ 6.07 (d, *J* = 3.0 Hz, 1H), 5.26 (d, *J* = 2.5 Hz, 1H), 4.40 (dd, *J* = 8.5, 3.0 Hz, 1H), 4.25 (app t, *J* = 9.5 Hz, 1H), 4.18 (dd, *J* = 9.5,

2.5 Hz, 1H), 2.12 (s, 3H). $^{13}$C NMR (126 MHz, $D_2O$) δ 175.2, 167.3, 146.9, 107.5, 88.0, 79.4, 58.9, 48.8, 23.0. HRMS (ESI) calculated for $C_9H_9N_4O_5$ $[M-H]^-$, 253.0578, found 253.0578.

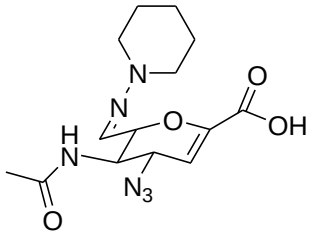


**5-acetamido-4-azido-5,6-dihydro-6-((piperidin-1-ylimino)methyl)-4*H*-pyran-2-carboxylic acid (3.30)**

**General procedure for coupling reaction of 3.30, 3.31**, **3.32**, and **3.33**.

To a solution of aldehyde **3.29** (1.6 mg, 0.0045 mmol) in MeOH (1 mL) was added 1-aminopiperidine (5 μL, 0.045 mmol) and HOAc (2 μL), and the mixture was stirred at room temperature overnight. Purification was performed by column chromatography (Iatrobeads) (MeOH/EtOAc) (28%). $^1$H NMR (500 MHz, $CD_3OD$) δ 6.80 (d, *J* = 6.5 Hz, 1H), 5.80 (d, *J* = 3.0 Hz, 1H), 4.36 (dd, *J* = 9.5, 7.0 Hz, 1H), 4.20 (dd, *J* = 8.5, 2.5 Hz, 1H), 4.14 (app t, *J*=9.0 Hz, 1H), 3.02 – 2.97 (m, 4H), 1.92 (s, 3H), 1.69 – 1.64 (m, 4H), 1.53 – 1.49 (m, 2H). $^{13}$C NMR (126 MHz, $CD_3OD$) δ 173.3, 163.3, 145.1, 134.2, 108.4, 80.4, 59.3, 52.9, 51.2, 25.9, 25.1, 22.8. HRMS (ESI) calculated for $C_{14}H_{19}N_6O_4$ $[M-H]^-$, 335.1473, found 335.1477.

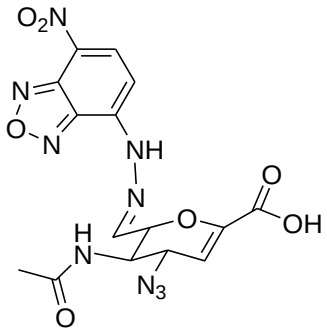

**(3R,4S)-3-acetamido-4-azido-2-((E)-(2-(7-nitrobenzo[c][1,2,5]oxadiazol-4-yl)hydrazono)methyl)-3,4-dihydro-2H-pyran-6-carboxylic acid** (**3.31**)

Compound **3.31** was generated by reaction of **3.29** with 2, 4-hydrazino-7-nitro-benzofurazan hydrazine (made by Dr. Jessie Key in our group) (5 equiv.), as described above (yield 36%). $^{1}$H NMR (700 MHz, $CD_3OD$) δ 8.59 (d, *J* = 8.4 Hz, 1H), 7.79 (d, *J* = 6.3 Hz, 1H), 7.12 (d, *J* = 8.4 Hz, 1H), 6.21 (d, *J* = 5.6 Hz, 1H), 4.78 – 4.77 (m, 1H), 4.50 – 4.46 (m, 1H), 4.11 – 4.09 (m, 1H), 1.94 (s, 3H). $^{13}$C NMR (176 MHz, $CD_3OD$) δ 173.6, 164.9, 148.5, 147.2, 145.4, 144.4, 141.8, 137.3, 126.8, 103.3, 96.8, 75.1, 56.3, 47.5, 22.3. HRMS (ESI) calculated for $C_{15}H_{12}N_9O_7$ $[M-H]^-$, 430.0865, found 430.0866.

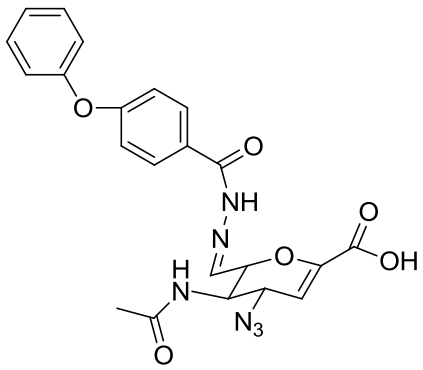

**(3R,4S)-3-acetamido-4-azido-2-((2-(4-phenoxybenzoyl)hydrazono)methyl)-3,4-dihydro-2H-pyran-6-carboxylic acid** (**3.32**)

Compound **3.32** was generated by reaction of **3.29** with 4-phenoxybenzohydrazide (5 equiv.), as described above. HRMS (ESI) calculated for $C_{22}H_{19}N_6O_6$ $[M-H]^-$, 463.1372, found 463.1367.

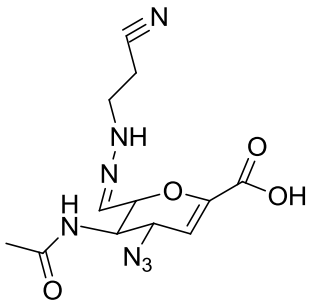


**(3R,4S)-3-acetamido-4-azido-2-((2-(2-cyanoethyl)hydrazono)methyl)-3,4-dihydro-2H-pyran-6-carboxylic acid** (**3.33)**

Cyanide **3.33** was generated by reaction of **3.29** with 2-Cyanoethylhydrazine (5 equiv.), as described above. HRMS (ESI) calculated for $C_{12}H_{14}N_7O_4$ $[M-H]^-$, 320.1113, found 320.1118.

**Table 3.1 Summary of Hydrazone derivatives.**

| *Compound* | *HRMS* | *NMR* | *Comments* |
|---|---|---|---|
| **3.21** 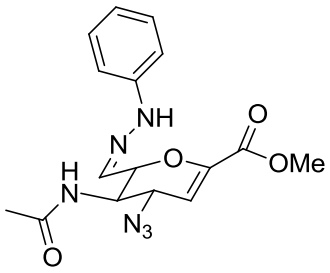 | Yes | Yes | **3.21** was generated by reaction of **3.5** with phenyl hydrazine in 36% yield. |
| **3.22** 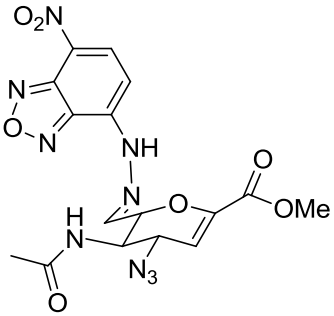 | Yes | Yes | **3.22** was generated by reaction of **3.5** with 2, 4-hydrazino-7-nitro-benzofurazan hydrazine in 25% yield. |
| **3.31** 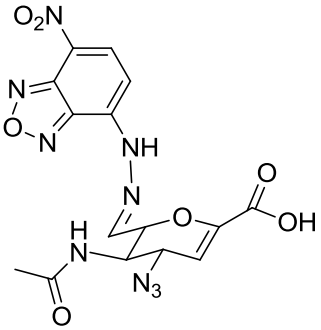 | Yes | Yes | **3.31** was generated by reaction of **3.29** with 2, 4-hydrazino-7-nitro-benzofurazan hydrazine in 36% yield. |

| Compound | HRMS | NMR | Comments |
|---|---|---|---|
| **3.23** 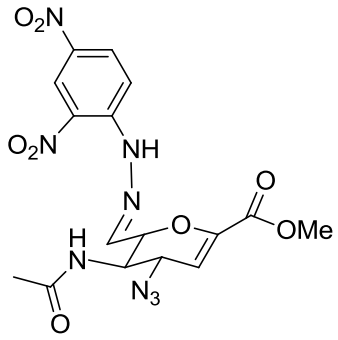 | Yes | Yes | **3.23** was generated by reaction of **3.5** with 2,4-dinitrophenyl hydrazine in 22% yield |
| **3.24** 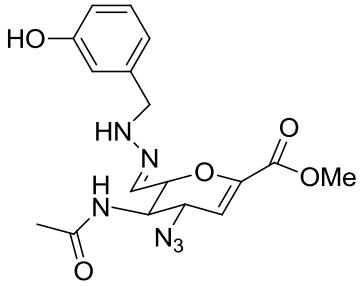 | Yes | No | Further purification required for characterization. |
| **3.25** 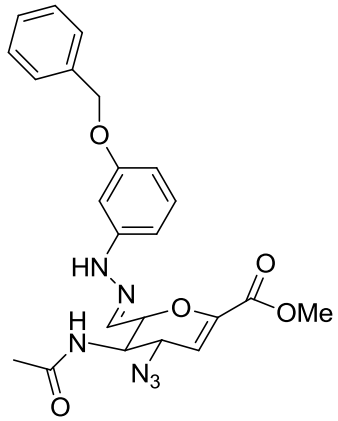 | Yes | No | Further purification required for characterization. |

| Compound | HRMS | NMR | Comments |
|---|---|---|---|
| **3.32** 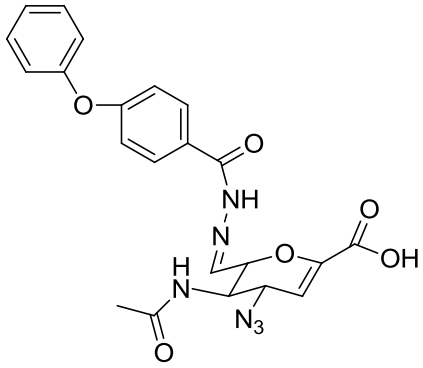 | Yes | No | Further purification required for characterization. |
| **3.33** 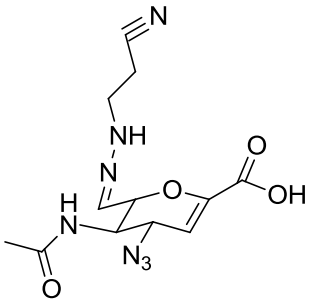 | Yes | No | Further purification required for characterization. |

### *3.5 Reference*


Achyuthan KE, Achyuthan AM. (2001). Comparative enzymology, biochemistry and pathophysiology of human exo-[alpha]-sialidases (neuraminidases). *Comparative Biochemistry and Physiology Part B: Biochemistry and Molecular Biology*, 129:29-64.

Ajit Varki RDC, Jeffrey D Esko, Hudson H Freeze, Pamela Stanley, Carolyn R Bertozzi, Gerald W Hart, and Marilynn E Etzler.2009.Essentials of Glycobiology, 2nd edition.

Albohy A, Li MD, Zheng RB, Zou C, Cairo CW. (2010). Insight into recognition and catalysis of the mammalian neuraminidase 3 (NEU3) through molecular modeling and site directed mutagenesis. *Glycobiology*, 20:1127-1138.

Albohy A, Mohan S, Pinto BM, Cairo CW. (2011). Inhibitor selectivity of a new class of oseltamivir analogs against viral neuraminidase over human neuraminidase enzymes. *Bioorg. Med. Chem.*, 19:2817-2822.

Anastasia L, Papini N, Colazzo F, Palazzolo G, Tringali C, Dileo L, Piccoli M, Conforti E, Sitzia C, Monti E, Sampaolesi M, *et al.* (2008). NEU3 Sialidase Strictly Modulates GM3 Levels in Skeletal Myoblasts C2C12 Thus Favoring Their Differentiation and Protecting Them from Apoptosis. *J. Biol. Chem.*, 283:36265-36271.

Andrews DM, Cherry PC, Humber DC, Jones PS, Keeling SP, Martin PF, Shaw CD, Swanson S. (1999). Synthesis and influenza virus sialidase inhibitory activity of analogues of 4-Guanidino-Neu5Ac2en (Zanamivir) modified in the glycerol side-chain. *Eur. J. Med. Chem.*, 34:563-574.

Azuma Y, Sato H, Higai K, Matsumoto K. (2007). Enhanced Expression of Membrane-Associated Sialidase Neu3 Decreases GD3 and Increases GM3 on the Surface of Jurkat Cells during Etoposide-Induced Apoptosis. *Biol. Pharm. Bull.*, 30:1680-1684.

Bagriacik EU, Miller KS. (1999). Cell surface sialic acid and the regulation of immune cell interactions: the neuraminidase effect reconsidered. *Glycobiology*, 9:267-275.

Bhaskar K V, Duggan PJ, Humphrey DG, Krippner GY, McCarl V, Offermann DA. (2001). Phenylboronic acid as a labile protective agent: the selective derivatisation of 1,2,3-triols. *J. Chem. Soc., Perkin Trans. 1*:1098-1102.

Bissantz C, Kuhn B, Stahl M. (2010). A Medicinal Chemist's Guide to Molecular Interactions. *J. Med. Chem.*, 53:5061-5084.

Bolitt V, Mioskowski C, Lee SG, Falck JR. (1990). Direct preparation of 2-deoxy-D-glucopyranosides from glucals without Ferrier rearrangement. *The Journal of Organic Chemistry*, 55:5812-5813.
Burmeister WP, Henrissat B, Bosso C, Cusack S, Ruigrok RWH. (1993). Influenza-B virus neuraminidase can synthesize its own inhibitor.. *Structure*, 1:19-26.

Buschiazzo A, Alzari PM. (2008). Structural insights into sialic acid enzymology. *Curr. Opin. Chem. Biol.*, 12:565-572.

Cabezas JA. (1991). Some questions and suggestions on the type references of the official nomenclature (IUB) for sialidase(s) and endosialidase. *Biochem. J*, 278:311-310.

Caciotti A, Di Rocco M, Filocamo M, Grossi S, Traverso F, d'Azzo A, Cavicchi C, Messeri A, Guerrini R, Zammarchi E, Donati M, *et al.* (2009). Type II sialidosis: review of the clinical spectrum and identification of a new splicing defect with chitotriosidase assessment in two patients. *Journal of Neurology*, 256:1911-1915.

Cantarel BL, Coutinho PM, Rancurel C, Bernard T, Lombard V, Henrissat B. (2009). The Carbohydrate-Active EnZymes database (CAZy): an expert resource for Glycogenomics. *Nucleic Acids Res.*, 37:D233-D238.

Carubelli I, Venerando B, Stamatos NM. (2006). Sialidases Neu1 and Neu3 on the surface of human monocyte-derived dendritic cells may influence cell activity by desialylating GM3 ganglioside. *Glycobiology*, 16:285.

Chandler M, Bamford MJ, Conroy R, Lamont B, Patel B, Patel VK, Steeples IP, Storer R, Weir NG, Wright M, Williamson C. (1995). Synthesis of the potent influenza neuraminidase inhibitor 4-guanidino Neu5Ac2en. X-Ray molecular structure of 5-acetamido-4-amino-2,6-anhydro-3,4,5-trideoxy-D-erythro-L-gluco-nononic acid. *J. Chem. Soc., Perkin Trans. 1*:1173-1180.

Chavas LMG, Tringali C, Fusi P, Venerando B, Tettamanti G, Kato R, Monti E, Wakatsuki S. (2005). Crystal structure of the human cytosolic sialidase Neu2: Evidence for the dynamic nature of substrate recognition. *J. Biol. Chem.*, 280:469-475.

Chavas LMG, Tringali C, Fusi P, Venerando B, Tettamanti G, Kato R, Monti E, Wakatsuki S. (2005). Crystal structure of the human cytosolic sialidase Neu2 - Evidence for the dynamic nature of substrate recognition. *J. Biol. Chem.*, 280:469-475.

Chavas LMG, Kato R, Suzuki N, von Itzstein M, Mann MC, Thomson RJ, Dyason JC, McKimm-Breschkin J, Fusi P, Tringali C, Venerando B, *et al.* (2010). Complexity in Influenza Virus Targeted Drug Design: Interaction with Human Sialidases. *J. Med. Chem.*, 53:2998-3002.

Chen XP, Enioutina EY, Daynes RA. (1997). The control of IL-4 gene expression in activated murine T lymphocytes - A novel role for neu-1 sialidase. *J. Immunol.*, 158:3070-3080.

Chen XP, Enioutina EY, Daynes RA. (1997). The Control of IL-4 Gene Expression in Activated Murine T Lymphocytes: A Novel Role for neu-1 Sialidase. *J. Immunol.*, 158:3070-3080.

Cross AS, Sakarya S, Rifat S, Held TK, Drysdale BE, Grange PA, Cassels FJ, Wang LX, Stamatos N, Farese A, Casey D, *et al.* (2003). Recruitment of murine neutrophils in vivo through endogenous sialidase activity. *J. Biol. Chem.*, 278:4112-4120.

D. Burkart M, P. Vincent S, Wong C-H. (1999). An efficient synthesis of CMP-3-fluoroneuraminic acid. *Chem. Commun.*:1525-1526.

Dyason JC, von Itzstein M. (2001). Anti-Influenza Virus Drug Design: Sialidase Inhibitors. *Aust. J. Chem.*, 54:663-670.

Edwards JO, Pearson RG. (1962). The Factors Determining Nucleophilic Reactivities. *J. Am. Chem. Soc.*, 84:16-24.

Feng C, Zhang L, Almulki L, Faez S, Whitford M, Hafezi-Moghadam A, Cross AS. (2011). Endogenous PMN sialidase activity exposes activation epitope on CD11b/CD18 which enhances its binding interaction with ICAM-1. *J. Leukocyte Biol.*, 90:313-321.

Gadhoum SZ, Sackstein R. (2008). CD15 expression in human myeloid cell differentiation is regulated by sialidase activity. *Nat. Chem. Biol.*, 4:751-757.

Gilson MK, Sharp KA, Honig BH. (1988). Calculating the electrostatic potential of molecules in solution: Method and error assessment. *J. Comput. Chem.*, 9:327-335.

Goodford PJ. (1985). A computational procedure for determining energetically favorable binding sites on biologically important macromolecules. *J. Med. Chem.*, 28:849-857.

Goodsell DS, Morris GM, Olson AJ. (1996). Automated docking of flexible ligands: Applications of autodock. *J. Mol. Recognit.*, 9:1-5.

Govorkova EA, Fang H-B, Tan M, Webster RG. (2004). Neuraminidase Inhibitor-Rimantadine Combinations Exert Additive and Synergistic Anti-Influenza Virus Effects in MDCK Cells. *Antimicrob. Agents Chemother.*, 48:4855-4863.

Greffard A, Pairon JC, Terzidis-Trabelsi H, Heslan JM, Bignon J, Lambre CR, Pilatte Y. (1994). Initial characterization of human thymocyte sialidase activity: evidence that this enzymatic system is not altered during the course of T-cell maturation. *Int. J. Biochem.*, 26:769-776.

Ha KT, Lee YC, Cho SH, Kim JK, Kim CH. (2004). Molecular characterization of membrane type and ganglioside-specific sialidase (Neu3) expressed in E. coli. *Mol. Cells*, 17:267-273.

Han S, Collins BE, Bengtson P, Paulson JC. (2005). Homomultimeric complexes of CD22 in B cells revealed by protein-glycan cross-linking. *Nat. Chem. Biol.*, 1:93-97.

Hata K, Koseki K, Yamaguchi K, Moriya S, Suzuki Y, Yingsakmongkon S, Hirai G, Sodeoka M, von Itzstein M, Miyagi T. (2008). Limited Inhibitory Effects of Oseltamivir and Zanamivir on Human Sialidases. *Antimicrob. Agents Chemother.*, 52:3484-3491.

Helm RF, Ralph J, Anderson L. (1991). Regioselective protection strategies for D-xylopyranosides. *The Journal of Organic Chemistry*, 56:7015-7021.

Holzer CT, Itzstein M, Jin B, Pegg MS, Stewart WP, Wu W-Y. (1993). Inhibition of sialidases from viral, bacterial and mammalian sources by analogues of 2-deoxy-2,3-didehydro-<i>N</i>-acetylneuraminic acid modified at the C-4 position. *Glycoconjugate J.*, 10:40-44.

Johansson S, Nilsson E, Qian W, Guilligay D, Crepin T, Cusack S, Arnberg N, Elofsson M. (2009). Design, Synthesis, and Evaluation of N-Acyl Modified Sialic Acids as Inhibitors of Adenoviruses Causing Epidemic Keratoconjunctivitis†. *J. Med. Chem.*, 52:3666-3678.

Kajihara Y, Kamiyama D, Yamamoto N, Sakakibara T, Izumi M, Hashimoto H. (2004). Synthesis of 2-[(2-pyridyl)amino]ethyl [beta]-d-lactosaminide and evaluation of its acceptor ability for sialyltransferase: a comparison with 4-methylumbelliferyl and dansyl [beta]-d-lactosaminide. *Carbohydr. Res.*, 339:1545-1550.

Kakugawa Y, Wada T, Yamaguchi K, Yamanami H, Ouchi K, Sato I, Miyagi T. (2002). Up-regulation of plasma membrane-associated ganglioside sialidase (Neu3) in human colon cancer and its involvement in apoptosis suppression. *Proc. Natl. Acad. Sci. U. S. A.*, 99:10718-10723.

Kanwar YS, Farquhar MG. (1980). Detachment of endothelium and epithelium from the glomerular basement membrane produced by kidney perfusion with neuraminidase. *Lab. Invest.*, 42:375-384.

Kato K, Shiga K, Yamaguchi K, Hata K, Kobayashi T, Miyazaki K, Saijo S, Miyagi T. (2006). Plasma-membrane-associated sialidase (NEU3) differentially regulates integrin-mediated cell proliferation through laminin- and fibronectin-derived signalling. *Biochem. J*, 394:647-656.

Kim CU, Lew W, Williams MA, Liu H, Zhang L, Swaminathan S, Bischofberger N, Chen MS, Mendel DB, Tai CY, Laver WG, *et al.* (1997). Influenza Neuraminidase Inhibitors Possessing a Novel Hydrophobic Interaction in the Enzyme Active Site: Design, Synthesis, and Structural Analysis of Carbocyclic Sialic Acid Analogues with Potent Anti-Influenza Activity. *J. Am. Chem. Soc.*, 119:681-690.

Kim CU, Lew W, Williams MA, Wu H, Zhang L, Chen X, Escarpe PA, Mendel DB, Laver WG, Stevens RC. (1998). Structure−Activity Relationship Studies of Novel Carbocyclic Influenza Neuraminidase Inhibitors. *J. Med. Chem.*, 41:2451-2460.

Kuboki A, Sekiguchi T, Sugai T, Ohta H. (1998). A Facile Access to Aryl α-Sialosides: the Combination of a Volatile Amine Base and Acetonitrile in Glycosidation of Sialosyl Chlorides. *Synlett*, 1998:479,482.

Lane CF. (1975). Sodium Cyanoborohydride - A Highly Selective Reducing Agent for Organic Functional Groups. *Synthesis*:135-146.

Laurence M. von Izstein NFW-YW, Mount Waverley; Tho V. Phan, Carnegie; Basil Danylec, Box Hill; Betty Jin, Mount Waverley, all of Australia. 1994. Derivatives and Analogues of 2-deoxy-2,3-didehydro-*N*-acetyl Neuraminic Acid and Their Use as Antiviral AgentsNovember 1, 1994 of Patent

Lepage O, Kattnig E, Fürstner A. (2004). Total Synthesis of Amphidinolide X. *J. Am. Chem. Soc.*, 126:15970-15971.

Li C-Y, Yu Q, Ye Z-Q, Sun Y, He Q, Li X-M, Zhang W, Luo J, Gu X, Zheng X, Wei L. (2007). A nonsynonymous SNP in human cytosolic sialidase in a small Asian population results in reduced enzyme activity: potential link with severe adverse reactions to oseltamivir. *Cell Res.*, 17:357-362.

Li J, Zheng M, Tang W, He P-L, Zhu W, Li T, Zuo J-P, Liu H, Jiang H. (2006). Syntheses of triazole-modified zanamivir analogues via click chemistry and anti-AIV activities. *Bioorg. Med. Chem. Lett.*, 16:5009-5013.

Li Y, Cao H, Yu H, Chen Y, Lau K, Qu J, Thon V, Sugiarto G, Chen X. (2011). Identifying selective inhibitors against the human cytosolic sialidase NEU2 by substrate specificity studies. *Mol. BioSyst.,* 7:1060-1072.

Loka RS, Sadek CM, Romaniuk NA, Cairo CW. (2010). Conjugation of Synthetic N-Acetyl-Lactosamine to Azide-Containing Proteins Using the Staudinger Ligation. *Bioconjugate Chem.,* 21:1842-1849.

Lu Y, Gervay-Hague J. (2007). Synthesis of C-4 and C-7 triazole analogs of zanamivir as multivalent sialic acid containing scaffolds. *Carbohydr. Res.,* 342:1636-1650.

Magesh S, Suzuki T, Miyagi T, Ishida H, Kiso M. (2006). Homology modeling of human sialidase enzymes NEU1, NEU3 and NEU4 based on the crystal structure of NEU2: Hints for the design of selective NEU3 inhibitors. *J. Mol. Graphics Modell.,* 25:196-207.

Magesh S, Moriya S, Suzuki T, Miyagi T, Ishida H, Kiso M. (2008). Design, synthesis, and biological evaluation of human sialidase inhibitors. Part 1: Selective inhibitors of lysosomal sialidase (NEU1). *Bioorg. Med. Chem. Lett.,* 18:532-537.

Magesh S, Savita V, Moriya S, Suzuki T, Miyagi T, Ishida H, Kiso M. (2009). Human sialidase inhibitors: Design, synthesis, and biological evaluation of 4-acetamido-5-acylamido-2-fluoro benzoic acids. *Bioorg. Med. Chem.,* 17:4595-4603.

Magesh S, Sriwilaijaroen N, Moriya S, Ando H, Miyagi T, Suzuki Y, Ishida H, Kiso M. (2011). Evaluation of a Set of C9 N-acyl Neu5Ac2en Mimetics as Viral Sialidase Selective Inhibitors. *International Journal of Medicinal Chemistry*, 2011.

Marra A, Sinay P. (1989). Acetylation of N-acetylneuraminic acid and its methyl ester. *Carbohydr. Res.*, 190:317-322.

Martin R, Witte KL, Wong C-H. (1998). The synthesis and enzymatic incorporation of sialic acid derivatives for use as tools to study the structure, activity, and inhibition of glycoproteins and other glycoconjugates. *Biorg. Med. Chem.*, 6:1283-1292.

Matrosovich M, Klenk H-D. (2003). Natural and synthetic sialic acid-containing inhibitors of influenza virus receptor binding. *Rev. Med. Virol.*, 13:85-97.

Meindl P, Bodo G, Palese P, Schulman J, Tuppy H. (1974). Inhibition of neuraminidase activity by derivatives of 2-deoxy-2,3-dehydro-N-acetylneuraminic acid. *Virology*, 58:457-463.

Meldal M, Tornøe CW. (2008). Cu-Catalyzed Azide−Alkyne Cycloaddition. *Chem. Rev.*, 108:2952-3015.

Miyagi T, Wada T, Iwamatsu A, Hata K, Yoshikawa Y, Tokuyama S, Sawada M. (1999). Molecular cloning and characterization of a plasma membrane-associated sialidase specific for gangliosides. *J. Biol. Chem.*, 274:5004-5011.

Miyagi T, Wada T, Yamaguchi K, Hata K. (2003). Sialidase and malignancy: A minireview. *Glycoconjugate J.*, 20:189-198.

Miyagi T, Wada T, Moriya S, Ueno S, Kato K, Yamaguchi K. (2004). A crucial role of plasma membrane-associated sialidase (NEU3) in the survival of human cancer cells. *Glycobiology*, 14:436.

Miyagi T, Wada T, Yamaguchi K, Hata K, Shiozaki K. (2008). Plasma Membrane-associated Sialidase as a Crucial Regulator of Transmembrane Signalling. *J. Biochem.*, 144:279-285.

Miyagi T. (2010). Mammalian sialidases and their functions. *Trends in Glycoscience and Glycotechnology*, 22:162-172.

Monti E, Preti A, Venerando B, Borsani G. (2002). Recent Development in Mammalian Sialidase Molecular Biology. *Neurochem. Res.*, 27:649-663.

Monti E, Bonten E, D'Azzo A, Bresciani R, Venerando B, Borsani G, Schauer R, Tettamanti G. 2010. Sialidases in Vertebrates: A Family Of Enzymes Tailored For Several Cell Functions. In: Derek H editor. Adv. Carbohydr. Chem. Biochem.: Academic Press. p. 403-479.

Monti E, Bonten E, D'Azzo A, Bresciani R, Venerando B, Borsani G, Schauer R, Tettamanti G, Derek H. 2010. Sialidases in Vertebrates: A Family Of Enzymes Tailored For Several Cell Functions*. Adv. Carbohydr. Chem. Biochem.: Academic Press. p. 403-479.

Morais GR, Oliveira RS, Falconer RA. (2009). Selective synthesis of Neu5Ac2en and its oxazoline derivative using BF3 Et2O. *Tetrahedron Lett.*, 50:1642-1644.

Moscona A. (2005). Neuraminidase Inhibitors for Influenza. *New Engl. J. Med.*, 353:1363-1373.

Papini N, Anastasia L, Tringali C, Croci G, Bresciani R, Yamaguchi K, Miyagi T, Preti A, Prinetti A, Prioni S, Sonnino S, *et al.* (2004). The Plasma Membrane-associated Sialidase MmNEU3 Modifies the Ganglioside Pattern of Adjacent Cells Supporting Its Involvement in Cell-to-Cell Interactions. *J. Biol. Chem.*, 279:16989-16995.

Quinn MT, Swain SD, Parkos CA, Jutila KL, Siemsen DW, Kurk SL, Jesaitis AJ, Jutila MA. (2001). A carbohydrate neoepitope that is up-regulated on human mononuclear leucocytes by neuraminidase treatment or by cellular activation. *Immunology*, 104:185-197.

Roy R, Laferrière CA. (1990). Synthesis of protein conjugates and analogues of N-acetylneuraminic acid. *Can. J. Chem.*, 68:2045-2054.

Sasaki A, Hata K, Suzuki S, Sawada M, Wada T, Yamaguchi K, Obinata M, Tateno H, Suzuki H, Miyagi T. (2003). Overexpression of plasma membrane-associated sialidase attenuates insulin signaling in transgenic mice. *J. Biol. Chem.*, 278:27896-27902.

Schauer R. (2004). Victor Ginsburg's influence on my research of the role of sialic acids in biological recognition. *Arch. Biochem. Biophys.*, 426:132-141.

Schreiner E, Zbiral E, Kleineidam RG, Schauer R. (1991). Structural Variations on N-acetylneuraminic acid, 20. Synthesis of some 2,3-didehydro-2-deoxysialic Acids structurally varied at C-4 and their behavior towards Sialidase from Vibrio cholerae. *Liebigs Ann. Chem.*, 1991:129-134.

Seyrantepe V, Poupetova H, Froissart R, Zabot M-T, Maire I, Pshezhetsky AV. (2003). Molecular pathology of NEU1 gene in sialidosis. *Hum. Mutat.*, 22:343-352.

Seyrantepe V, Poupetova H, Froissart R, Zabot MT, Maire I, Pshezhetsky AV. (2003). Molecular pathology of NEU1 gene in sialidosis. *Hum. Mutat.*, 22:343-352.

Skehel JJ, Wiley DC. (2000). Receptor binding and membrane fusion in virus entry: the influenza hemagglutinin *Annu. Rev. Biochem*, 69:531-569.

Smith PW, Sollis SL, Howes PD, Cherry PC, Cobley KN, Taylor H, Whittington AR, Scicinski J, Bethell RC, Taylor N, Skarzynski T, *et al.* (1996). Novel inhibitors of influenza sialidases related to GG167 structure-activity, crystallographic and Molecular dynamics studies with 4H-pyran-2-carboxylic acid 6-carboxamides. *Bioorg. Med. Chem. Lett.*, 6:2931-2936.

Smith PW, Sollis SL, Howes PD, Cherry PC, Starkey ID, Cobley KN, Weston H, Scicinski J, Merritt A, Whittington A, Wyatt P, *et al.* (1998). Dihydropyrancarboxamides Related to Zanamivir: A New Series of Inhibitors of Influenza Virus Sialidases. 1. Discovery, Synthesis, Biological Activity, and Structure−Activity Relationships of 4-Guanidino- and 4-Amino-4H-pyran-6-carboxamides. *J. Med. Chem.*, 41:787-797.

Smith PW, Robinson JE, Evans DN, Sollis SL, Howes PD, Trivedi N, Bethell RC. (1999). Sialidase inhibitors related to zanamivir: Synthesis and biological evaluation of 4H-pyran 6-ether and ketone. *Bioorg. Med. Chem. Lett.*, 9:601-604.

Sollis SL, Smith PW, Howes PD, Cherry PC, Bethell RC. (1996). Novel inhibitors of influenza sialidase related to GG167 Synthesis of 4-amino and guanidino-4H-pyran-2-carboxylic acid-6-propylamides; selective inhibitors of influenza a virus sialidase. *Bioorg. Med. Chem. Lett.*, 6:1805-1808.

Sun X-L, Kai T, Takayanagi H, Furuhata K. (1997). Syntheses of sialic acid analogues with acylamino groups at C-4 (N-acyl regioisomers of sialic acids). *Carbohydr. Res.*, 298:181-189.

Taylor NR, von Itzstein M. (1994). Molecular Modeling Studies on Ligand Binding to Sialidase from Influenza Virus and the Mechanism of Catalysis. *J. Med. Chem.*, 37:616-624.

Taylor NR, Cleasby A, Singh O, Skarzynski T, Wonacott AJ, Smith PW, Sollis SL, Howes PD, Cherry PC, Bethell R, Colman P, *et al.* (1998). Dihydropyrancarboxamides Related to Zanamivir: A New Series of Inhibitors of Influenza Virus Sialidases. 2. Crystallographic and Molecular Modeling Study of Complexes of 4-Amino-4H-pyran-6-carboxamides and Sialidase from Influenza Virus Types A and B. *J. Med. Chem.*, 41:798-807.

Uemura T, Shiozaki K, Yamaguchi K, Miyazaki S, Satomi S, Kato K, Sakuraba H, Miyagi T. (2009). Contribution of sialidase NEU1 to suppression of metastasis of human colon cancer cells through desialylation of integrin [beta]4. *Oncogene*, 28:1218-1229.

Ueno S, Saito S, Wada T, Yamaguchi K, Satoh M, Arai Y, Miyagi T. (2006). Plasma Membrane-associated Sialidase Is Up-regulated in Renal Cell Carcinoma and Promotes Interleukin-6-induced Apoptosis Suppression and Cell Motility. *J. Biol. Chem.*, 281:7756-7764.

Valaperta R, Chigorno V, Basso L, Prinetti A, Bresciani R, Preti A, Miyagi T, Sonnino S. (2006). Plasma membrane production of ceramide from ganglioside GM3 in human fibroblasts. *The FASEB Journal*, 20:1227-1229.

Varghese JN. (1999). Development of neuraminidase inhibitors as anti-influenza virus drugs. *Drug Dev. Res.*, 46:176-196.

Varki NM, Varki A. (2007). Diversity in cell surface sialic acid presentations: implications for biology and disease. *Lab. Invest.*, 87:851-857.

von Itzstein M, Jin B, Wu W-Y, Chandler M. (1993). A convenient method for the introduction of nitrogen and sulfur at C-4 on a sialic acid analogue. *Carbohydr. Res.*, 244:181-185.

von Itzstein M, Wu W-Y, Kok GB, Pegg MS, Dyason JC, Jin B, Phan TV, Smythe ML, White HF, Oliver SW, Colman PM, *et al.* (1993). Rational design of potent sialidase-based inhibitors of influenza virus replication. *Nature*, 363:418-423.

von Itzstein M. (2007). The war against influenza: discovery and development of sialidase inhibitors. *Nat. Rev. Drug Discov.*, 6:967-974.

Watson DC, Leclerc S, Wakarchuk WW, Young NM. (2010). Enzymatic synthesis and properties of glycoconjugates with legionaminic acid as a replacement for neuraminic acid. *Glycobiology*, 21:99-108.

Weiss L. (1963). Studies on cellular adhesion in tissue-culture. V. Some effects of enzymes on cell-detachment. *Exp. Cell Res.*, 30:509-520.

We ïwer M, Chen C-C, Kemp MM, Linhardt RJ. (2009). Synthesis and Biological Evaluation of Non-Hydrolyzable 1,2,3-Triazole-Linked Sialic Acid Derivatives as Neuraminidase Inhibitors. *Eur. J. Org. Chem.*, 2009:2611-2620.

Wen W-H, Wang S-Y, Tsai K-C, Cheng Y-SE, Yang A-S, Fang J-M, Wong C-H. (2010). Analogs of zanamivir with modified C4-substituents as the inhibitors against the group-1 neuraminidases of influenza viruses. *Biorg. Med. Chem.*, 18:4074-4084.

Yoo S-E, Hye RK, Kyu YY. (1990). Oxidative debenzylation of 4-methoxy-[alpha]-methylbenzyl esters. *Tetrahedron Lett.*, 31:5913-5916.

Yu H, Huang S, Chokhawala H, Sun M, Zheng H, Chen X. (2006). Highly Efficient Chemoenzymatic Synthesis of Naturally Occurring and Non-Natural α-2,6-Linked Sialosides: A P. damsela α-2,6-Sialyltransferase with Extremely Flexible Donor–Substrate Specificity. *Angew. Chem. Int. Ed.*, 45:3938-3944.

Zou Y, Albohy A, Sandbhor M, Cairo CW. (2010). Inhibition of human neuraminidase 3 (NEU3) by C9-triazole derivatives of 2,3-didehydro-N-acetyl-neuraminic acid. *Bioorg. Med. Chem. Lett.*, 20:7529-7533.

# Appendix

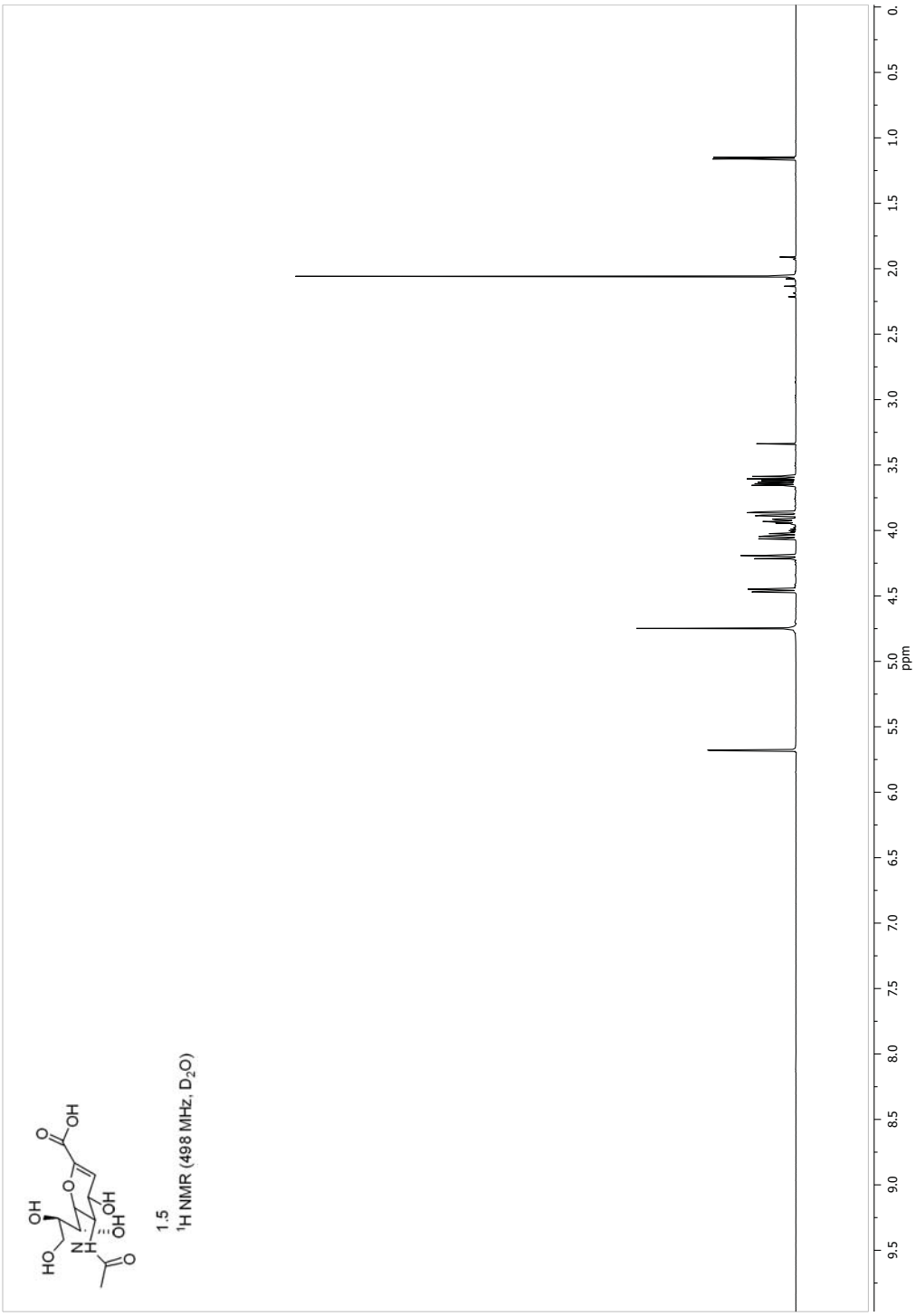
1.5
$^1$H NMR (498 MHz, $D_2O$)
ppm

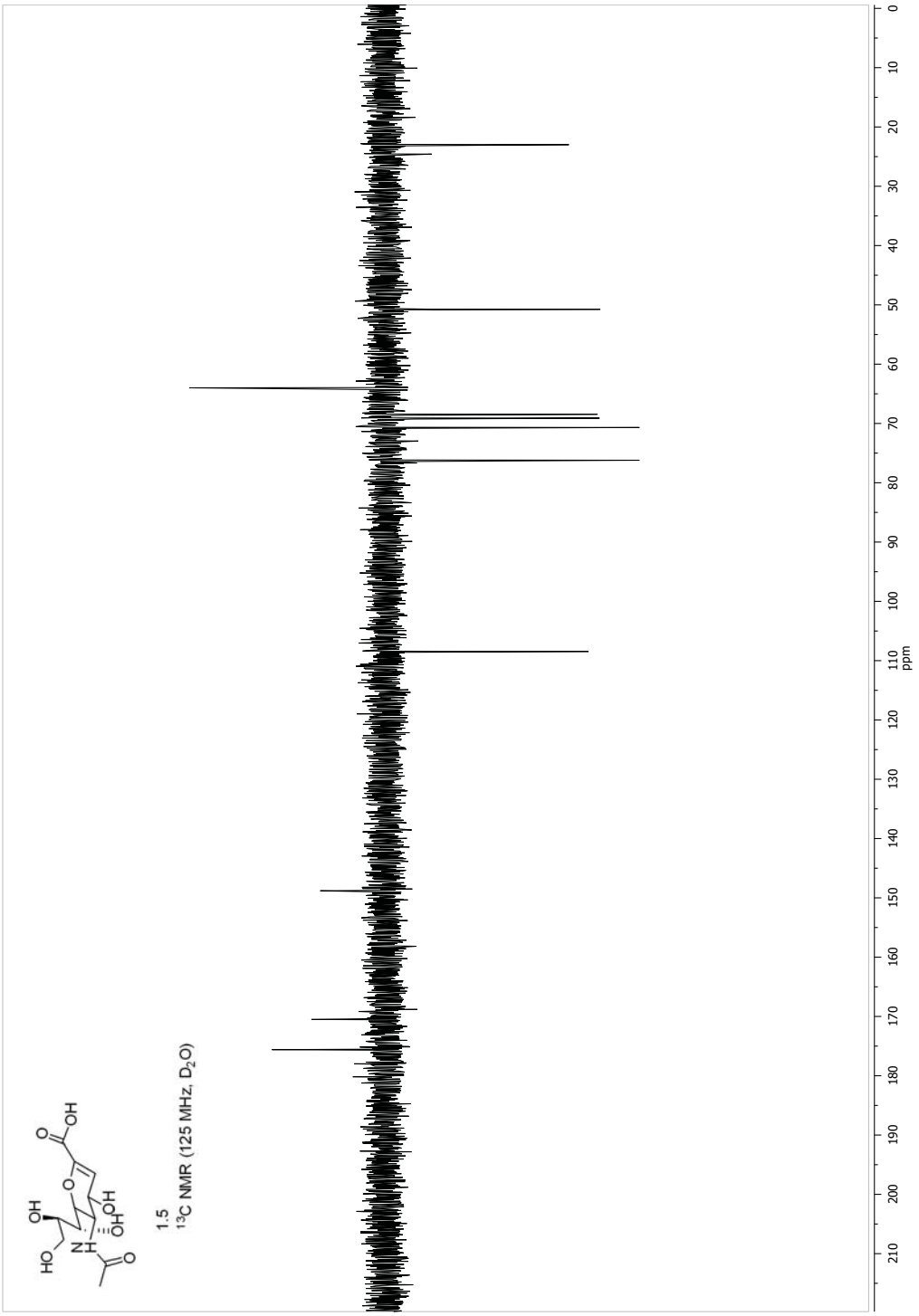
1.5
$^{13}$C NMR (125 MHz, $D_2O$)
ppm

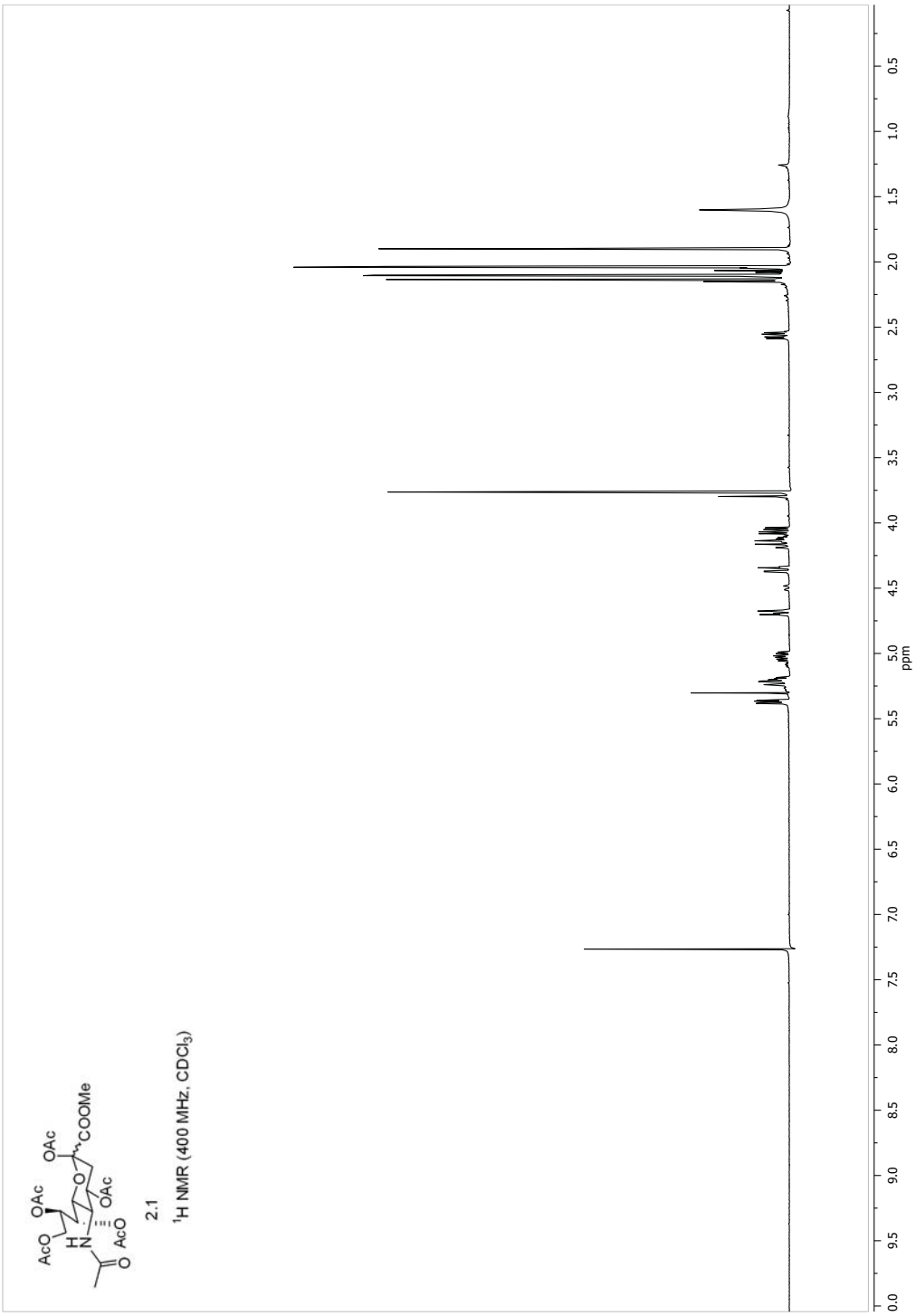
AcO
OAc
OAc
COOMe
OAc
AcO
O
2.1
$^1$H NMR (400 MHz, $CDCl_3$)
0.0
0.5
1.0
1.5
2.0
2.5
3.0
3.5
4.0
4.5
5.0
5.5
6.0
6.5
7.0
7.5
8.0
8.5
9.0
9.5
ppm

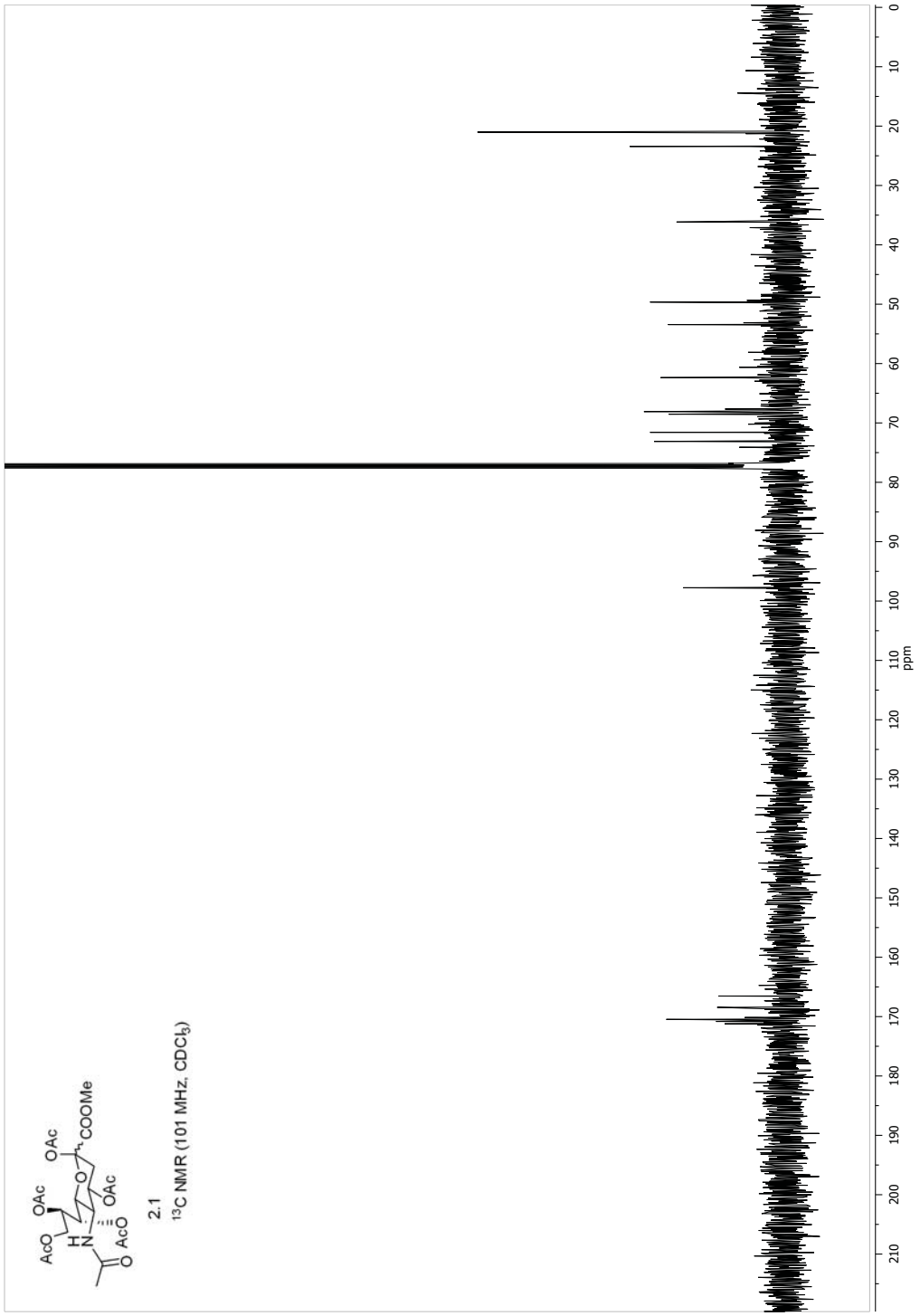
AcO
OAc
OAc
COOMe
AcO
OAc
2.1
$^{13}$C NMR (101 MHz, $CDCl_3$)
ppm

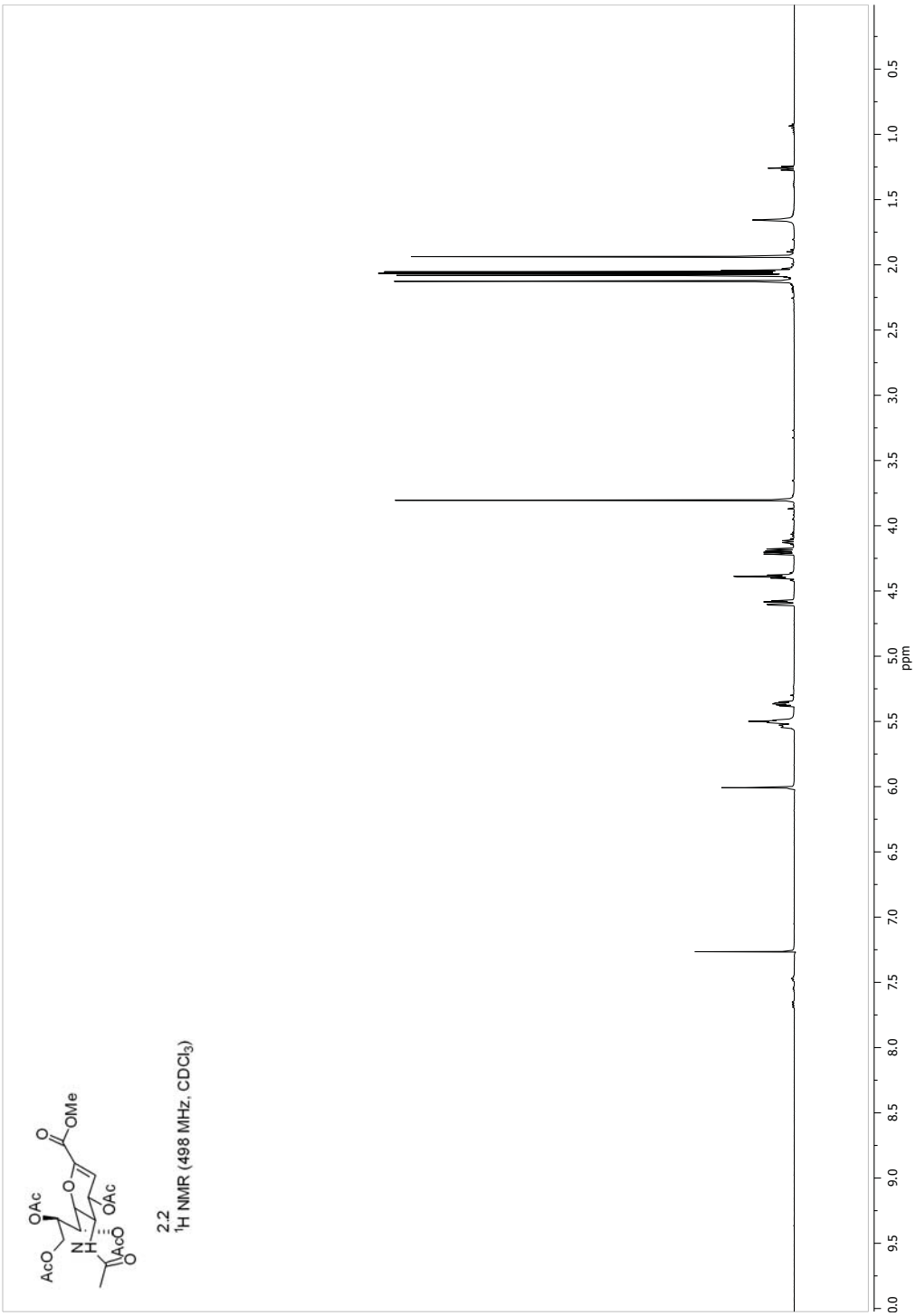
AcO
OAc
N
H
AcO
O
OAc
O
O
OMe
2.2
$^1$H NMR (498 MHz, $CDCl_3$)
0.0
0.5
1.0
1.5
2.0
2.5
3.0
3.5
4.0
4.5
5.0
5.5
6.0
6.5
7.0
7.5
8.0
8.5
9.0
9.5
ppm

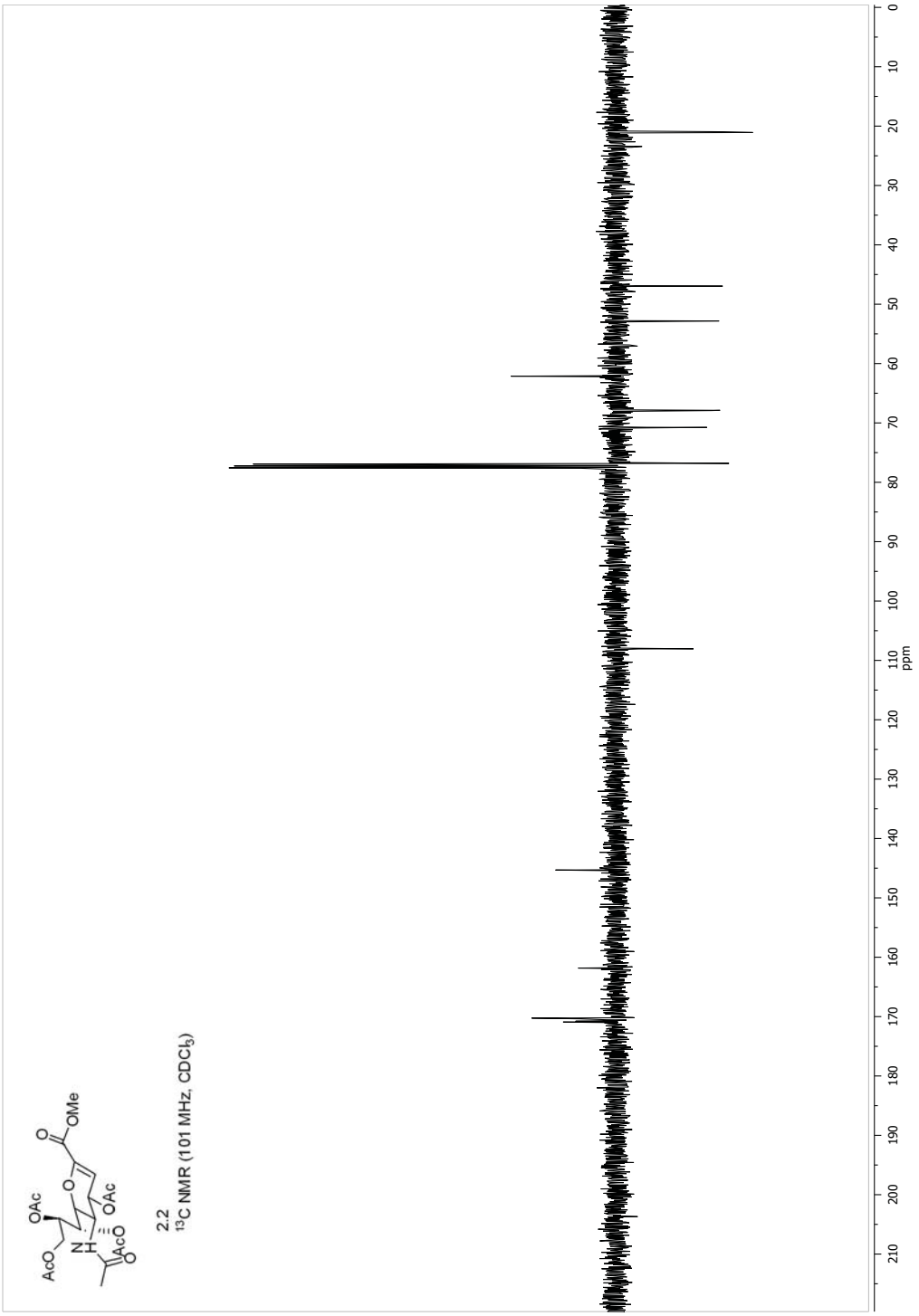
2.2
$^{13}$C NMR (101 MHz, $CDCl_3$)
ppm

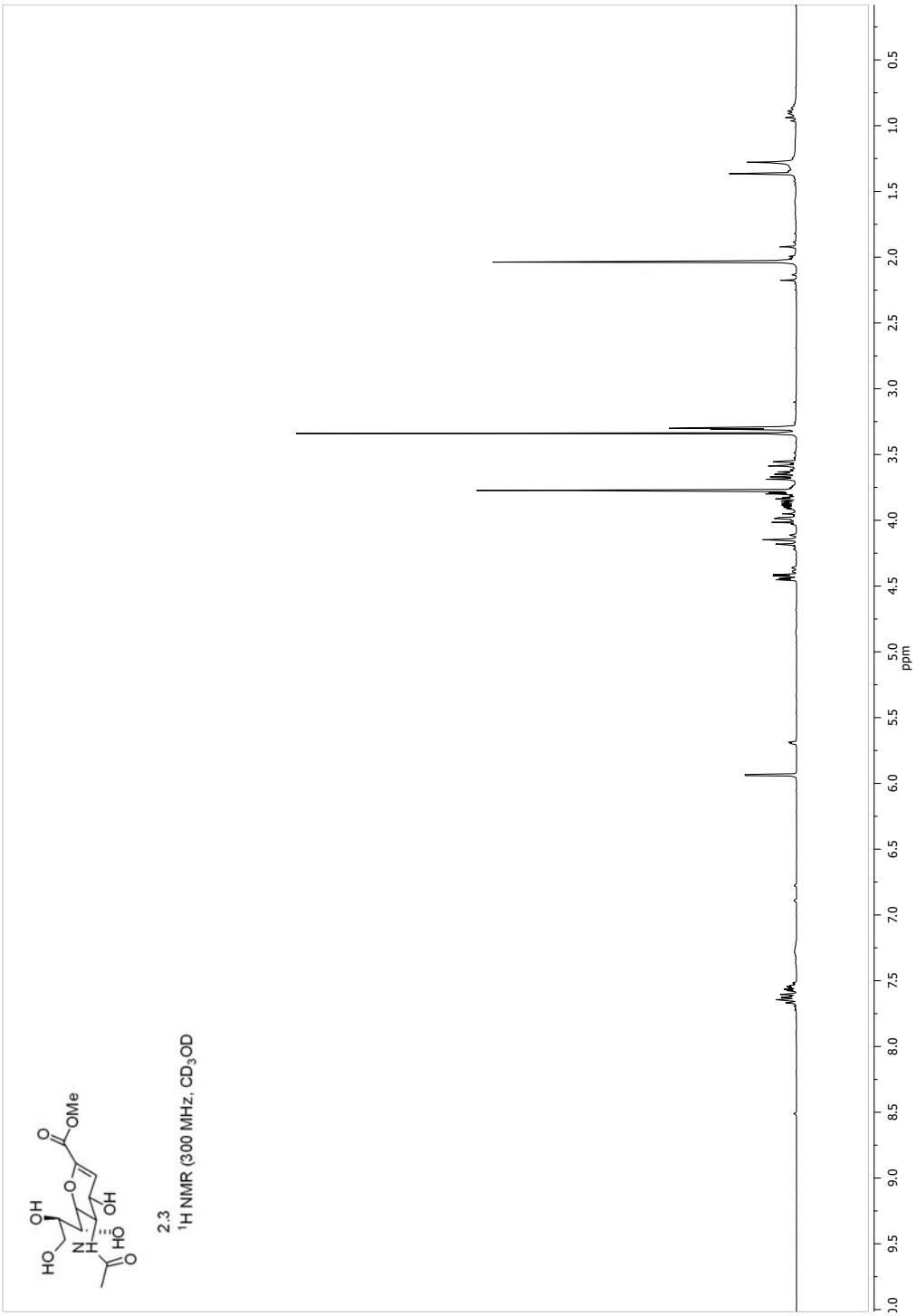
OMe
O
OH
HO
O
N
H
OH
HO
O
2.3
$^1$H NMR (300 MHz, $CD_3OD$)
ppm

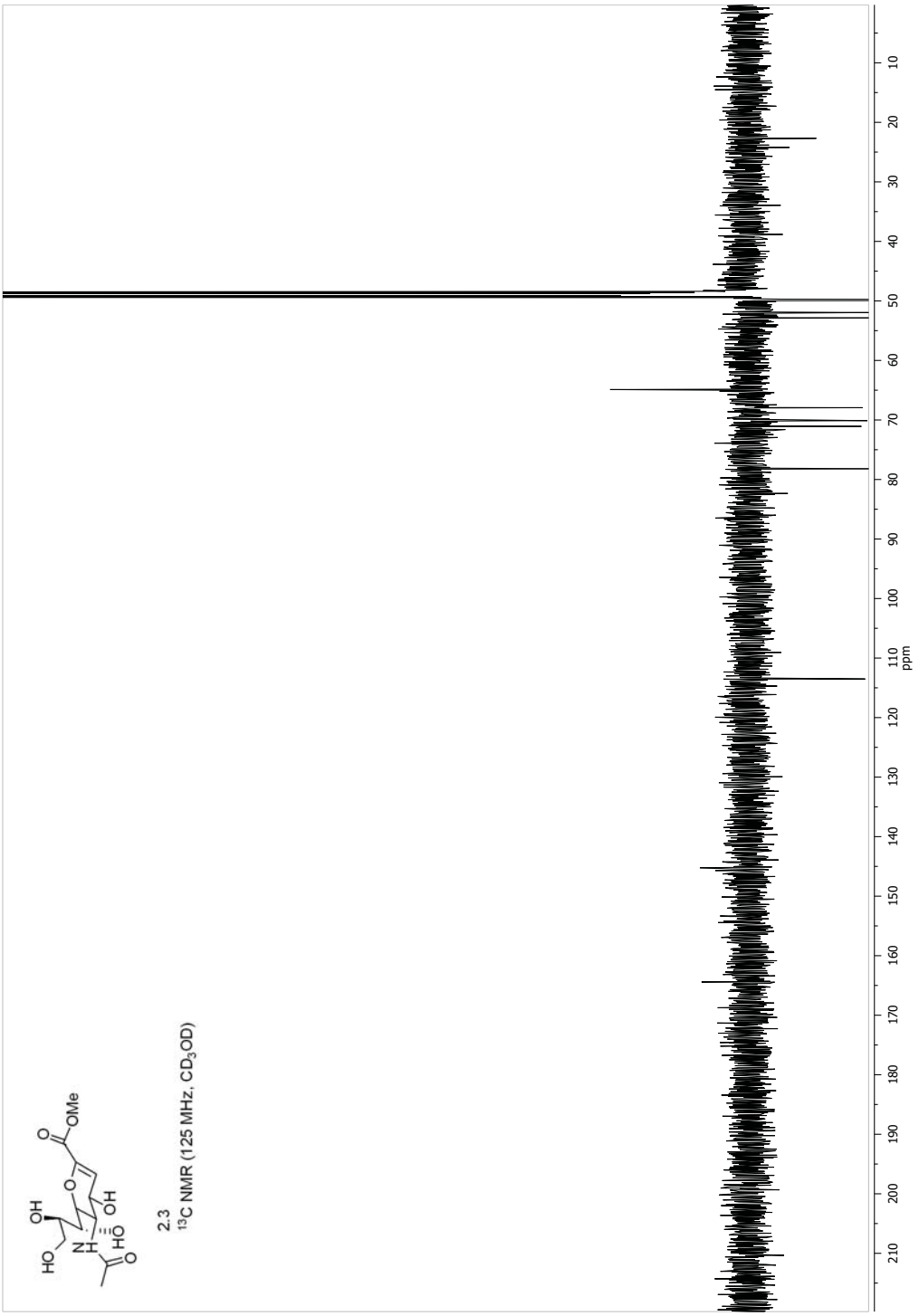
2.3
$^{13}$C NMR (125 MHz, $CD_3OD$)
ppm

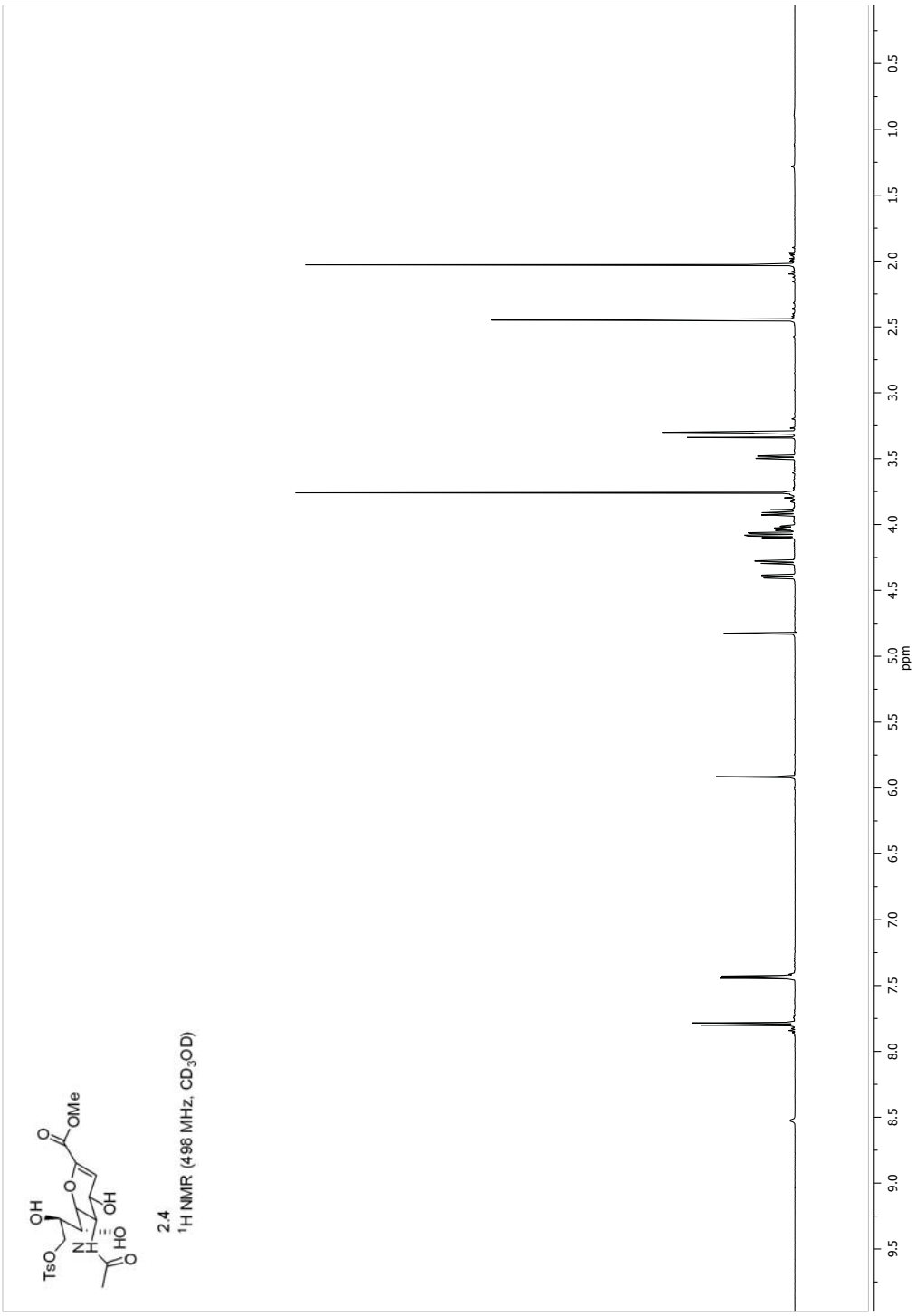
2.4
$^1$H NMR (498 MHz, $CD_3OD$)
ppm

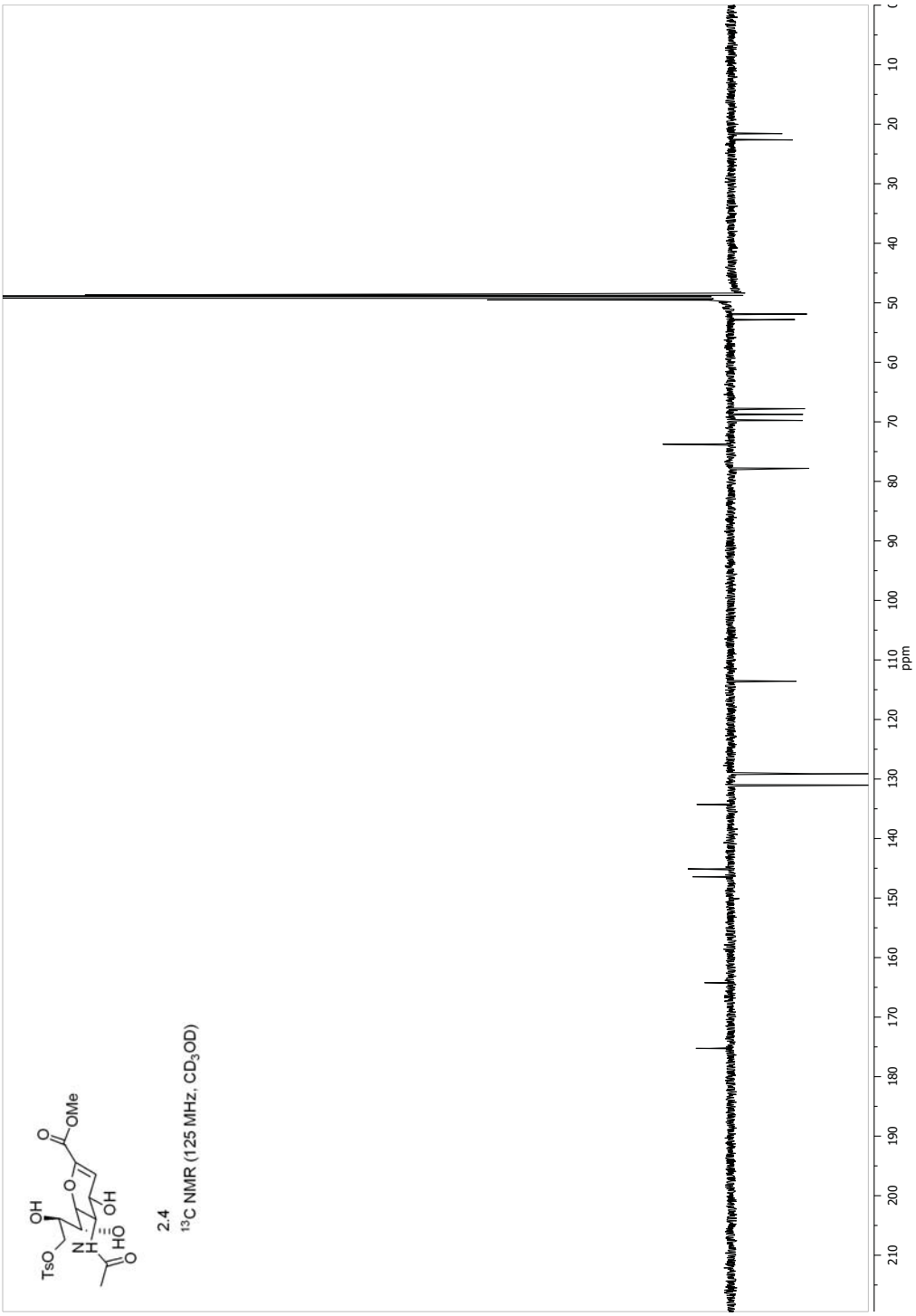
2.4
$^{13}$C NMR (125 MHz, $CD_3OD$)
ppm

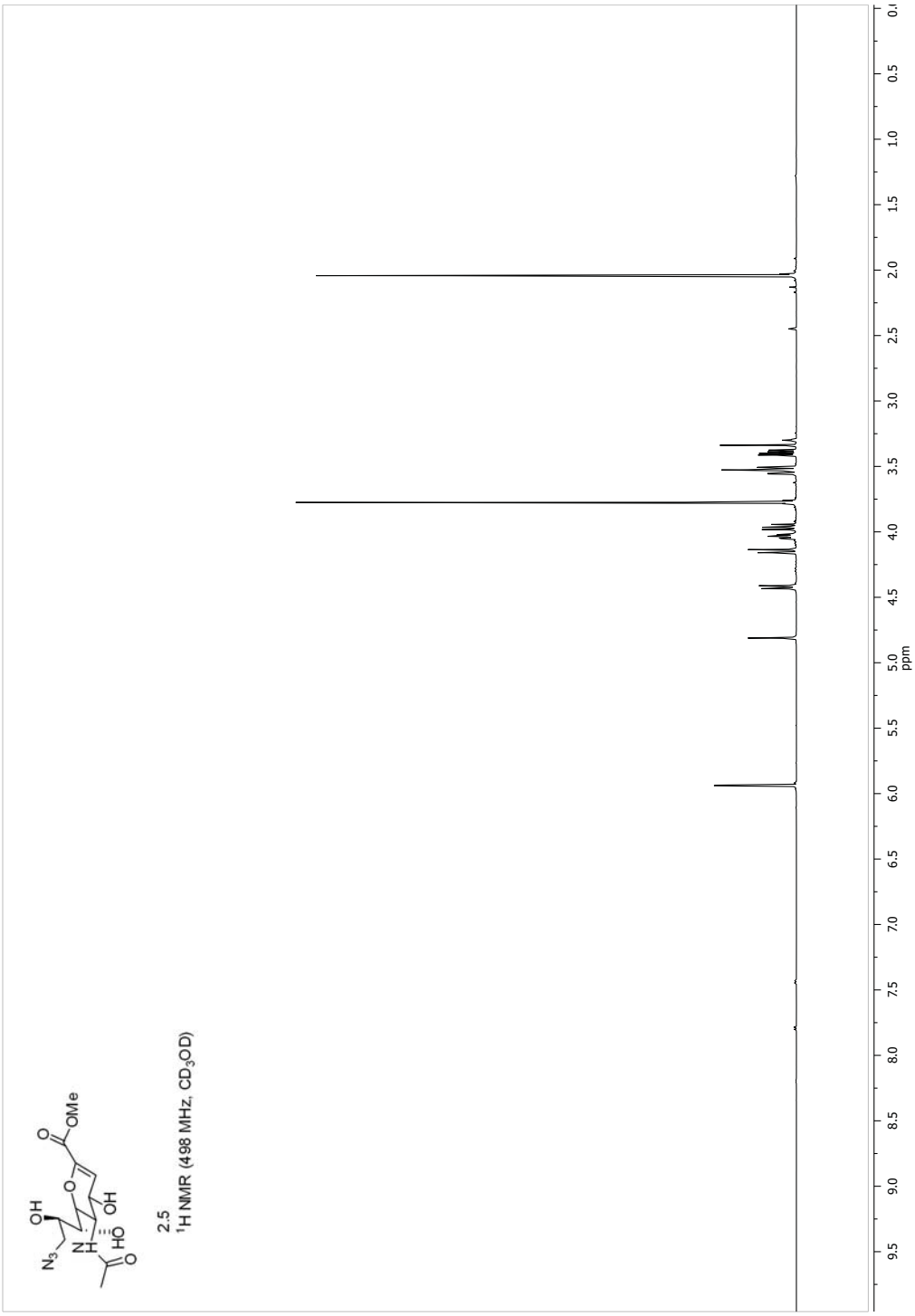
2.5
$^1$H NMR (498 MHz, $CD_3OD$)
ppm

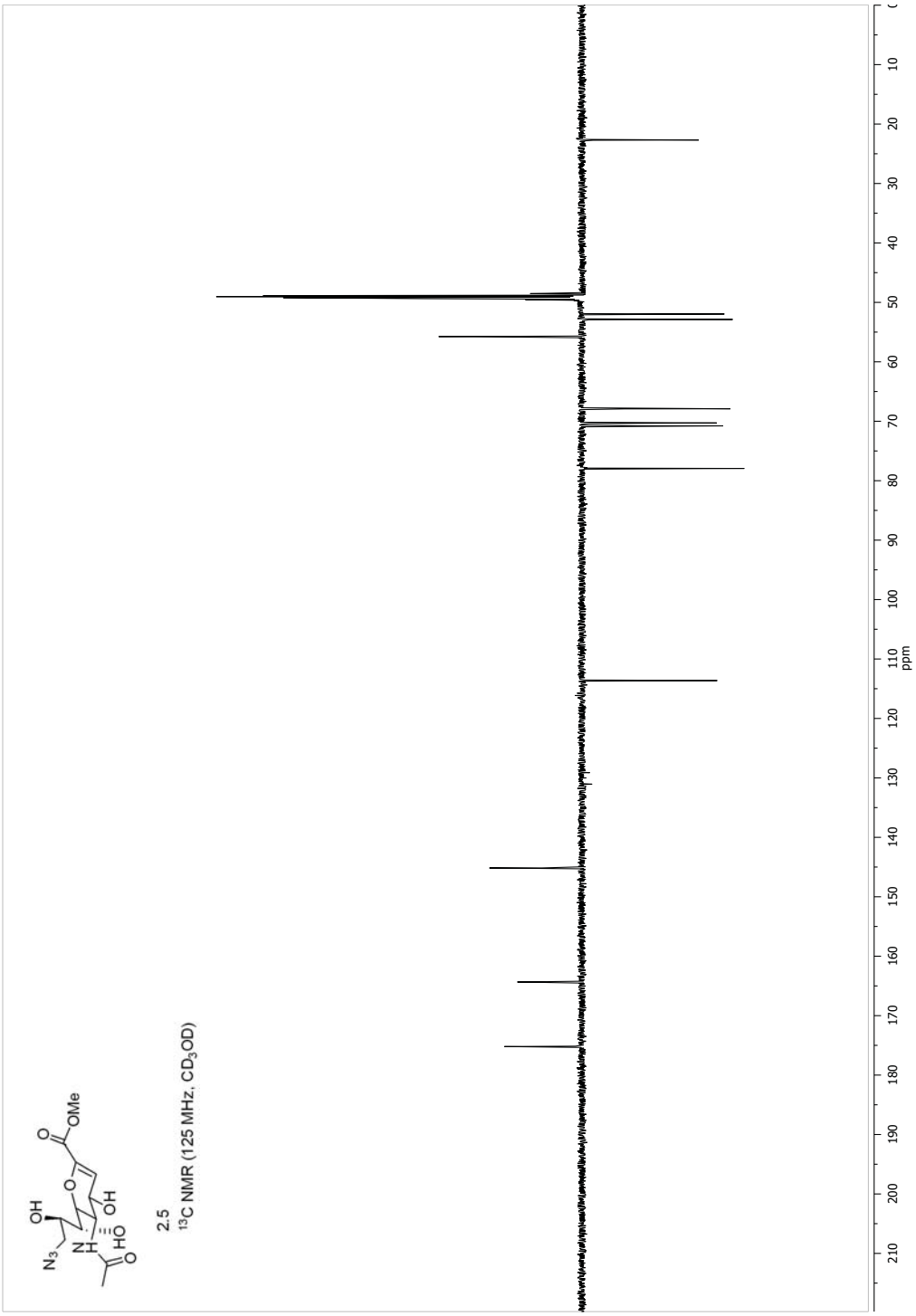
2.5
$^{13}$C NMR (125 MHz, $CD_3OD$)
ppm

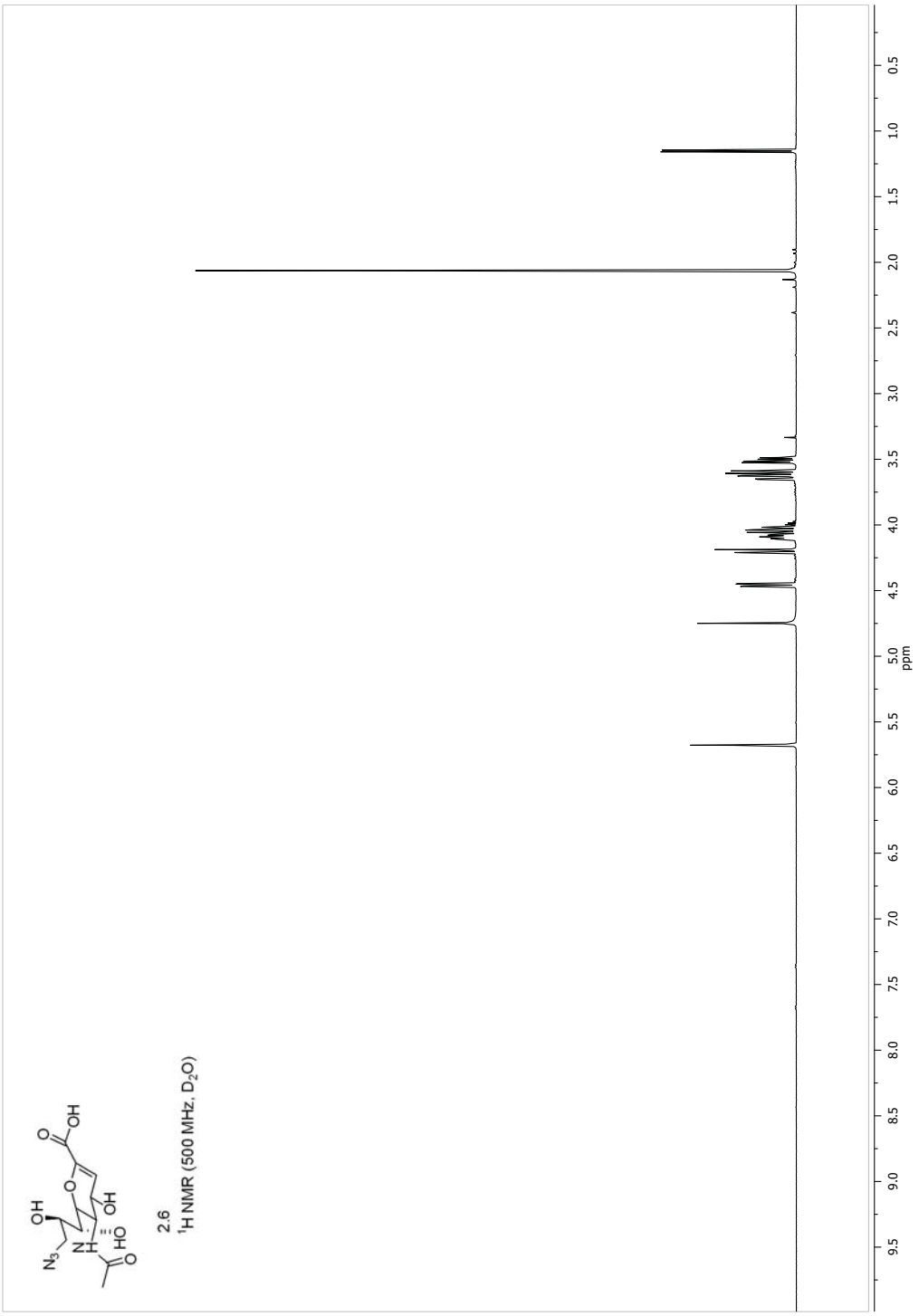
2.6
$^1$H NMR (500 MHz, $D_2O$)
ppm

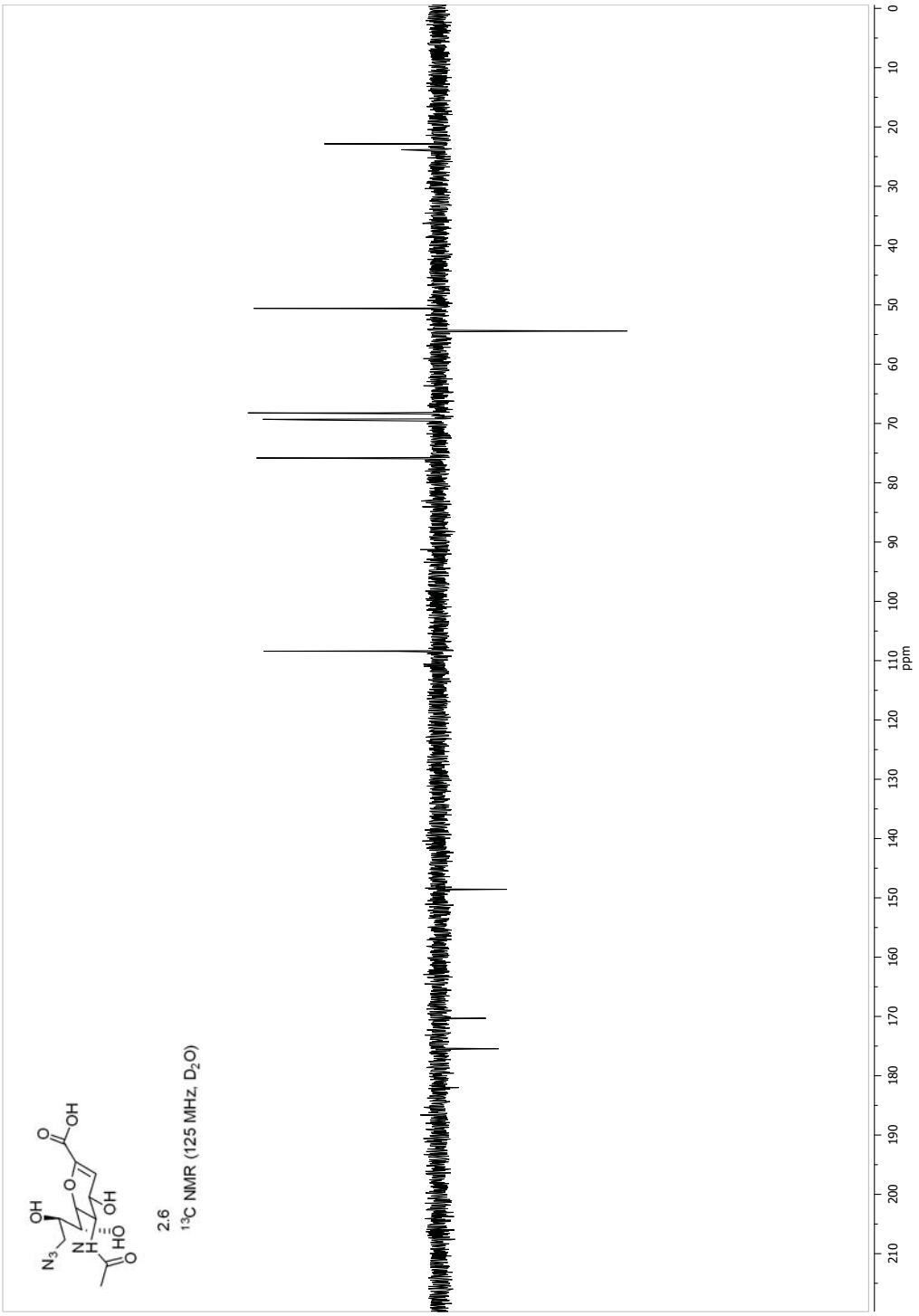
2.6
$^{13}$C NMR (125 MHz, $D_2O$)
ppm

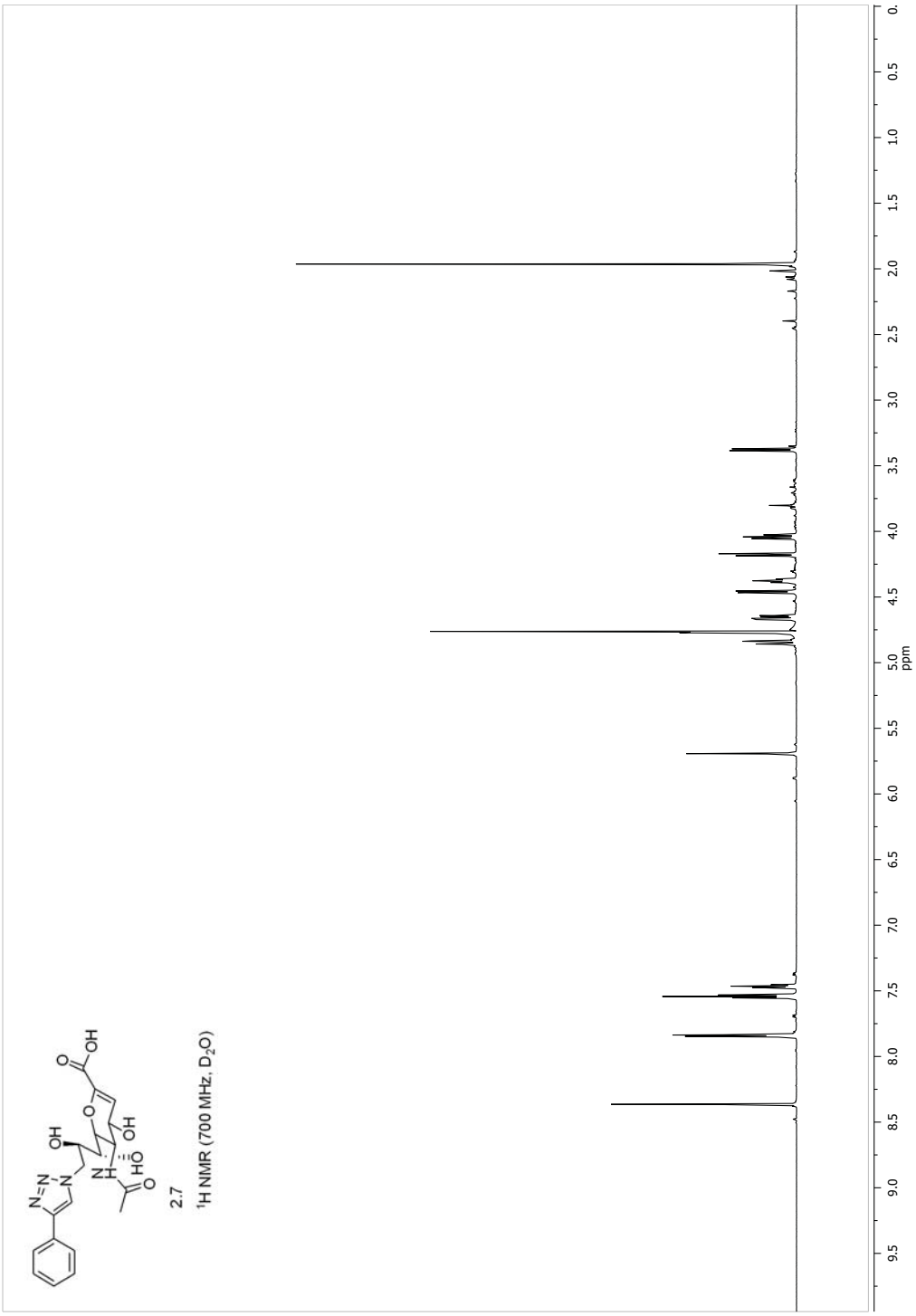
2.7
$^1$H NMR (700 MHz, $D_2O$)
ppm

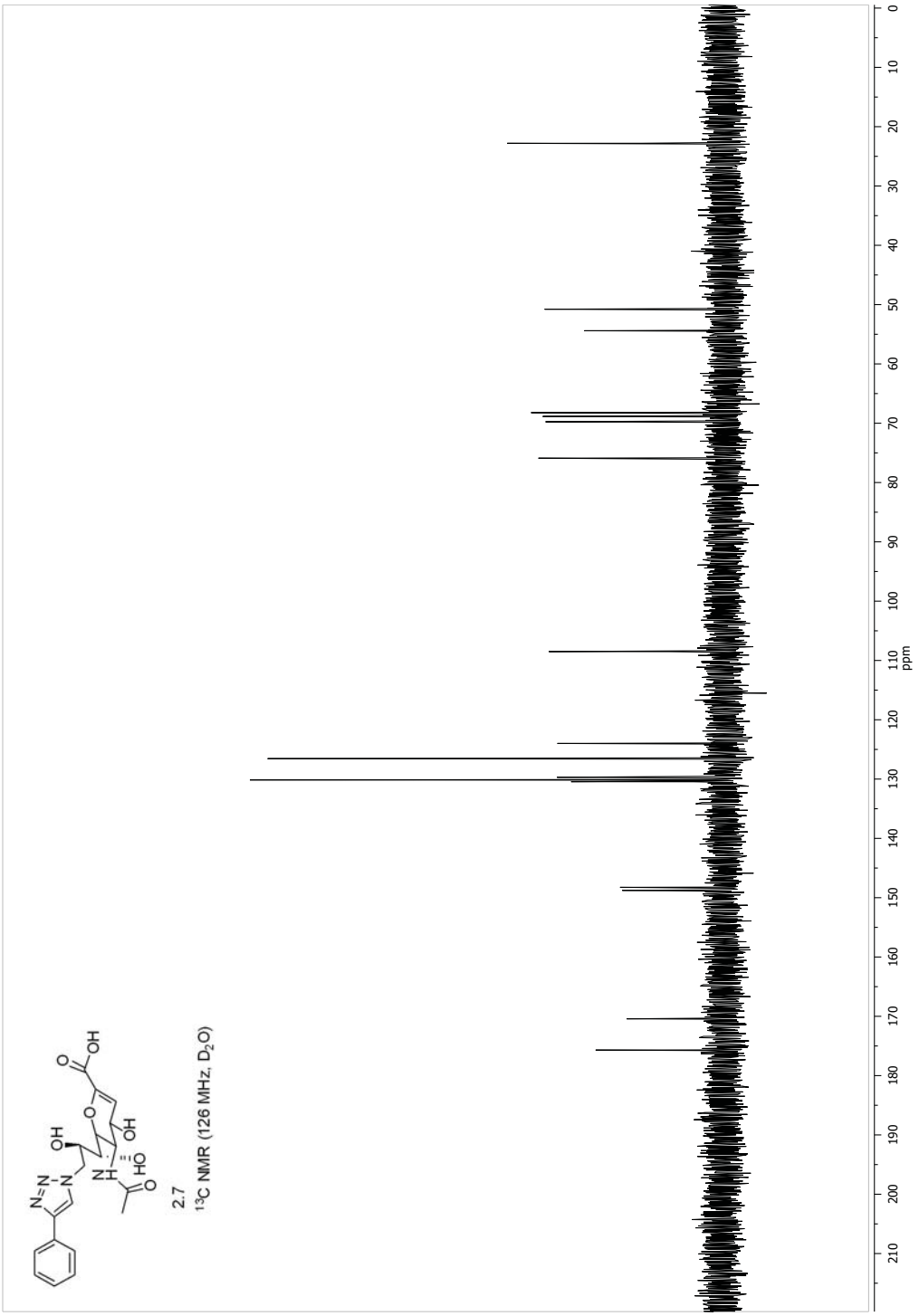
2.7
$^{13}$C NMR (126 MHz, $D_2O$)
ppm

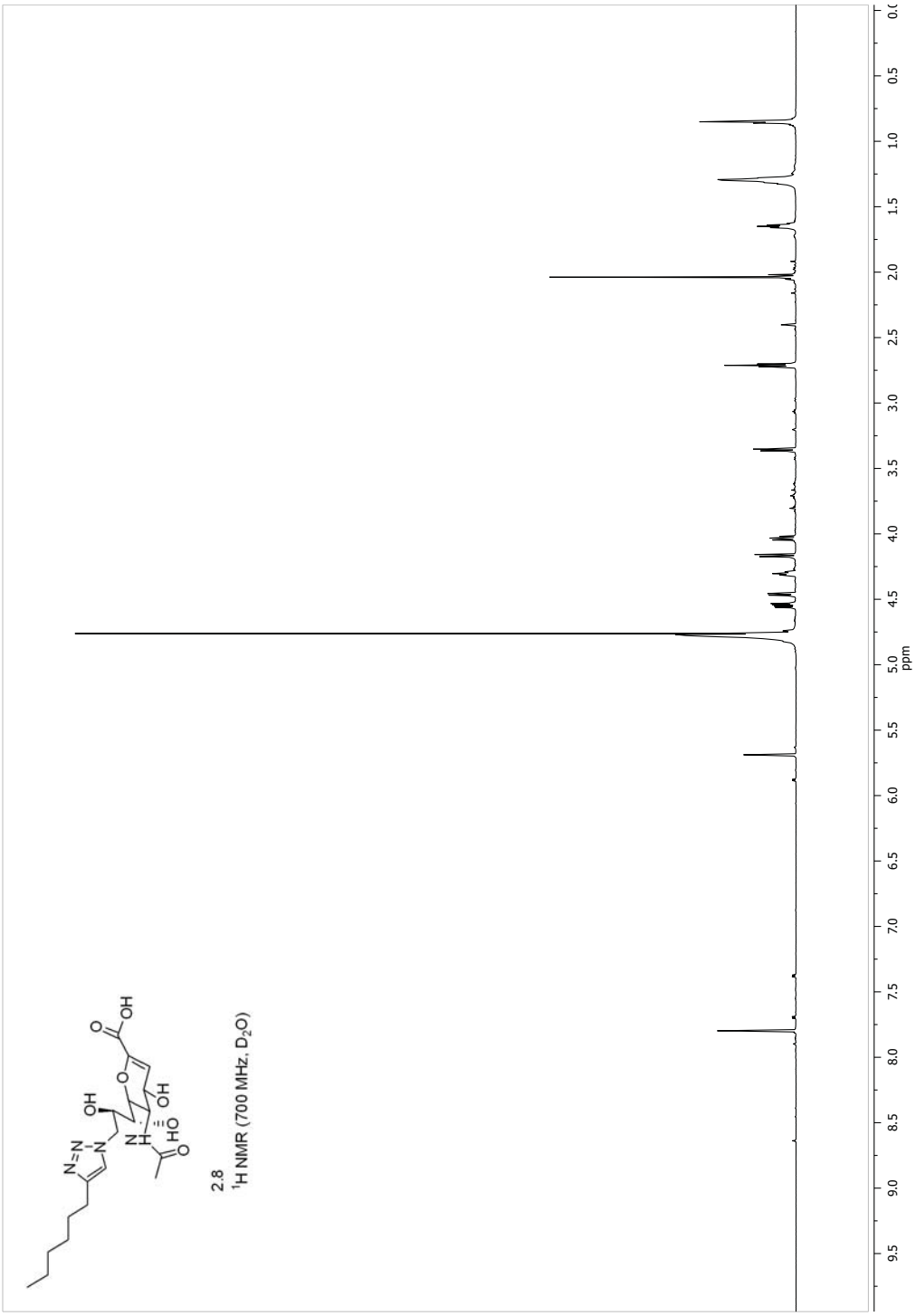
2.8
$^1$H NMR (700 MHz, $D_2O$)
ppm

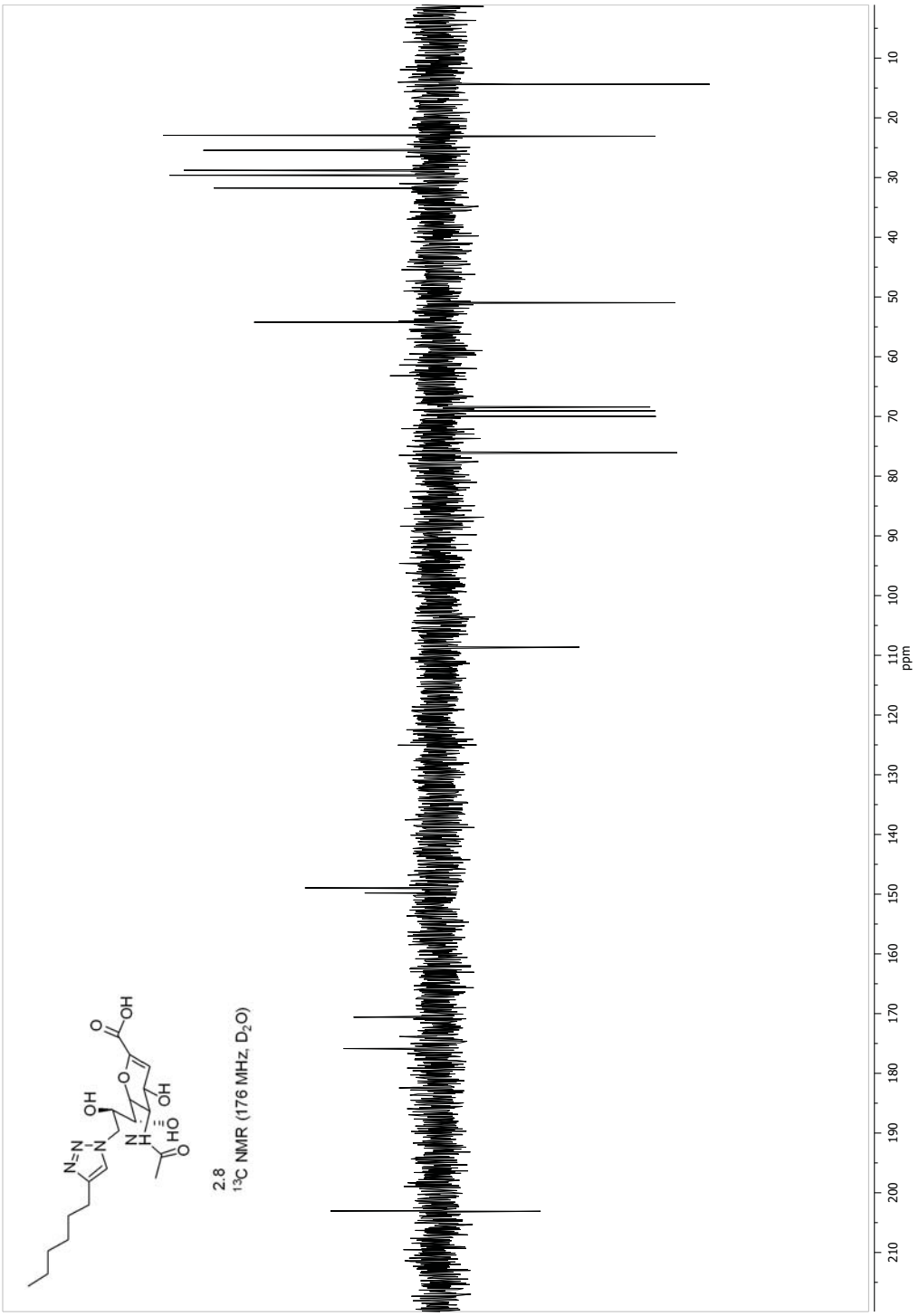
2.8
$^{13}$C NMR (176 MHz, $D_2O$)
ppm

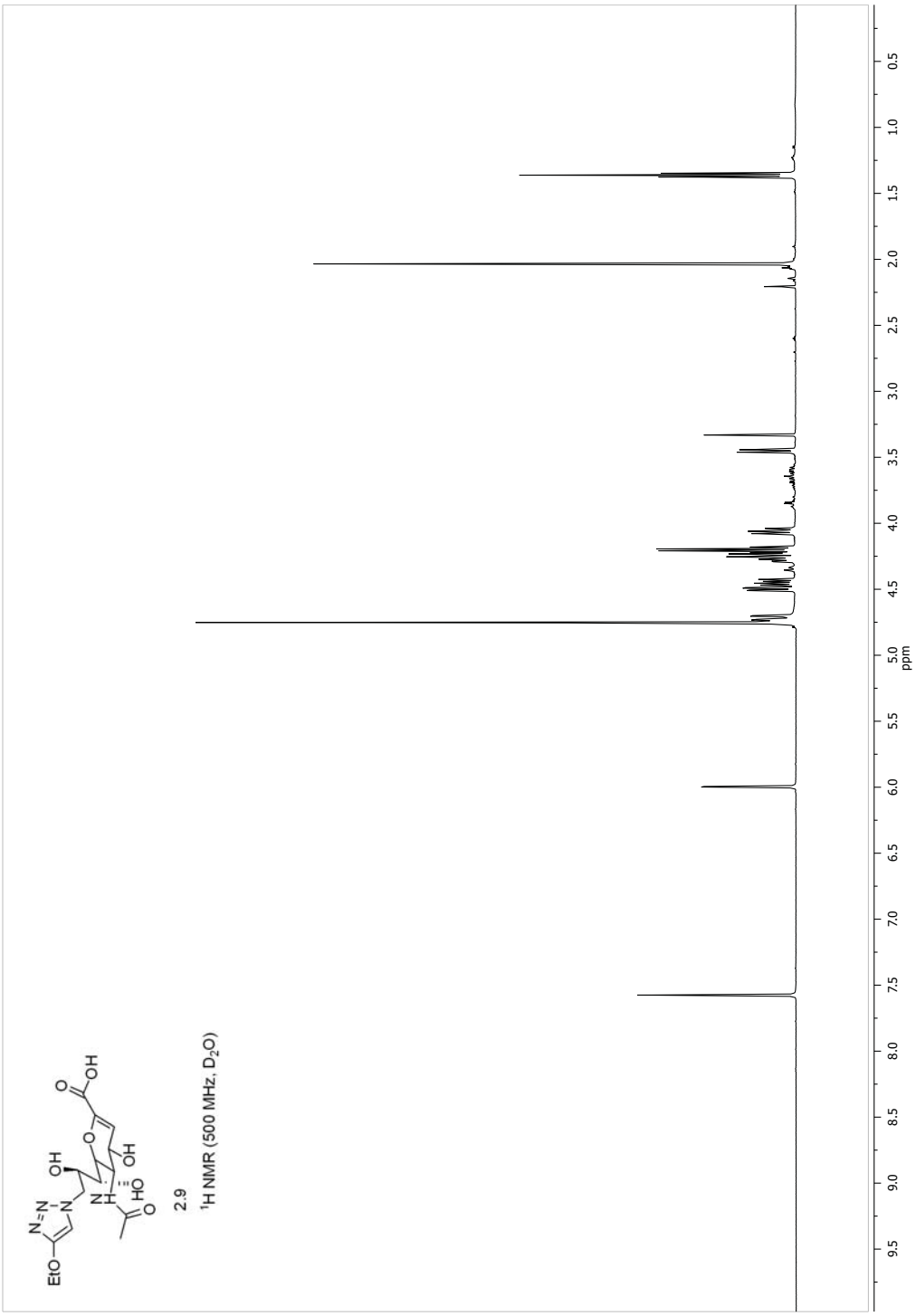
2.9
$^1$H NMR (500 MHz, $D_2O$)
ppm

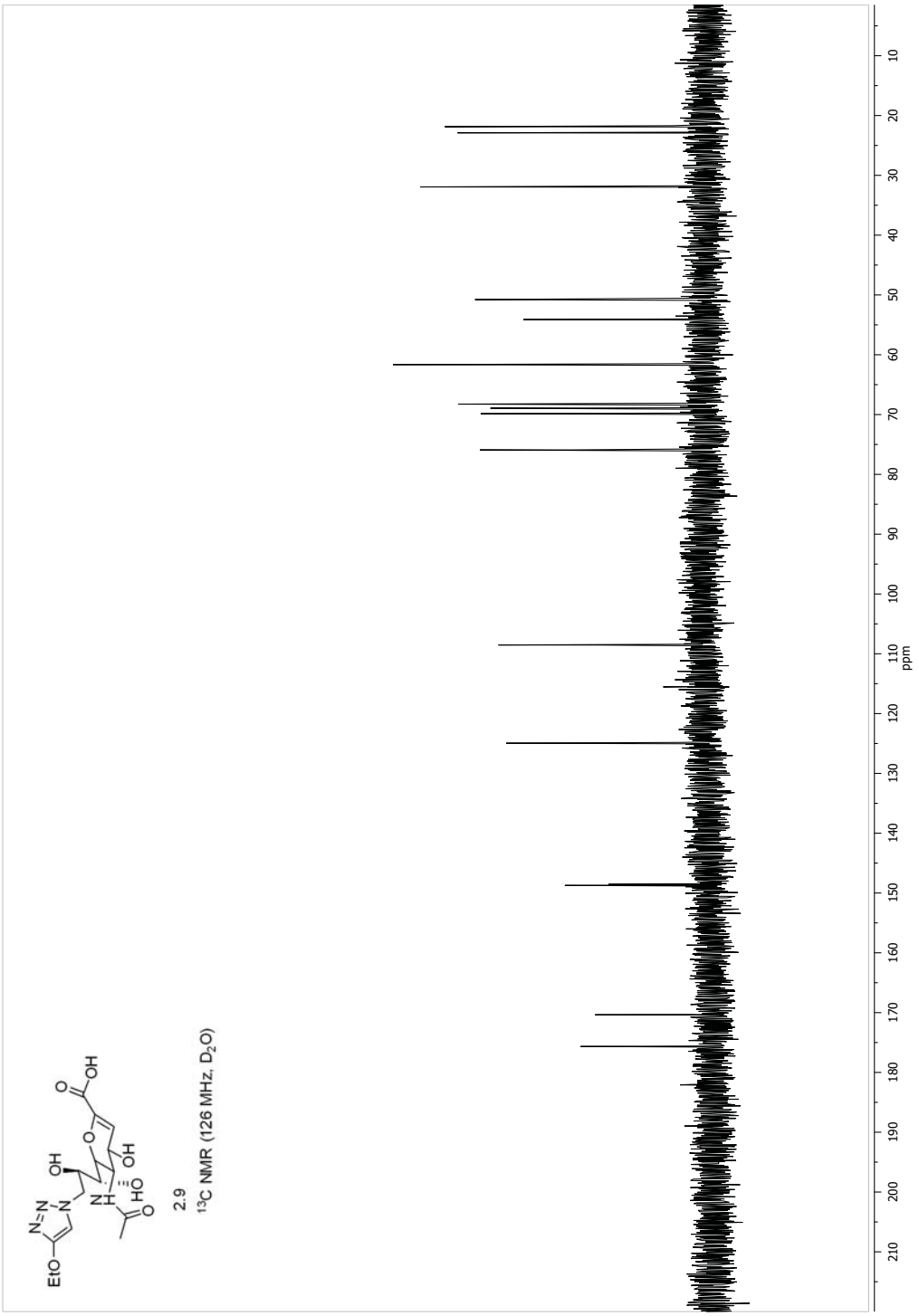
2.9
$^{13}$C NMR (126 MHz, $D_2O$)
ppm

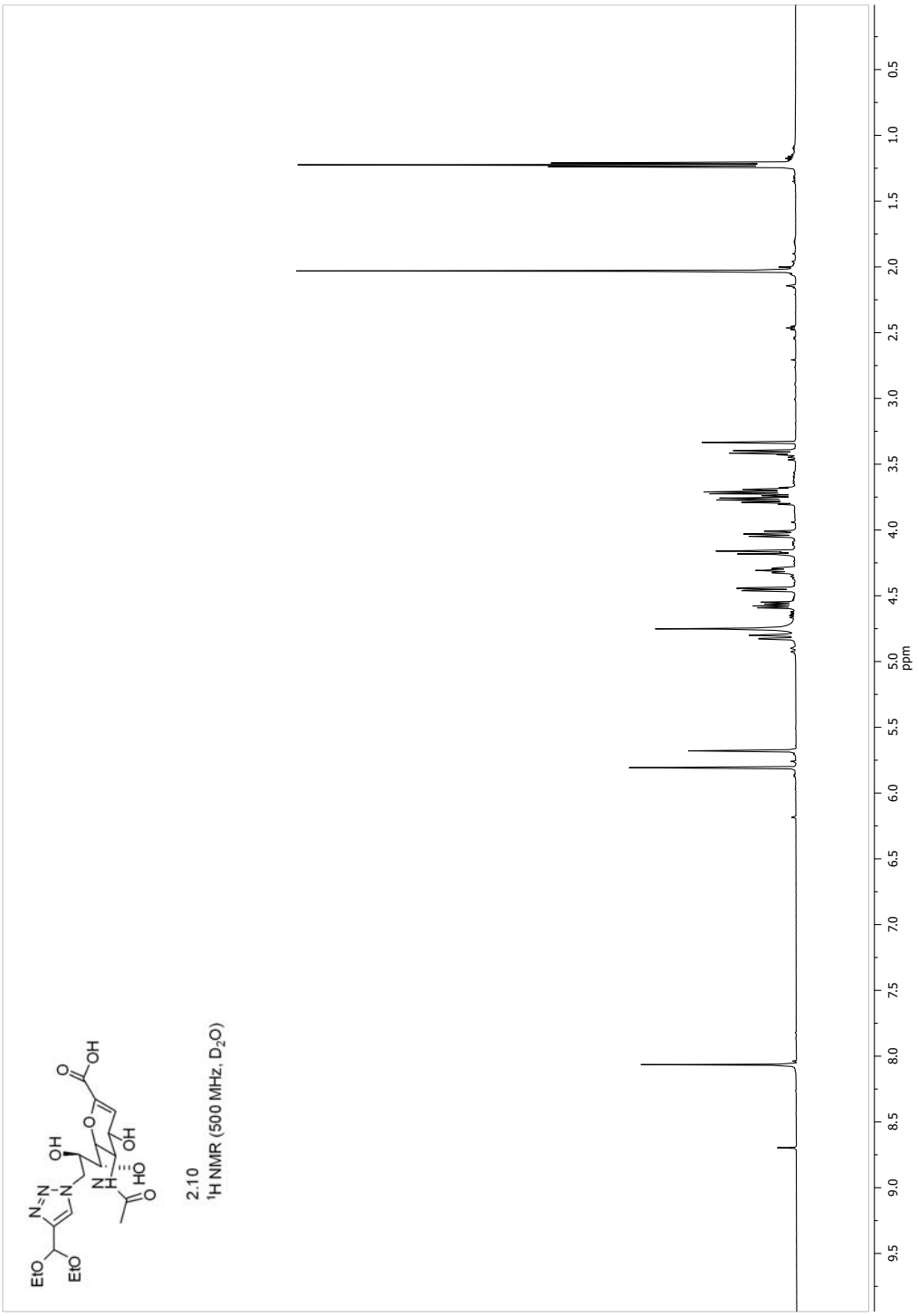
2.10
$^1$H NMR (500 MHz, $D_2O$)
ppm

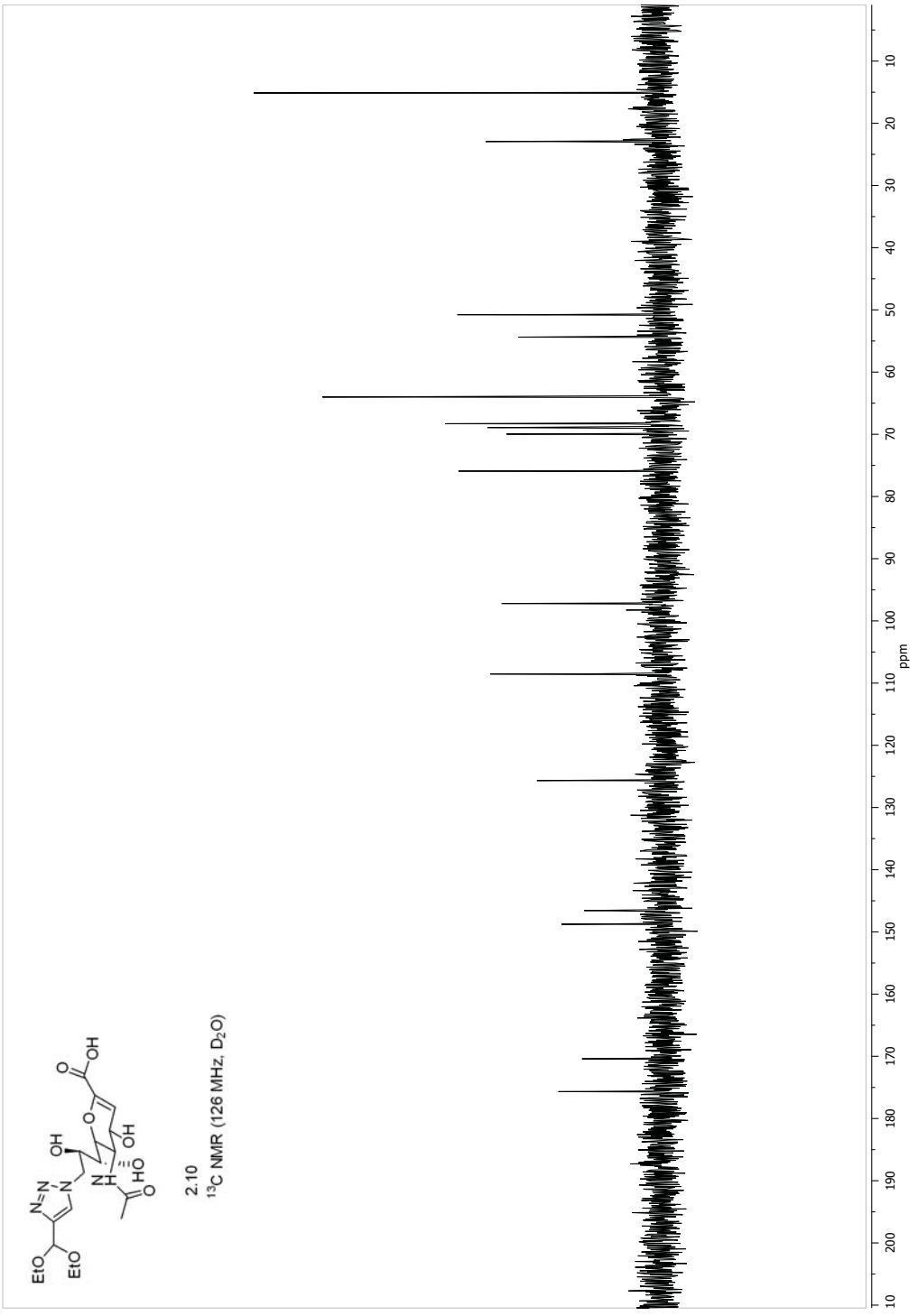
2.10
$^{13}$C NMR (126 MHz, $D_2O$)
ppm

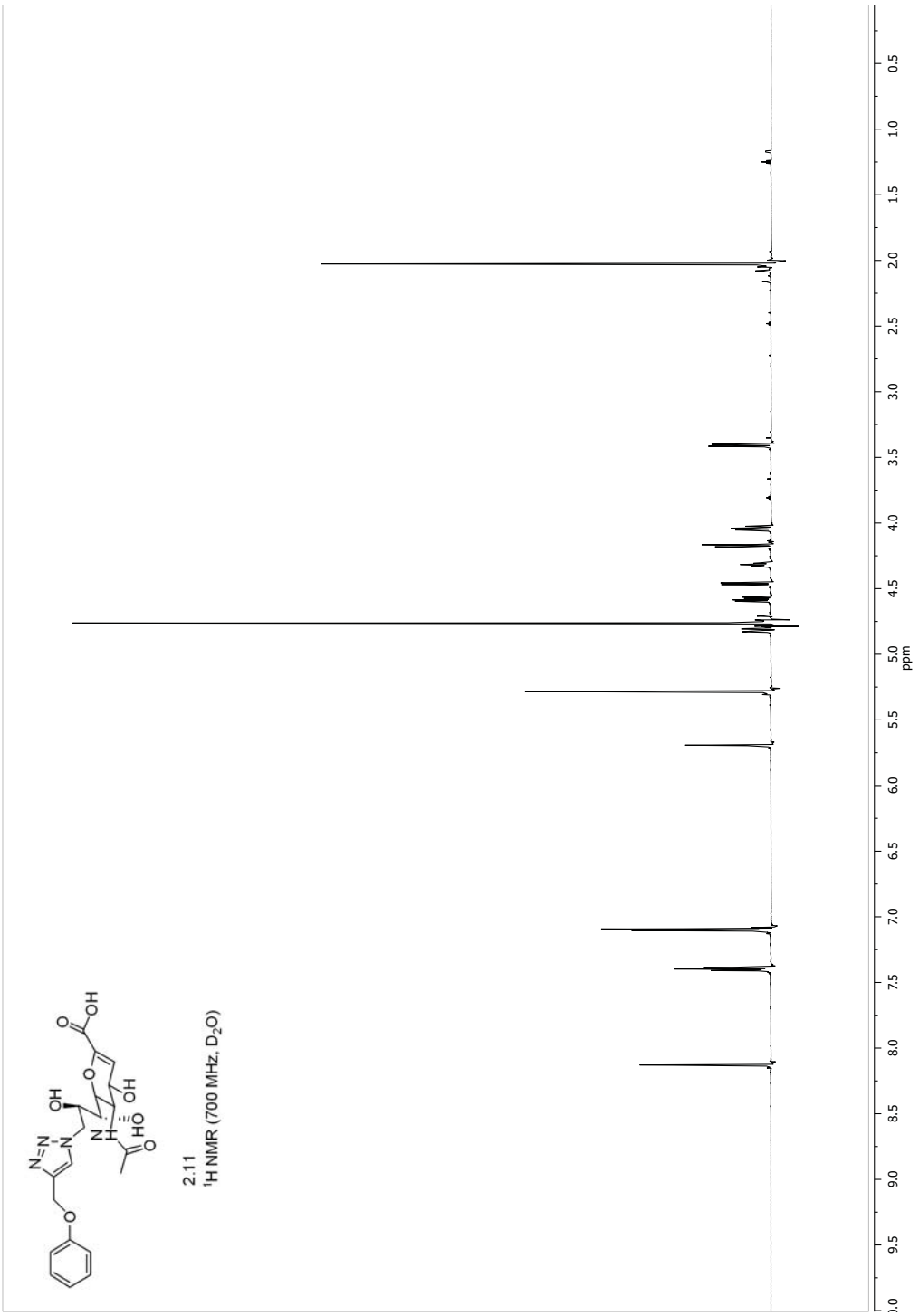
2.11
$^1$H NMR (700 MHz, $D_2O$)
ppm

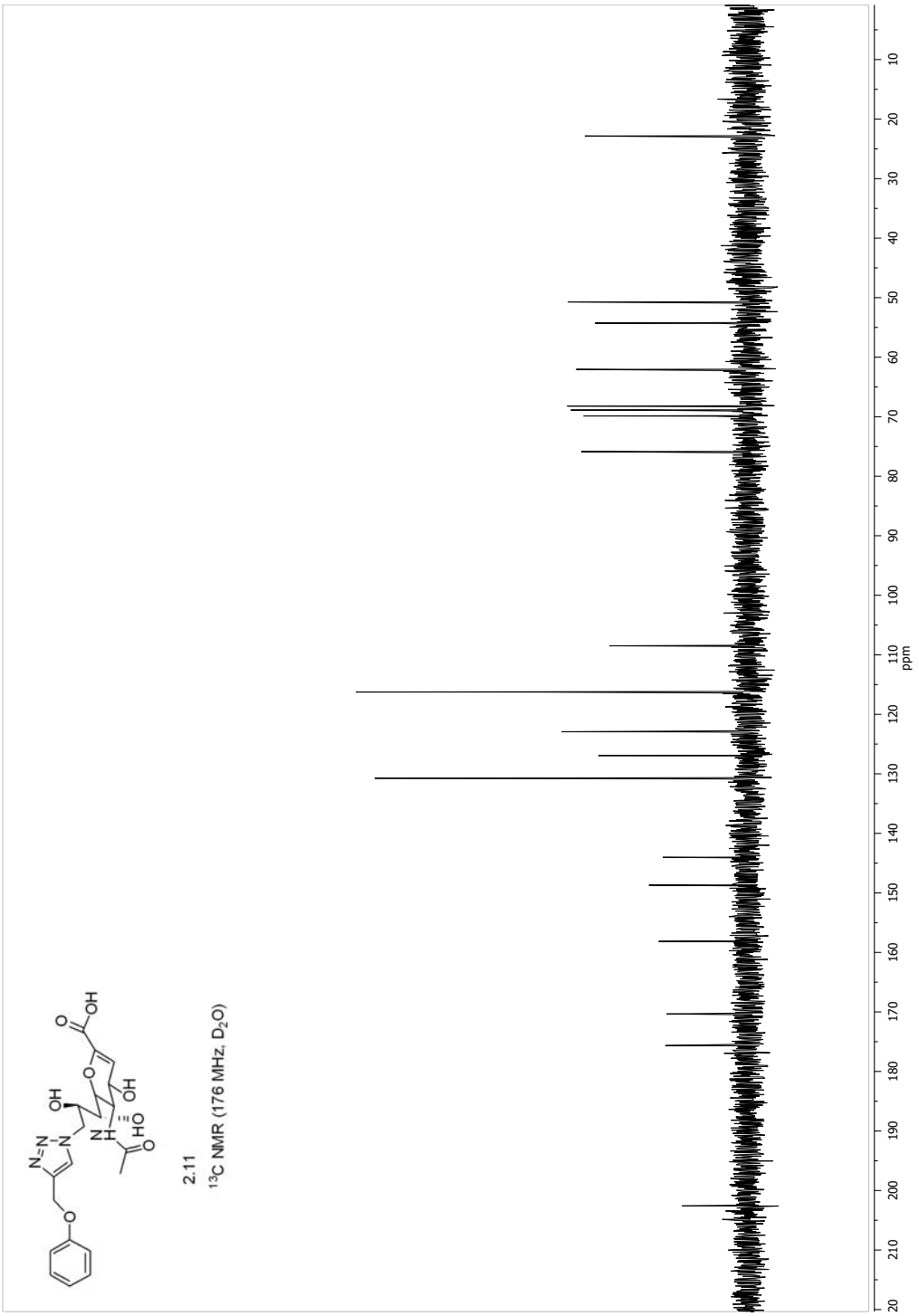
2.11
$^{13}$C NMR (176 MHz, $D_2O$)
ppm

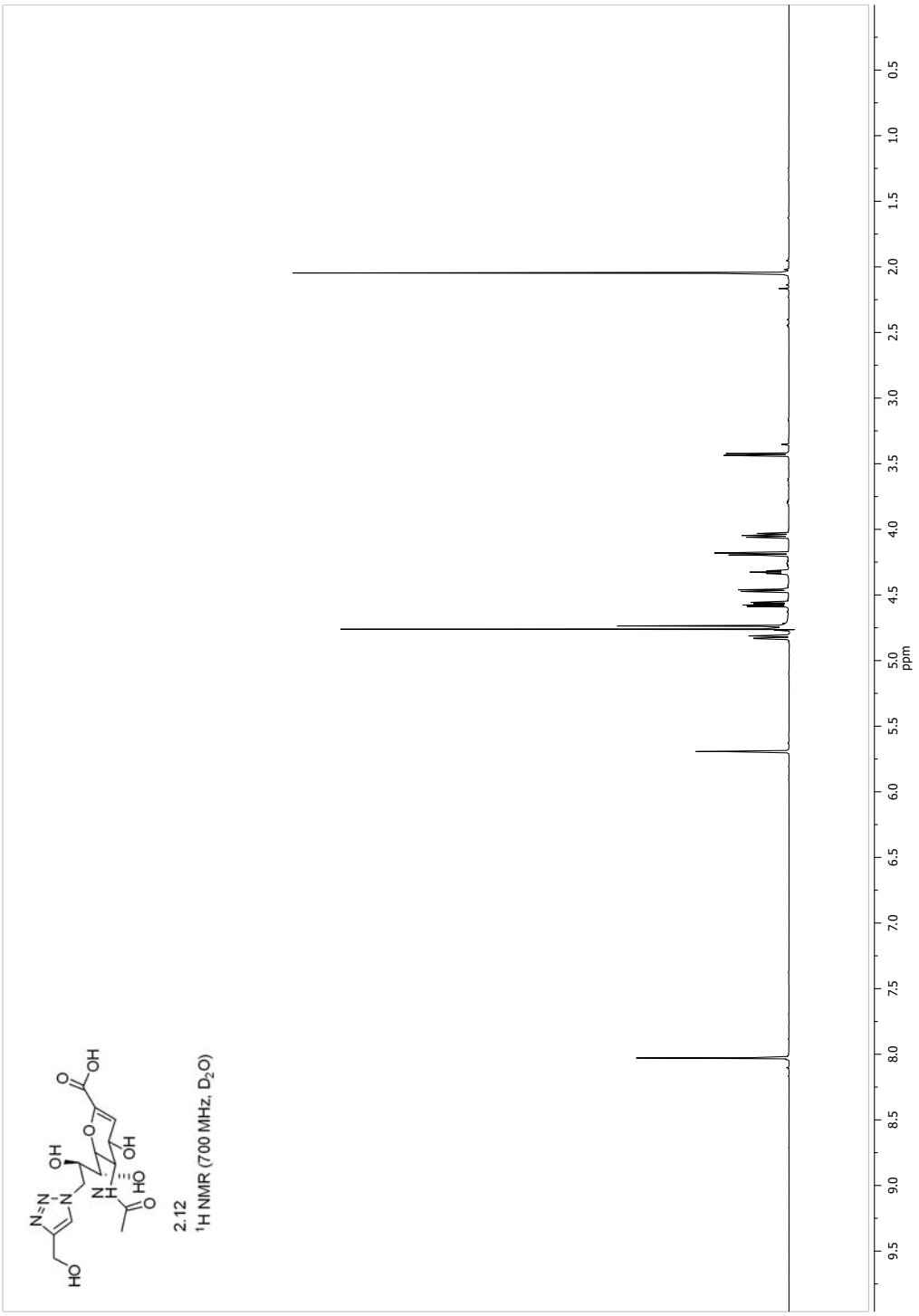
2.12
$^1$H NMR (700 MHz, $D_2O$)
ppm

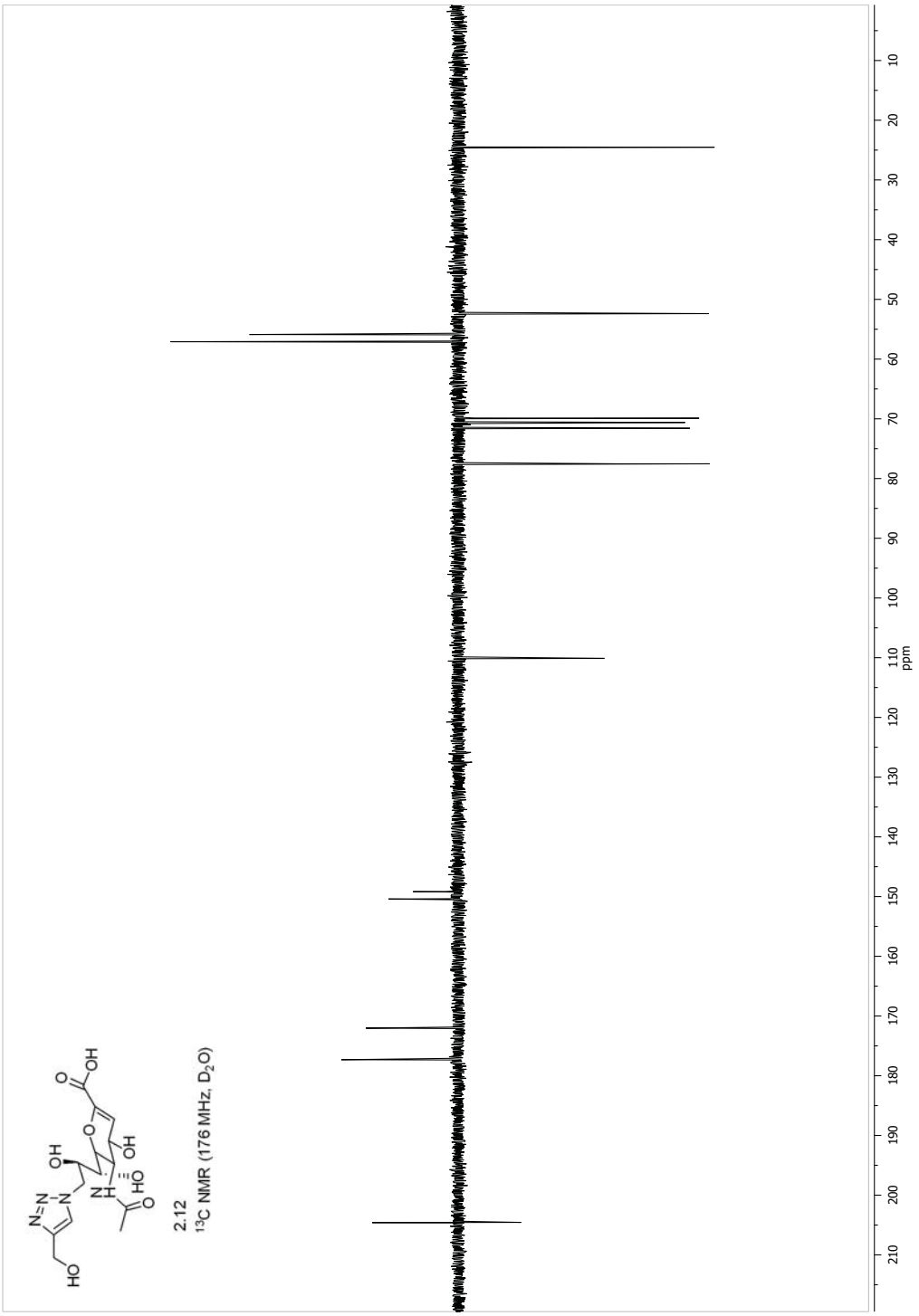
2.12
$^{13}$C NMR (176 MHz, $D_2O$)
ppm

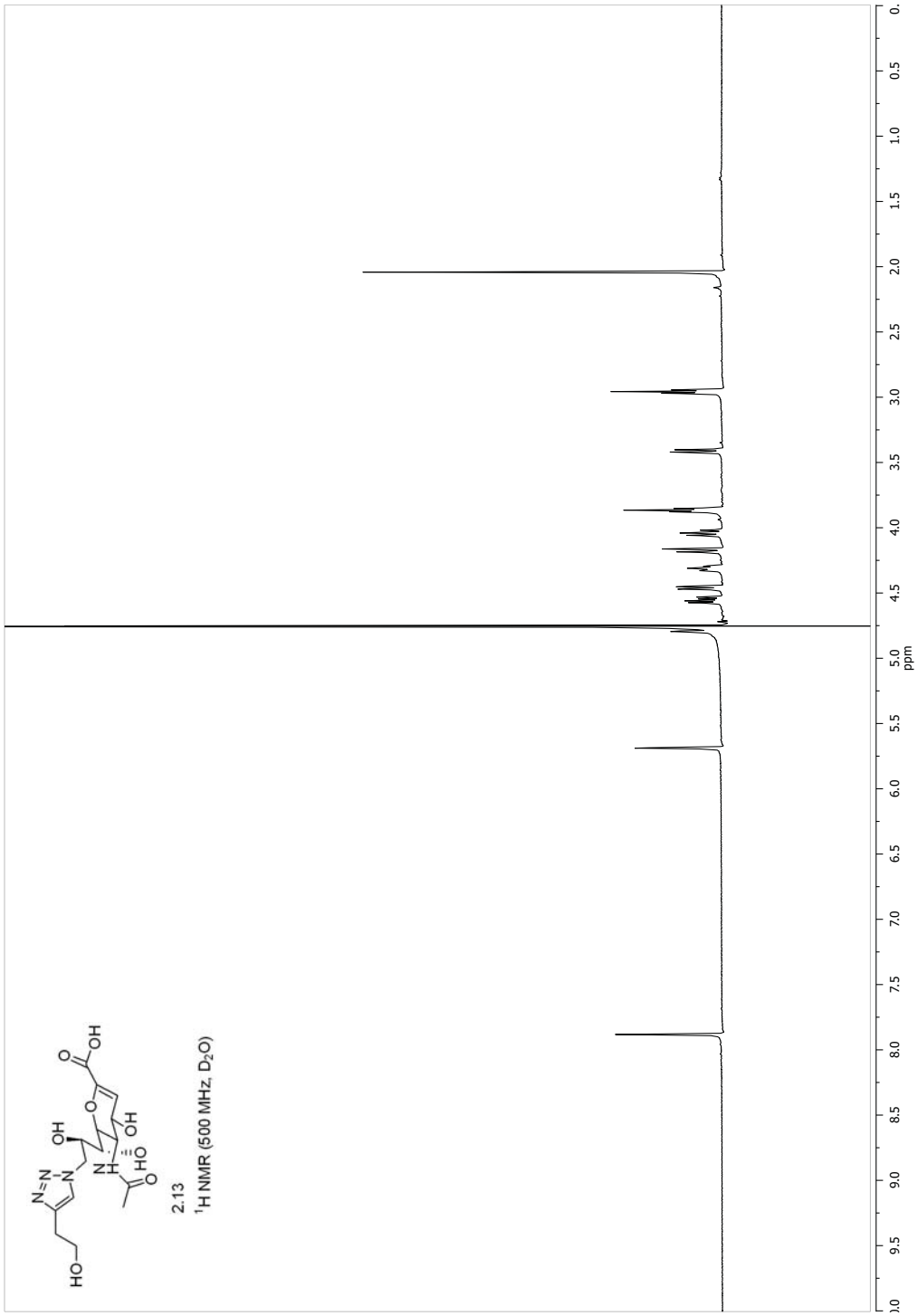
2.13
$^1$H NMR (500 MHz, $D_2O$)
ppm

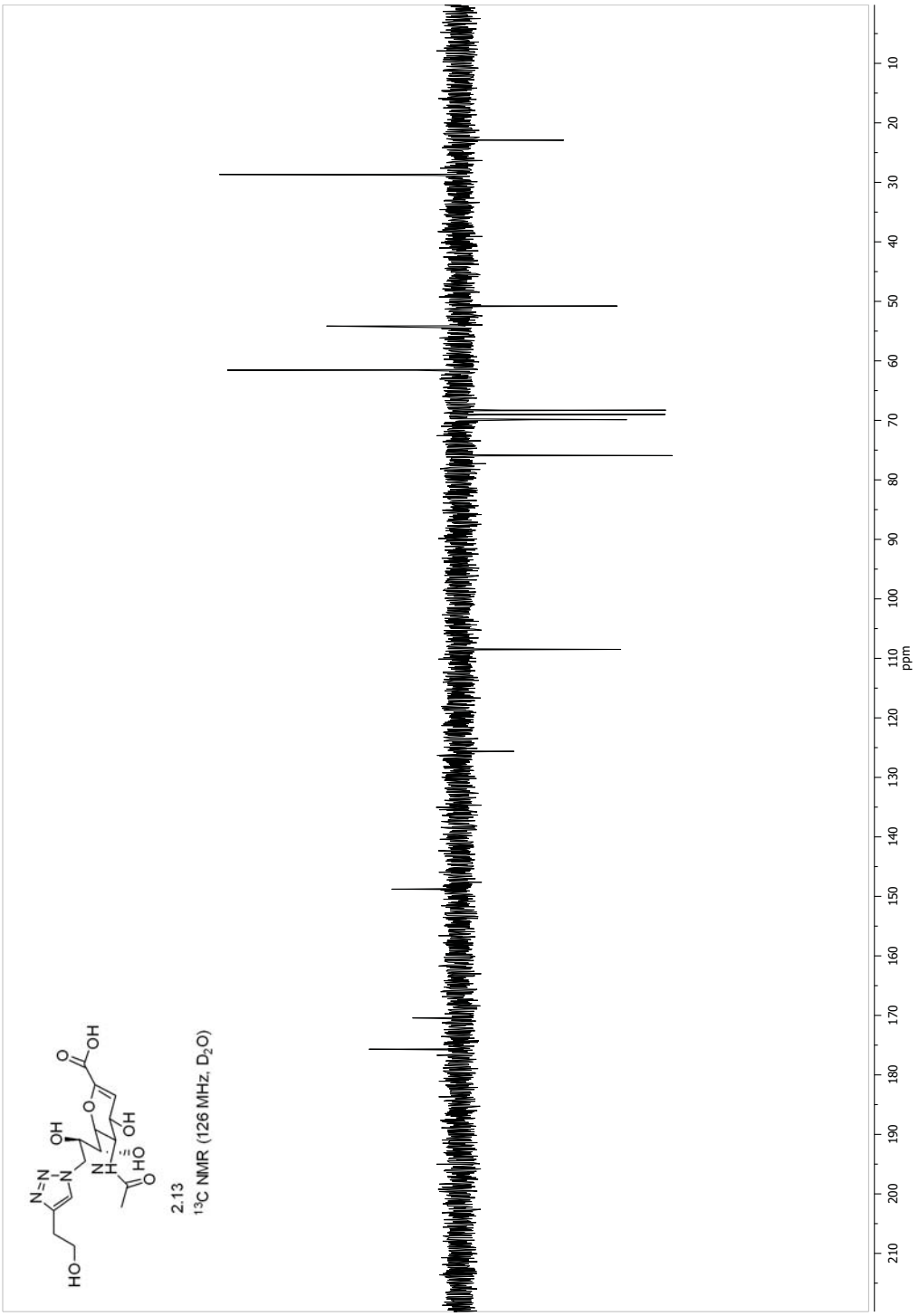
2.13
$^{13}$C NMR (126 MHz, $D_2O$)
ppm

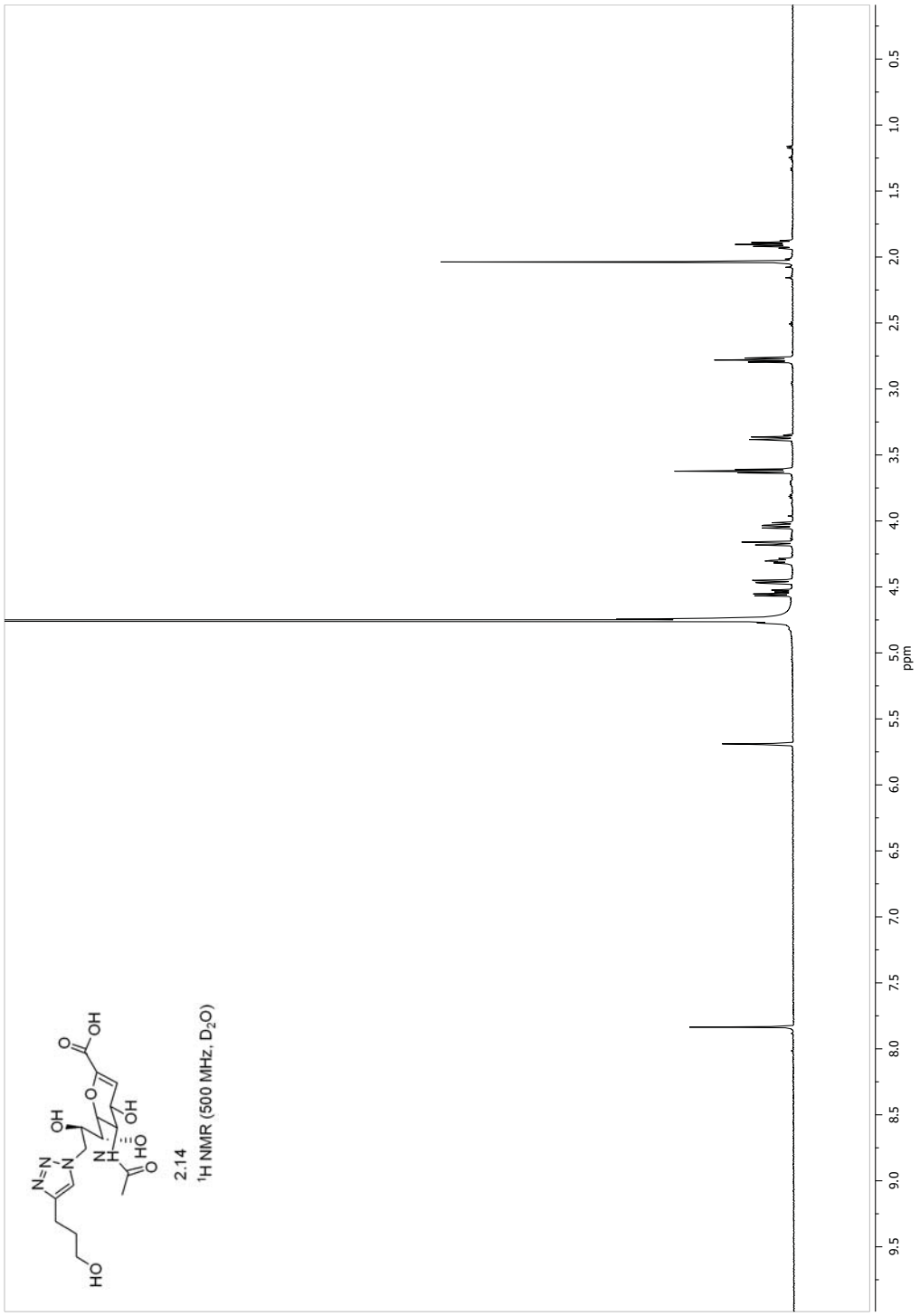
2.14
$^1$H NMR (500 MHz, $D_2O$)
ppm

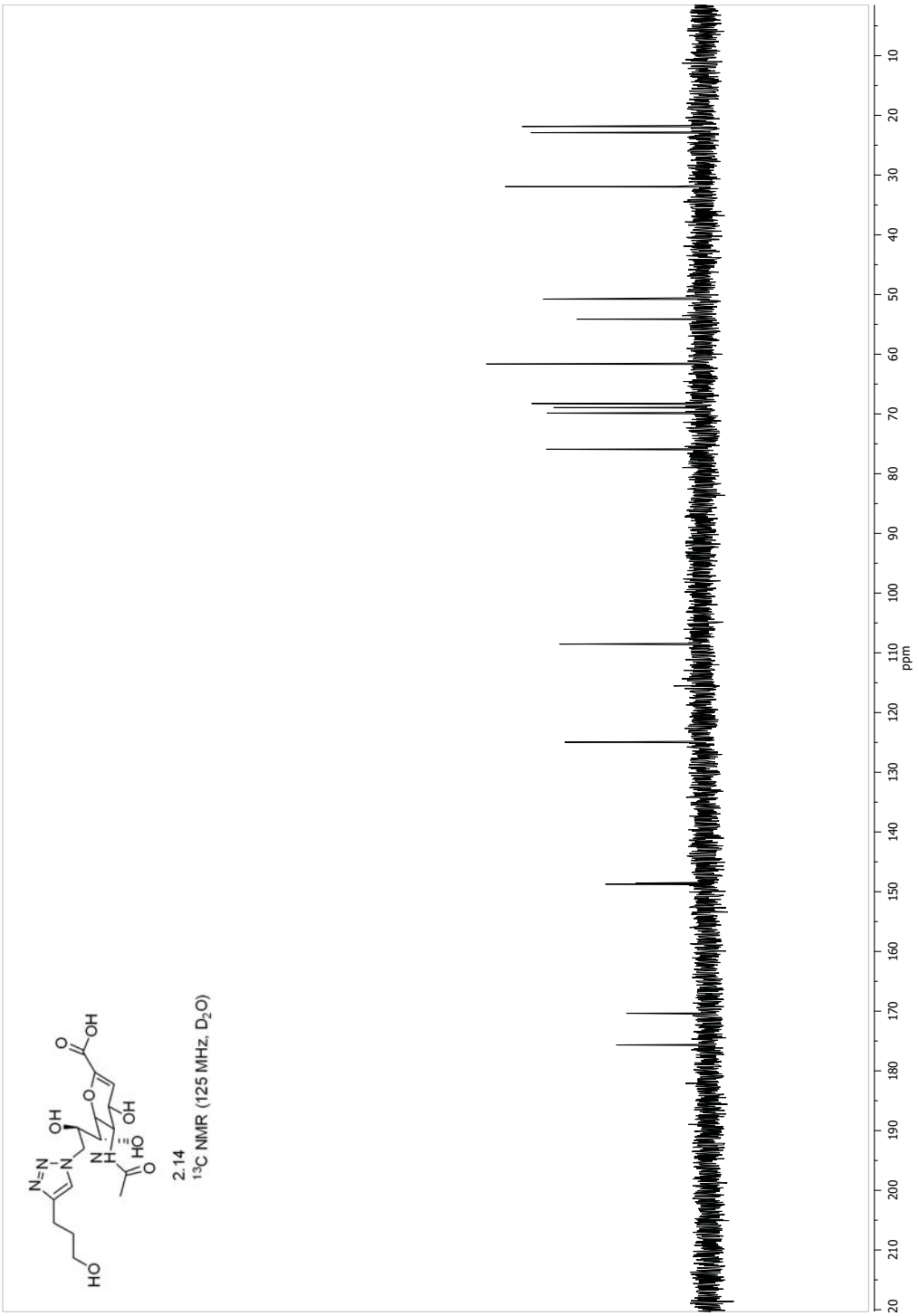
2.14
$^{13}$C NMR (125 MHz, $D_2O$)
ppm

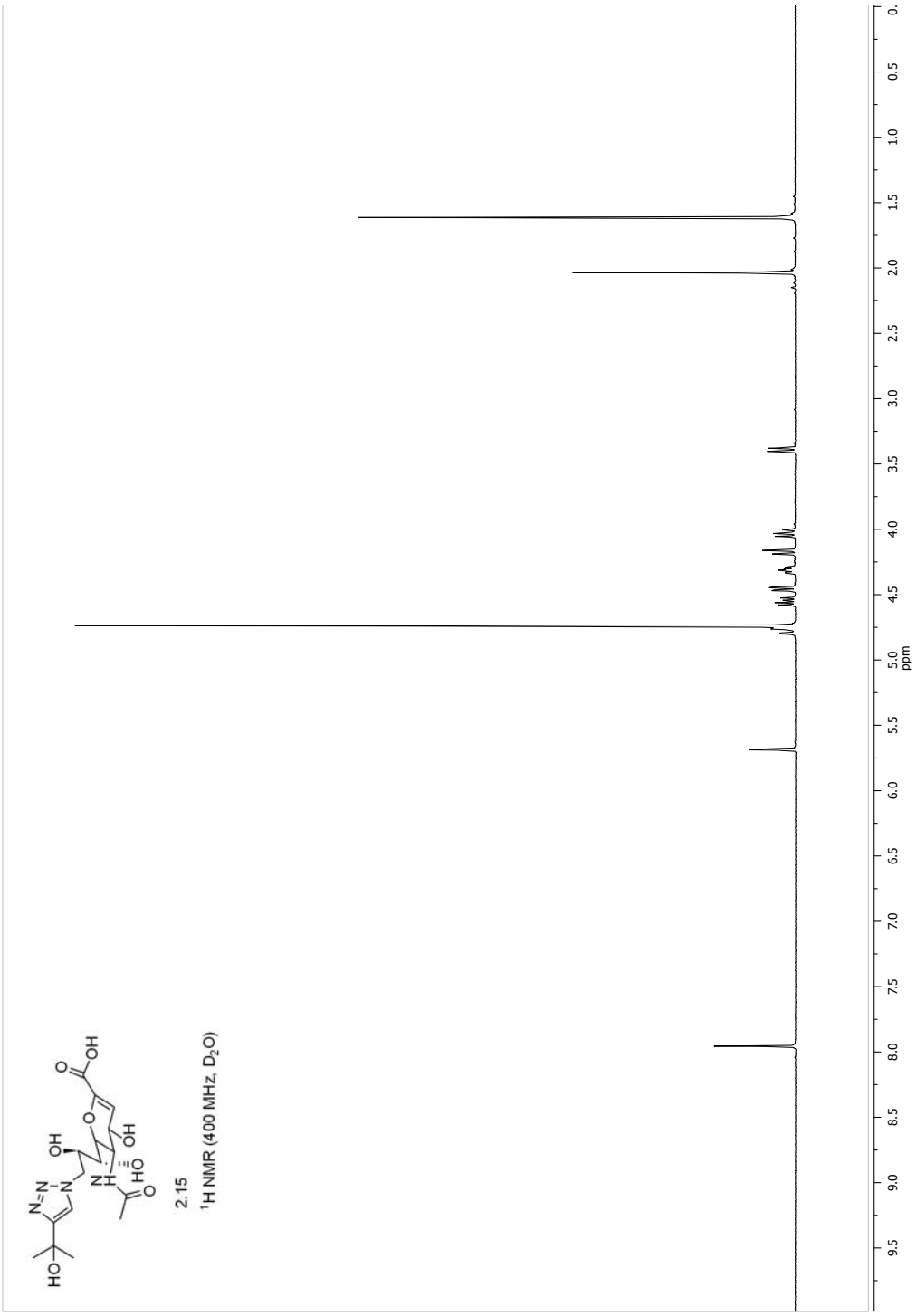
2.15
$^1$H NMR (400 MHz, $D_2O$)
ppm

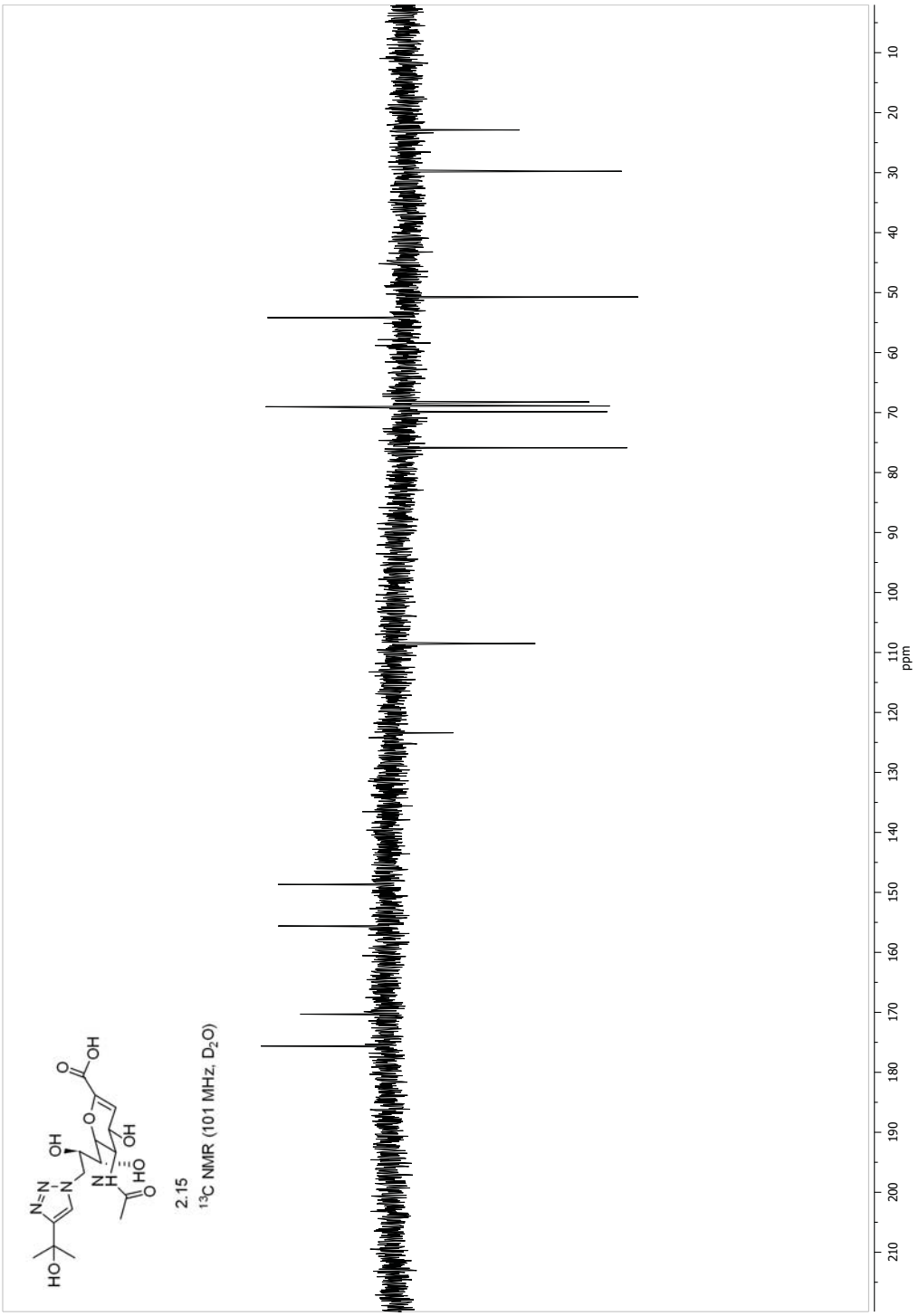
2.15
$^{13}$C NMR (101 MHz, $D_2O$)
ppm

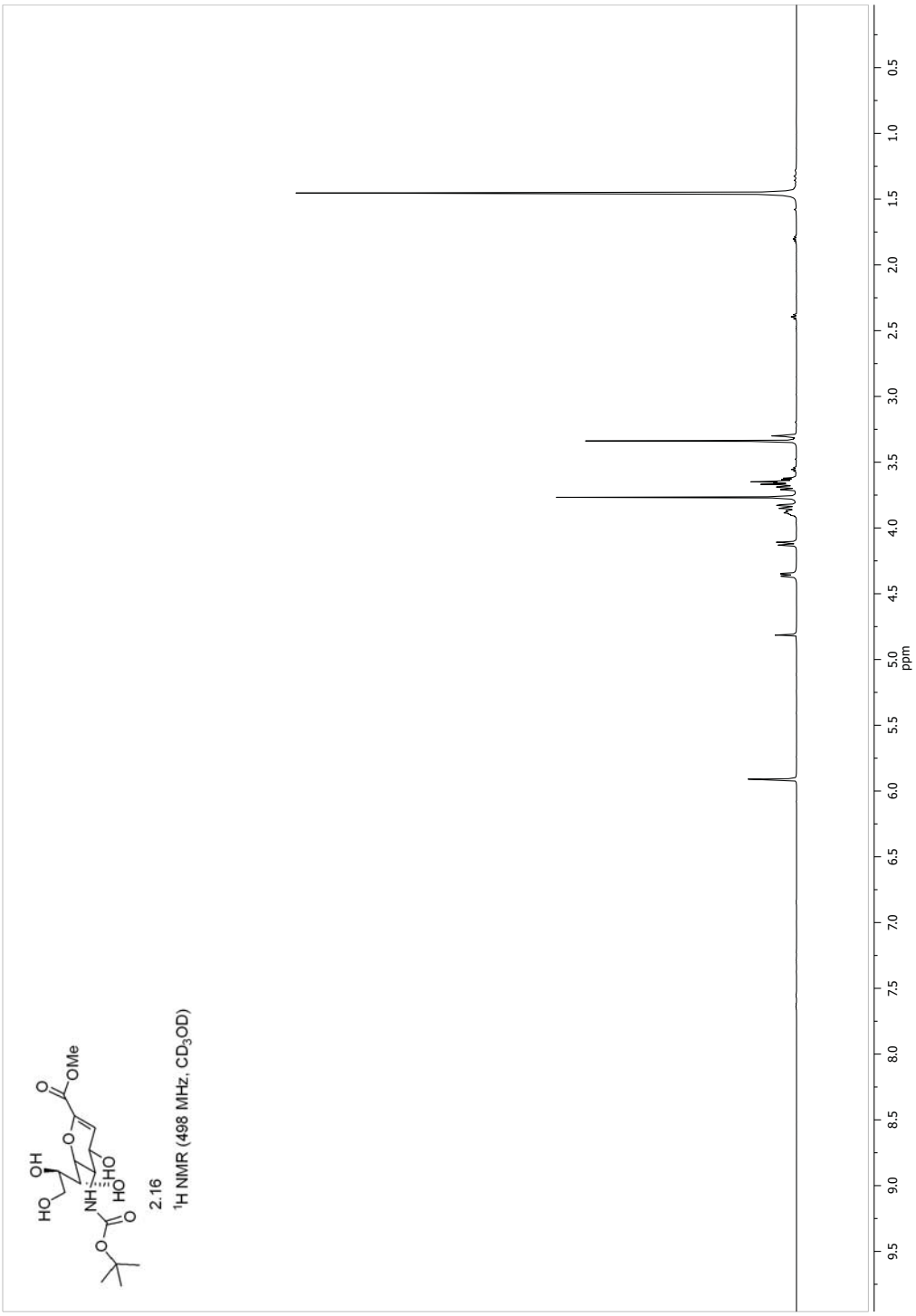
2.16
$^1$H NMR (498 MHz, $CD_3OD$)
ppm

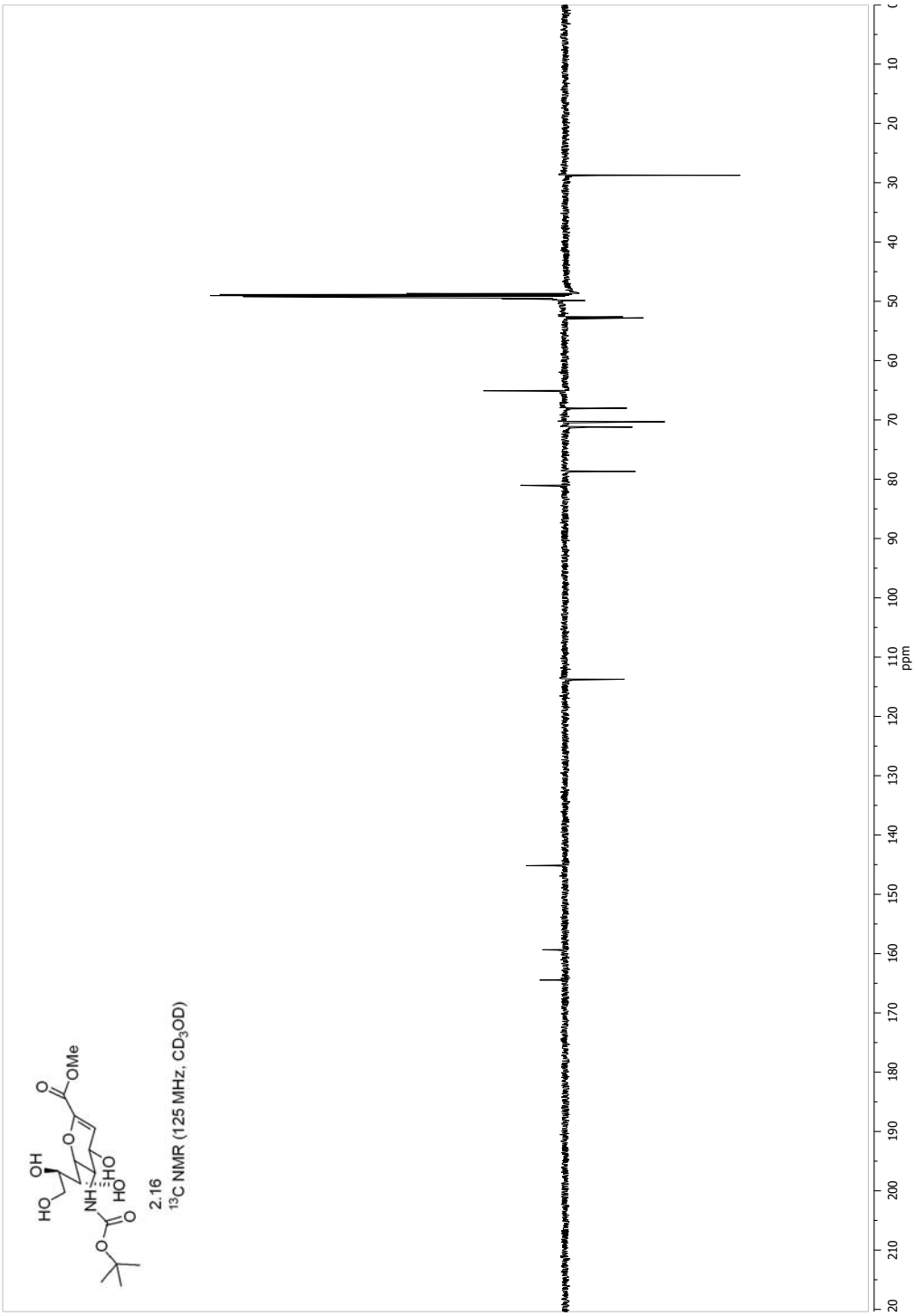
2.16
$^{13}$C NMR (125 MHz, $CD_3OD$)
ppm

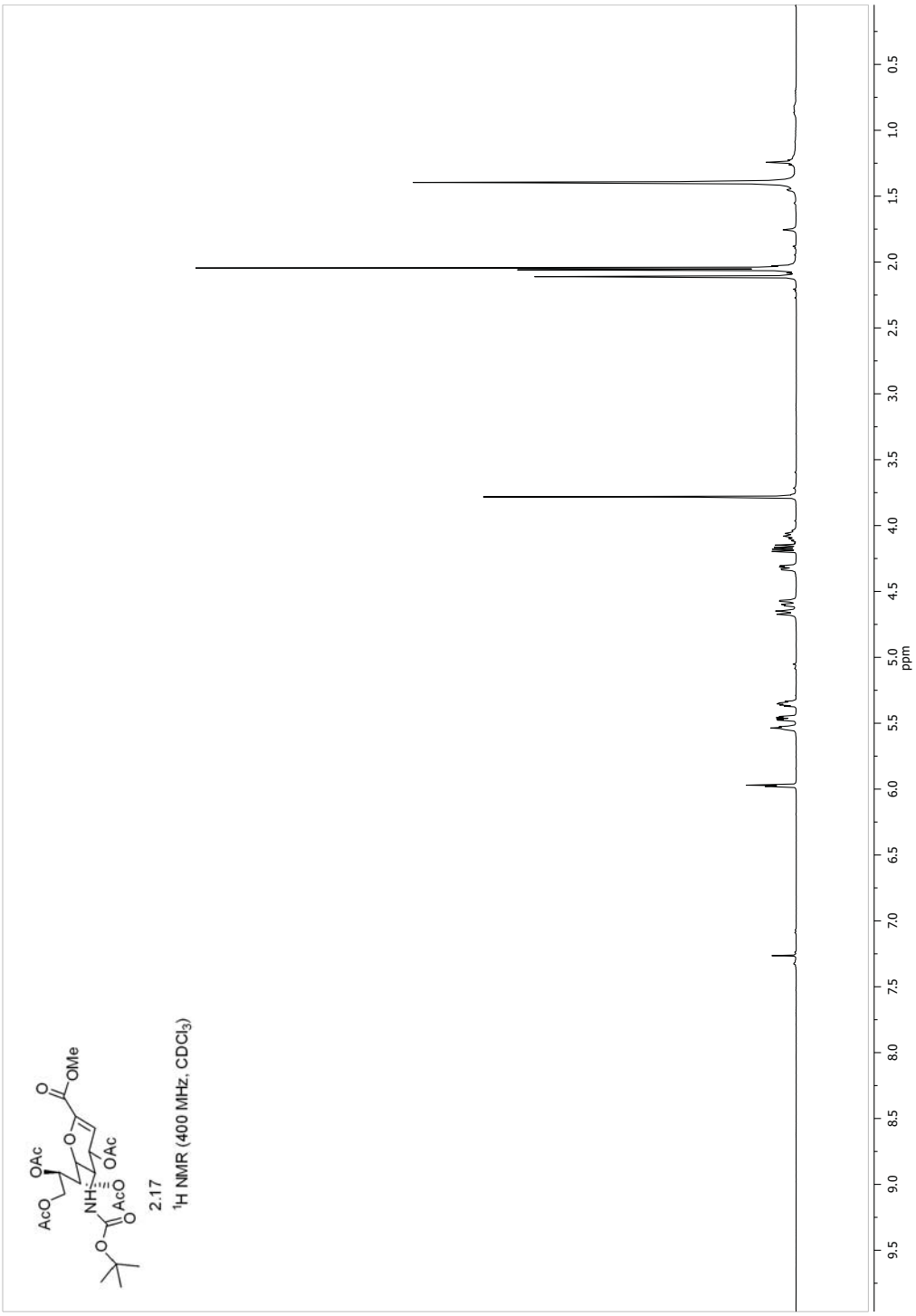
AcO
OAc
NH
AcO
OAc
OMe
O
O
O
O
O
2.17
$^1$H NMR (400 MHz, $CDCl_3$)
9.5
9.0
8.5
8.0
7.5
7.0
6.5
6.0
5.5
5.0
4.5
4.0
3.5
3.0
2.5
2.0
1.5
1.0
0.5
ppm

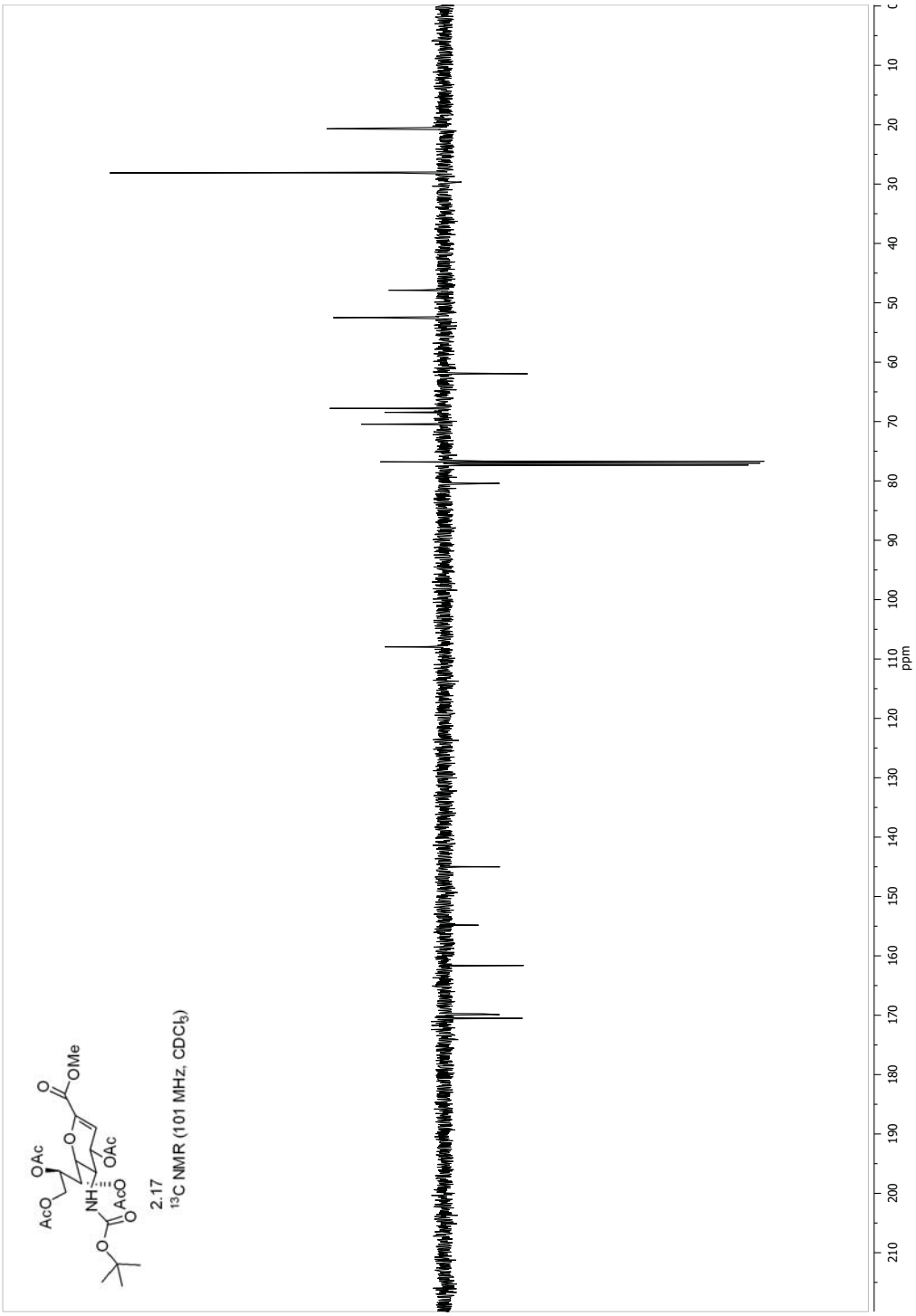
2.17
$^{13}$C NMR (101 MHz, $CDCl_3$)
ppm

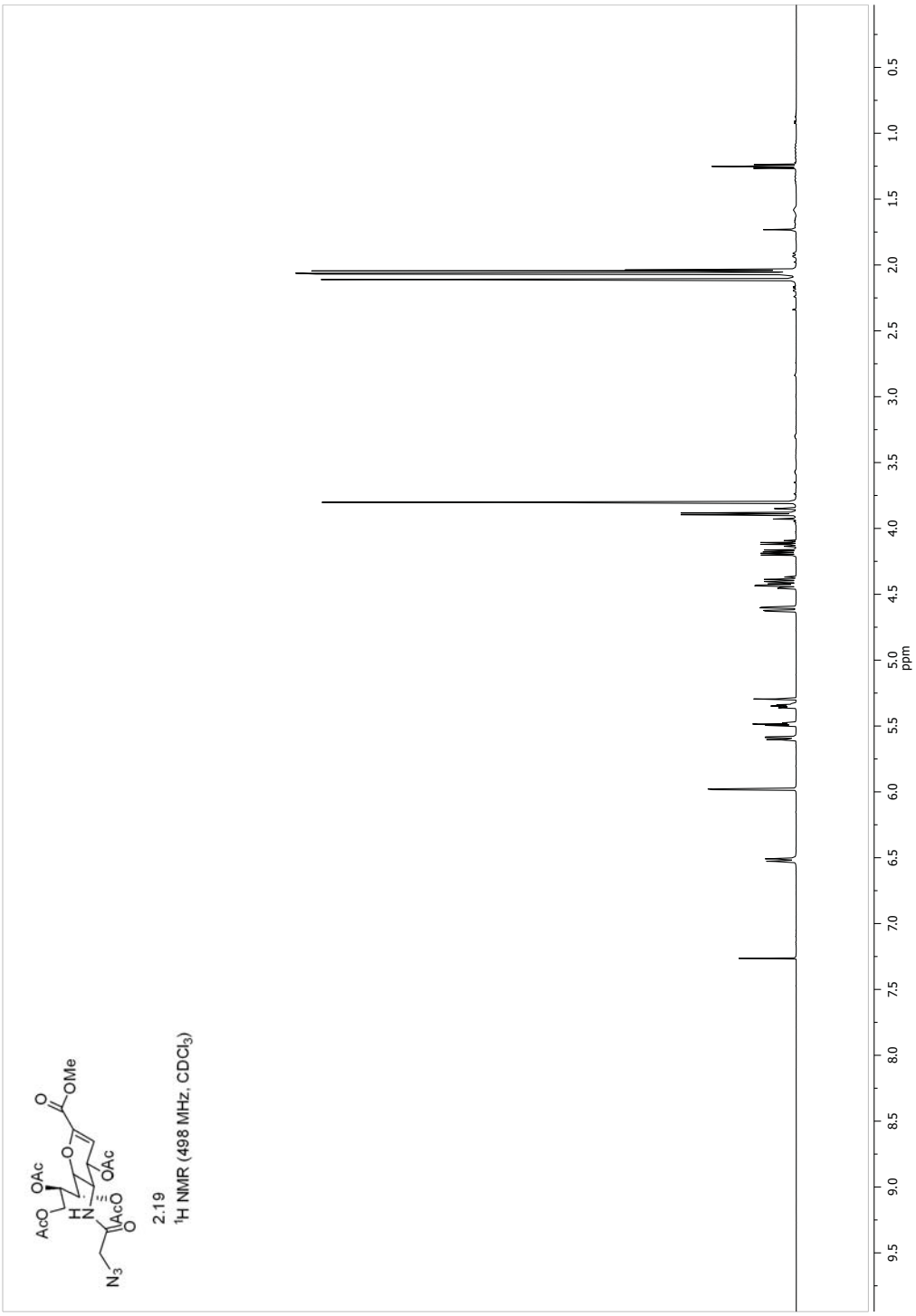
AcO
OAc
O
OMe
OAc
AcO
N3
2.19
1H NMR (498 MHz, CDCl3)
9.5
9.0
8.5
8.0
7.5
7.0
6.5
6.0
5.5
5.0
4.5
4.0
3.5
3.0
2.5
2.0
1.5
1.0
0.5
ppm

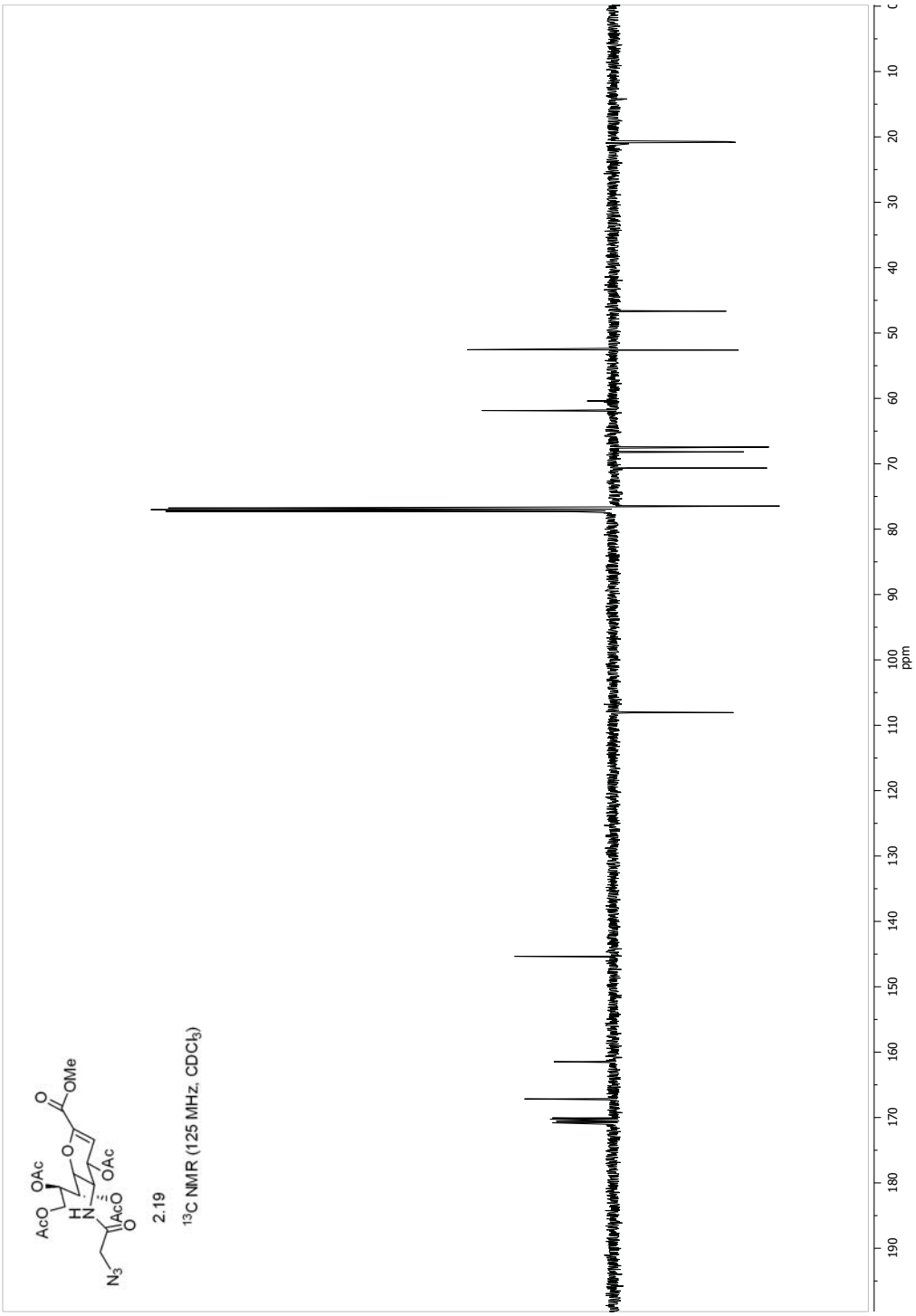
2.19
$^{13}$C NMR (125 MHz, $CDCl_3$)
ppm

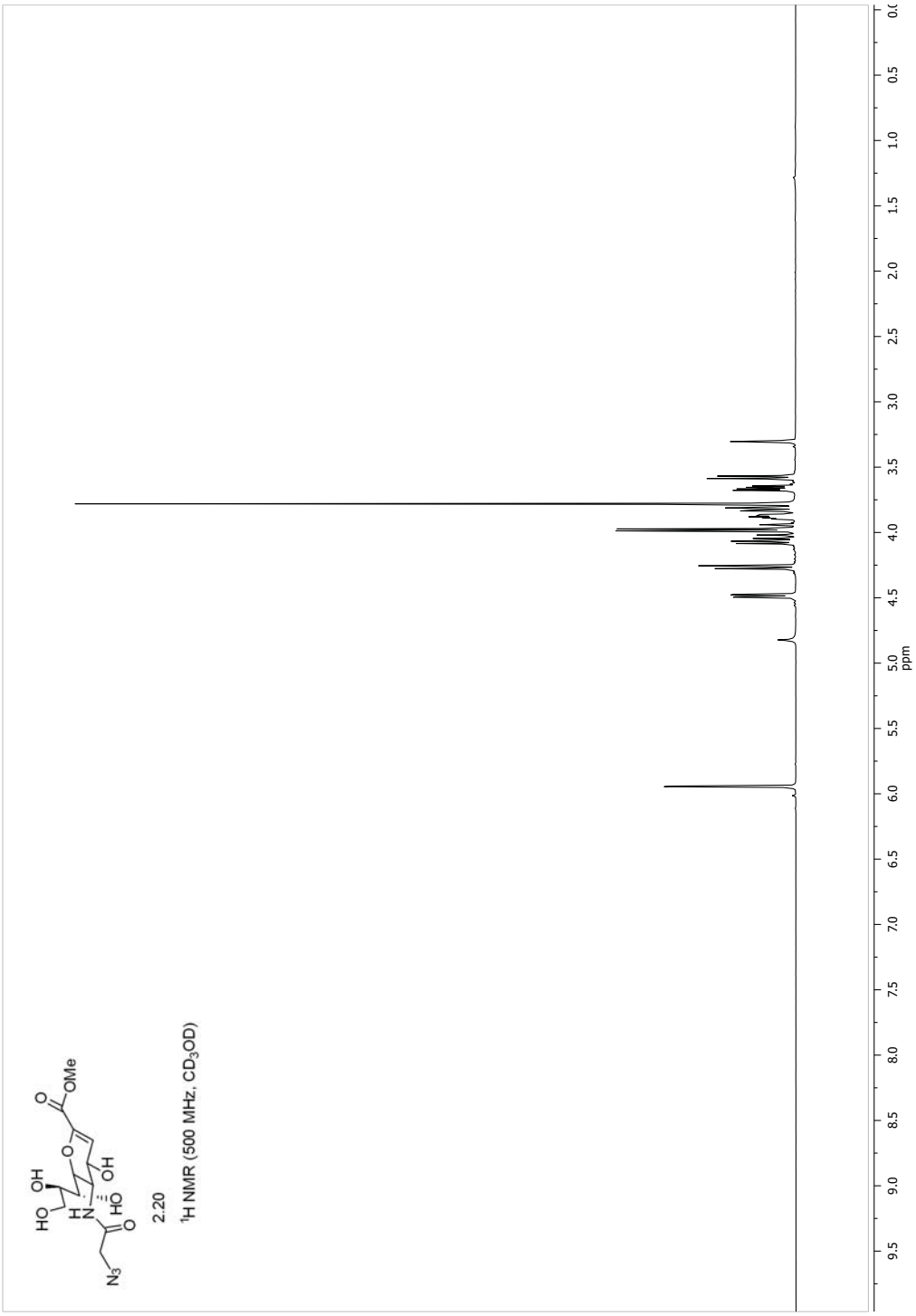
2.20
$^1$H NMR (500 MHz, $CD_3OD$)
ppm

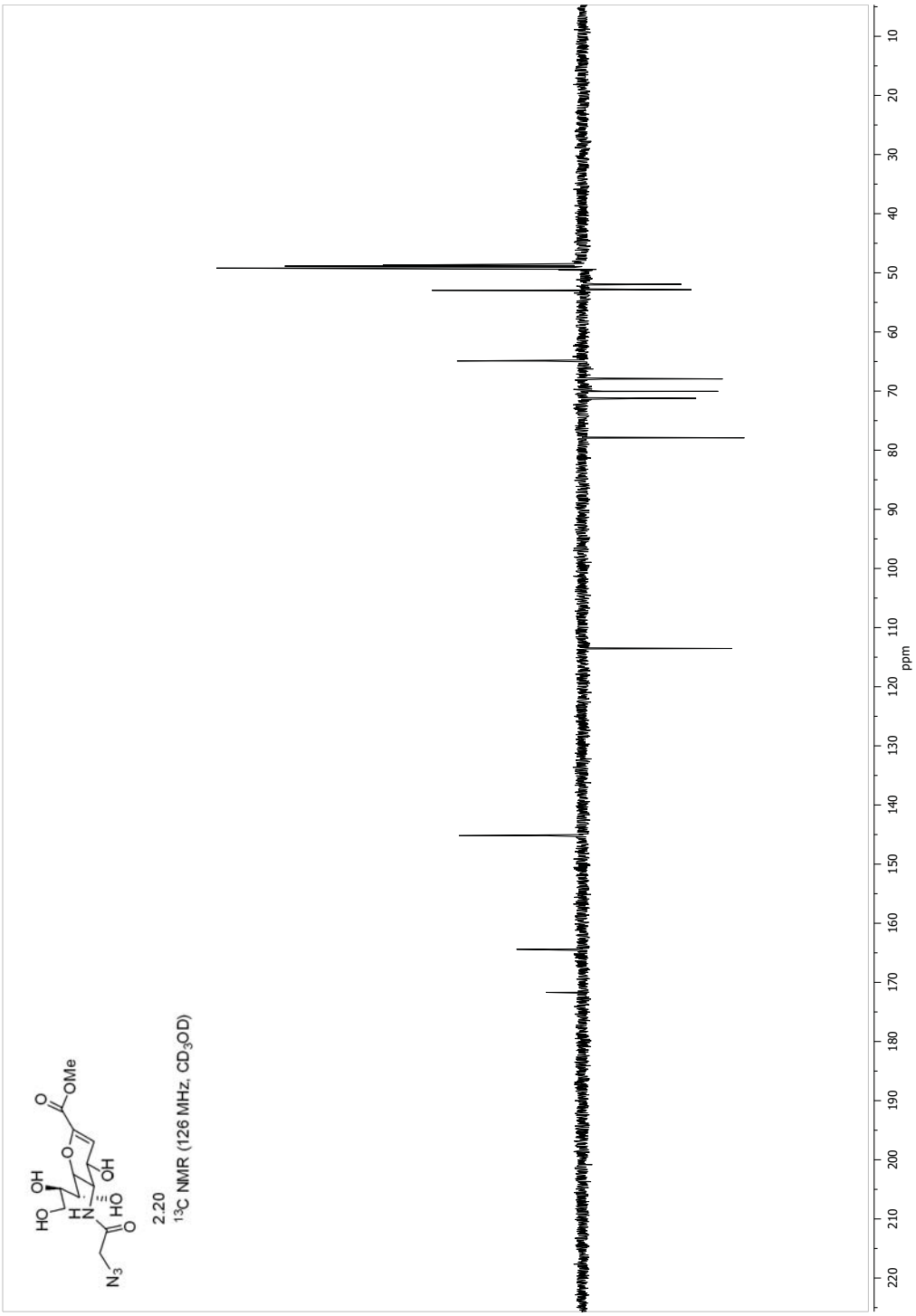
2.20
$^{13}$C NMR (126 MHz, $CD_3OD$)
ppm

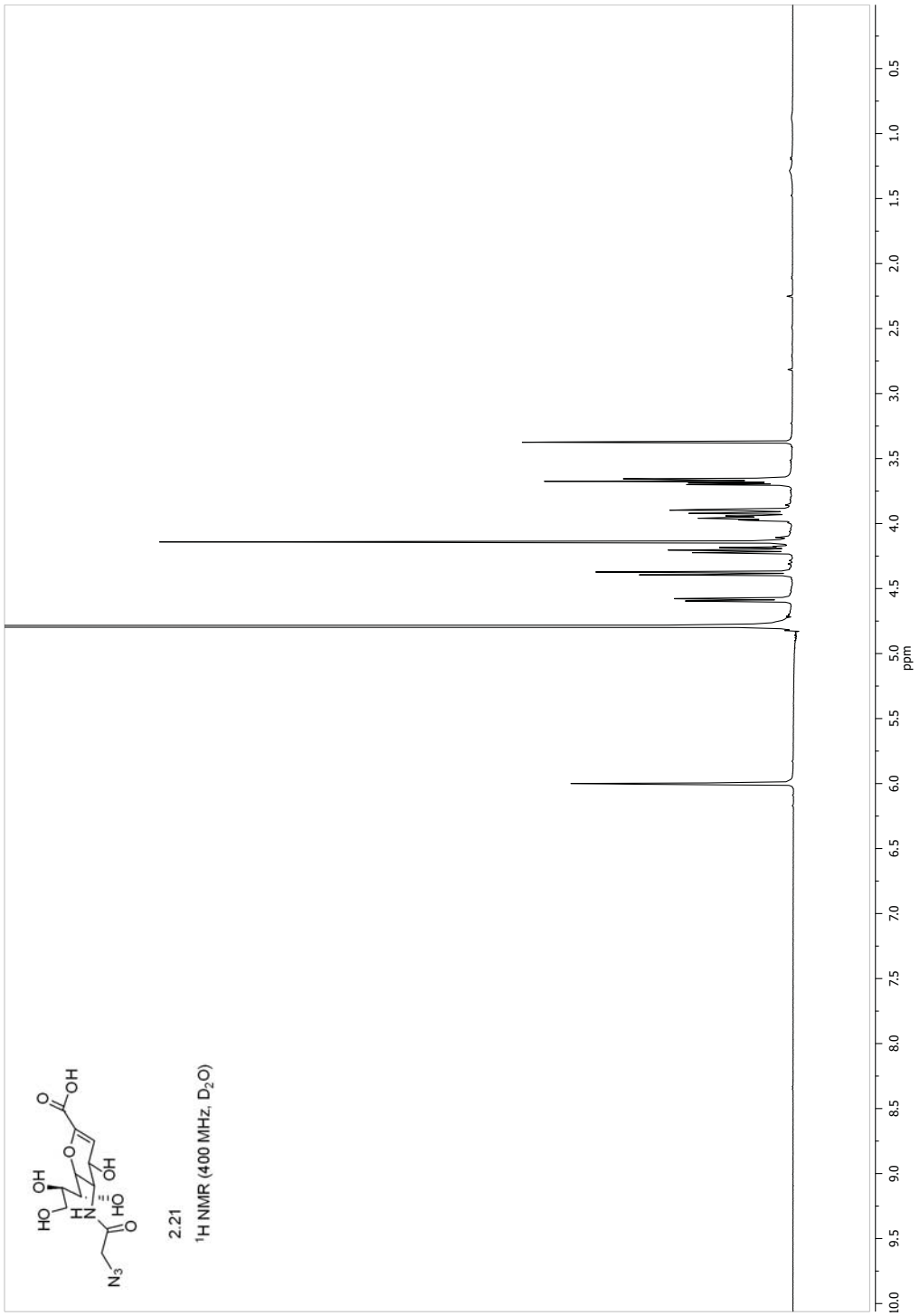
2.21
$^1$H NMR (400 MHz, $D_2O$)
ppm

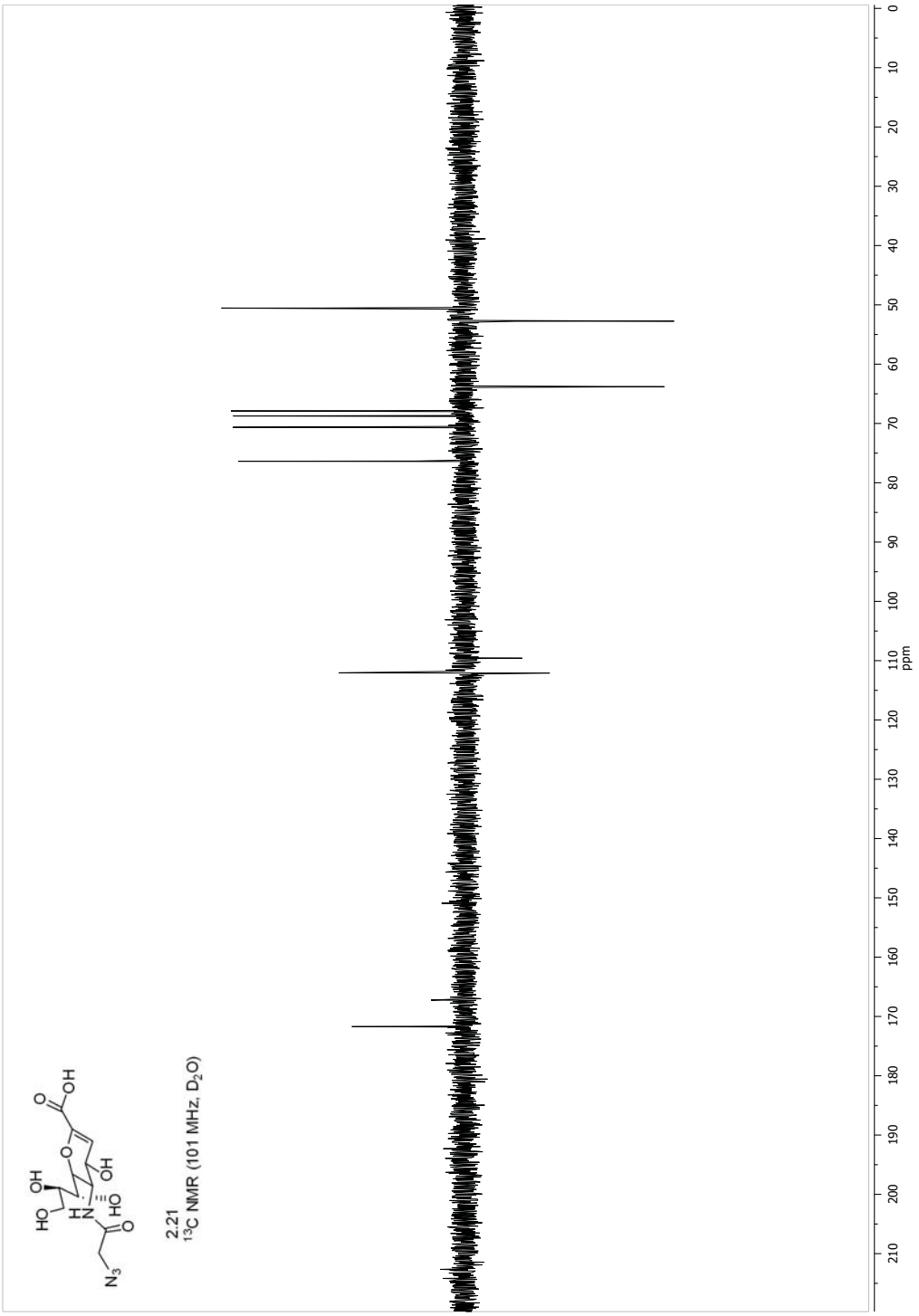
2.21
$^{13}$C NMR (101 MHz, $D_2O$)
ppm

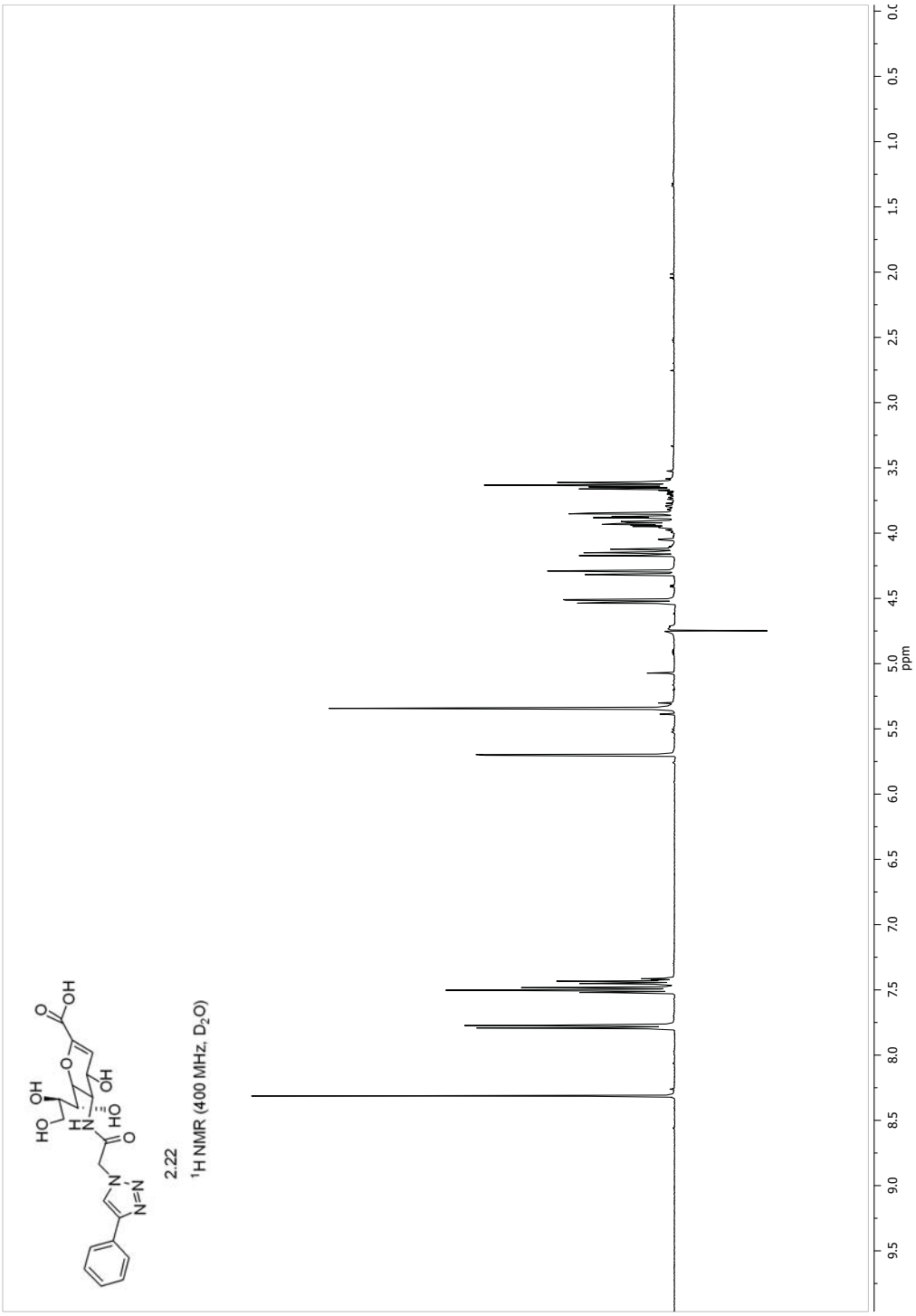
2.22
$^1$H NMR (400 MHz, $D_2O$)
ppm

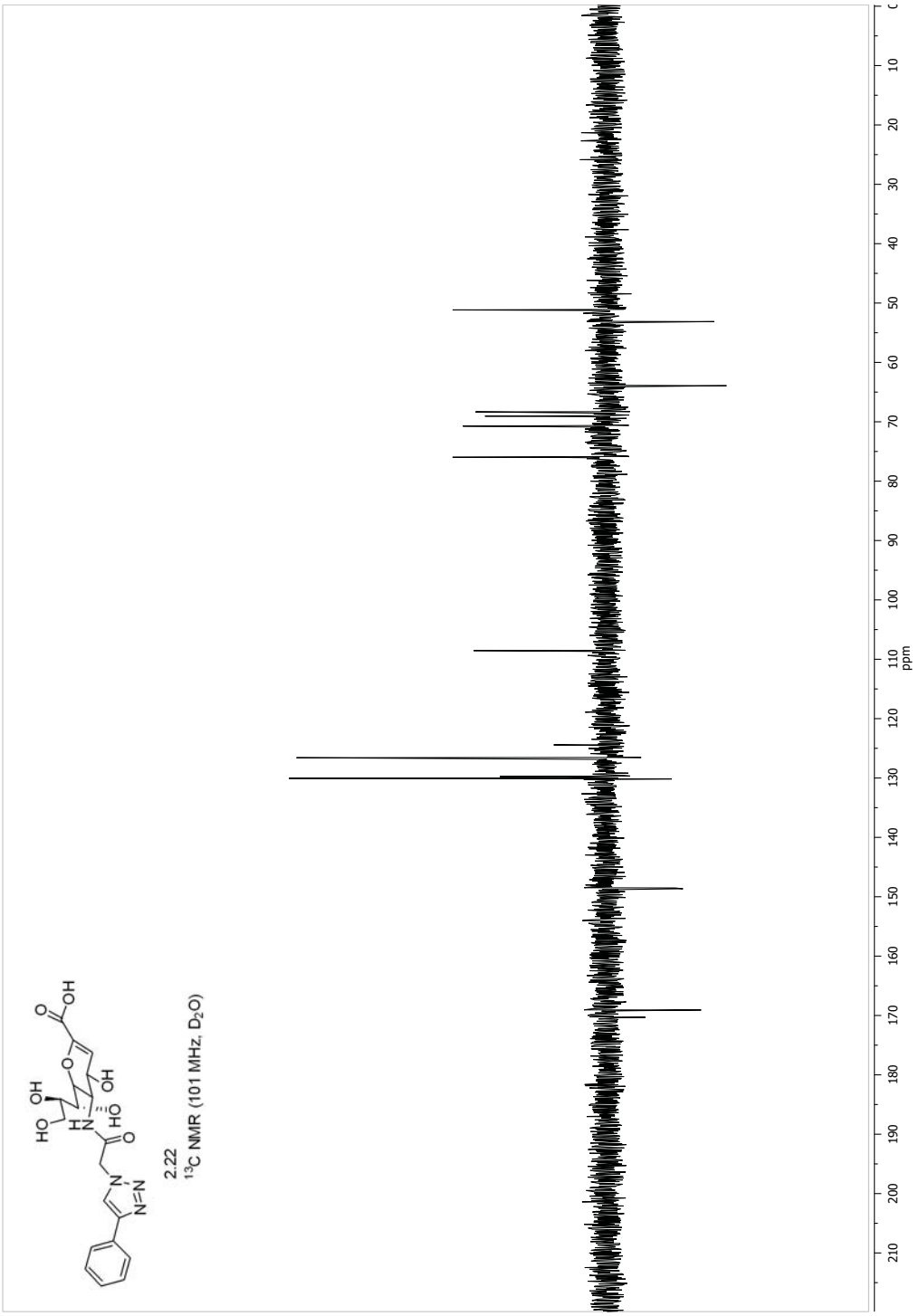
2.22
$^{13}$C NMR (101 MHz, $D_2O$)
ppm

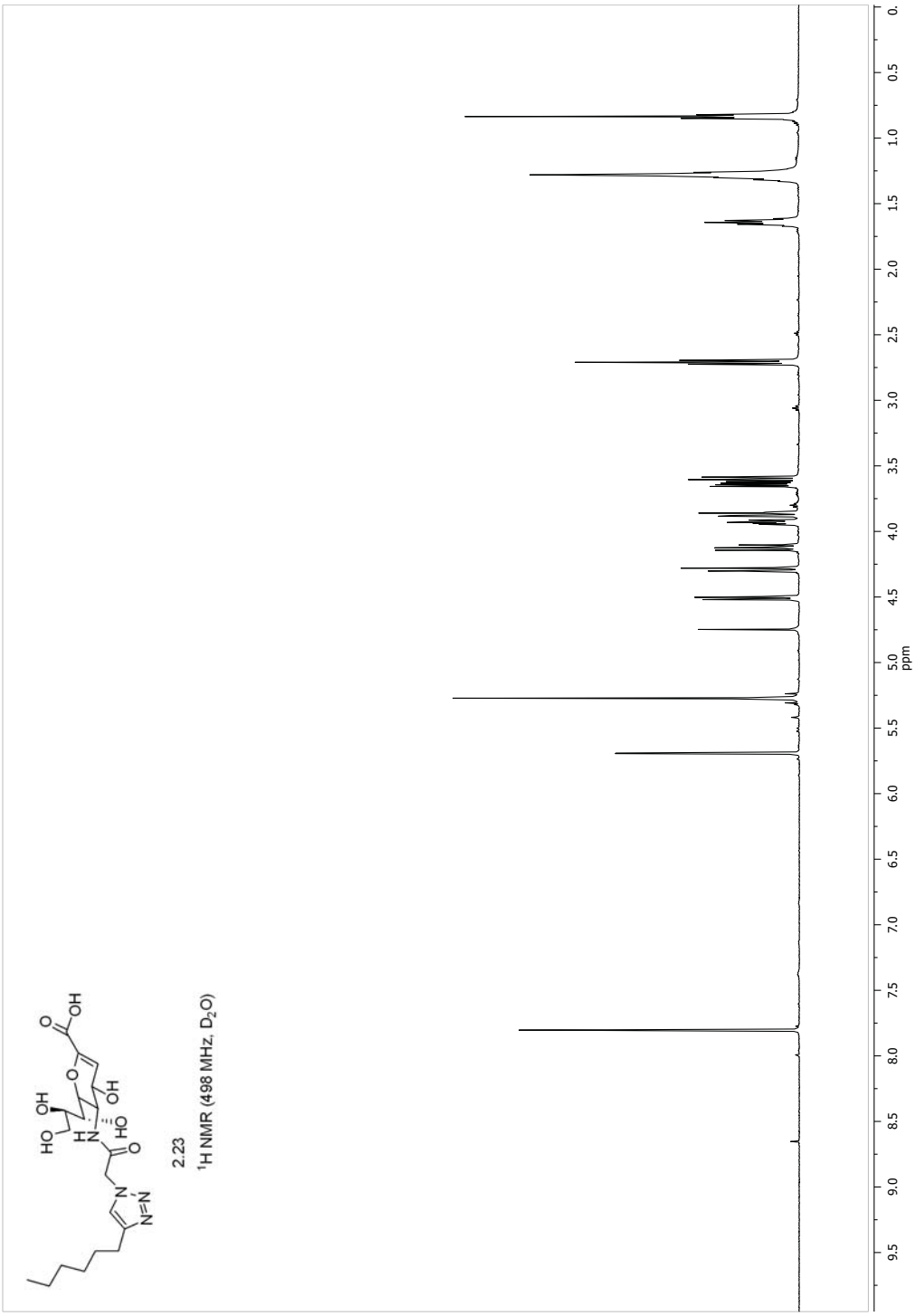
2.23
$^1$H NMR (498 MHz, $D_2O$)
ppm

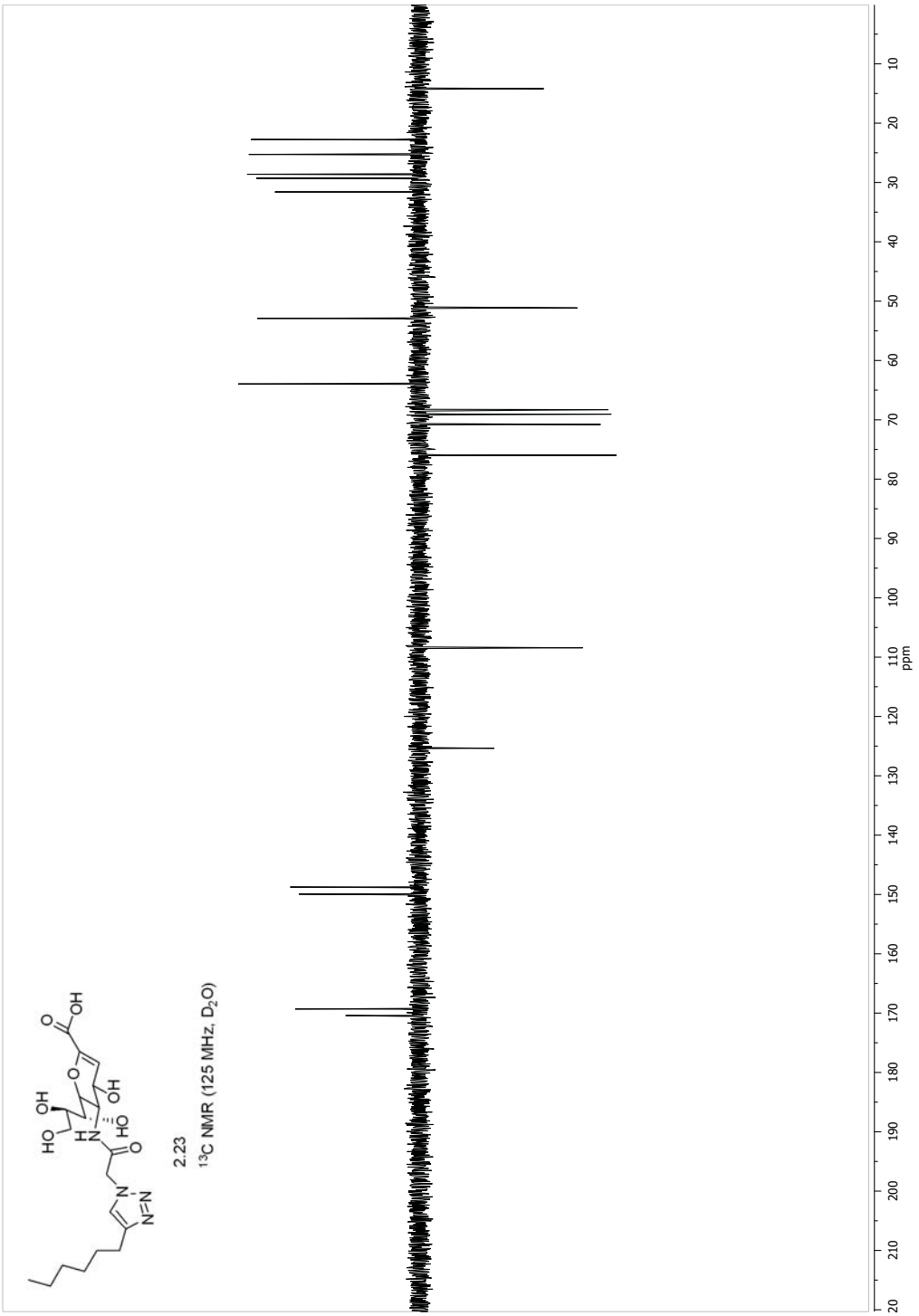
2.23
$^{13}$C NMR (125 MHz, $D_2O$)
ppm

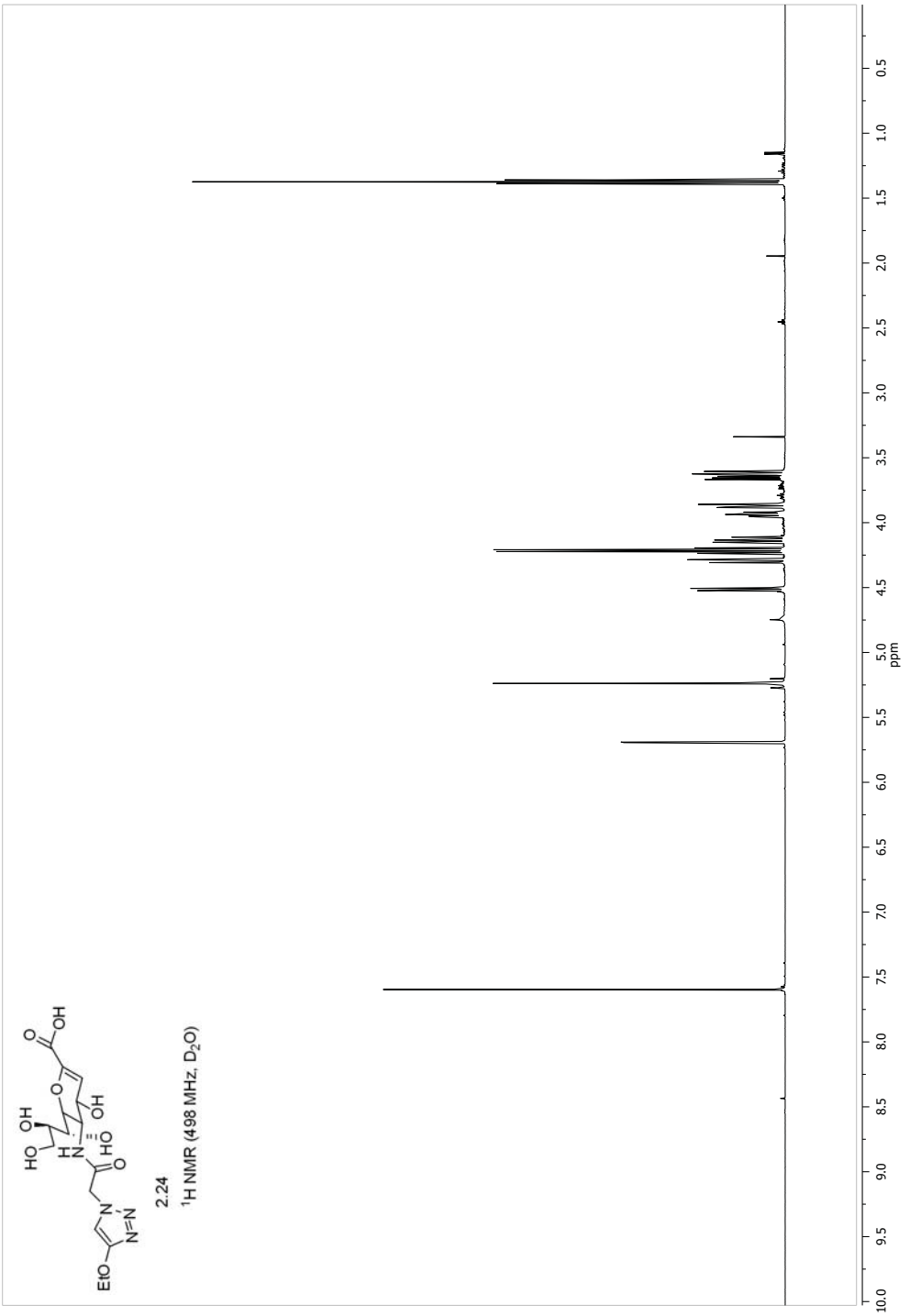
2.24
$^1$H NMR (498 MHz, $D_2O$)
ppm

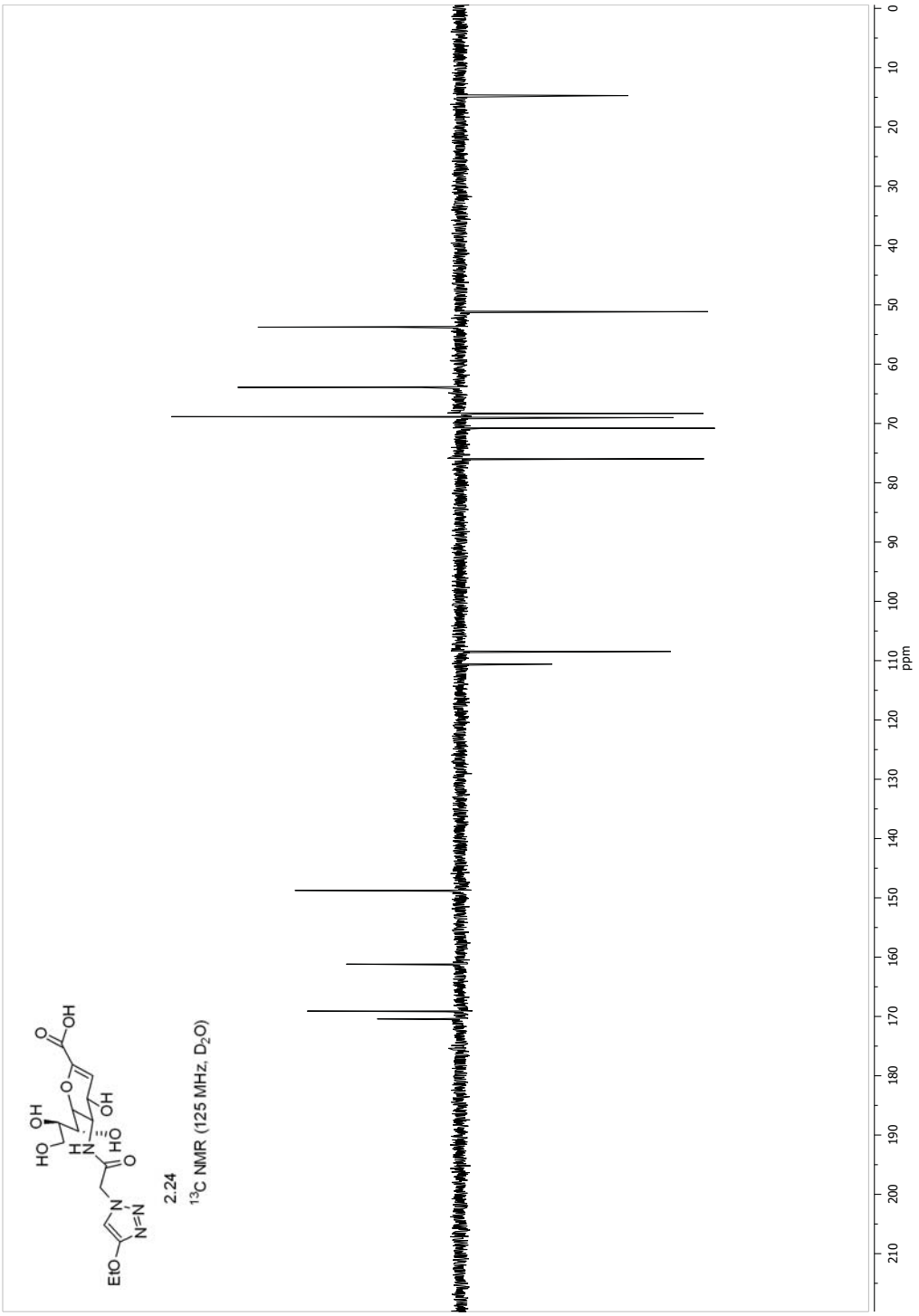
2.24
$^{13}$C NMR (125 MHz, $D_2O$)
ppm

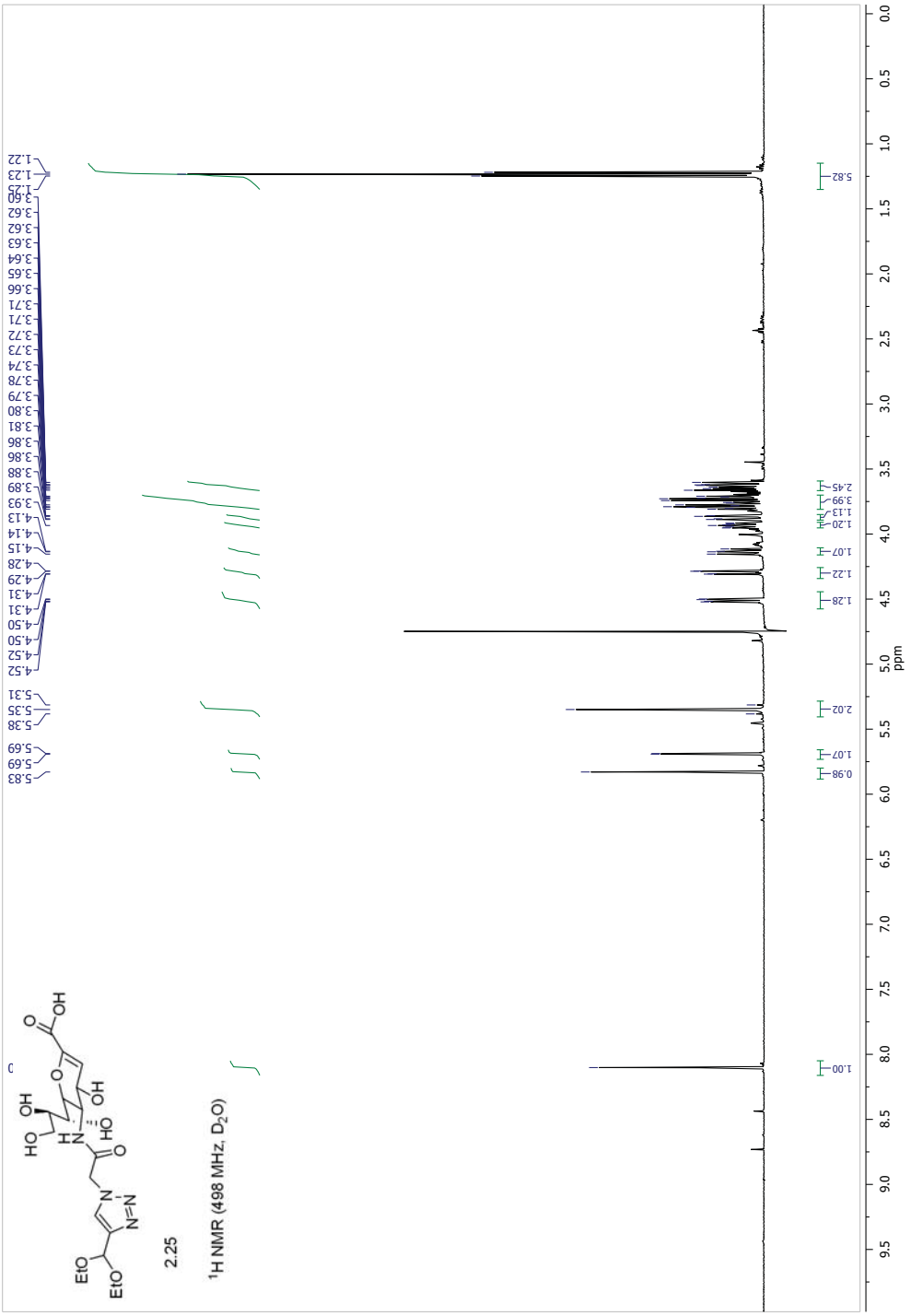
2.25
$^1$H NMR (498 MHz, $D_2O$)
ppm

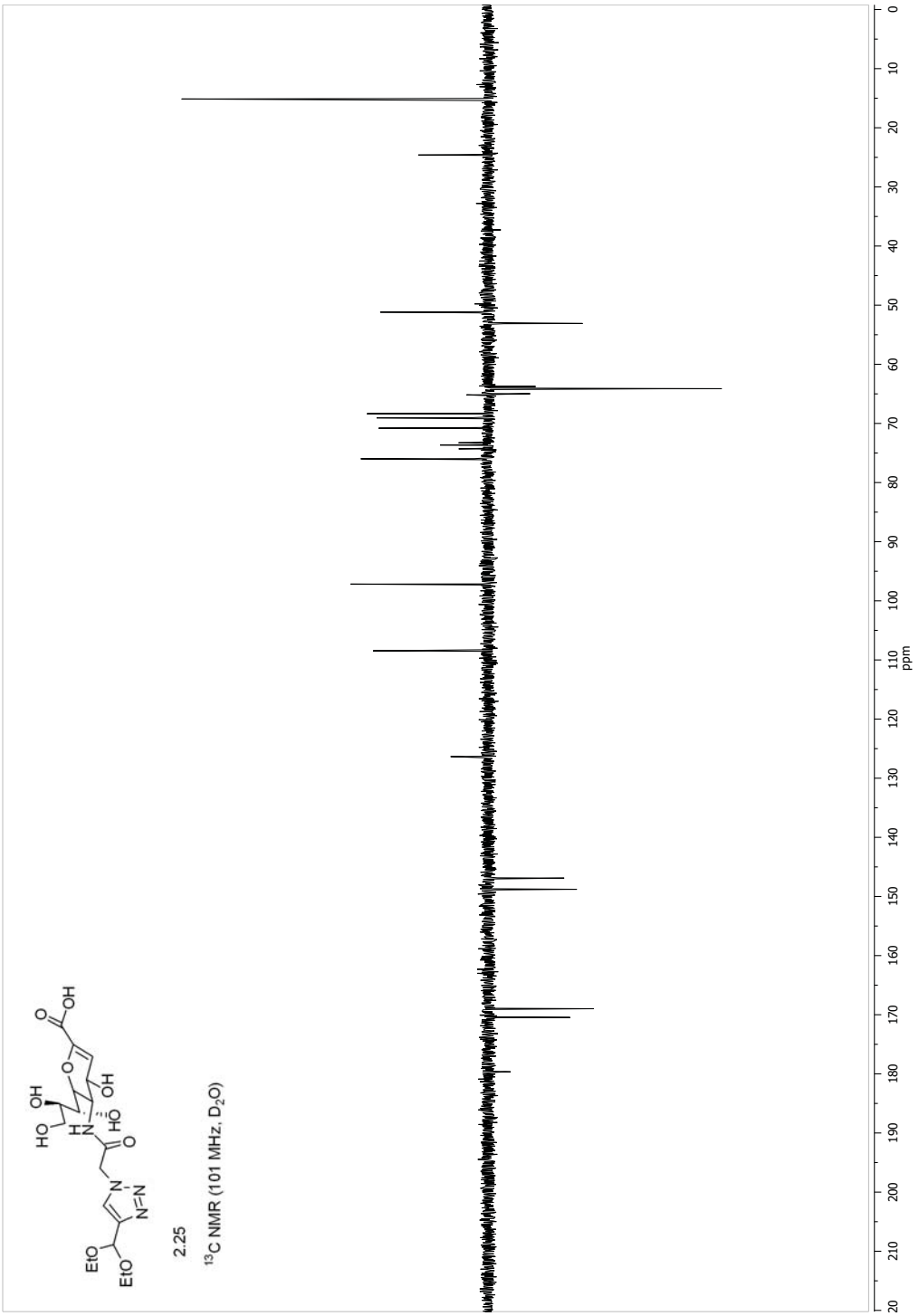
2.25
$^{13}$C NMR (101 MHz, $D_2O$)
ppm

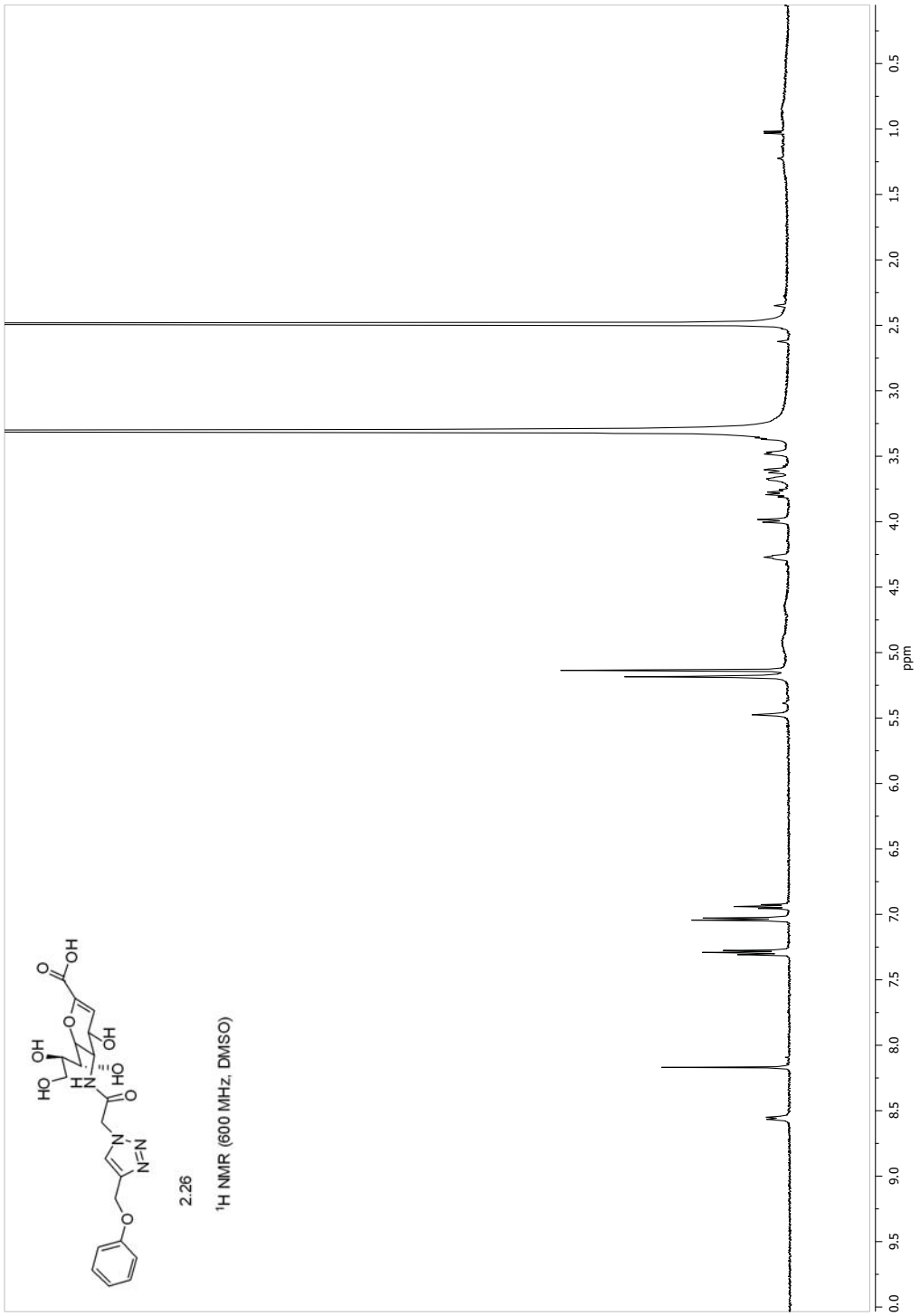
2.26
$^1$H NMR (600 MHz, DMSO)
ppm

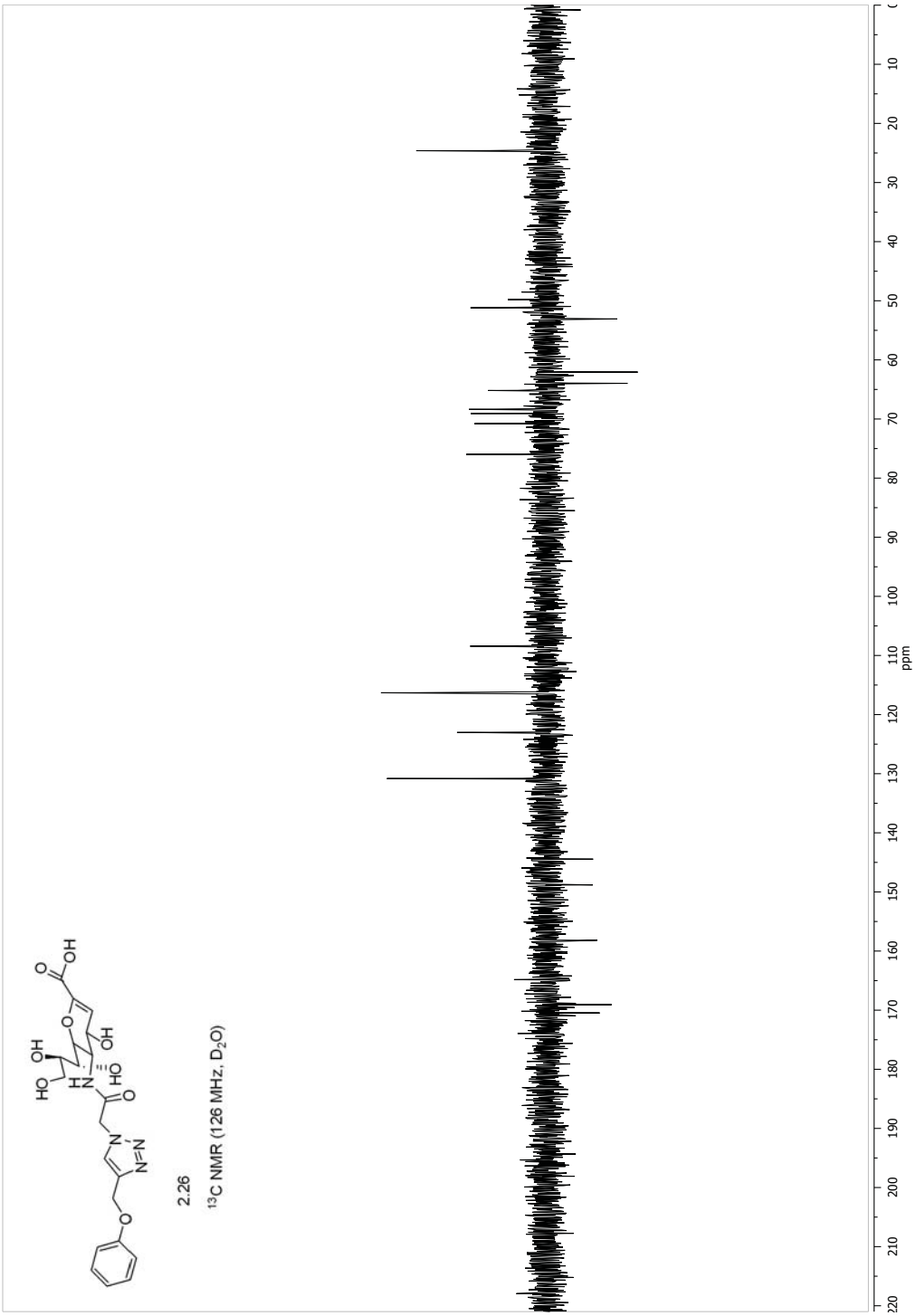
2.26
$^{13}$C NMR (126 MHz, $D_2O$)
ppm

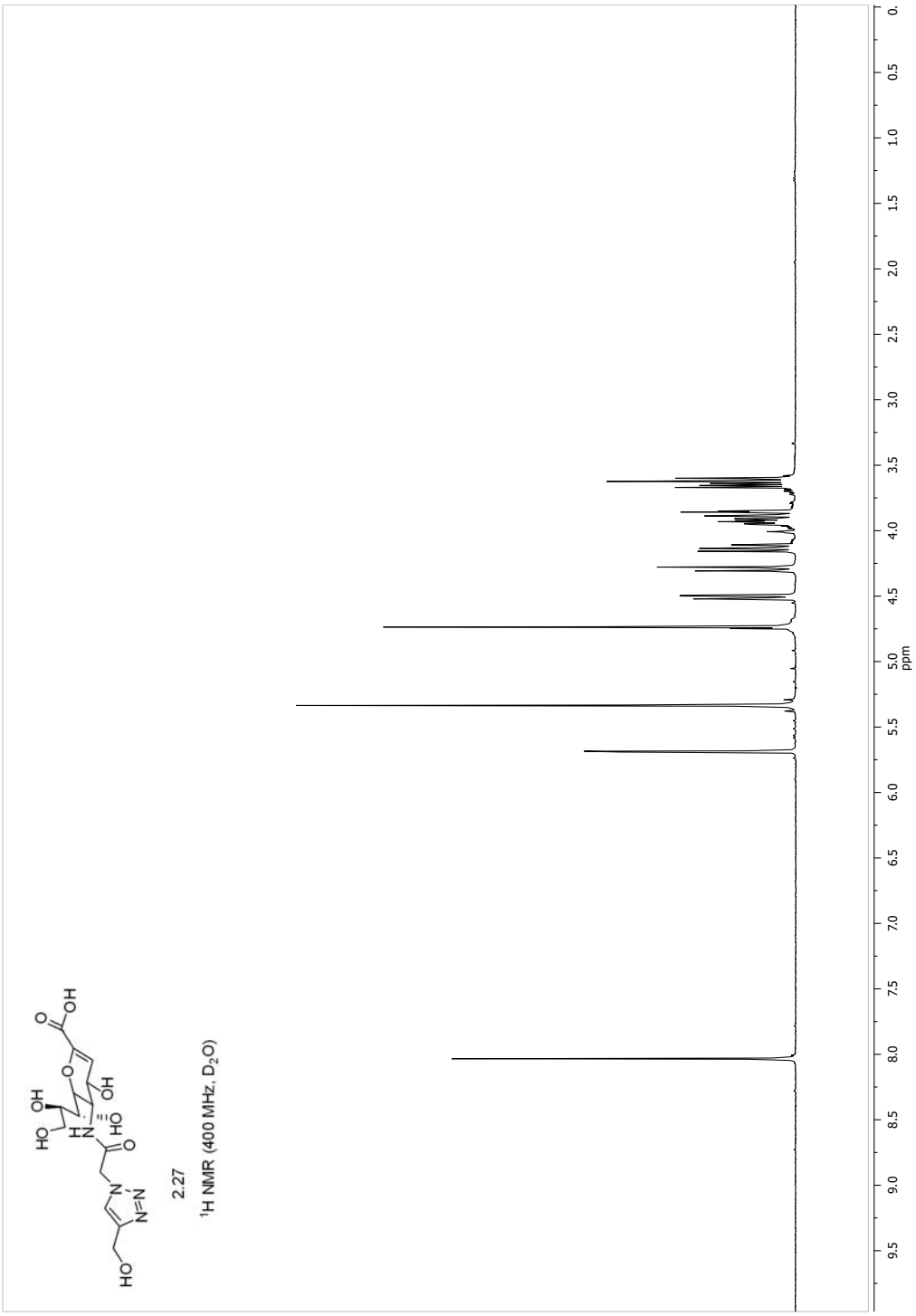
2.27
$^1$H NMR (400 MHz, $D_2O$)
ppm

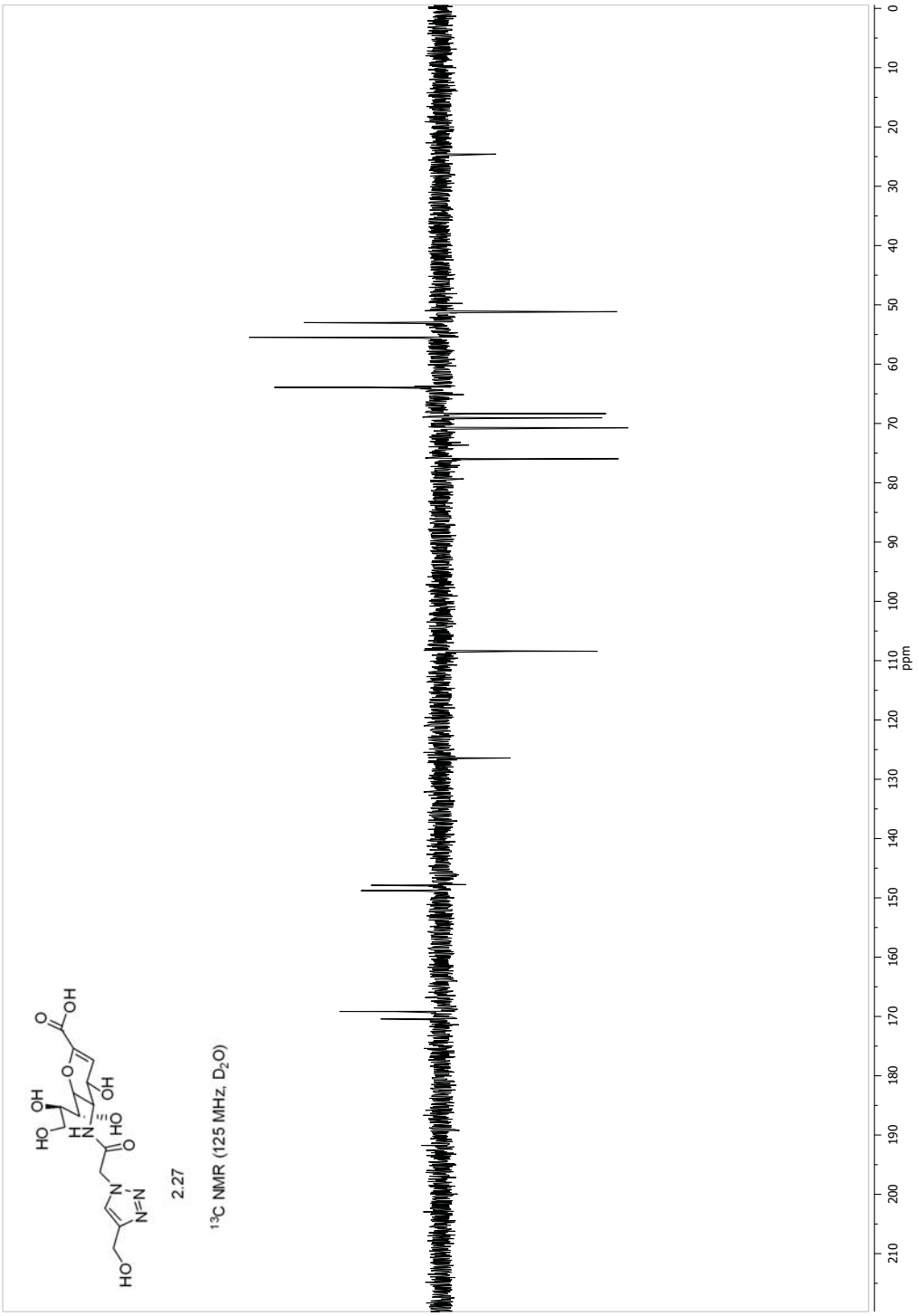
2.27
$^{13}$C NMR (125 MHz, $D_2O$)
ppm

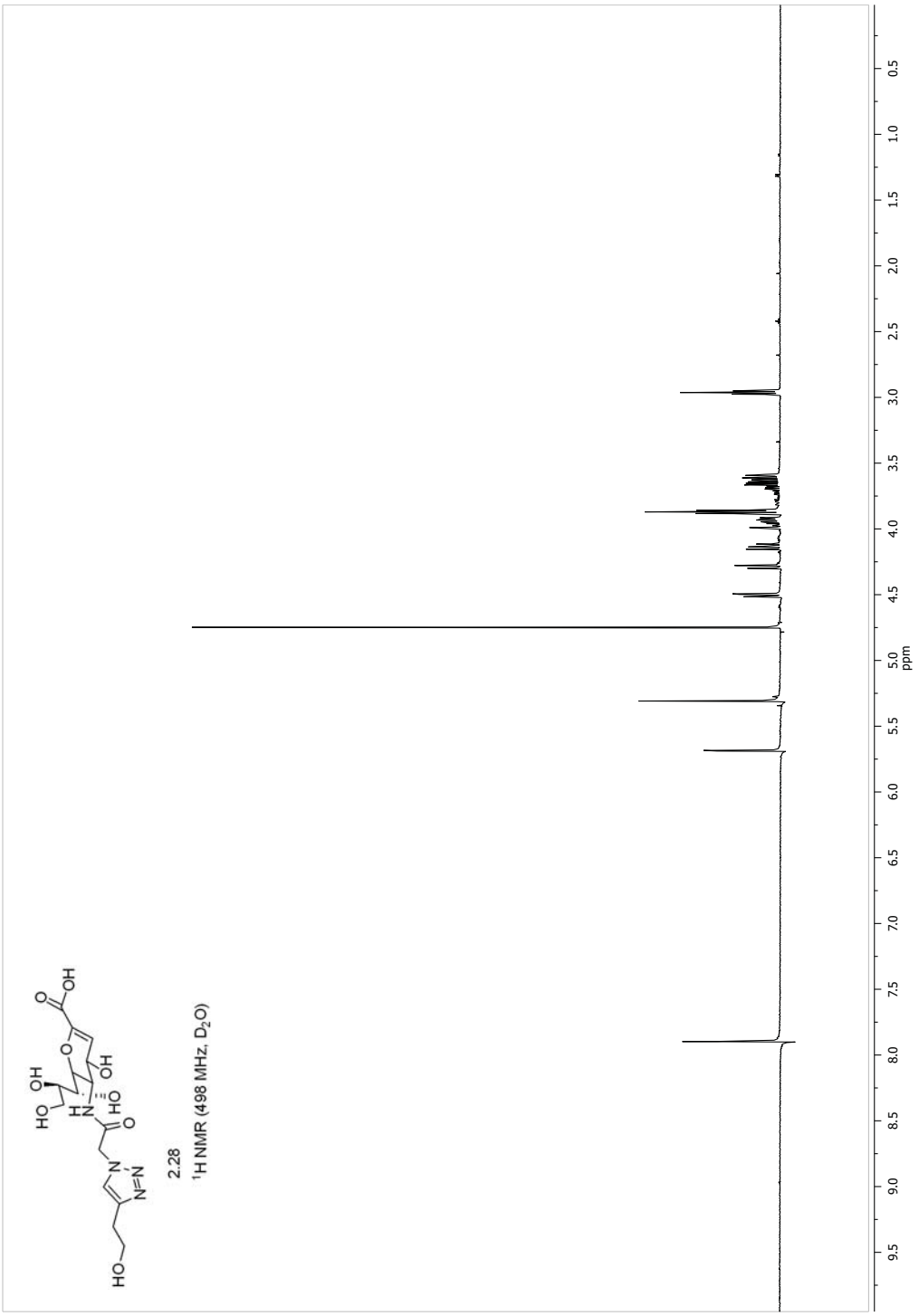
2.28
$^1$H NMR (498 MHz, $D_2O$)
ppm

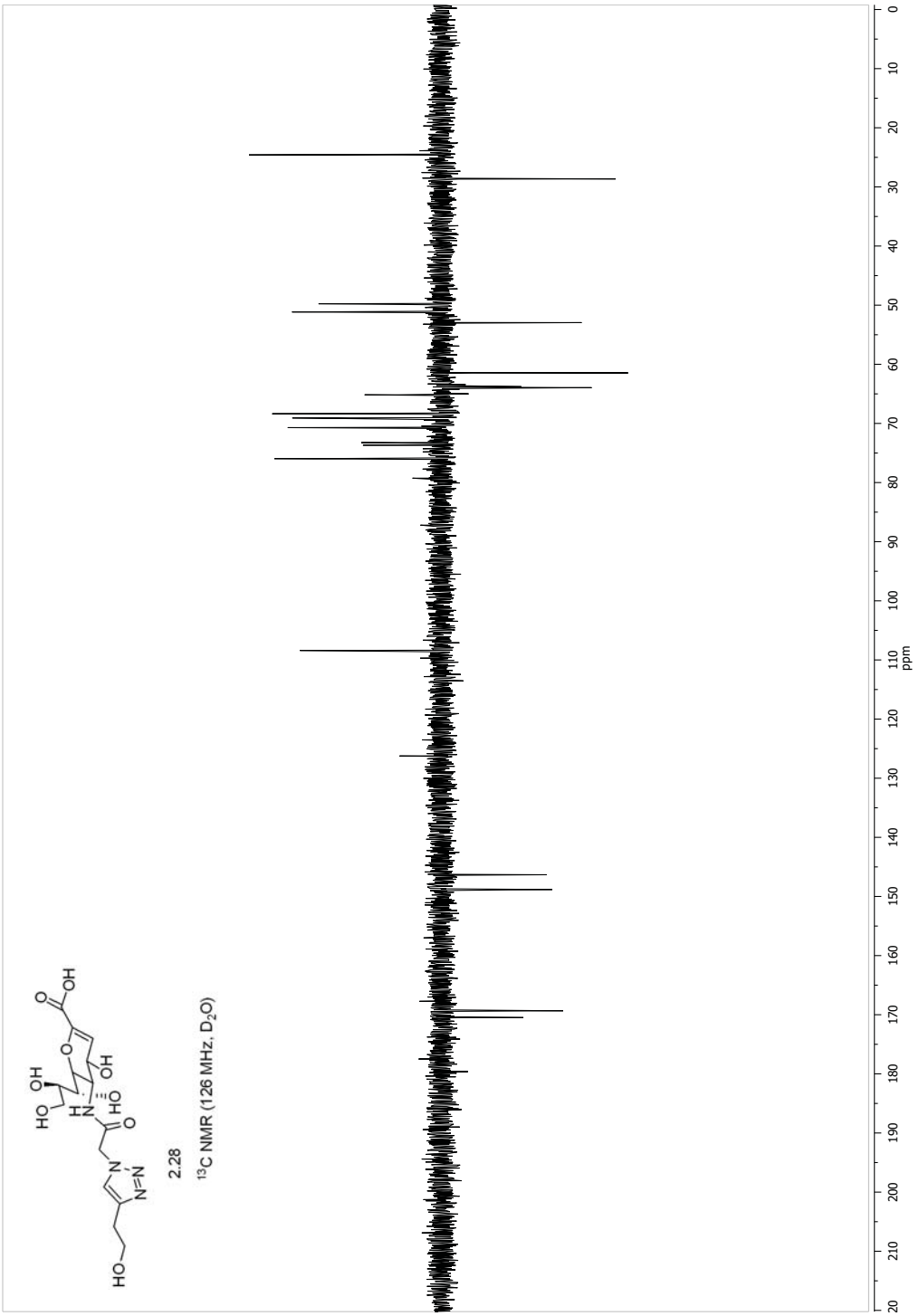
2.28
$^{13}$C NMR (126 MHz, $D_2O$)
ppm

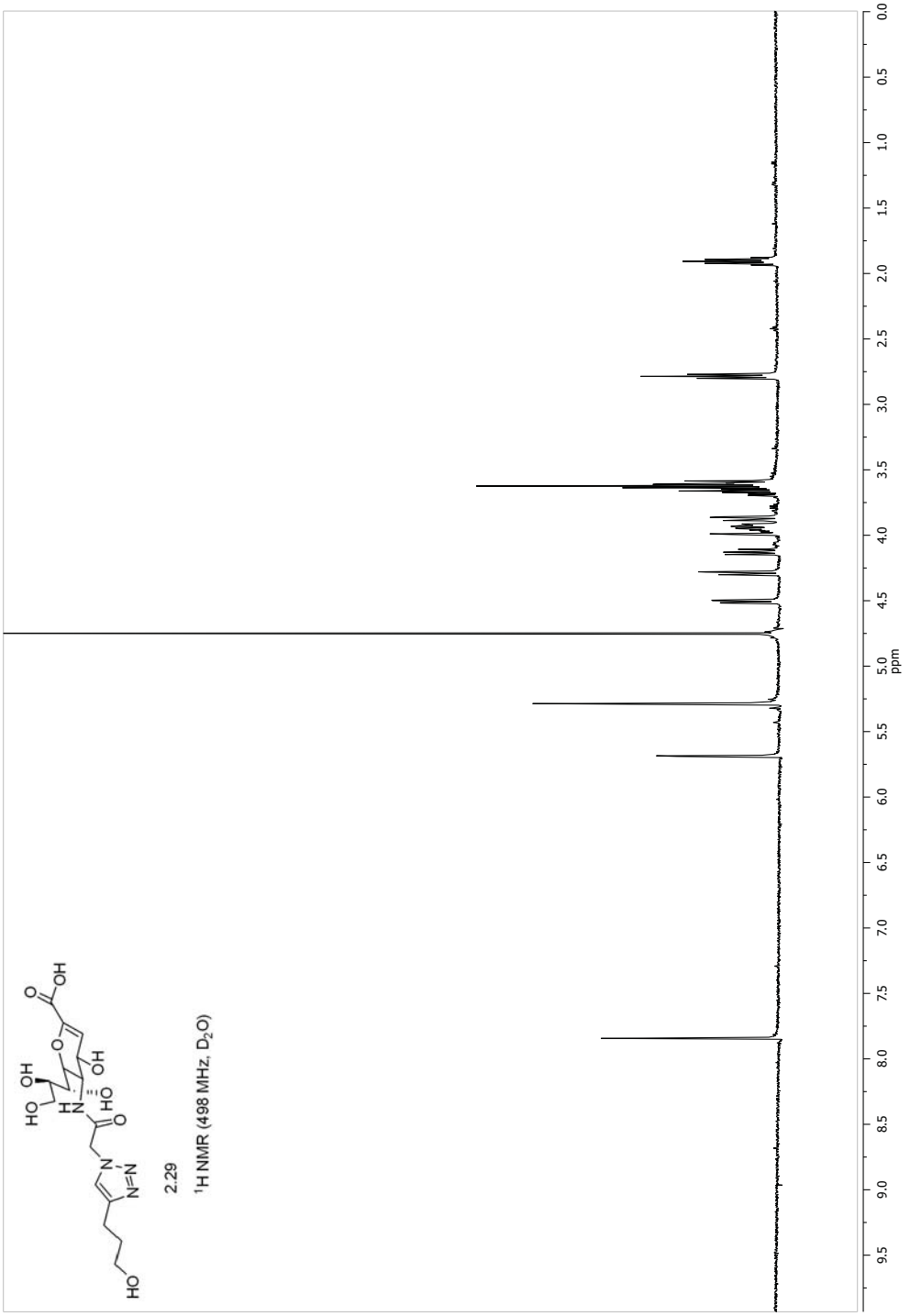
2.29
$^1$H NMR (498 MHz, $D_2O$)
ppm

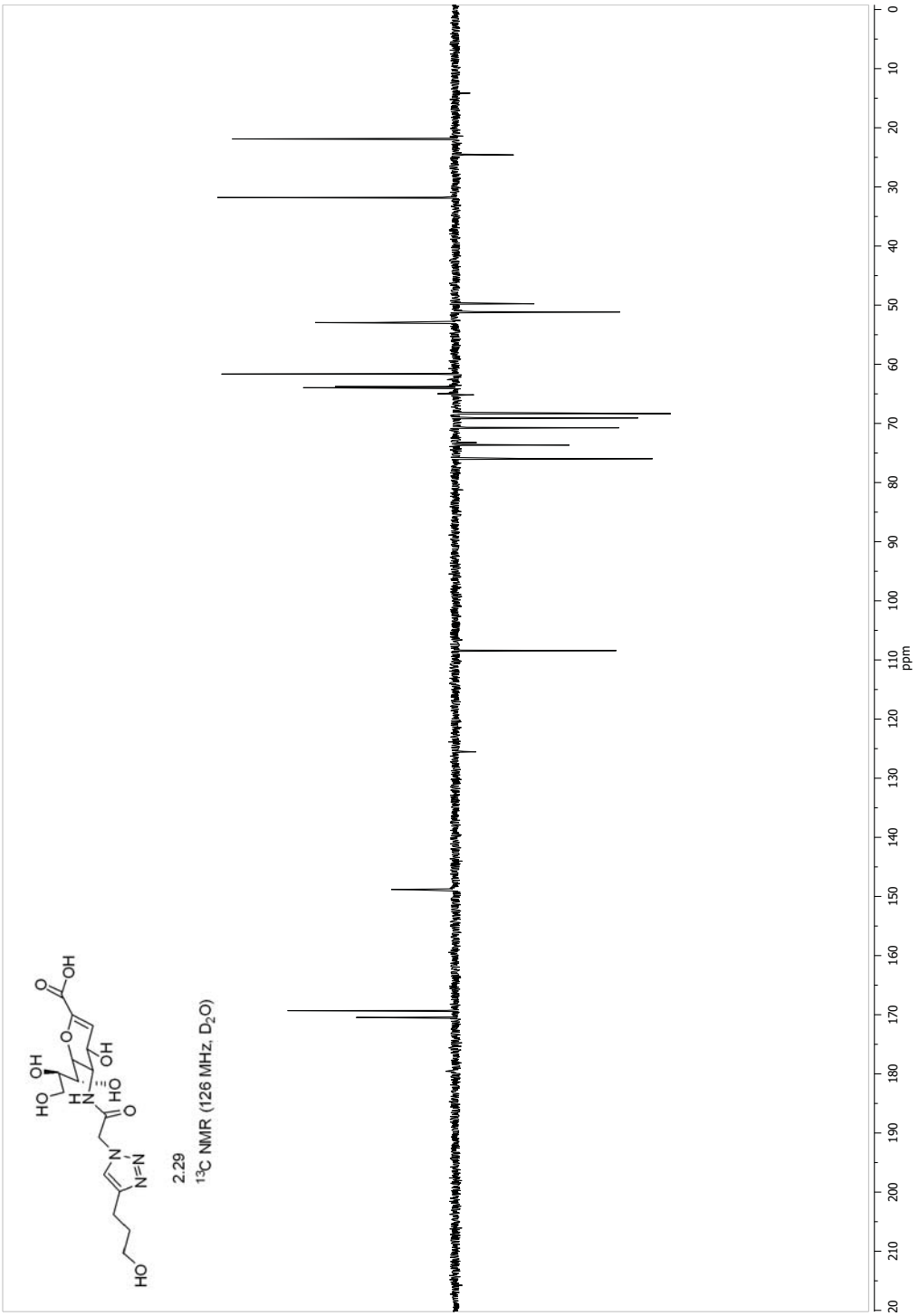
2.29
$^{13}$C NMR (126 MHz, $D_2O$)
ppm

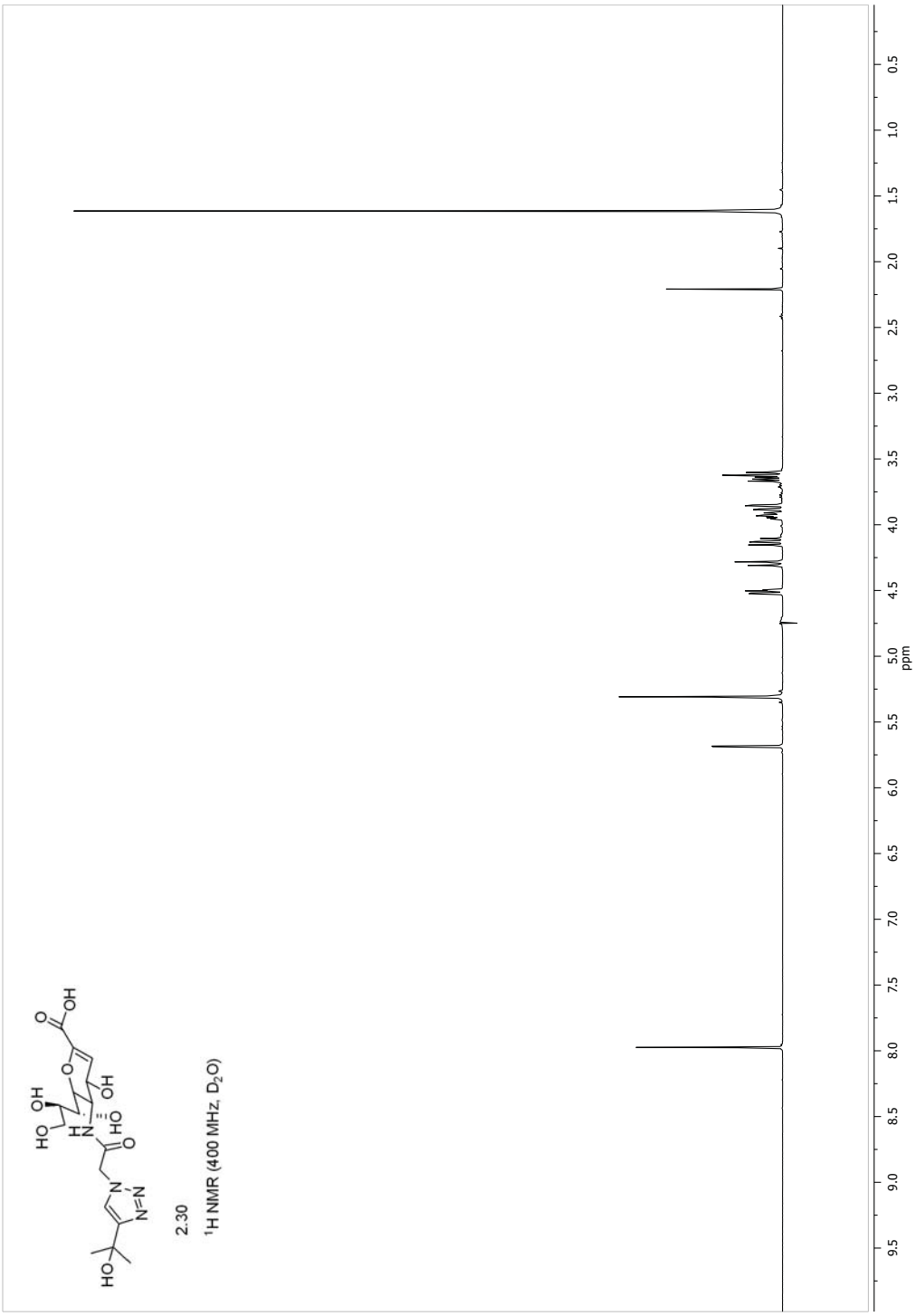
2.30
$^1$H NMR (400 MHz, $D_2O$)
ppm

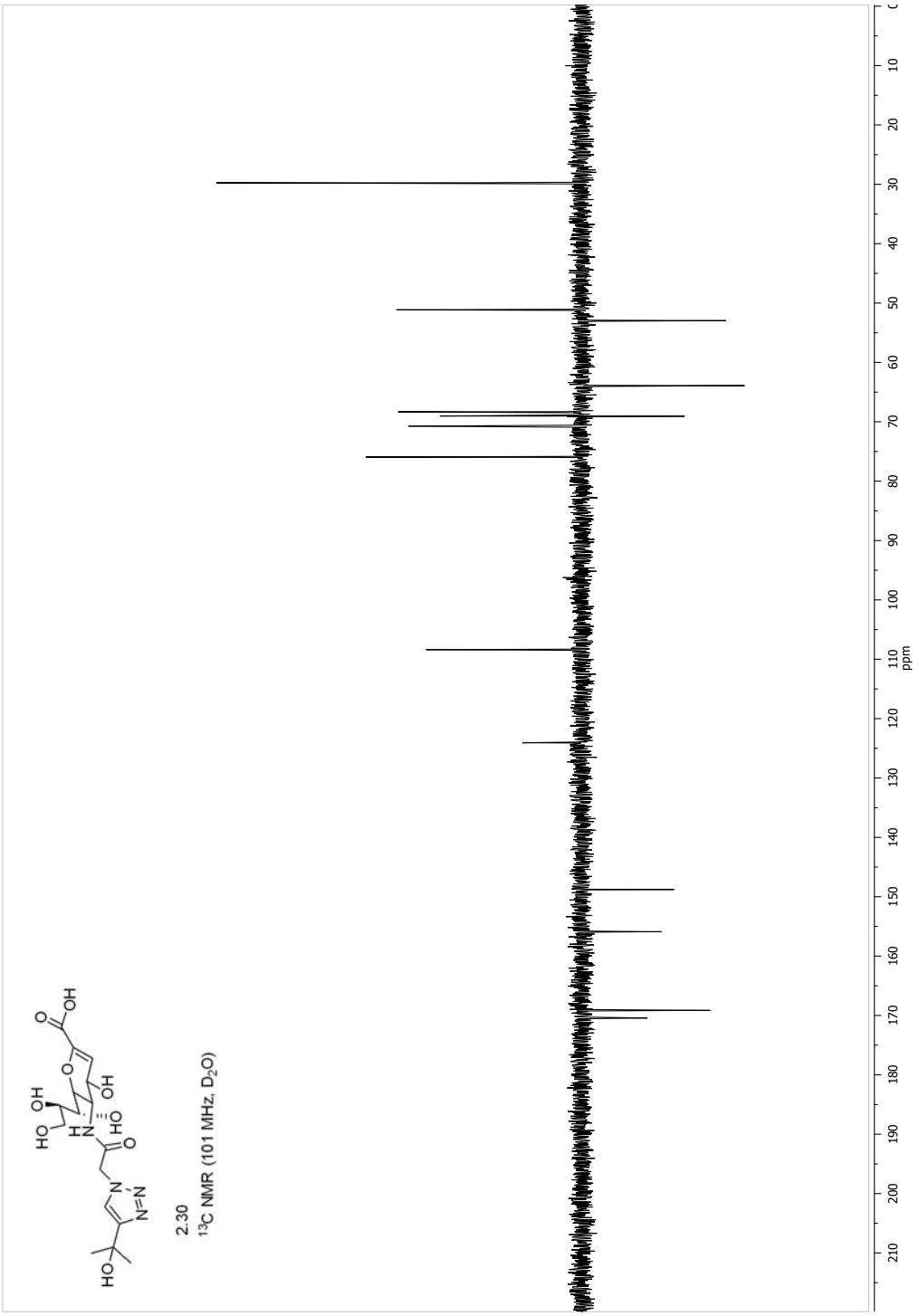
2.30
$^{13}$C NMR (101 MHz, $D_2O$)
ppm

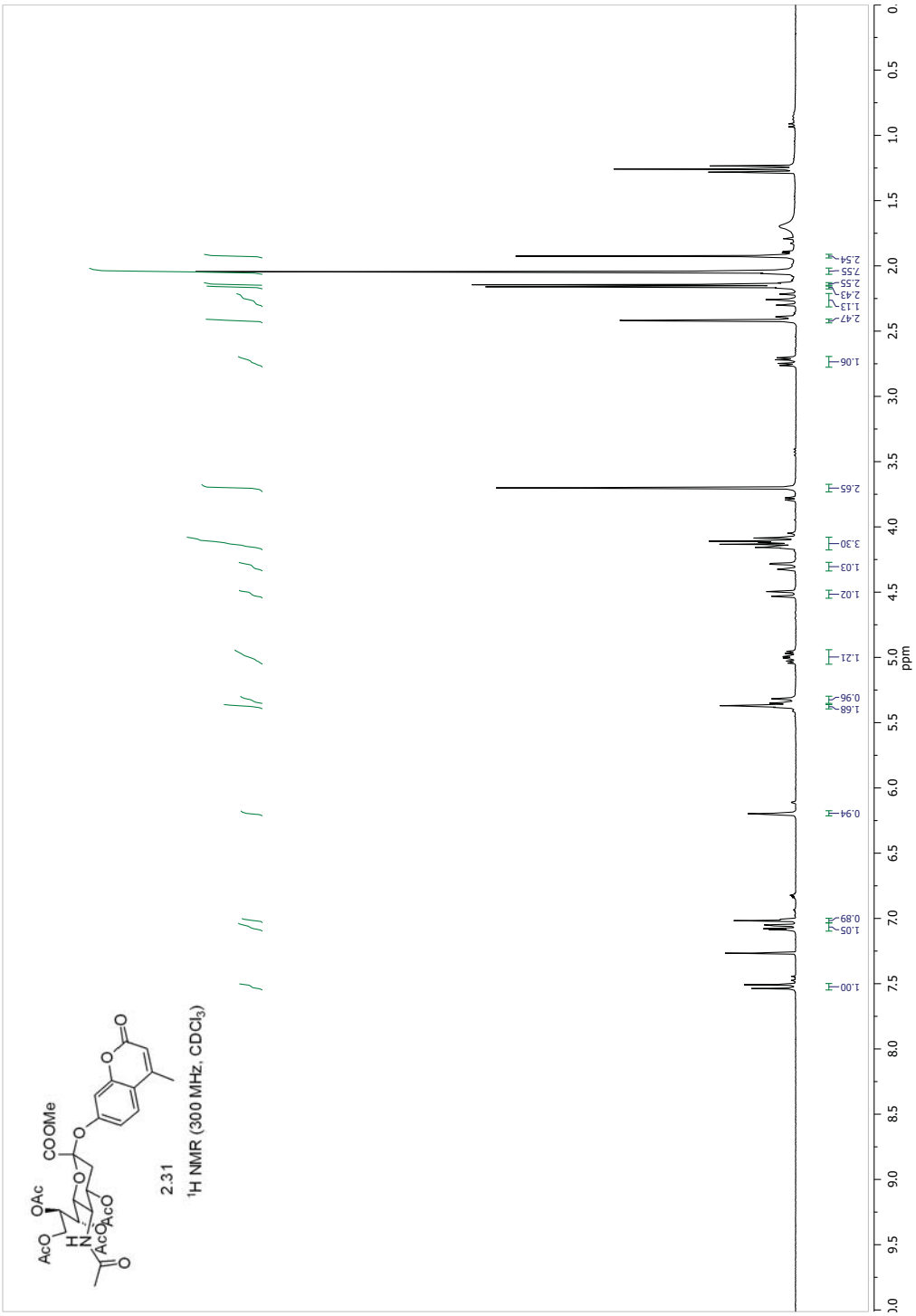
2.31
$^1$H NMR (300 MHz, $CDCl_3$)
ppm

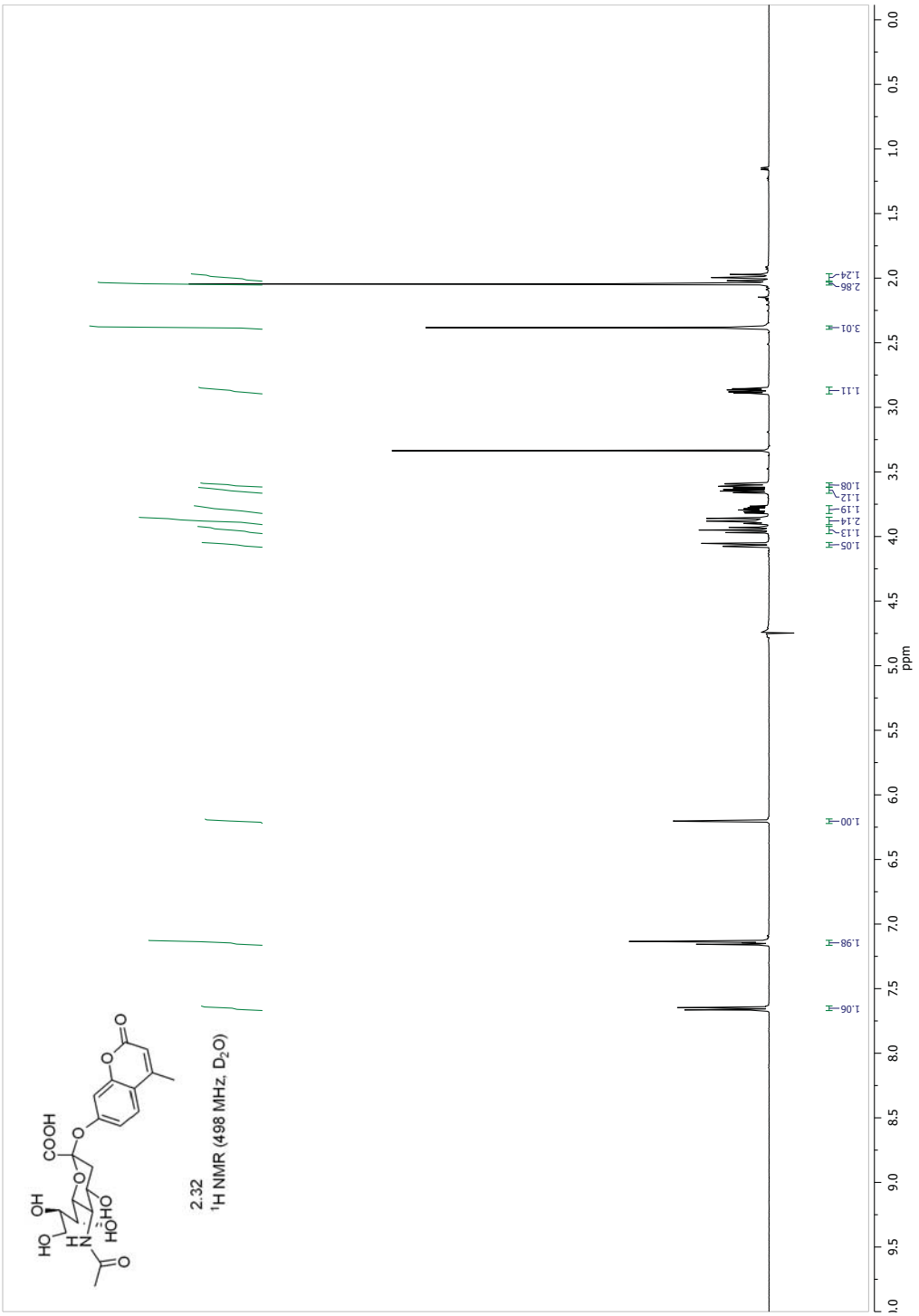
2.32
$^1$H NMR (498 MHz, $D_2O$)
1.06
1.98
1.00
3.01
1.11
1.08
1.12
1.19
2.14
1.13
1.05
2.86
1.24
ppm

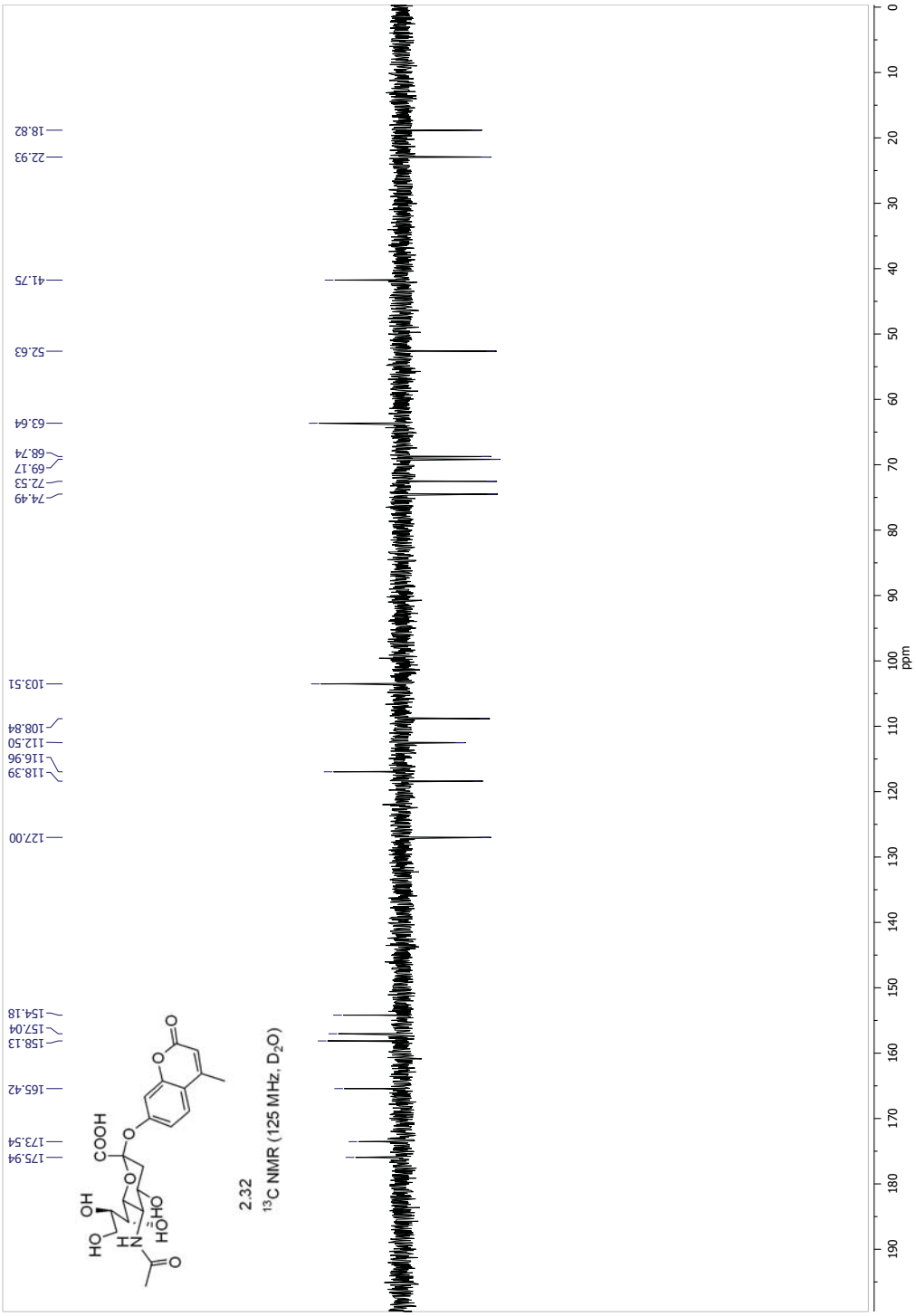
18.82
22.93
41.75
52.63
63.64
68.74
69.17
72.53
74.49
103.51
108.84
112.50
116.96
118.39
127.00
154.18
157.04
158.13
165.42
173.54
175.94
2.32
$^{13}$C NMR (125 MHz, $D_2O$)
ppm

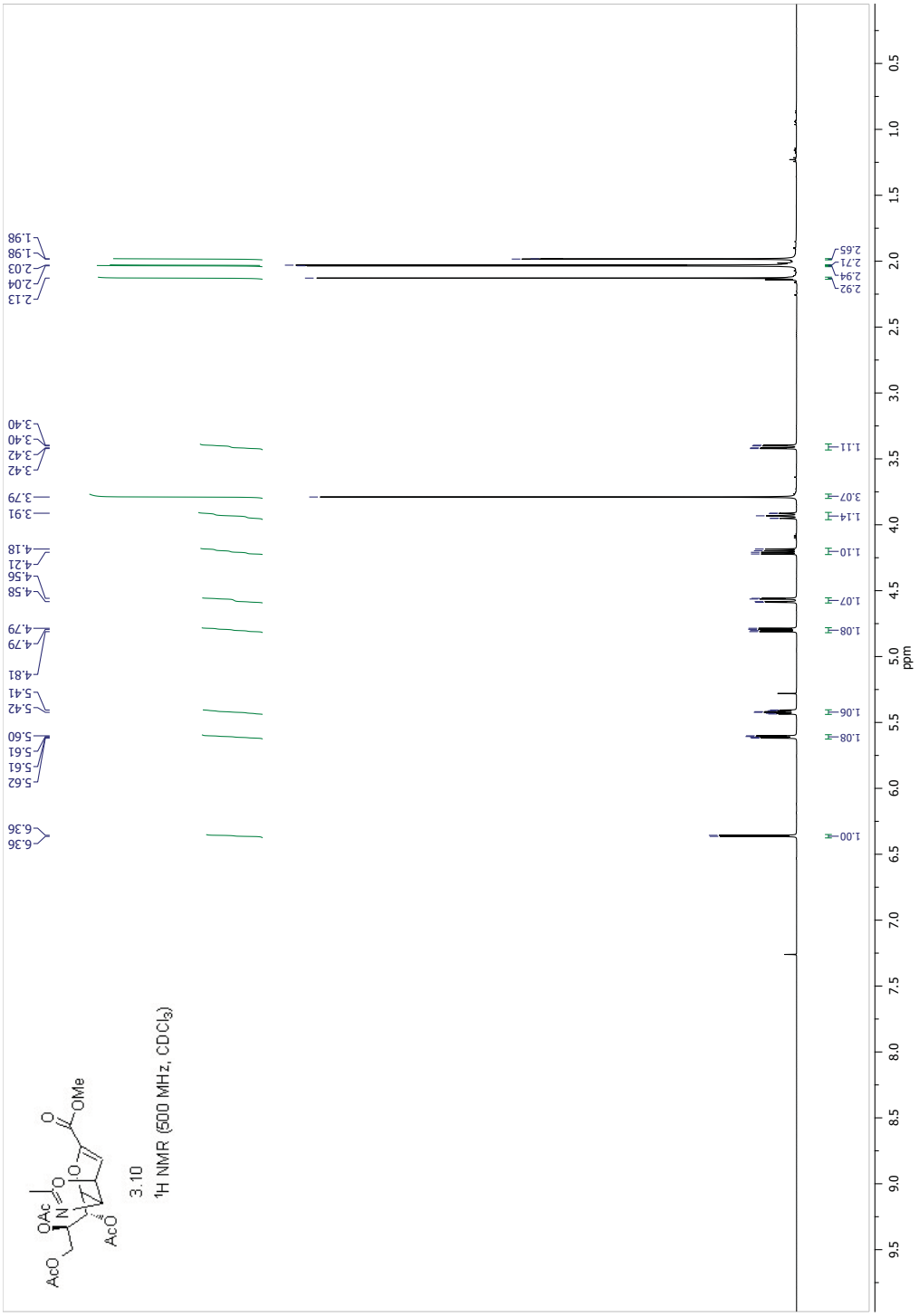
3.10
1H NMR (500 MHz, CDCl3)
OMe
OAc
AcO
AcO
1.98
1.98
2.03
2.04
2.13
3.40
3.40
3.42
3.42
3.79
3.91
4.18
4.21
4.56
4.58
4.79
4.79
4.81
5.41
5.42
5.60
5.61
5.61
5.62
6.36
6.36
2.92
2.94
2.71
2.65
1.11
3.07
1.14
1.10
1.07
1.08
1.06
1.08
1.00
ppm

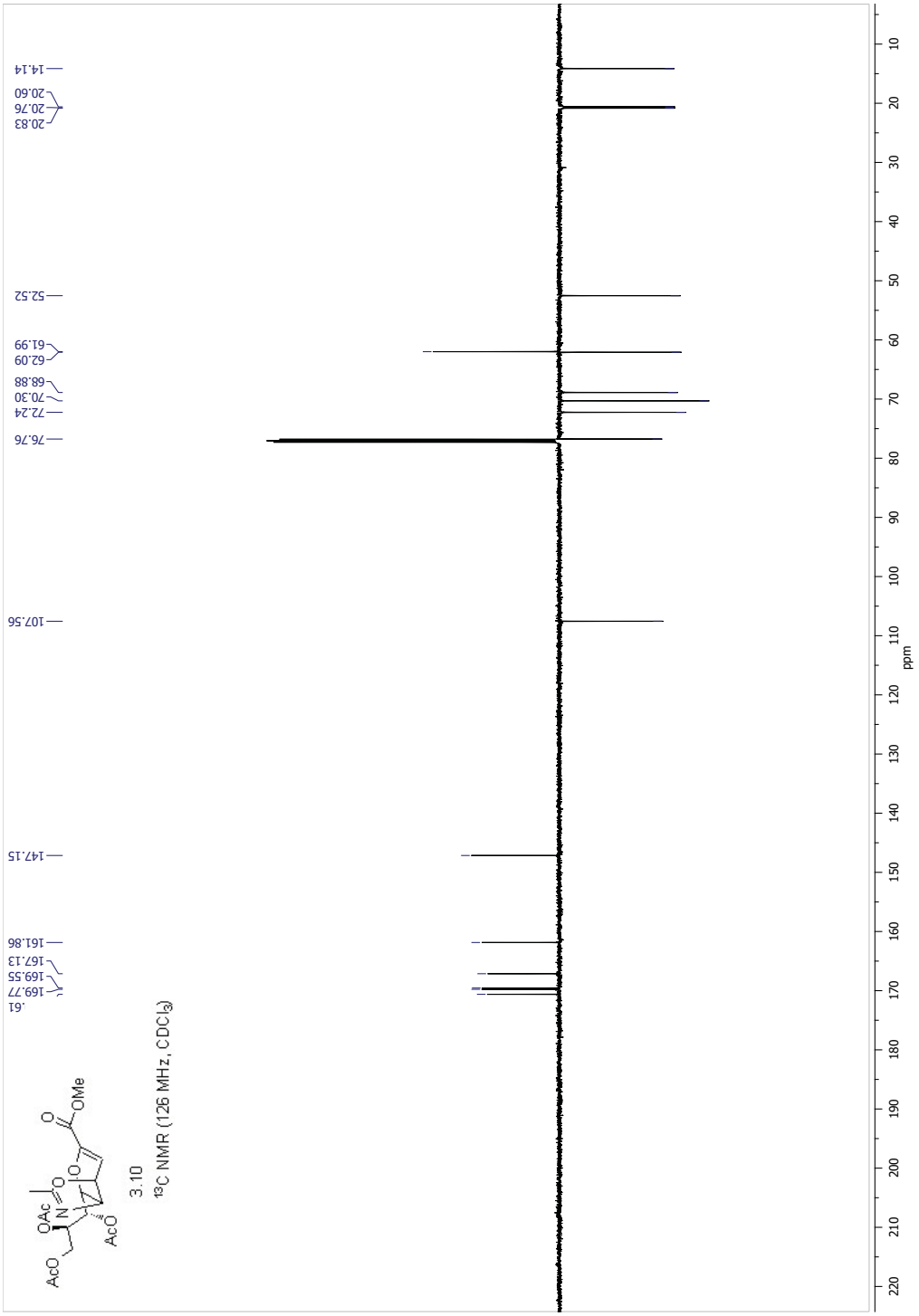
14.14
20.60
20.76
20.83
52.52
61.99
62.09
68.88
70.30
72.24
76.76
107.56
147.15
161.86
167.13
169.55
169.77
.61
3.10
$^{13}$C NMR (126 MHz, $CDCl_3$)
OMe
OAc
AcO
AcO
ppm

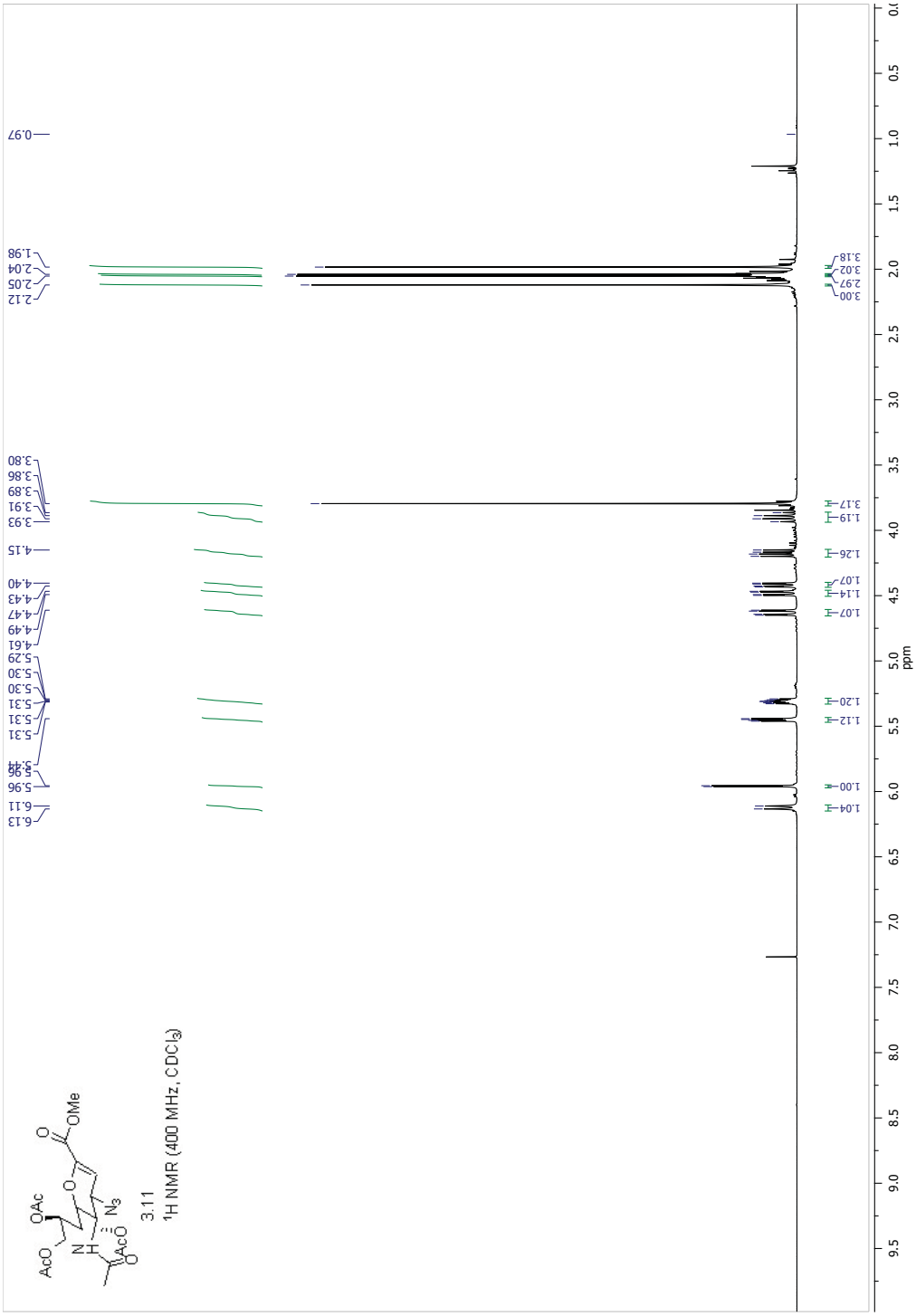
3.11
$^1$H NMR (400 MHz, CDCl$_3$)
ppm

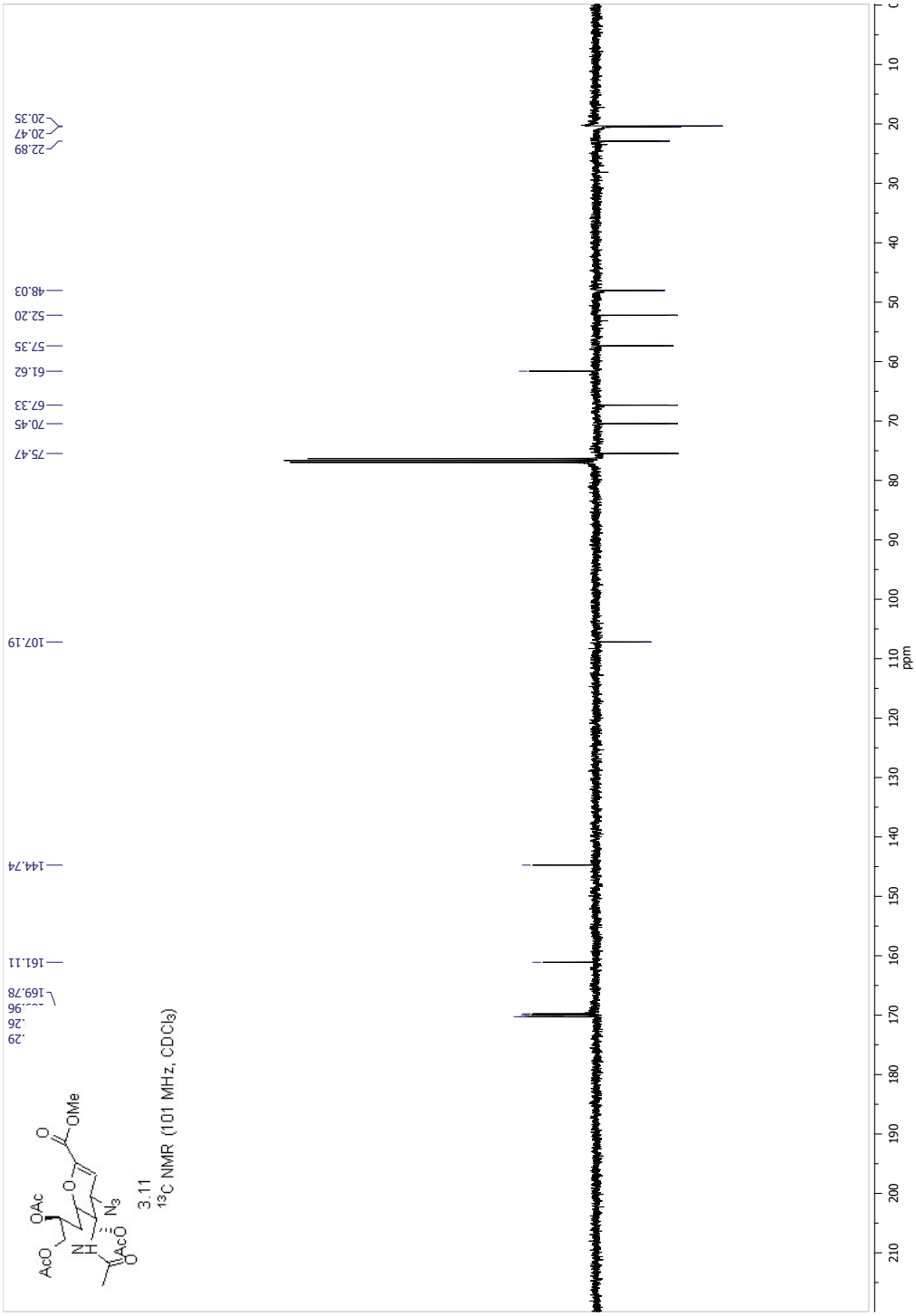
3.11
$^{13}$C NMR (101 MHz, CDCl$_3$)
22.89
20.47
20.35
48.03
52.20
57.35
61.62
67.33
70.45
75.47
107.19
144.74
161.11
169.78
ppm

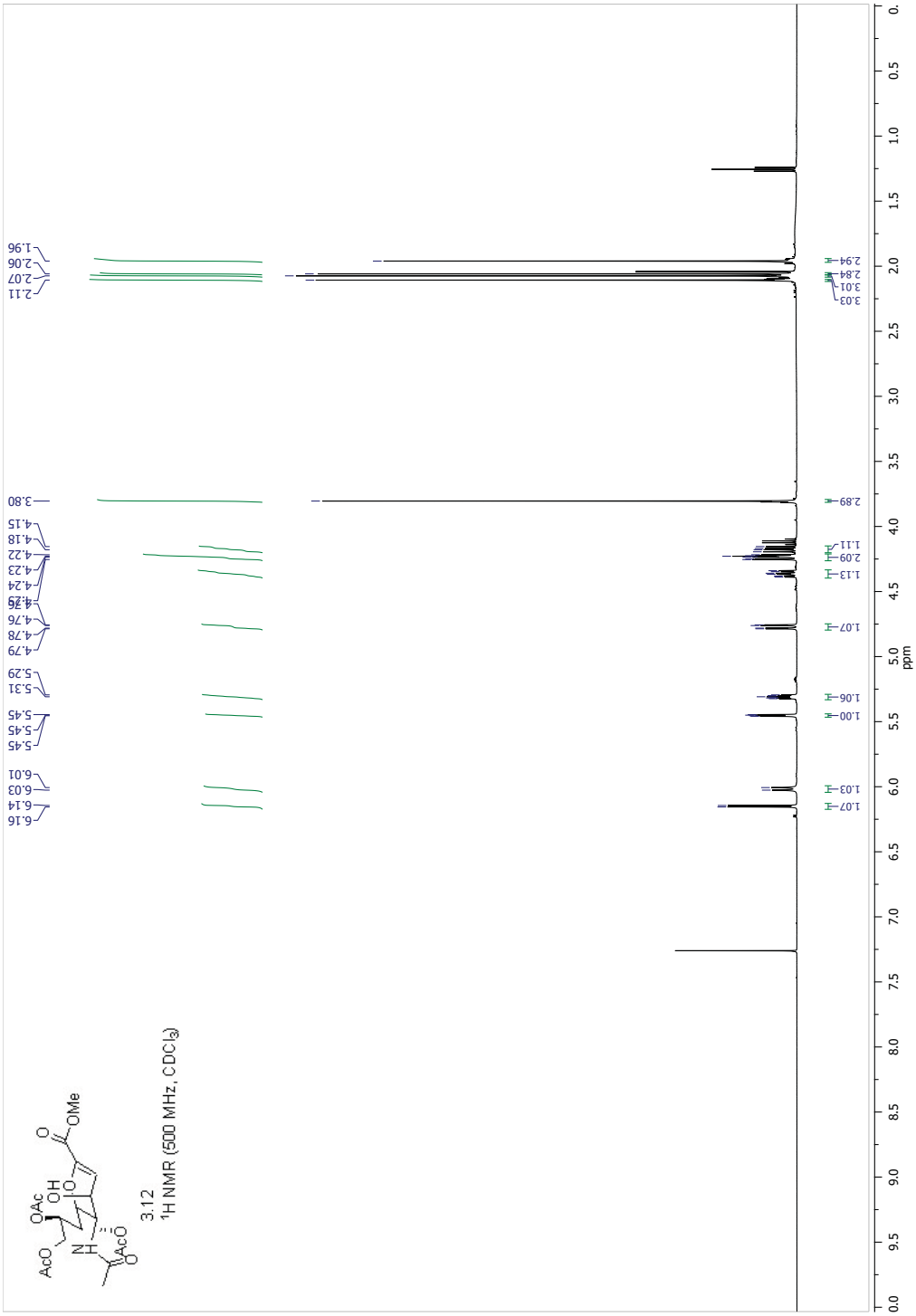
3.12
$^1$H NMR (500 MHz, CDCl$_3$)
ppm

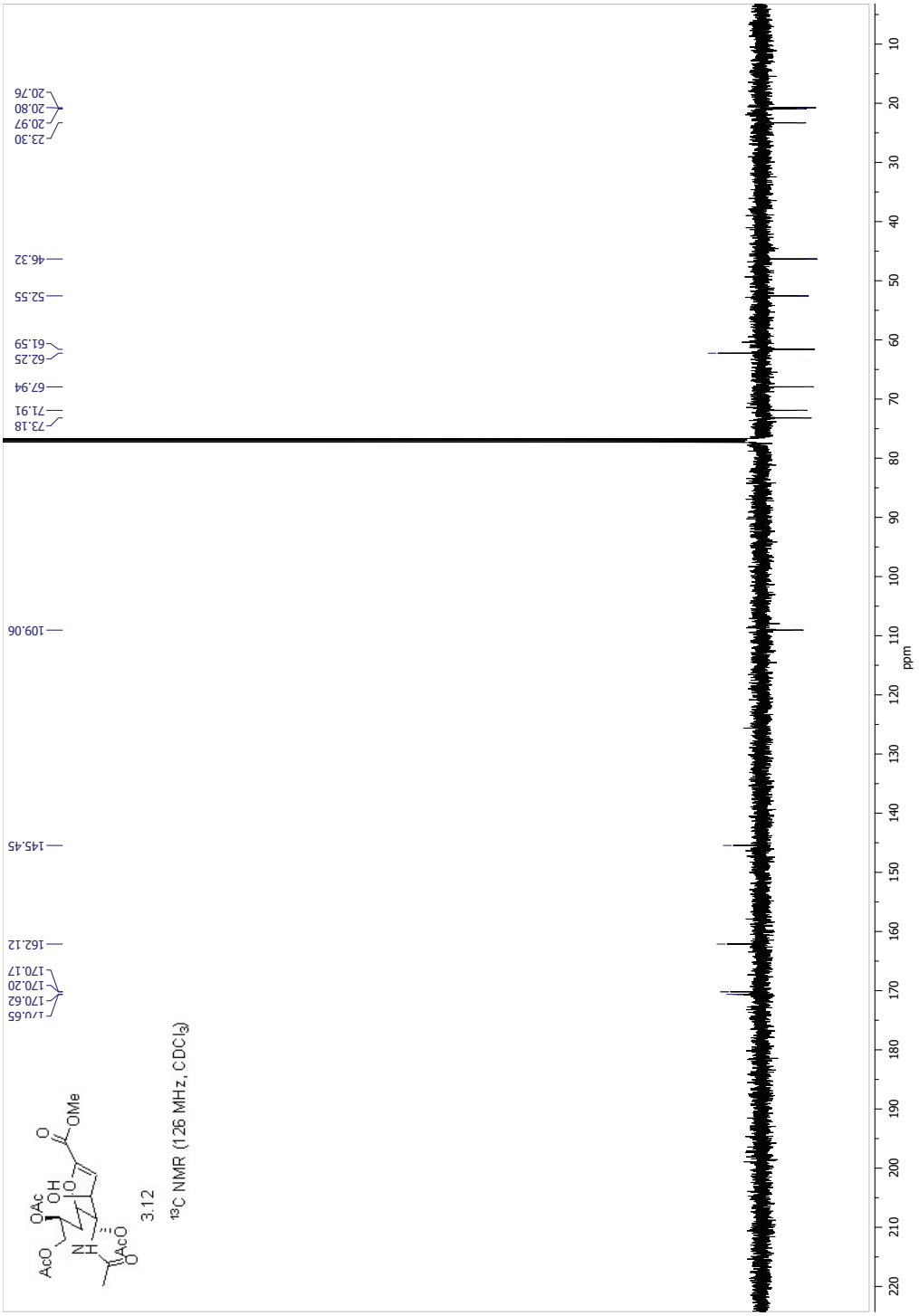
3.12
$^{13}$C NMR (126 MHz, CDCl$_3$)
170.65
170.62
170.20
170.17
162.12
145.45
109.06
73.18
71.91
67.94
62.25
61.59
52.55
46.32
23.30
20.97
20.80
20.76
ppm

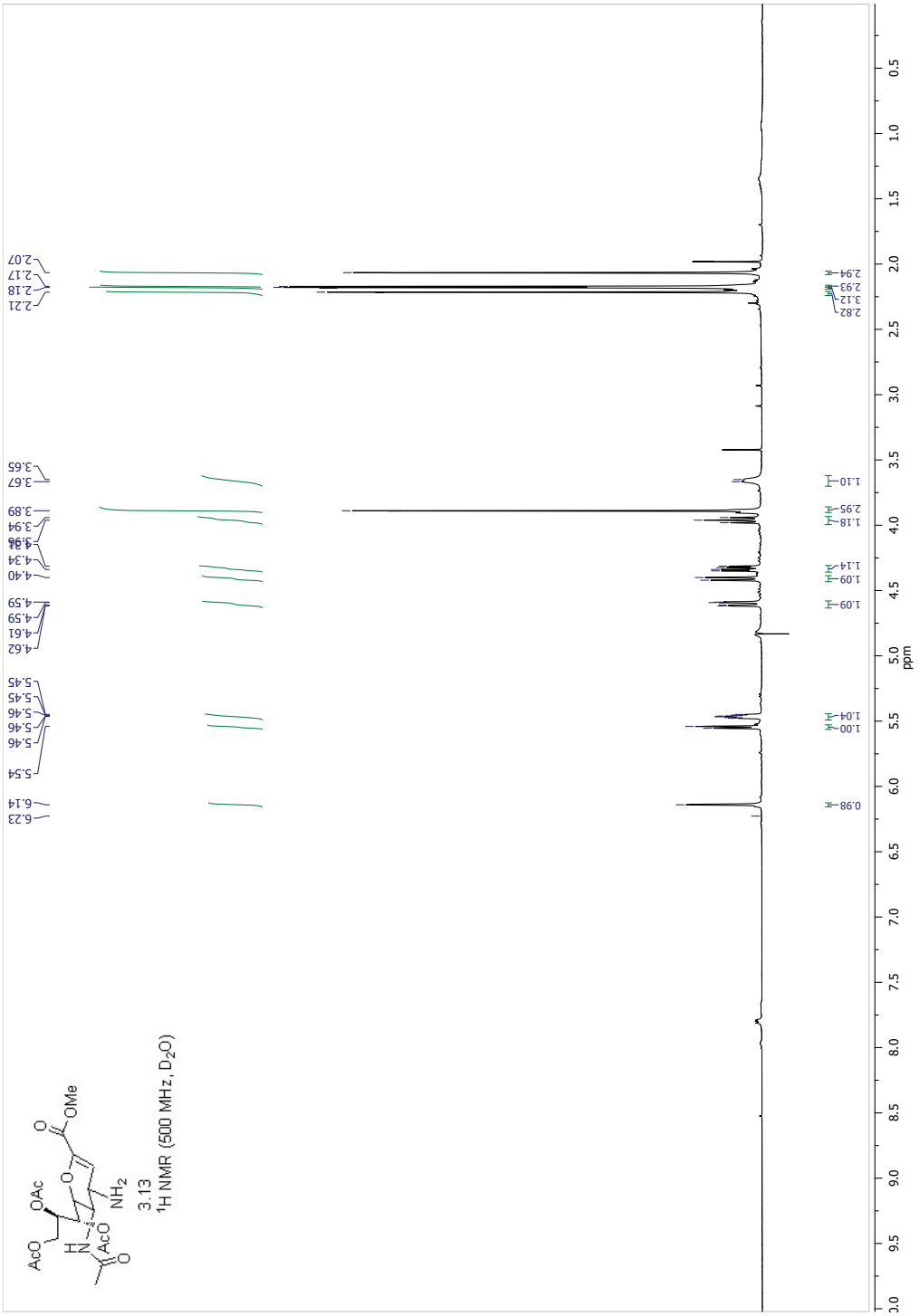
3.13
$^1$H NMR (500 MHz, $D_2O$)
ppm

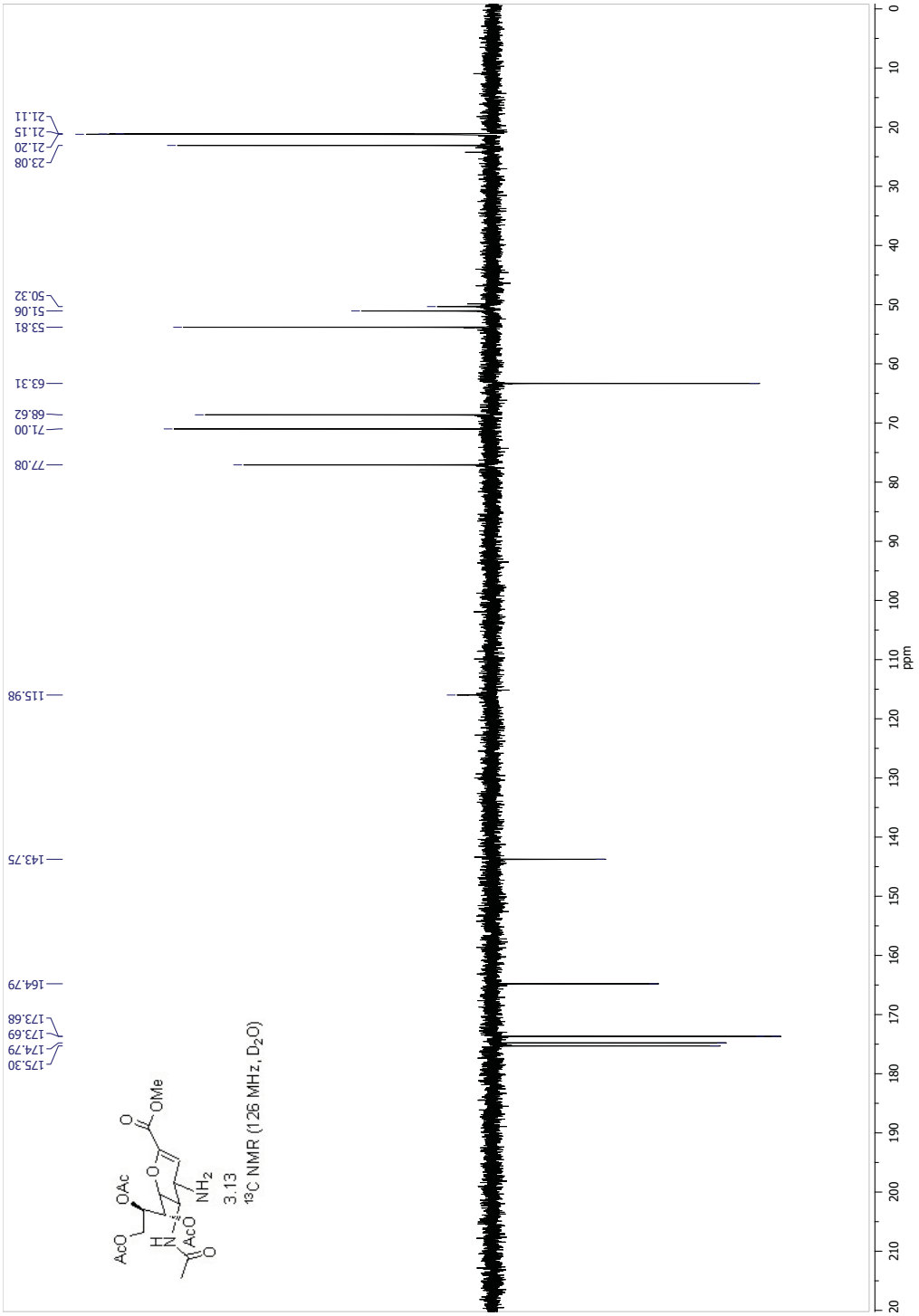
21.11
21.15
21.20
23.08
50.32
51.06
53.81
63.31
68.62
71.00
77.08
115.98
143.75
164.79
173.68
173.69
174.79
175.30
ppm
3.13
$^{13}$C NMR (126 MHz, $D_2O$)
AcO
OAc
O
OMe
O
$NH_2$
H
N
AcO
O

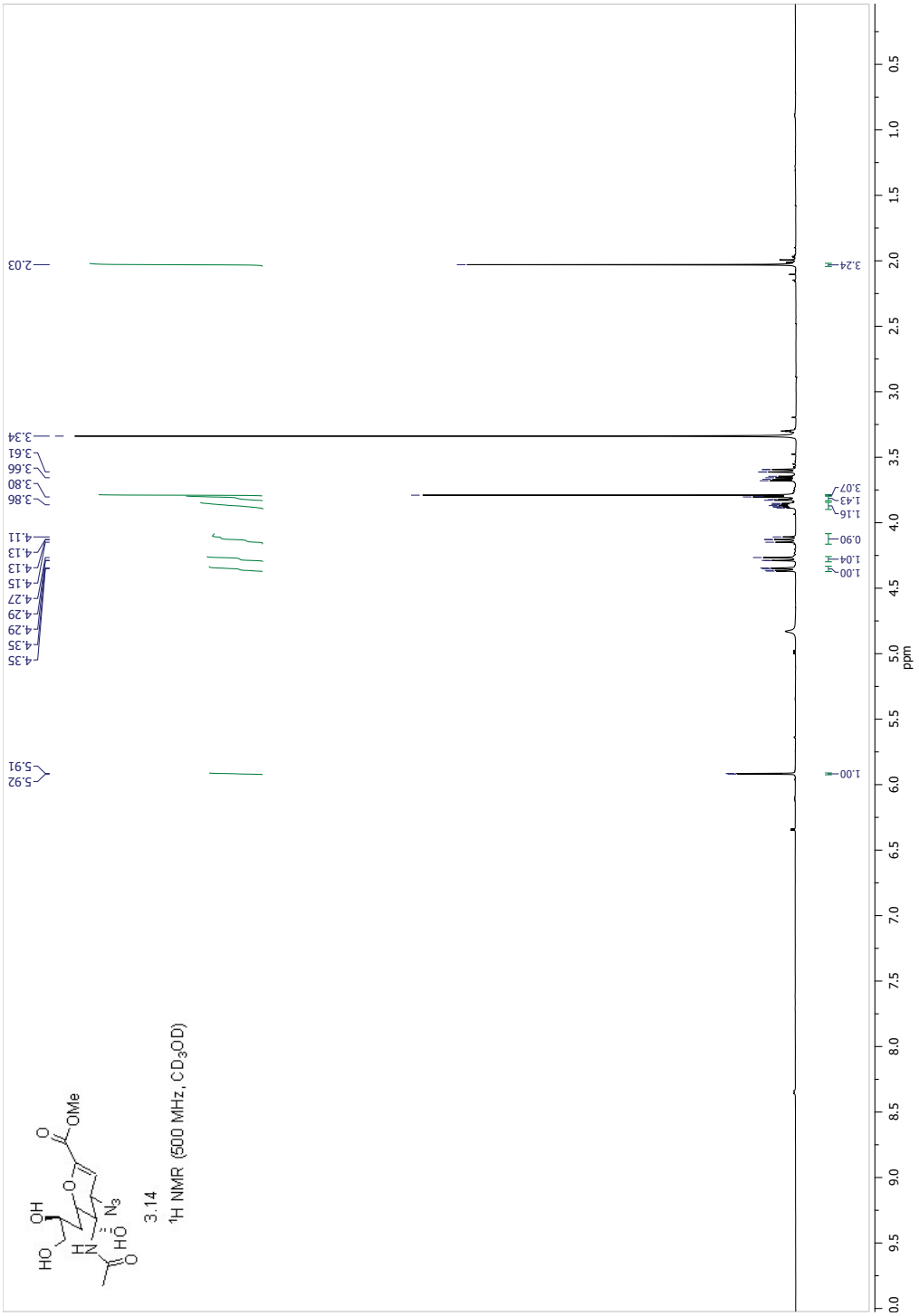
3.14
$^1$H NMR (500 MHz, $CD_3OD$)
5.92
5.91
4.35
4.35
4.29
4.29
4.27
4.15
4.13
4.13
4.11
3.86
3.80
3.66
3.61
3.34
2.03
1.00
3.24
1.16
1.43
3.07
0.90
1.04
1.00
ppm

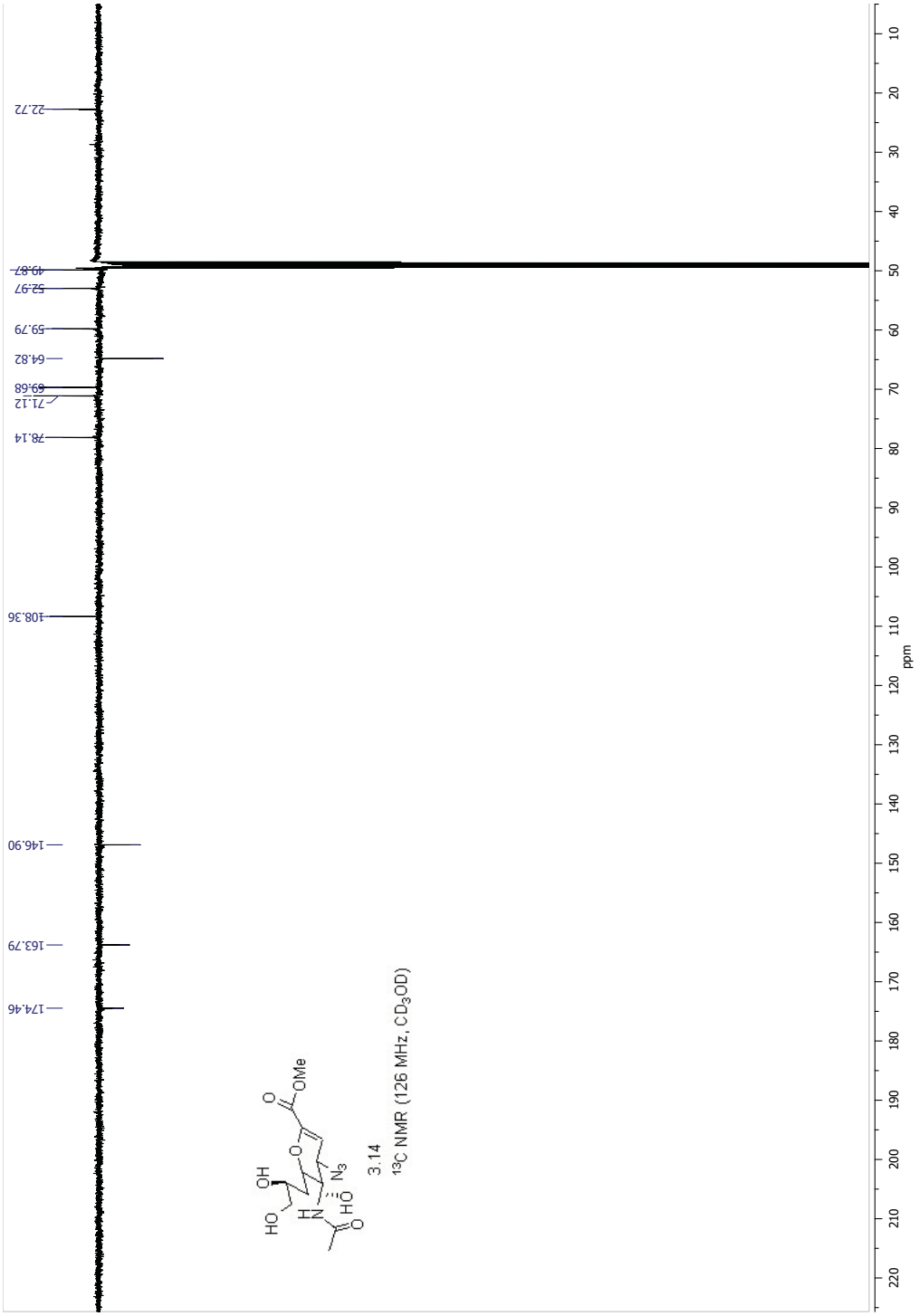
22.72
49.87
52.97
59.79
64.82
69.68
71.12
78.14
108.36
146.90
163.79
174.46
3.14
$^{13}$C NMR (126 MHz, $CD_3OD$)
ppm

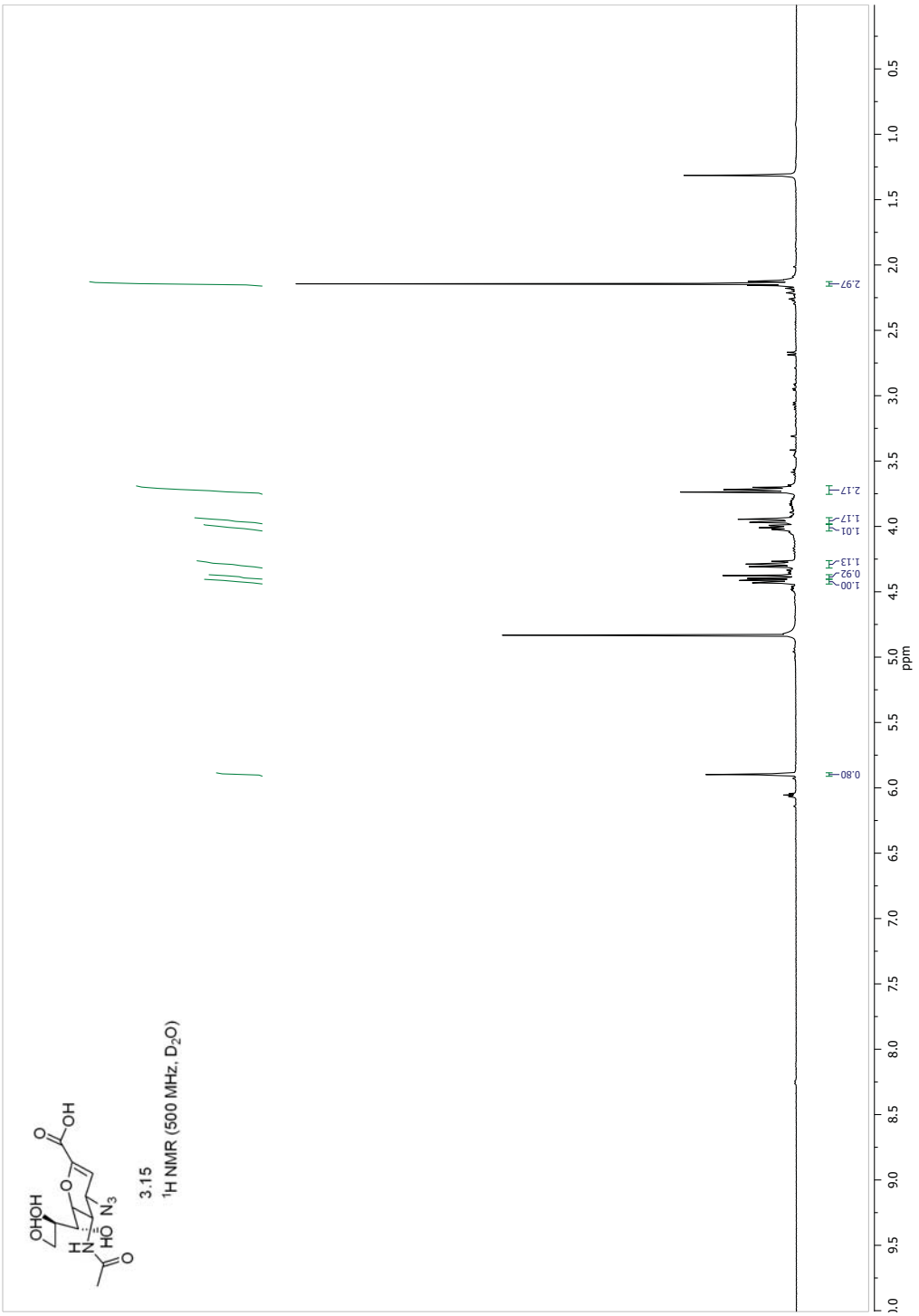
3.15
$^1$H NMR (500 MHz, $D_2O$)
2.97
2.17
1.01
1.17
1.13
0.92
1.00
0.80
ppm

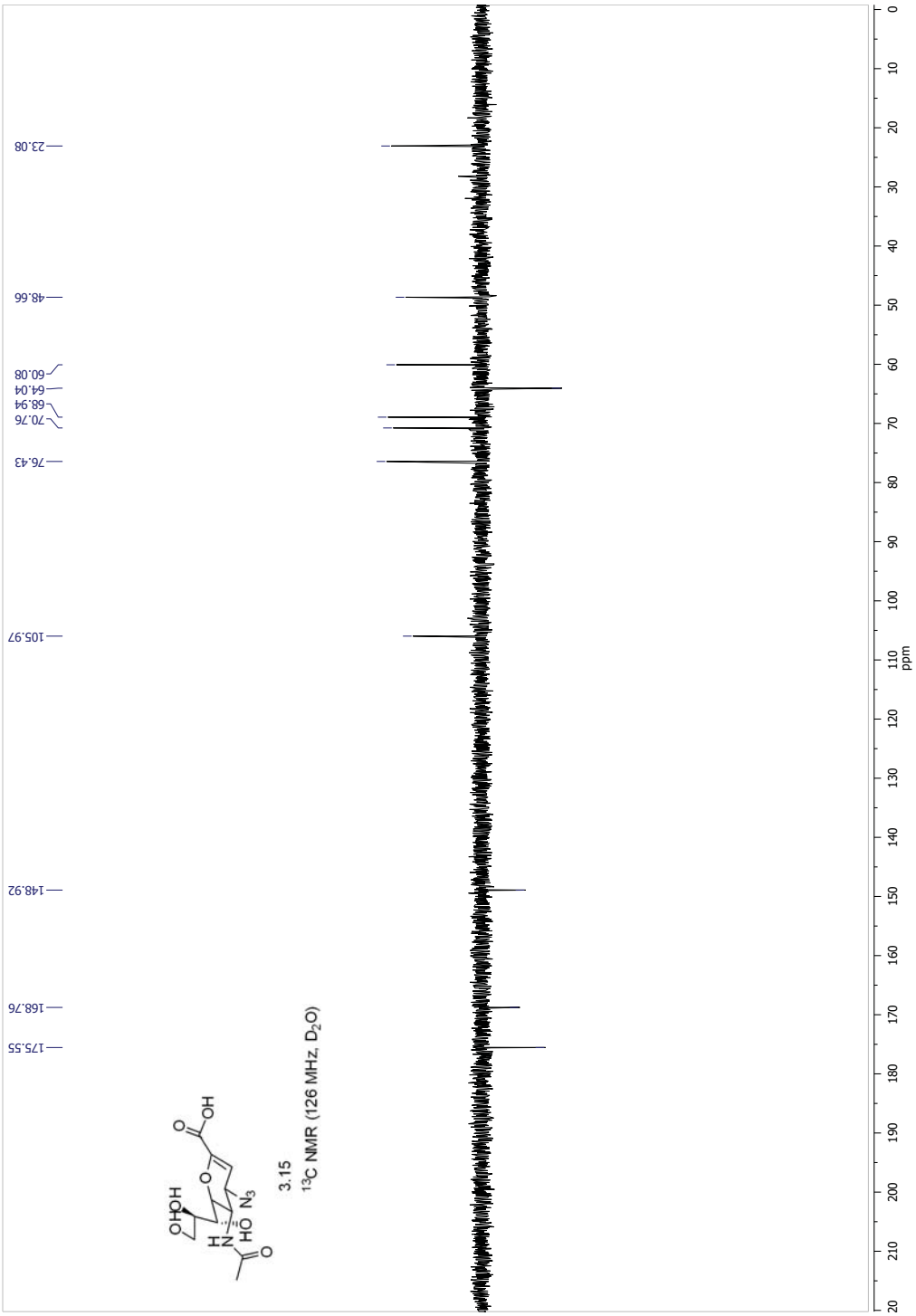
3,15
$^{13}$C NMR (126 MHz, $D_2O$)
175.55
168.76
148.92
105.97
76.43
70.76
68.94
64.04
60.08
48.66
23.08
ppm

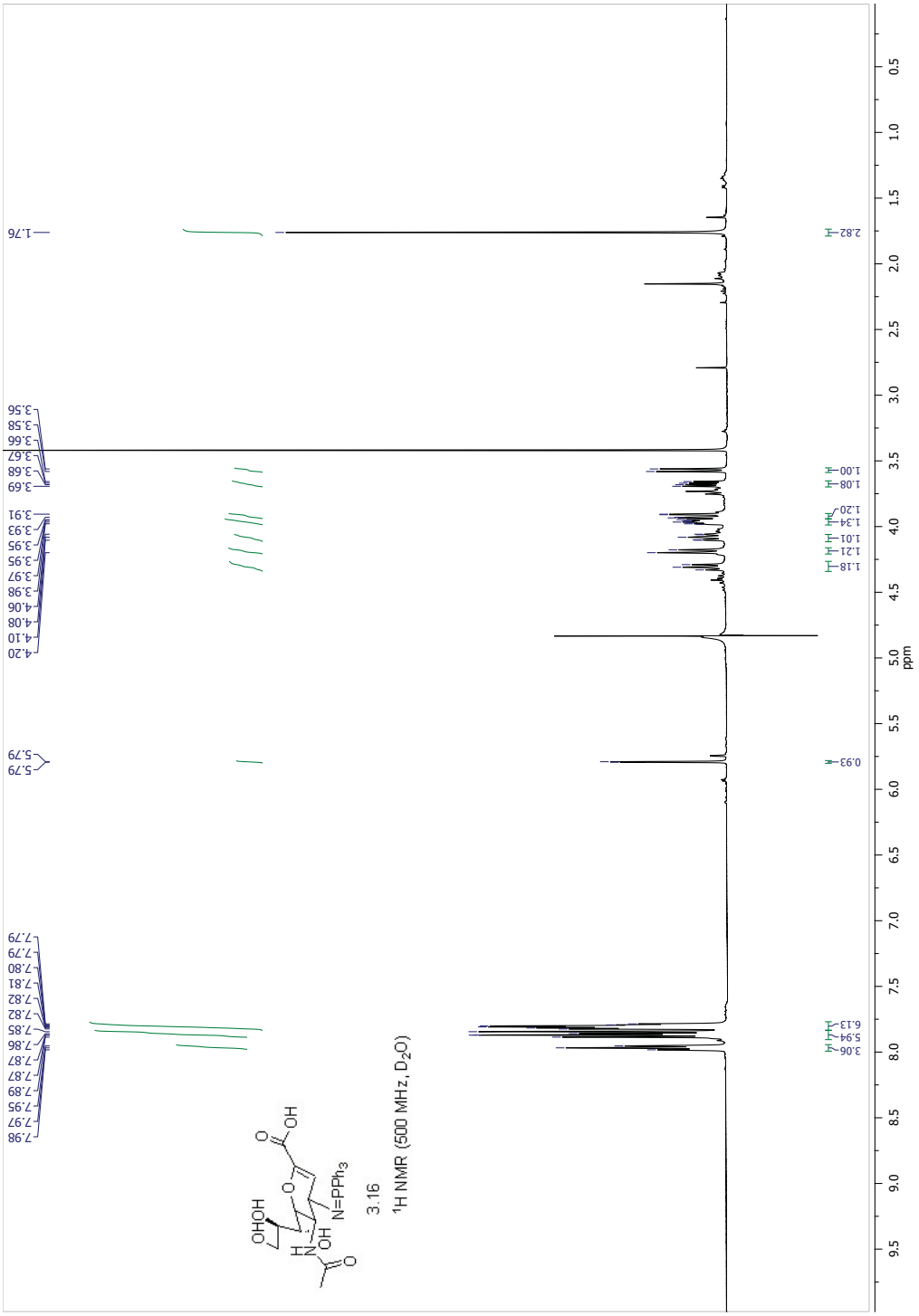
3.16
$^1$H NMR (500 MHz, $D_2O$)
ppm

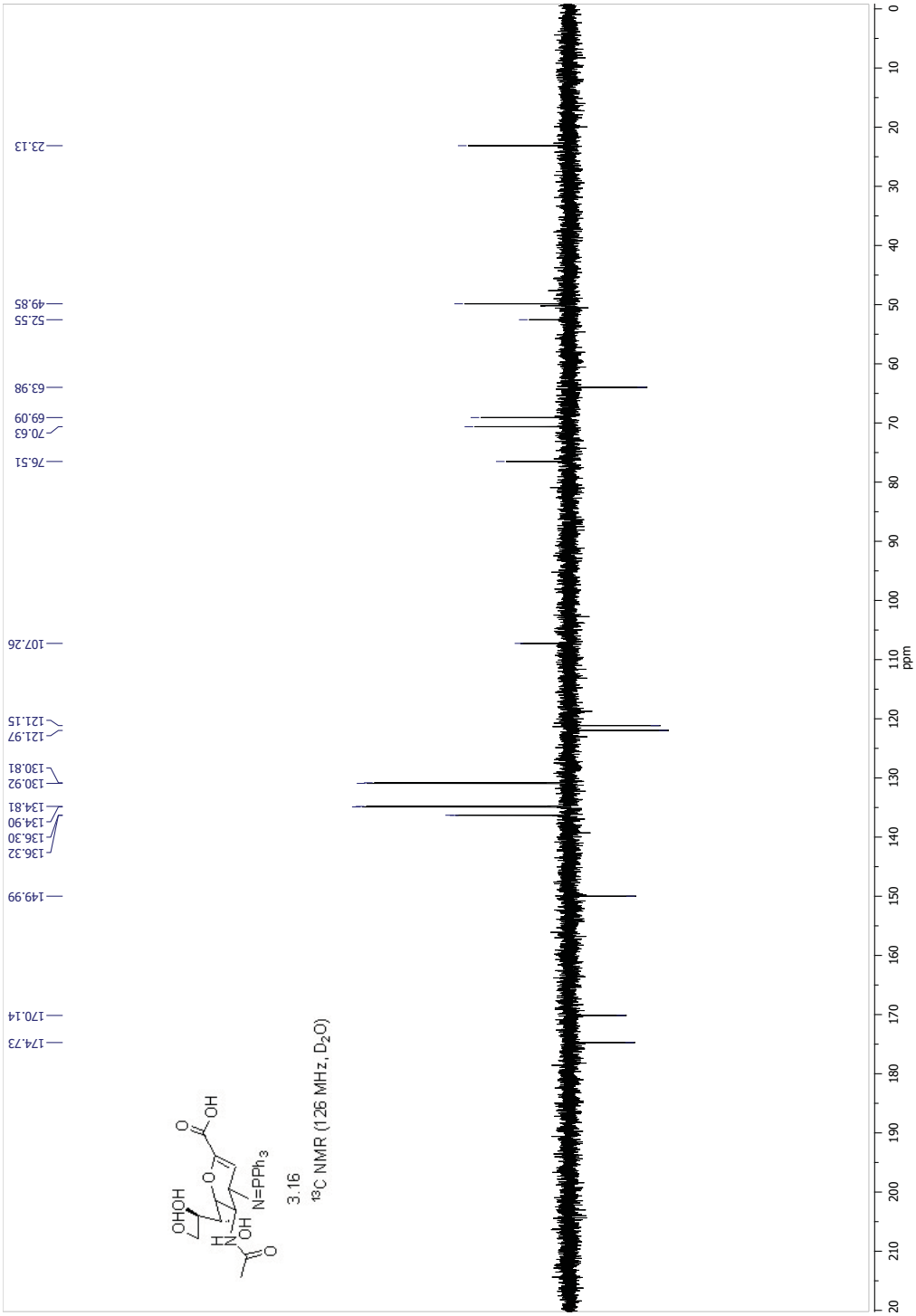
23.13
49.85
52.55
63.98
69.09
70.63
76.51
107.26
121.15
121.97
130.81
130.92
134.81
134.90
136.30
136.32
149.99
170.14
174.73
3.16
$^{13}$C NMR (126 MHz, $D_2O$)
ppm

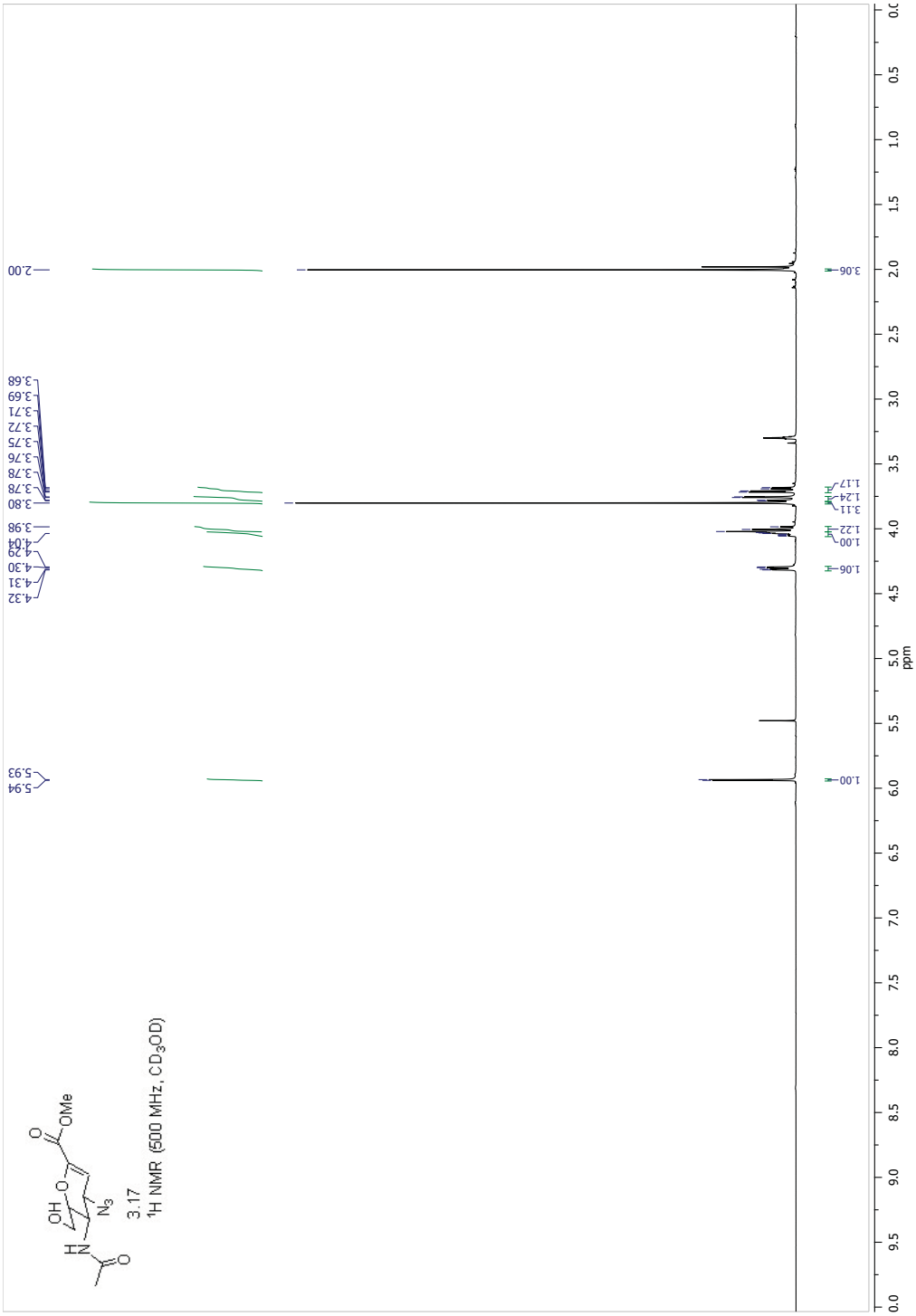
3.17
$^1$H NMR (500 MHz, $CD_3OD$)
5.94
5.93
4.32
4.31
4.30
4.29
4.04
3.98
3.80
3.78
3.78
3.76
3.75
3.72
3.71
3.69
3.68
2.00
3.06
1.17
1.24
3.11
1.22
1.00
1.06
1.00
ppm

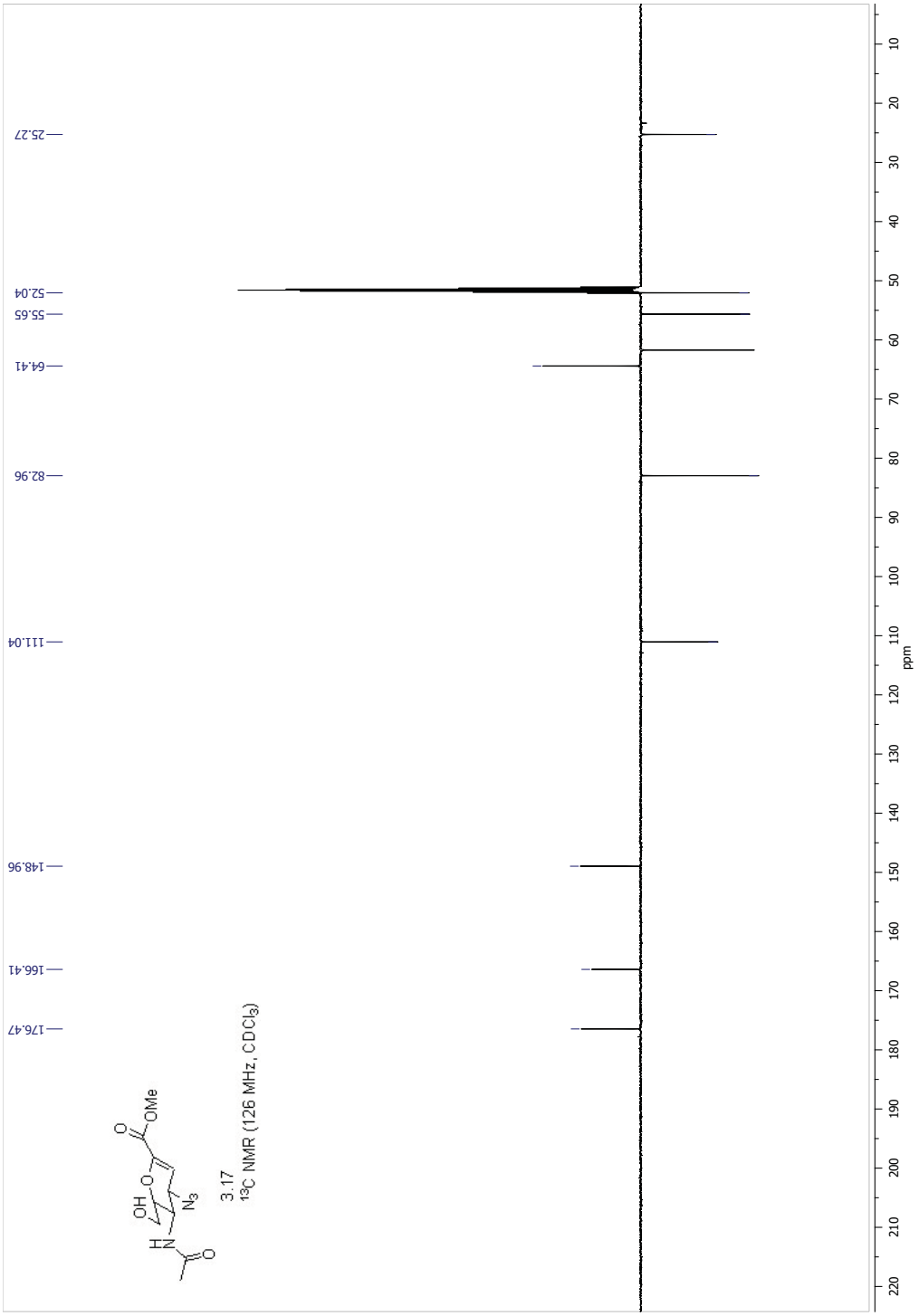
25.27
52.04
55.65
64.41
82.96
111.04
148.96
166.41
176.47
ppm
3.17
$^{13}$C NMR (126 MHz, $CDCl_3$)
OMe
OH
$N_3$

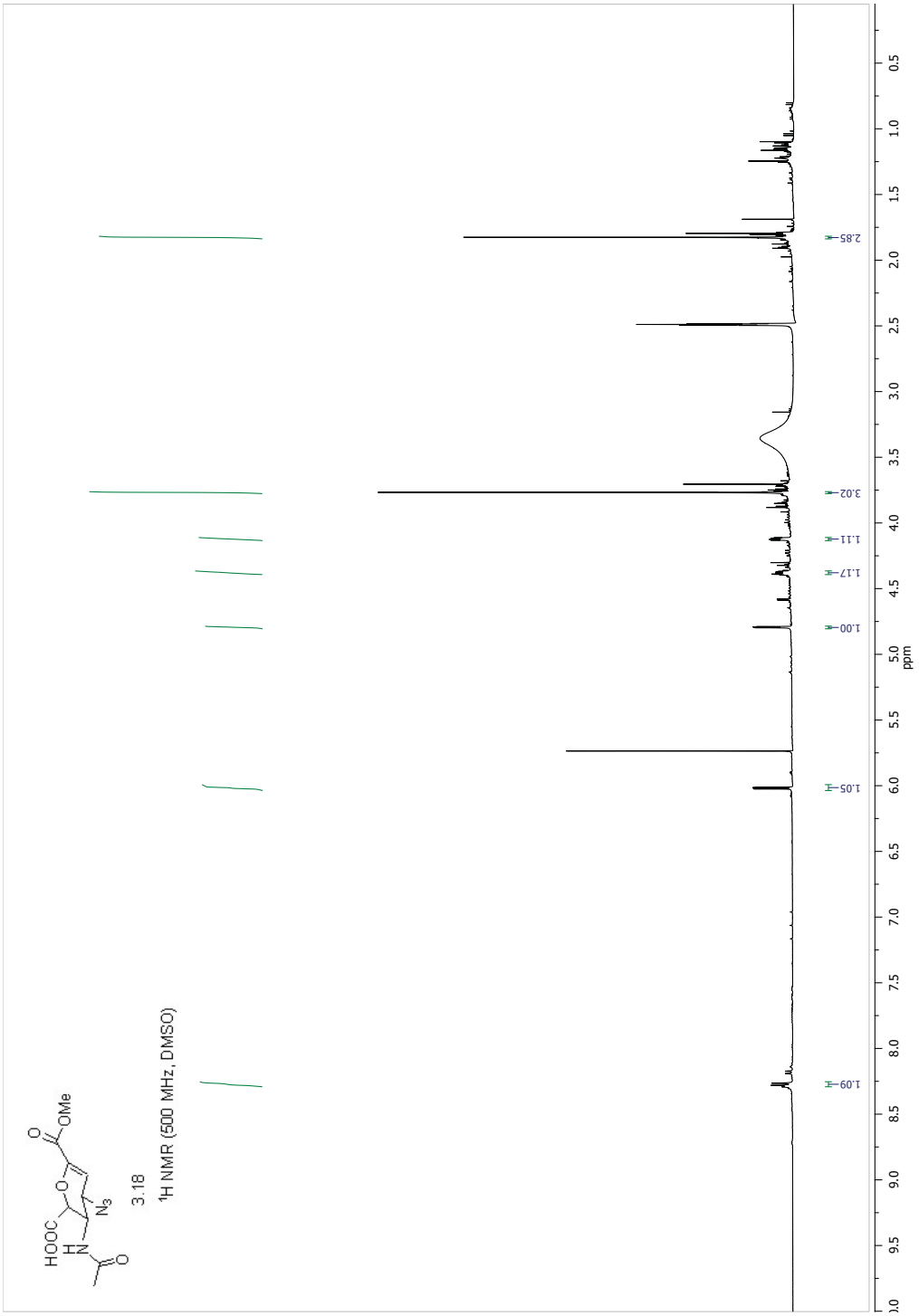
3.18
$^1$H NMR (500 MHz, DMSO)
1.09
1.05
1.00
1.17
1.11
3.02
2.85
ppm

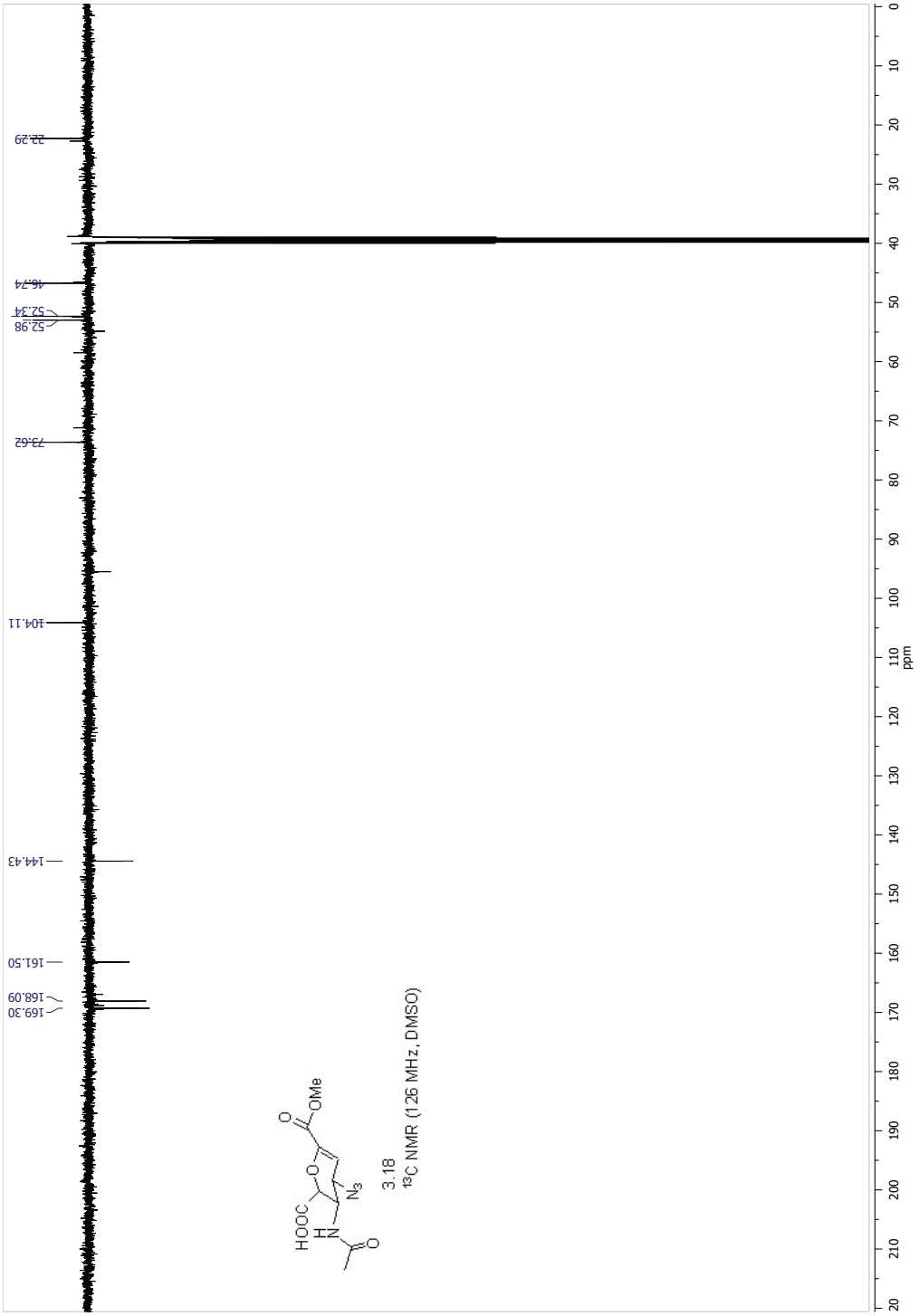
22.29
46.74
52.34
52.98
73.62
104.11
144.43
161.50
168.09
169.30
3.18
$^{13}$C NMR (126 MHz, DMSO)
HOOC
OMe
$N_3$
ppm

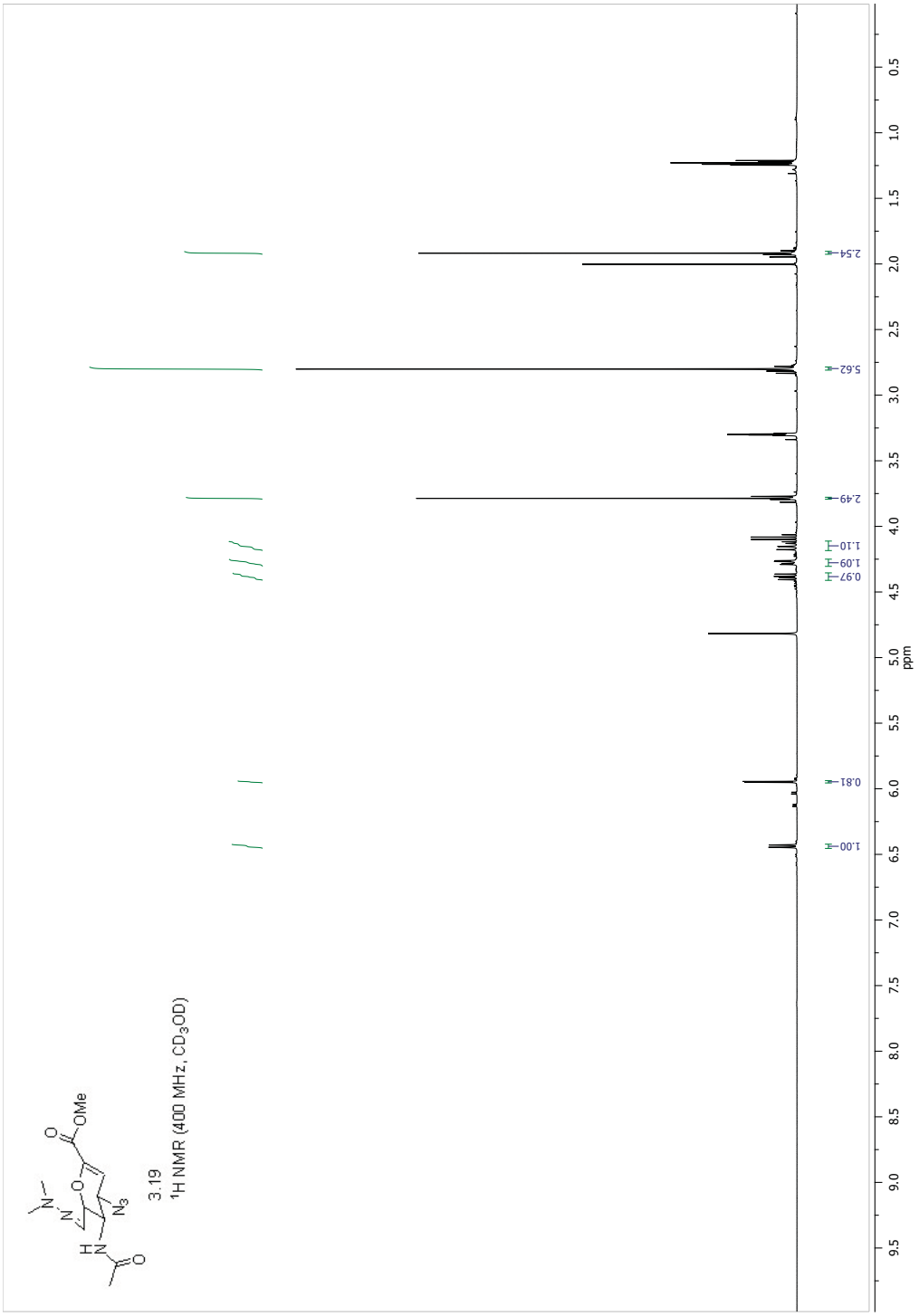
3.19
$^1$H NMR (400 MHz, $CD_3OD$)
OMe
$N_3$
2.54
5.62
2.49
1.10
1.09
0.97
0.81
1.00
ppm

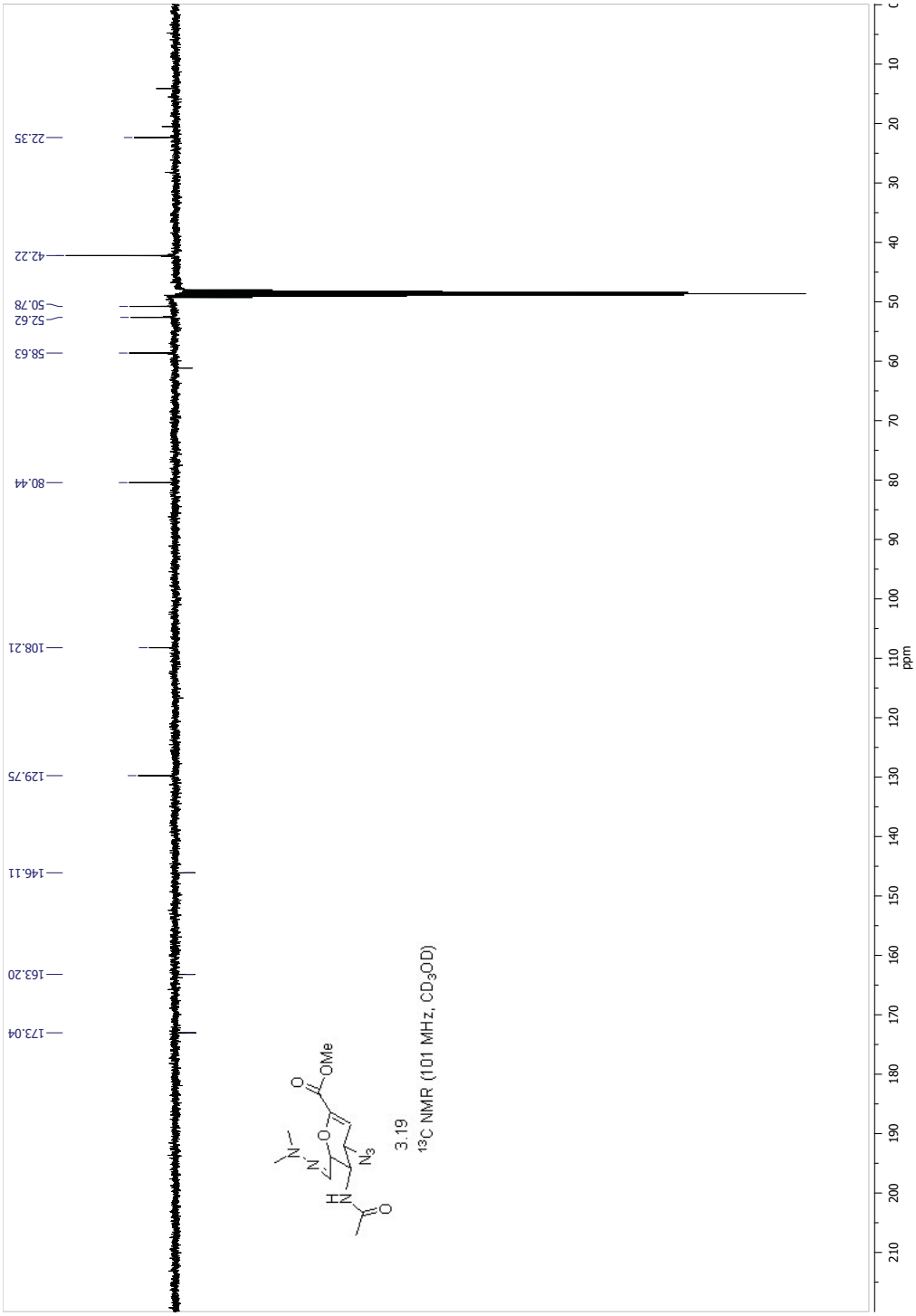
22.35
42.22
50.78
52.62
58.63
80.44
108.21
129.75
146.11
163.20
173.04
3.19
13C NMR (101 MHz, CD3OD)
ppm

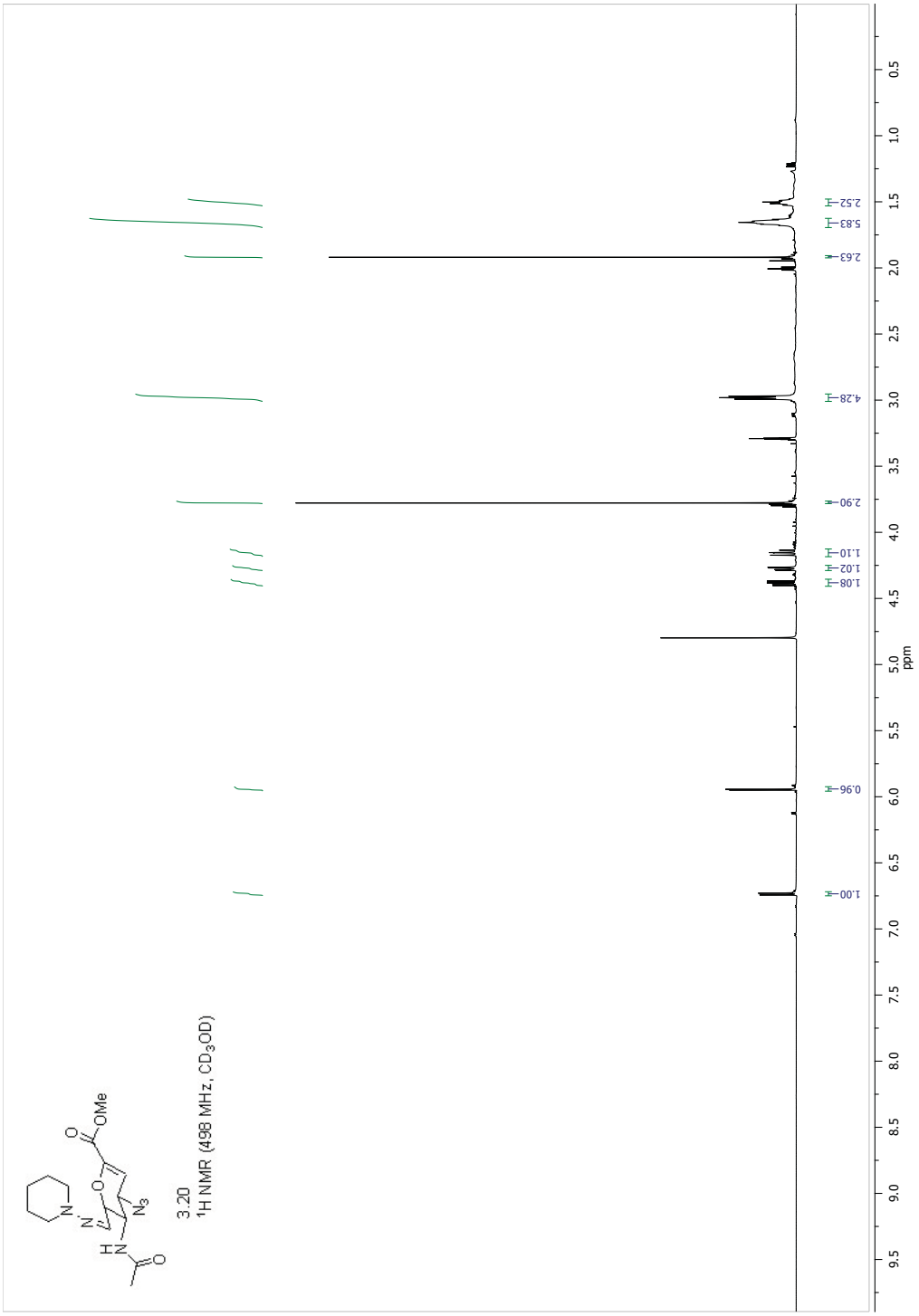
3.20
$^1$H NMR (498 MHz, $CD_3OD$)
OMe
$N_3$
2.52
5.83
2.63
4.28
2.90
1.10
1.02
1.08
0.96
1.00
ppm

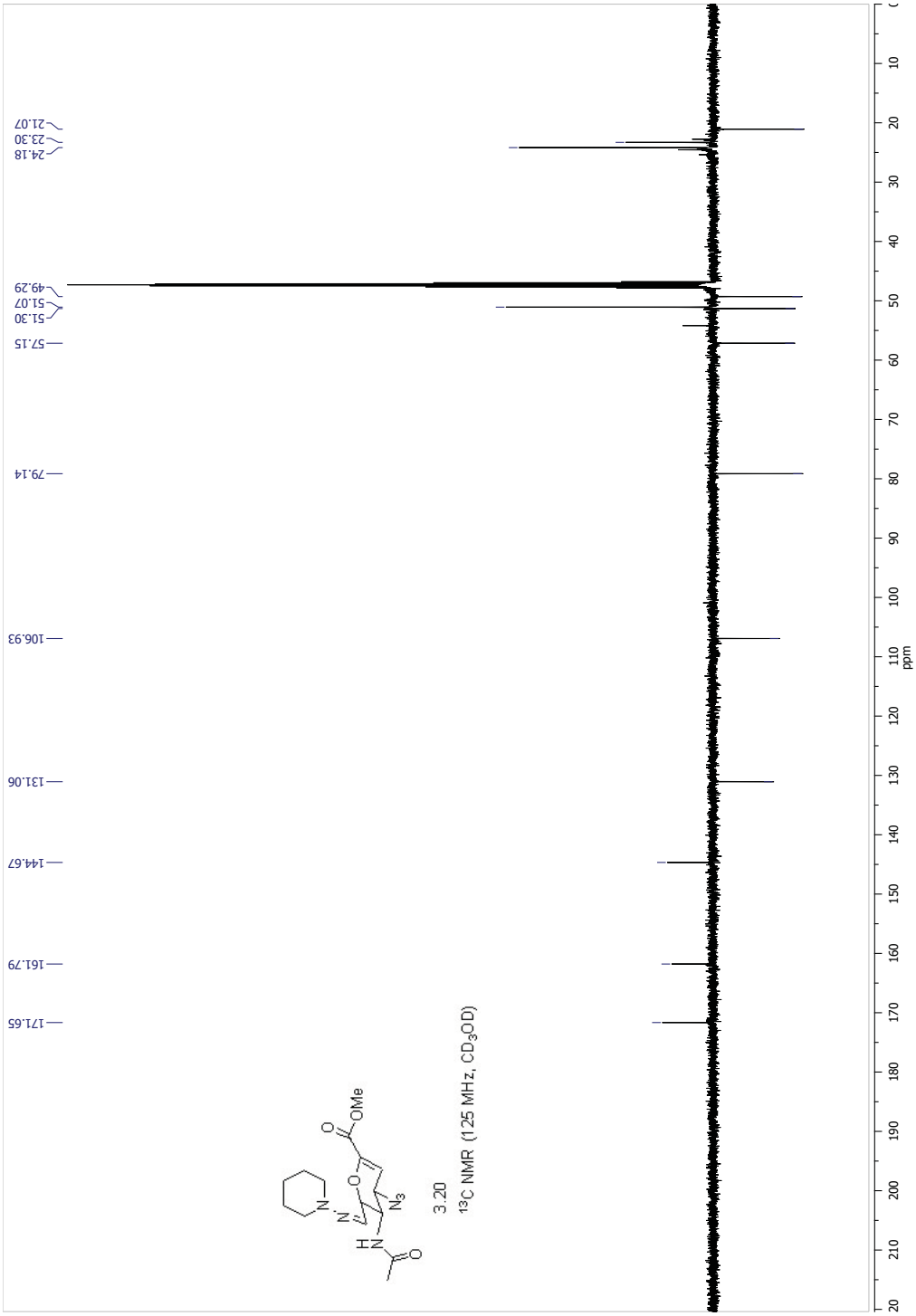
171.65
161.79
144.67
131.06
106.93
79.14
57.15
51.30
51.07
49.29
24.18
23.30
21.07
3.20
$^{13}$C NMR (125 MHz, $CD_3OD$)
ppm

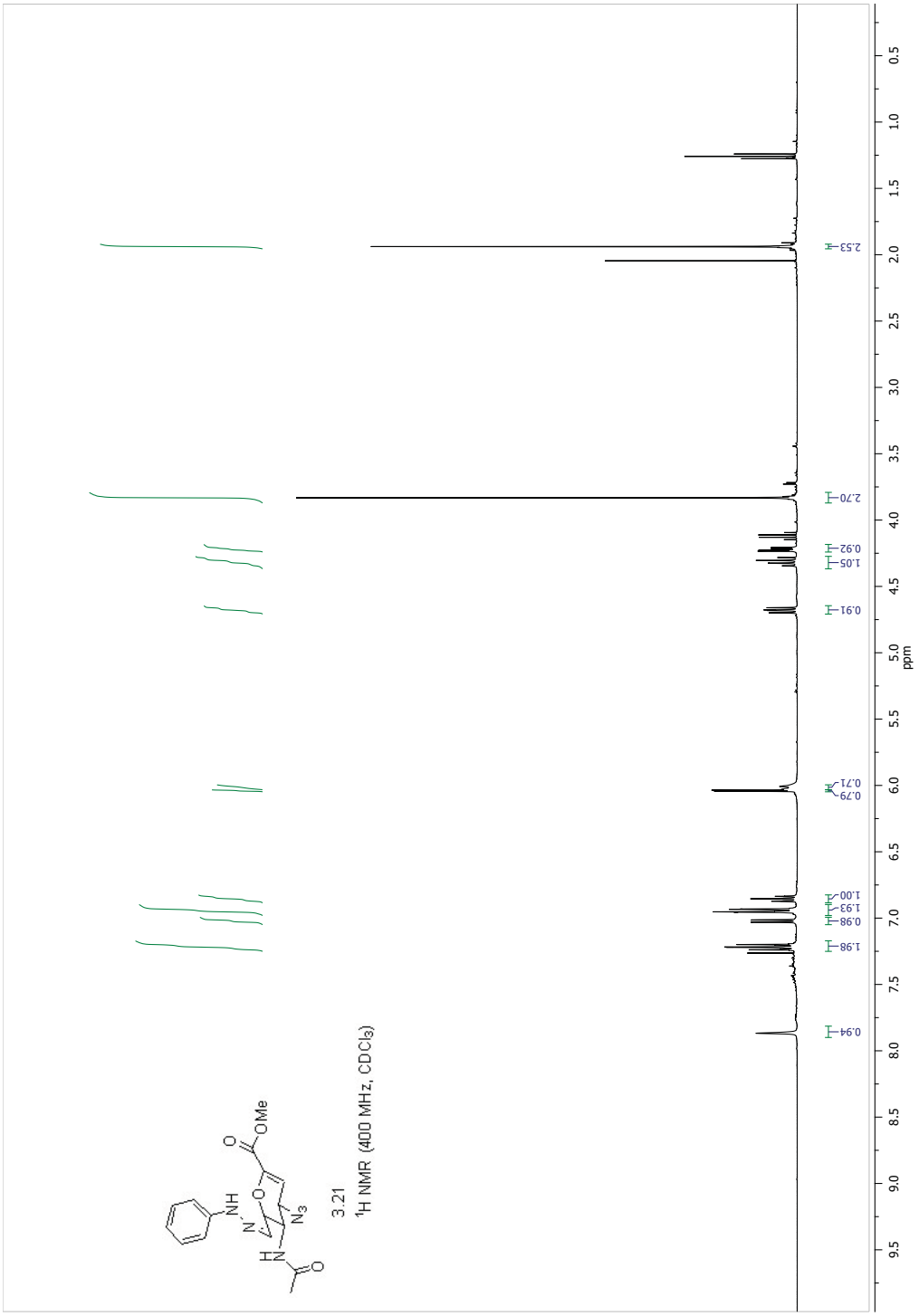
3.21
$^1$H NMR (400 MHz, CDCl$_3$)
2.53
2.70
0.92
1.05
0.91
0.79
0.71
1.00
1.93
0.98
1.98
0.94
ppm

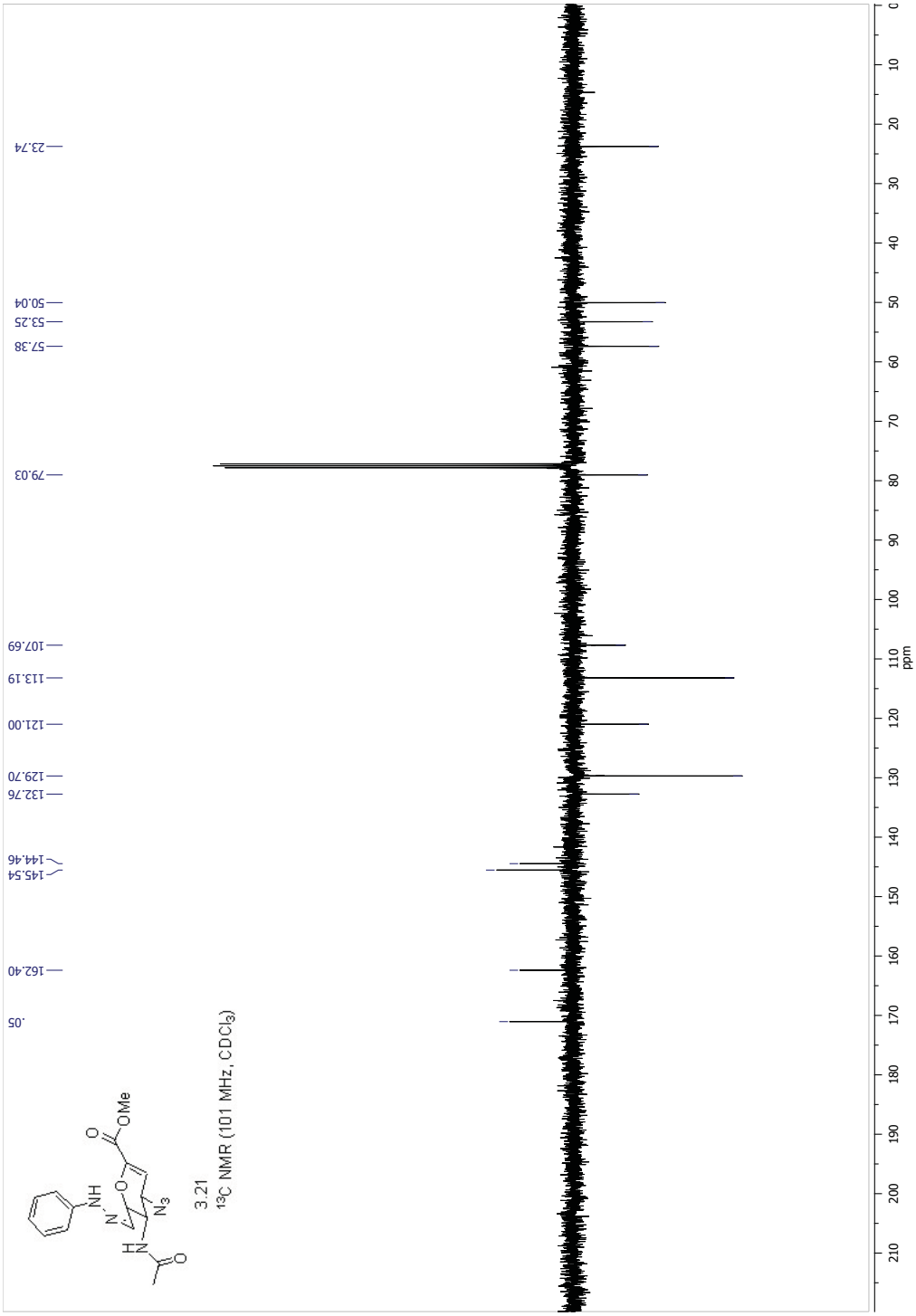
3.21
$^{13}$C NMR (101 MHz, CDCl$_3$)
23.74
50.04
53.25
57.38
79.03
107.69
113.19
121.00
129.70
132.76
144.46
145.54
162.40
.05
ppm

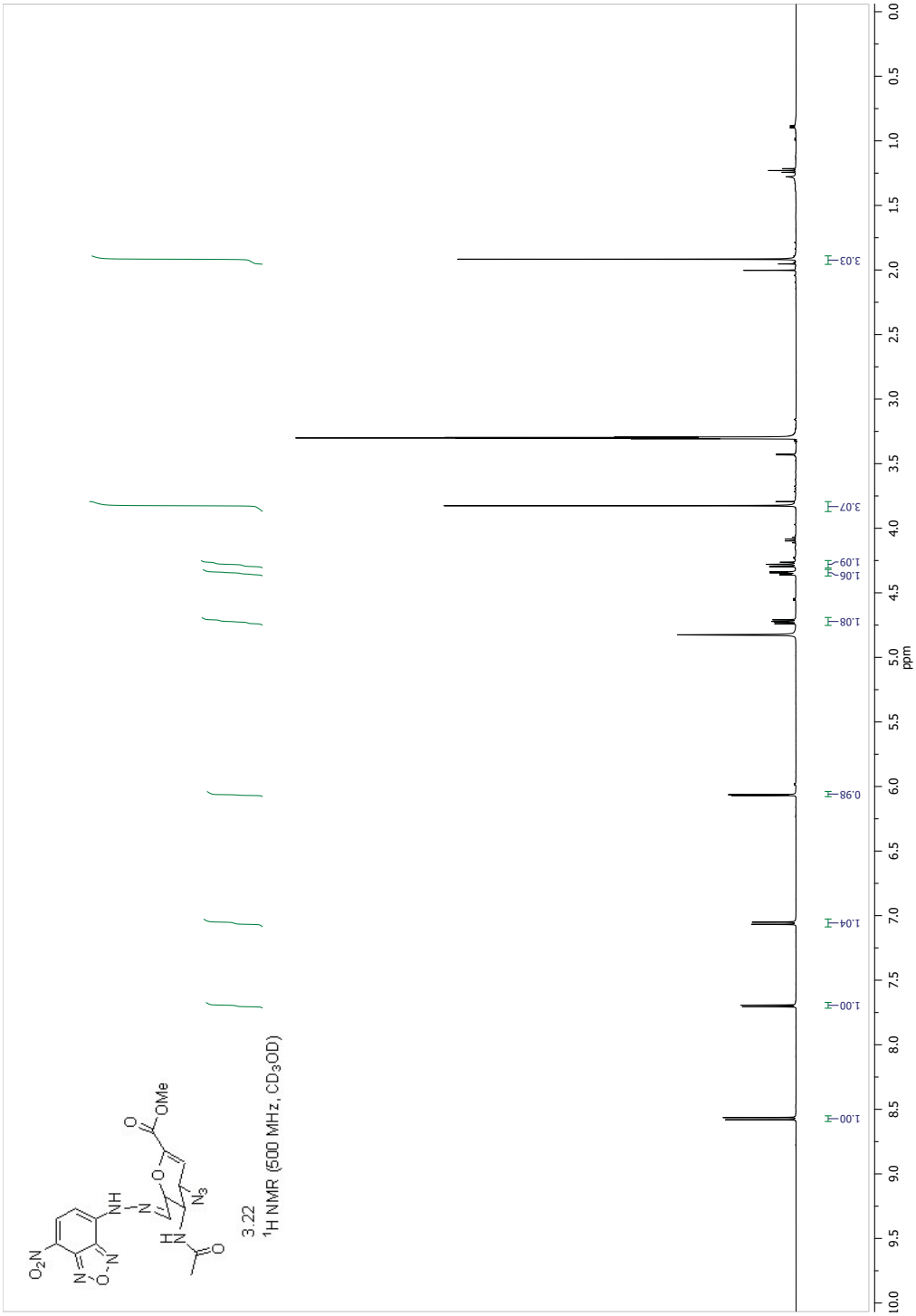
3.22
$^1$H NMR (500 MHz, $CD_3OD$)
3.03
3.07
1.09
1.06
1.08
0.98
1.04
1.00
1.00
ppm

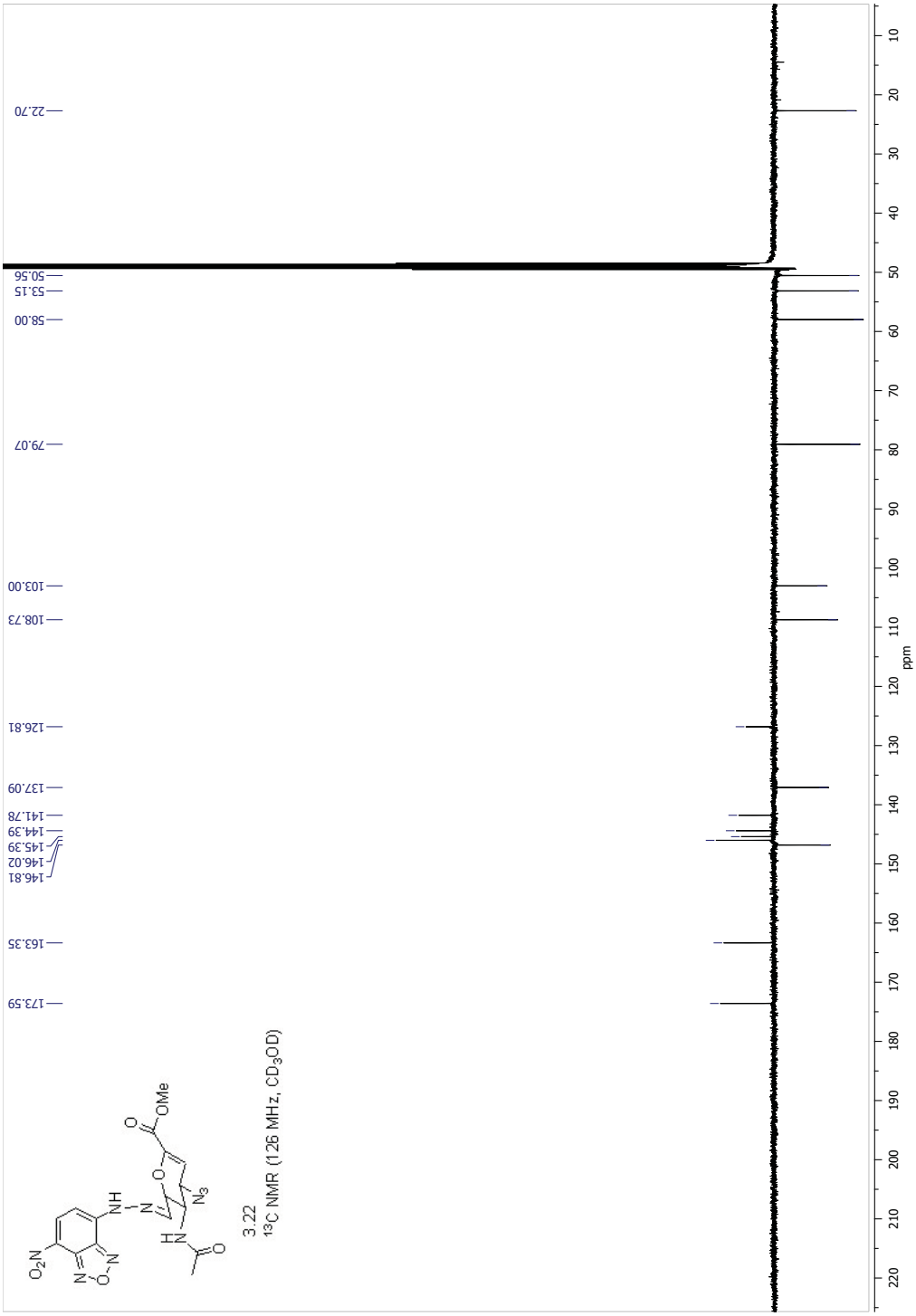
22.70
50.56
53.15
58.00
79.07
103.00
108.73
126.81
137.09
141.78
144.39
145.39
146.02
146.81
163.35
173.59
3.22
$^{13}$C NMR (126 MHz, $CD_3OD$)
ppm

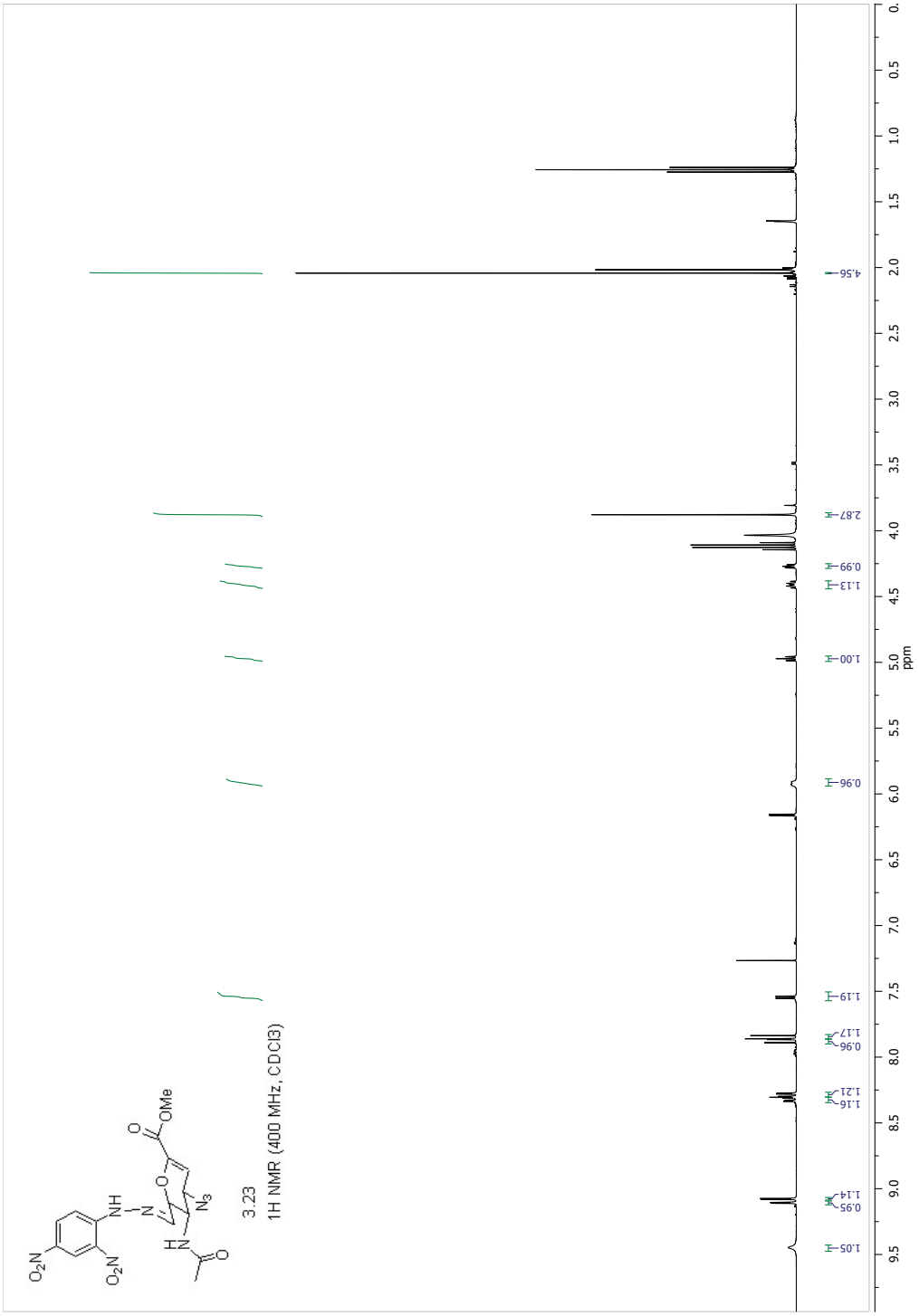
3.23
1H NMR (400 MHz, CDCl3)
4.56
2.87
0.99
1.13
1.00
0.96
1.19
0.96
1.17
1.16
1.21
0.95
1.14
1.05
ppm

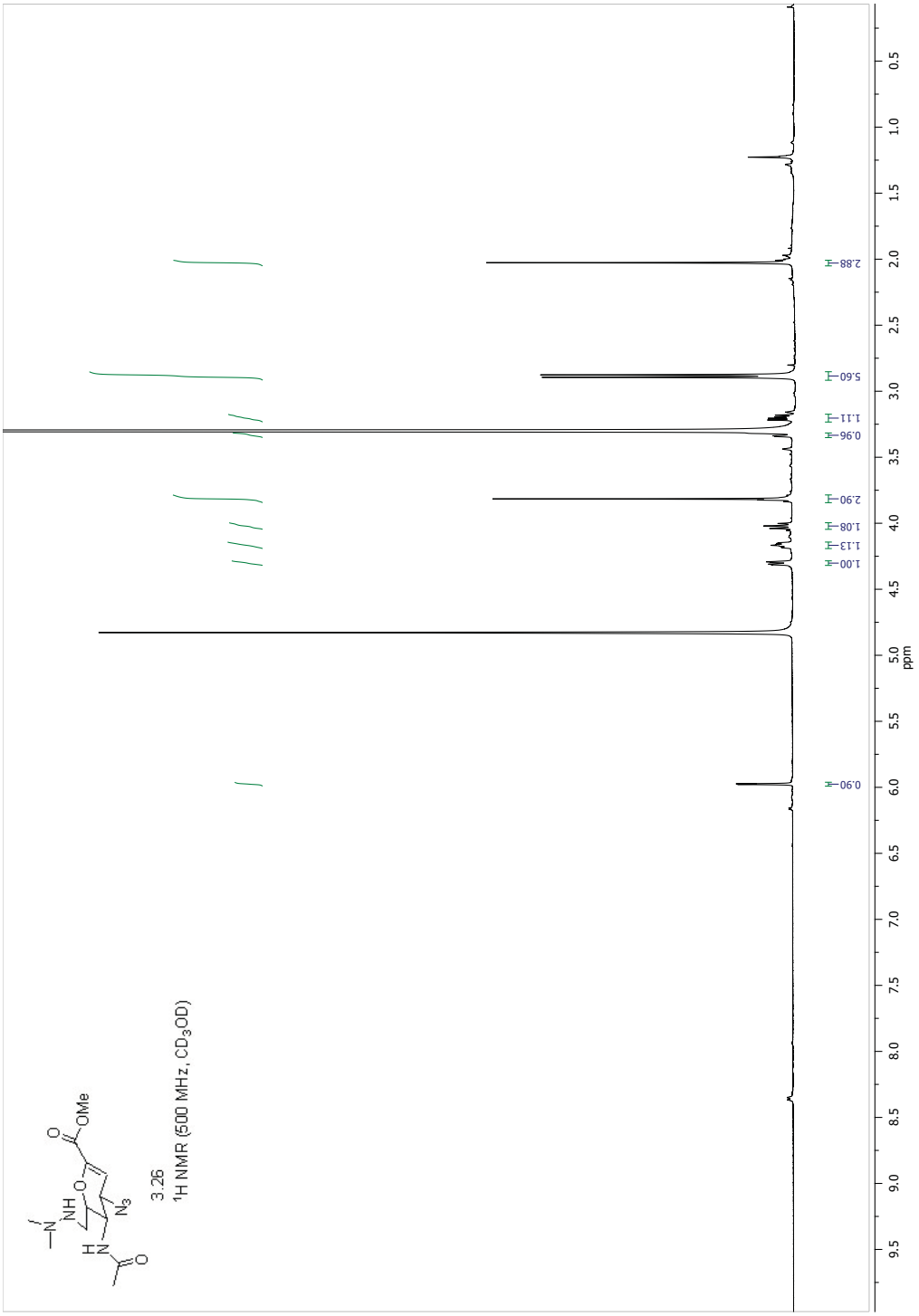
3.26
$^1$H NMR (500 MHz, $CD_3OD$)
2.88
5.60
1.11
0.96
2.90
1.08
1.13
1.00
0.90
ppm

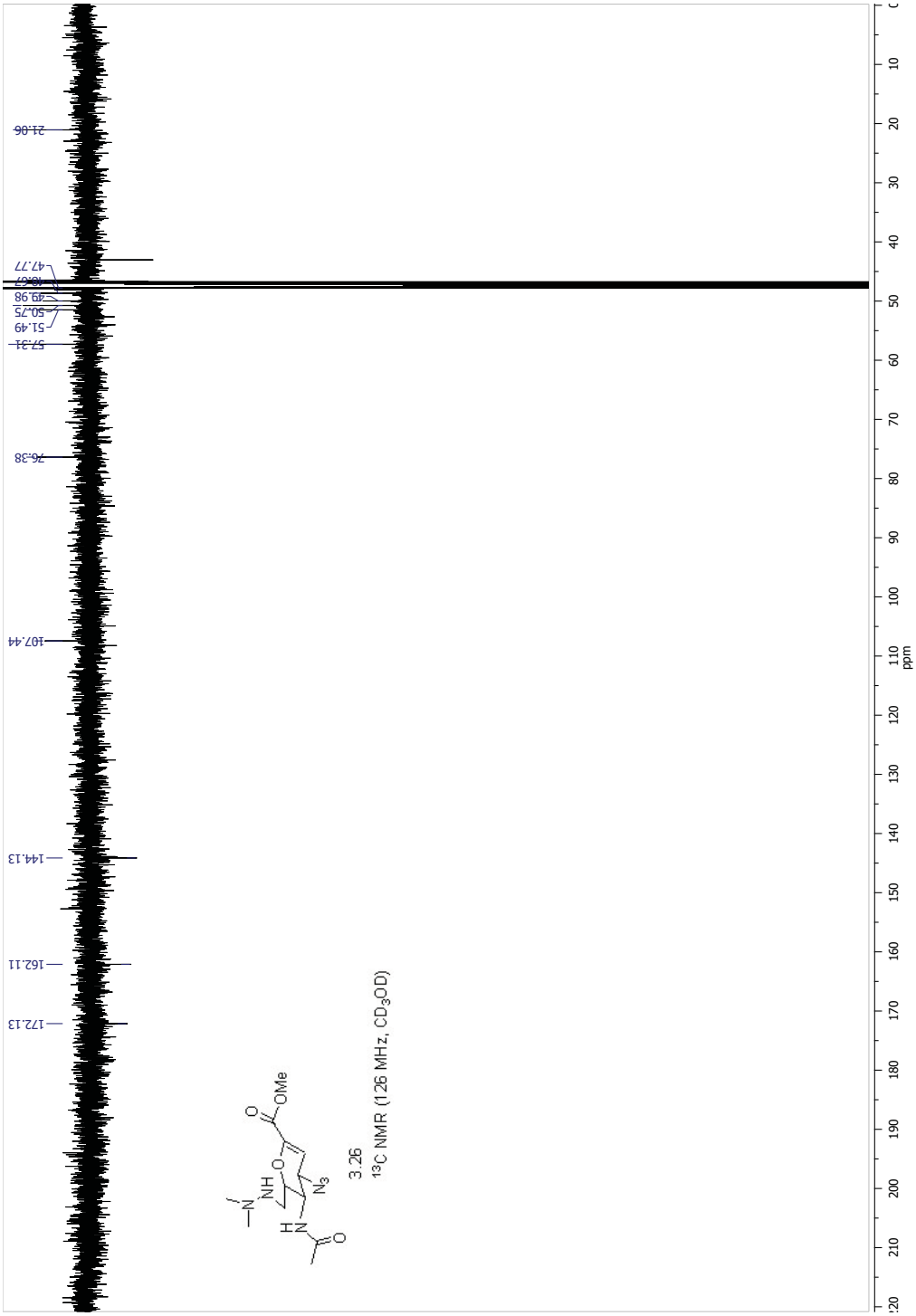
21.06
47.77
48.07
49.98
50.75
51.49
57.31
76.38
107.44
144.13
162.11
172.13
ppm
3.26
$^{13}$C NMR (126 MHz, $CD_3OD$)

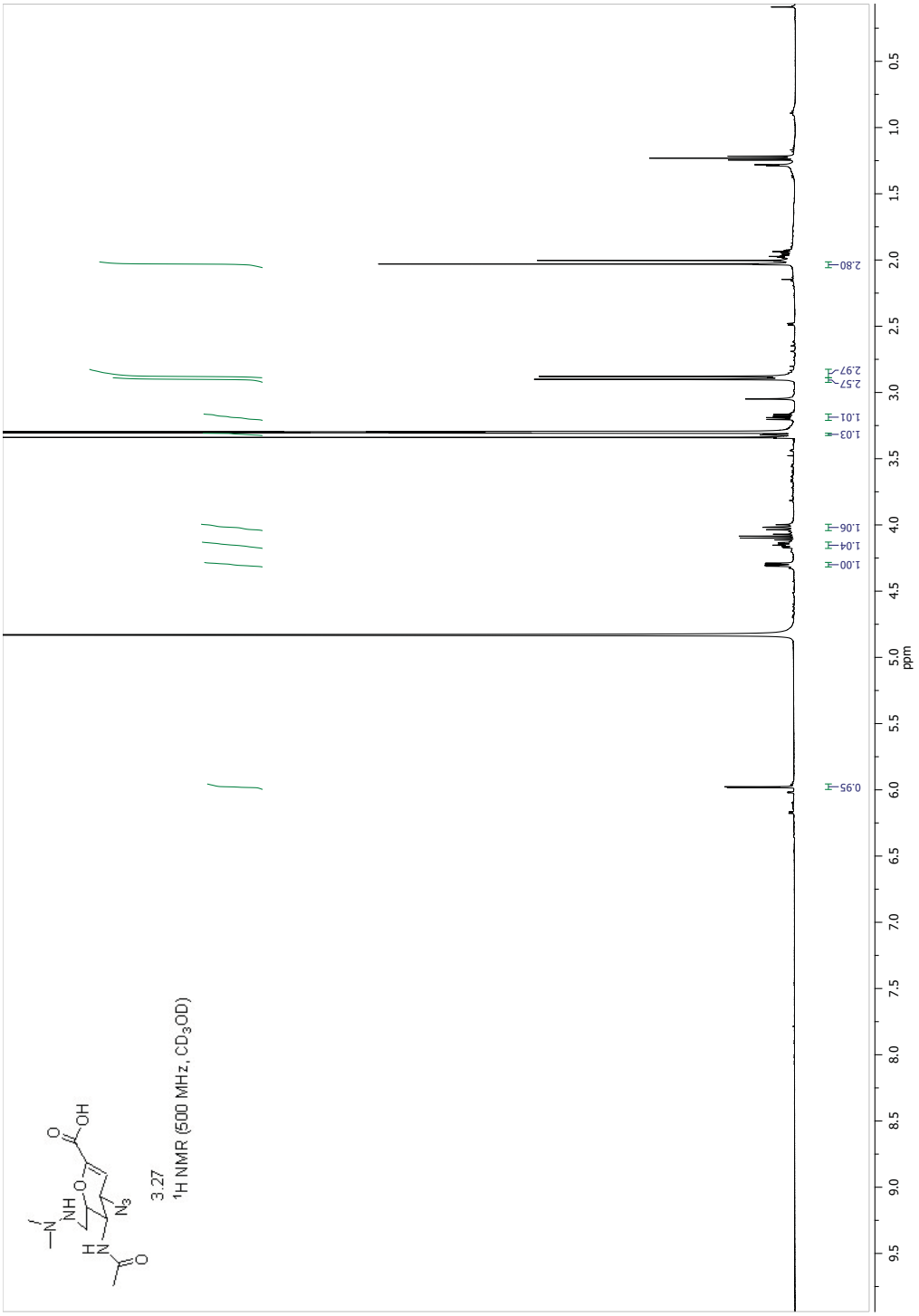
3.27
$^1$H NMR (500 MHz, $CD_3OD$)
2.80
2.97
2.57
1.01
1.03
1.06
1.04
1.00
0.95
ppm

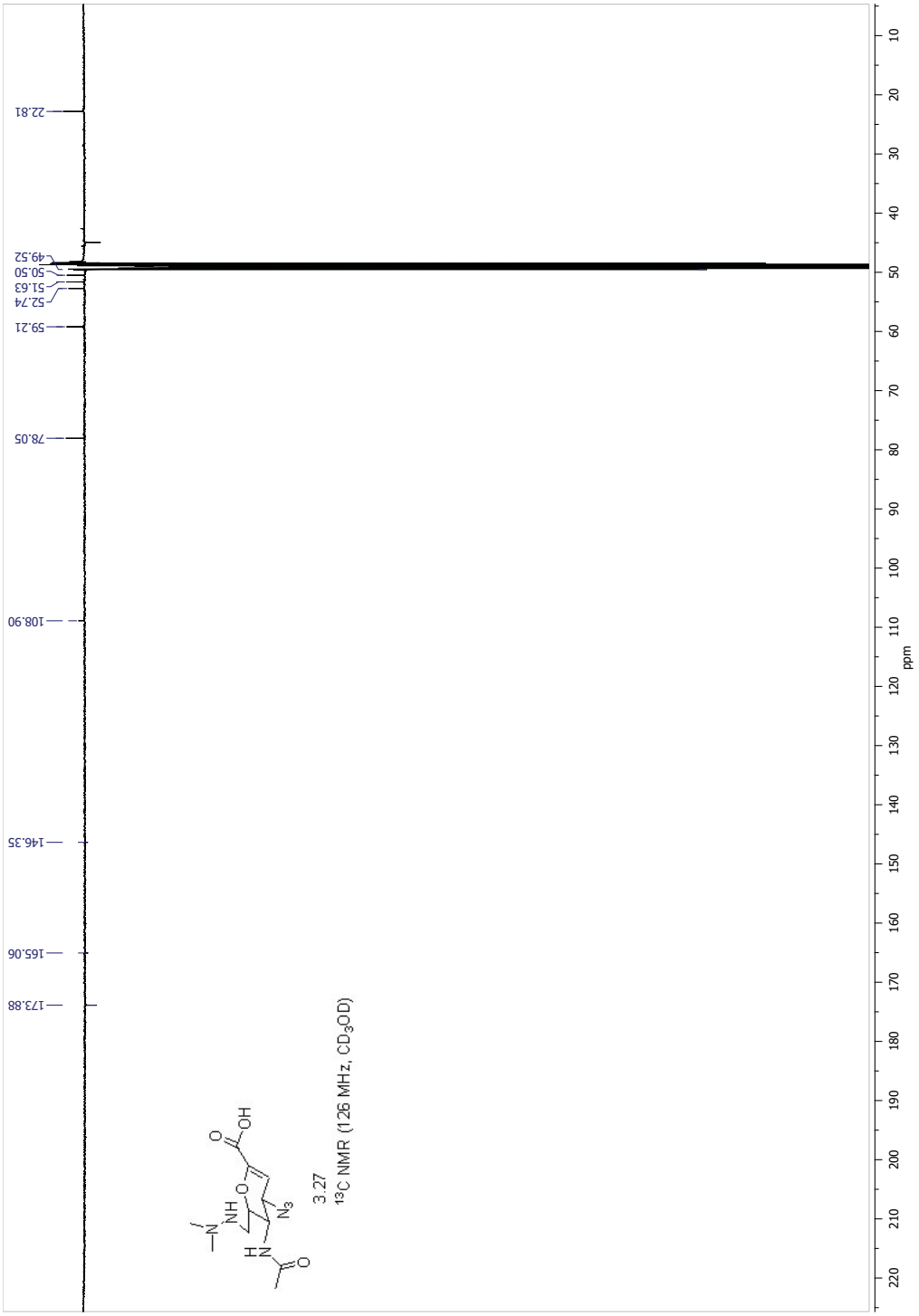
22.81
49.52
50.50
51.63
52.74
59.21
78.05
108.90
146.35
165.06
173.88
10
20
30
40
50
60
70
80
90
100
110
120
130
140
150
160
170
180
190
200
210
220
ppm
3.27
$^{13}$C NMR (126 MHz, $CD_3OD$)

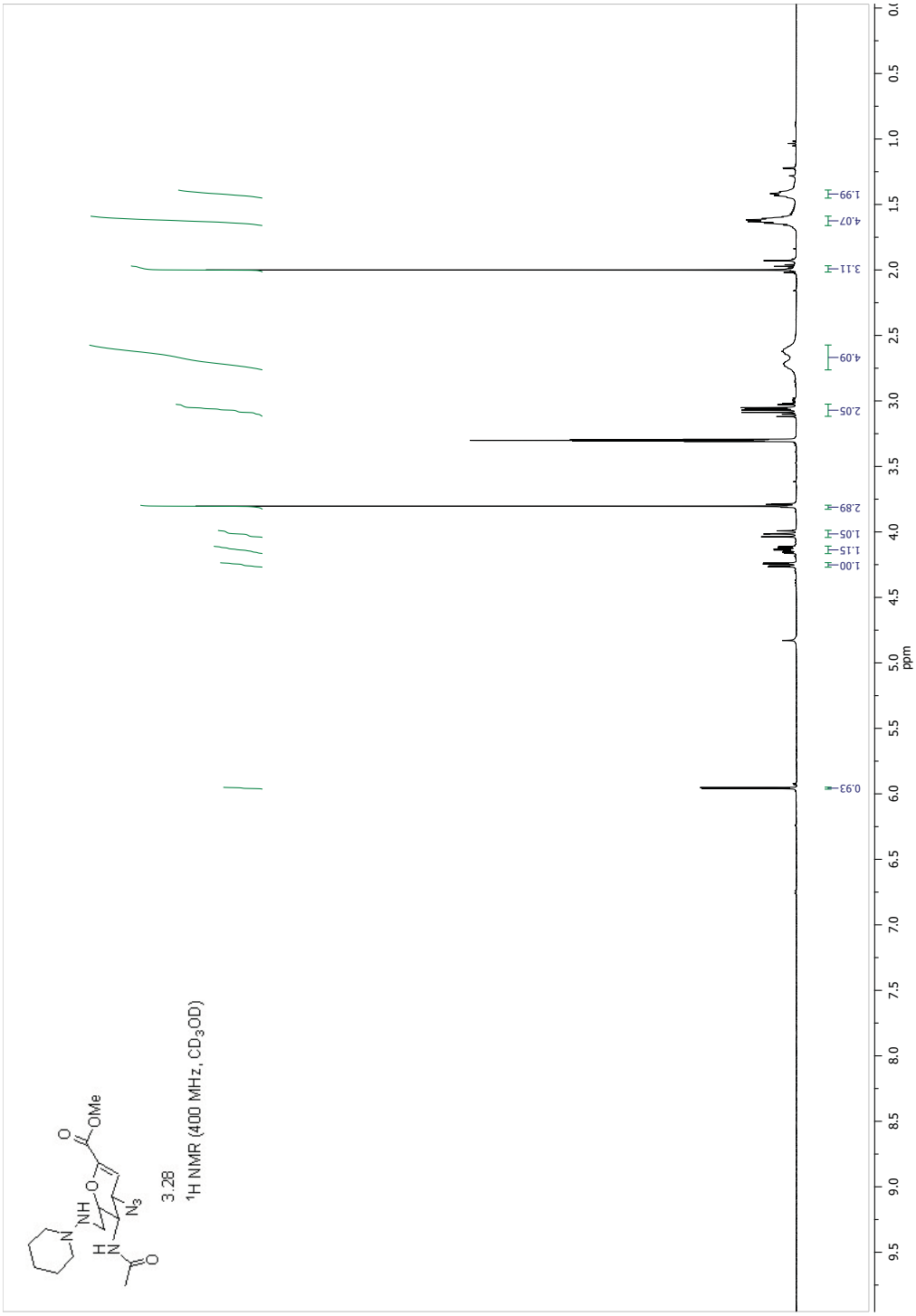
3.28
$^1$H NMR (400 MHz, $CD_3OD$)
OMe
O
NH
O
$N_3$
H
N
O
1.99
4.07
3.11
4.09
2.05
2.89
1.05
1.15
1.00
0.93
ppm

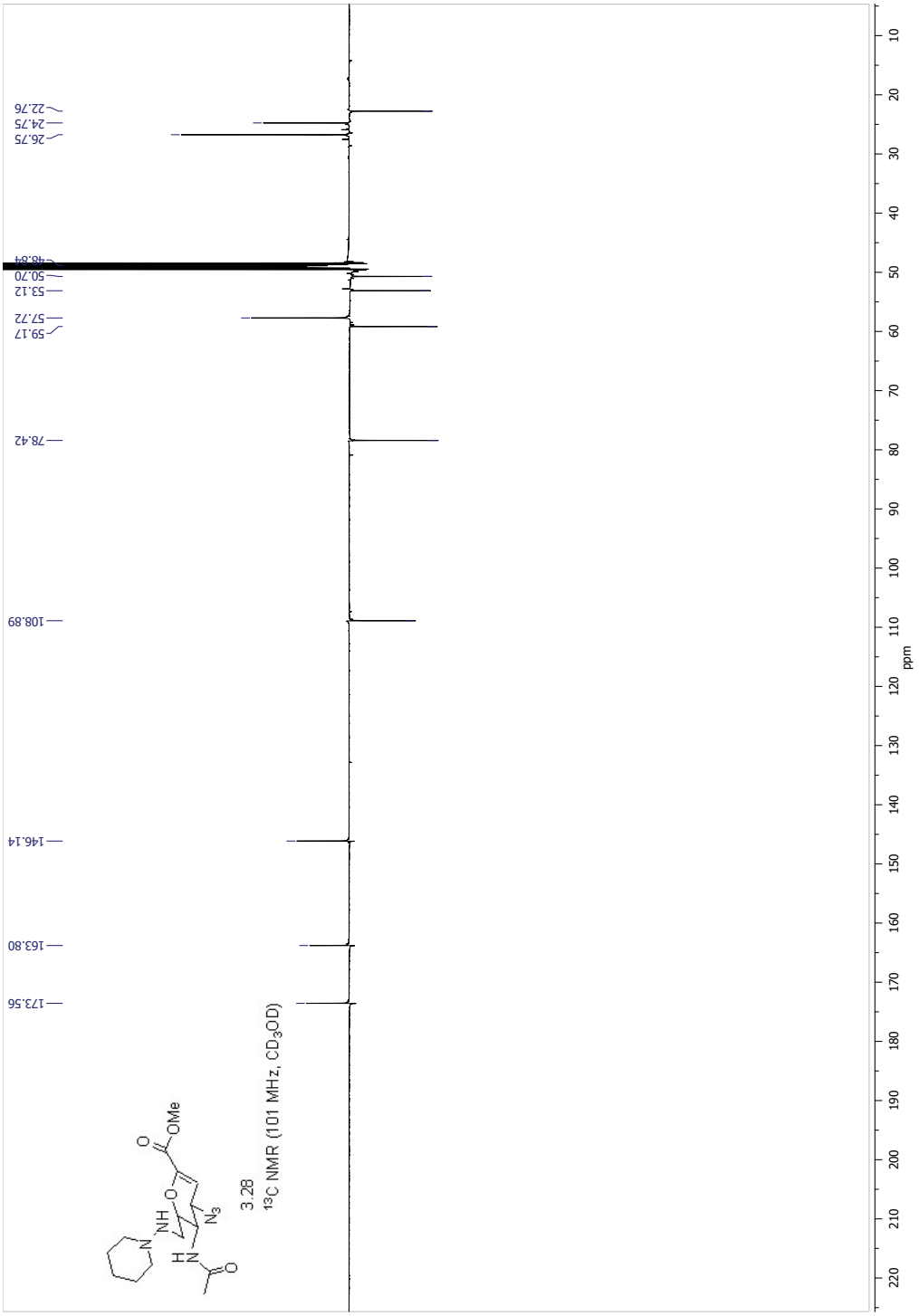
22.76
24.75
26.75
48.84
50.70
53.12
57.72
59.17
78.42
108.89
146.14
163.80
173.56
3.28
$^{13}$C NMR (101 MHz, $CD_3OD$)
ppm

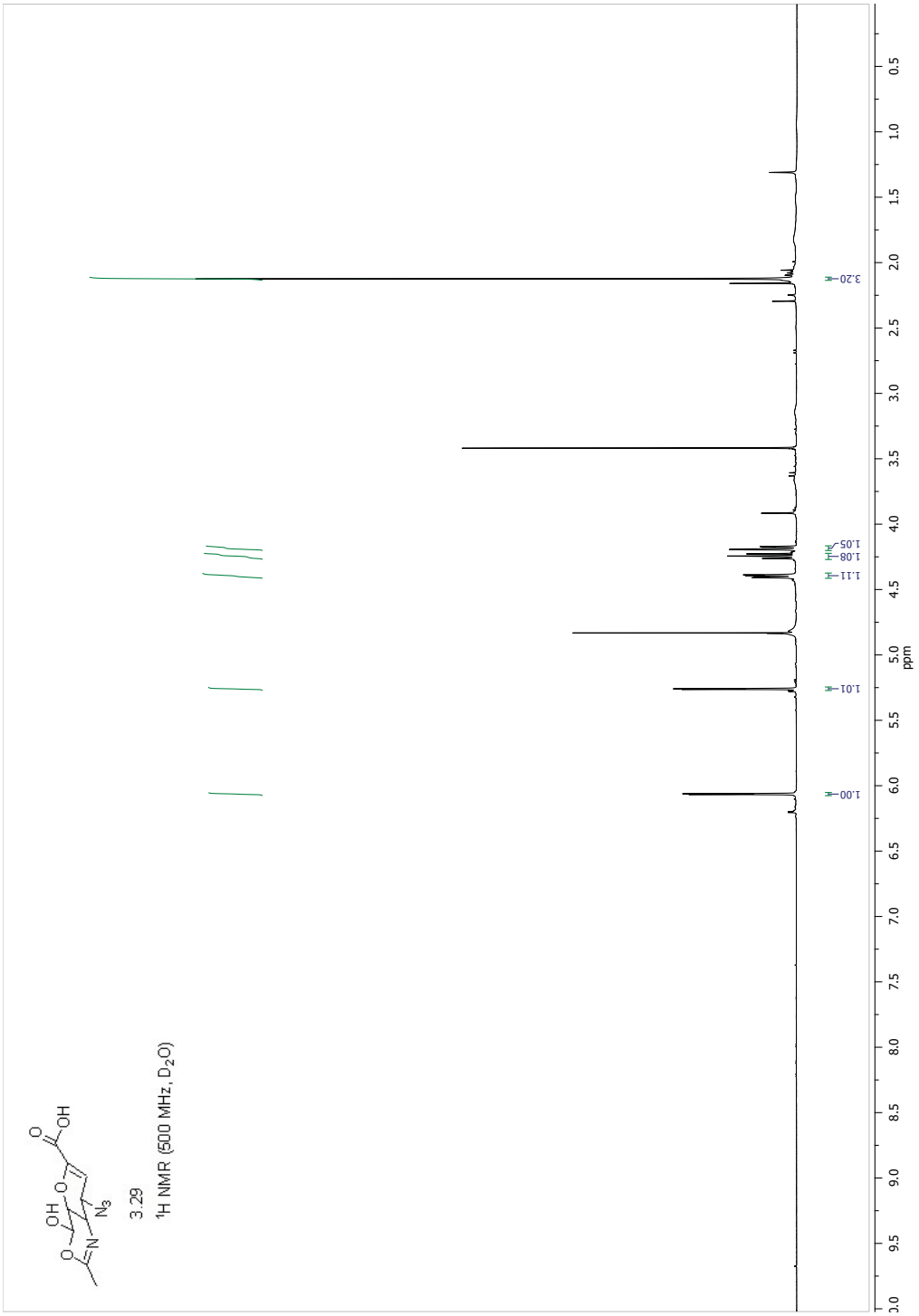
3.29
1H NMR (600 MHz, D2O)
3.20
1.08
1.05
1.11
1.01
1.00
ppm

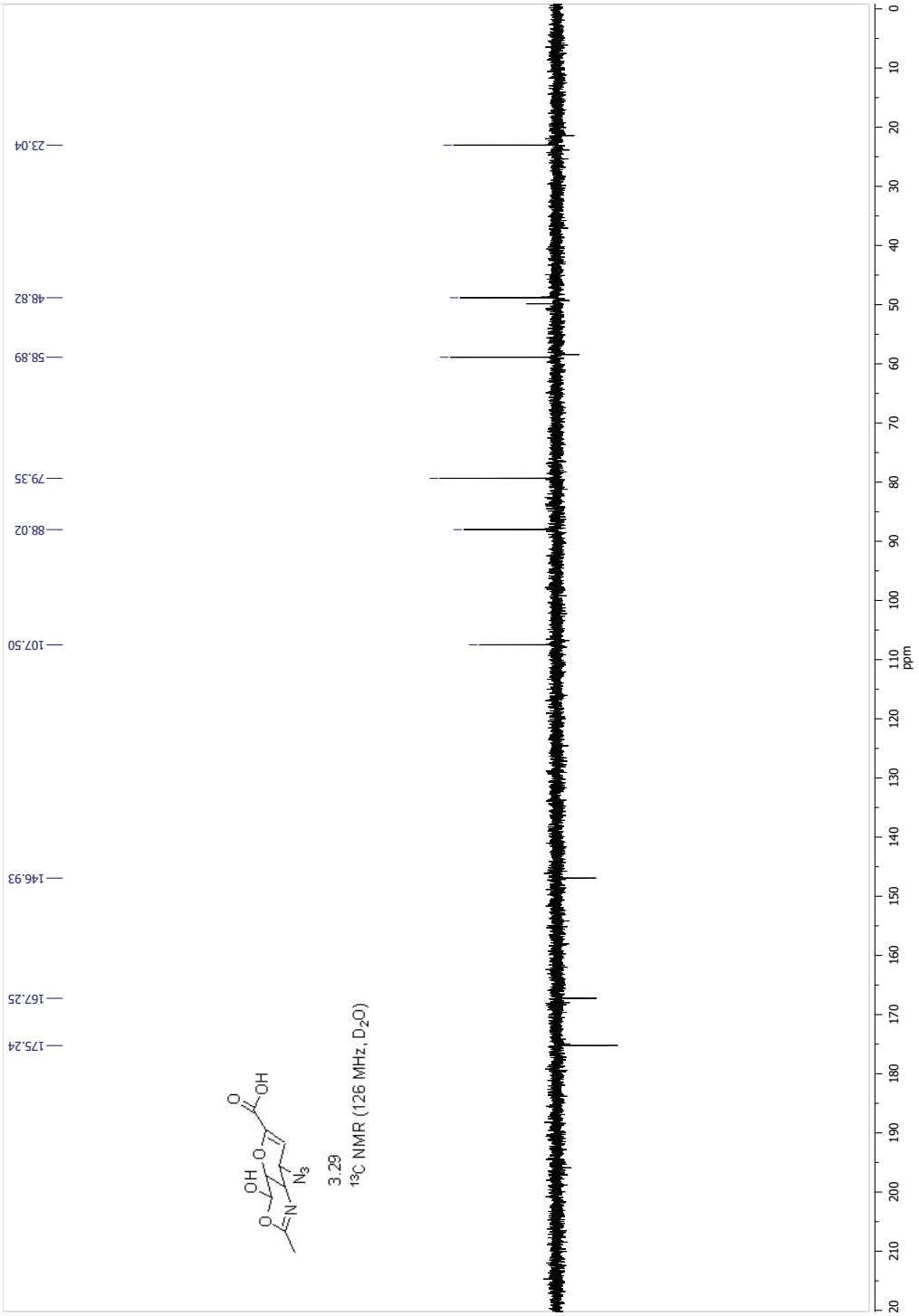
175.24
167.25
146.93
107.50
88.02
79.35
58.89
48.82
23.04
ppm
3.29
$^{13}$C NMR (126 MHz, $D_2O$)

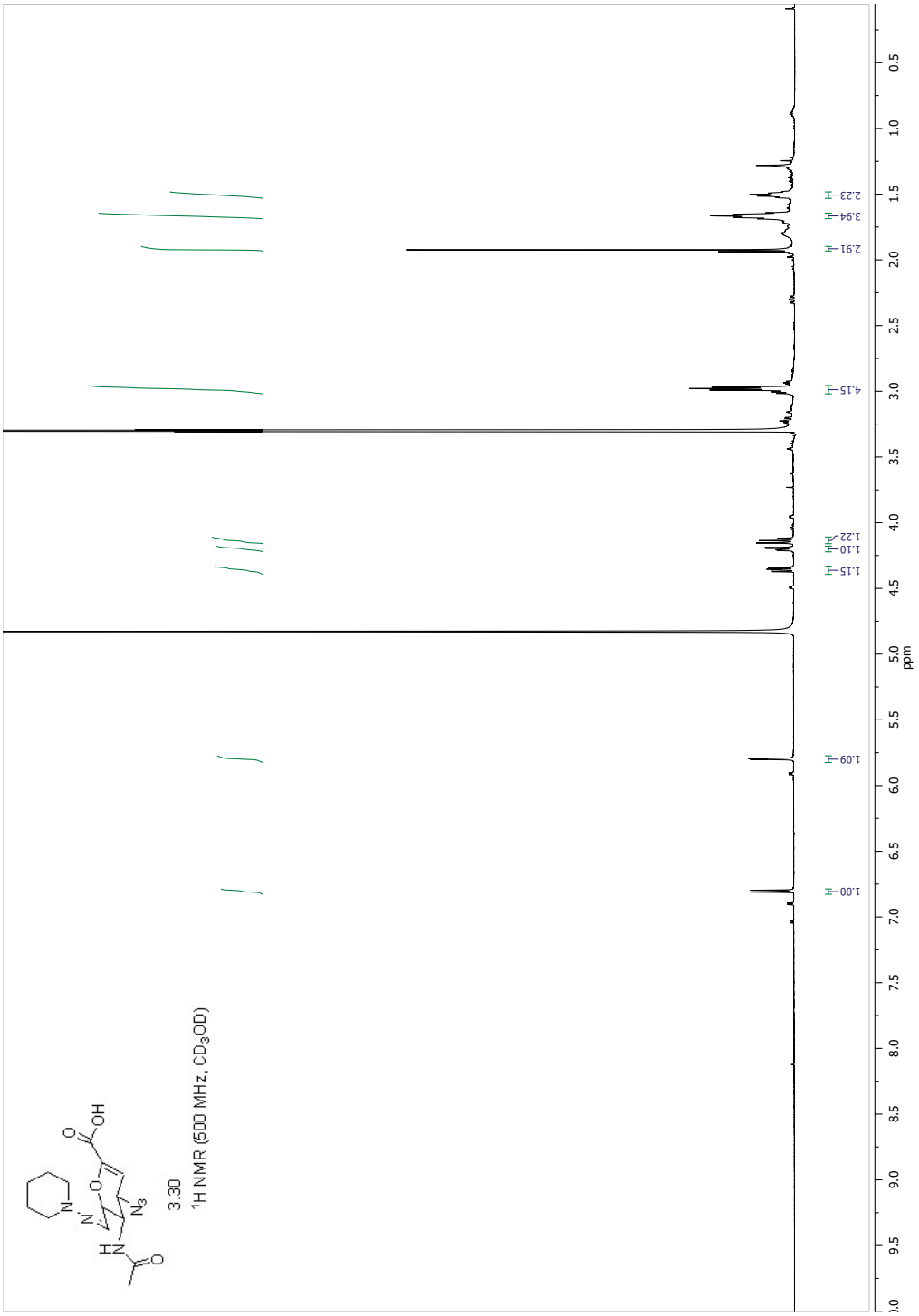
3.30
$^1$H NMR (500 MHz, $CD_3OD$)
1.00
1.09
1.15
1.10
1.22
4.15
2.91
3.94
2.23
ppm

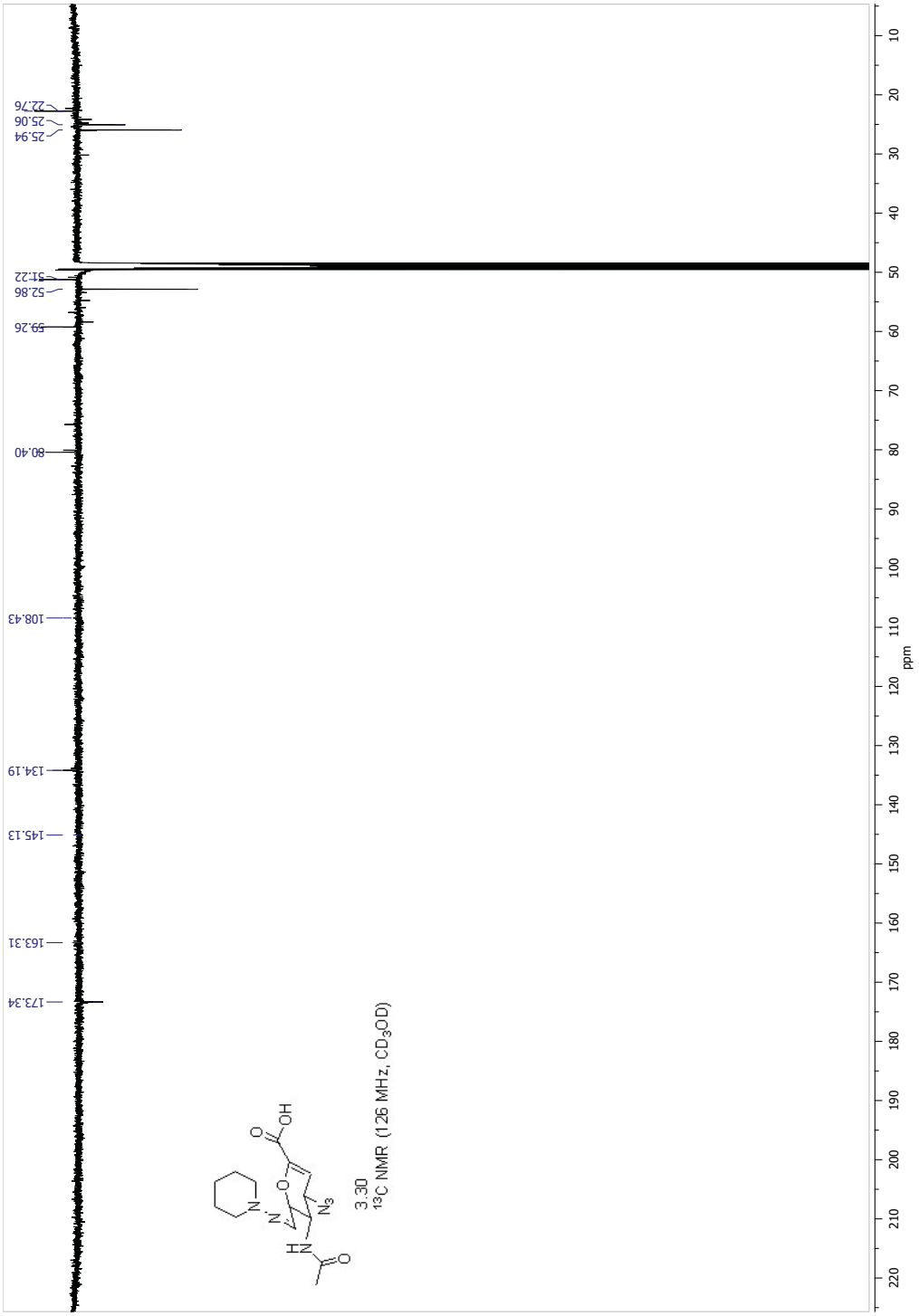
22.76
25.06
25.94
51.22
52.86
59.26
80.40
108.43
134.19
145.13
163.31
173.34
3.3D
13C NMR (126 MHz, CD3OD)
ppm

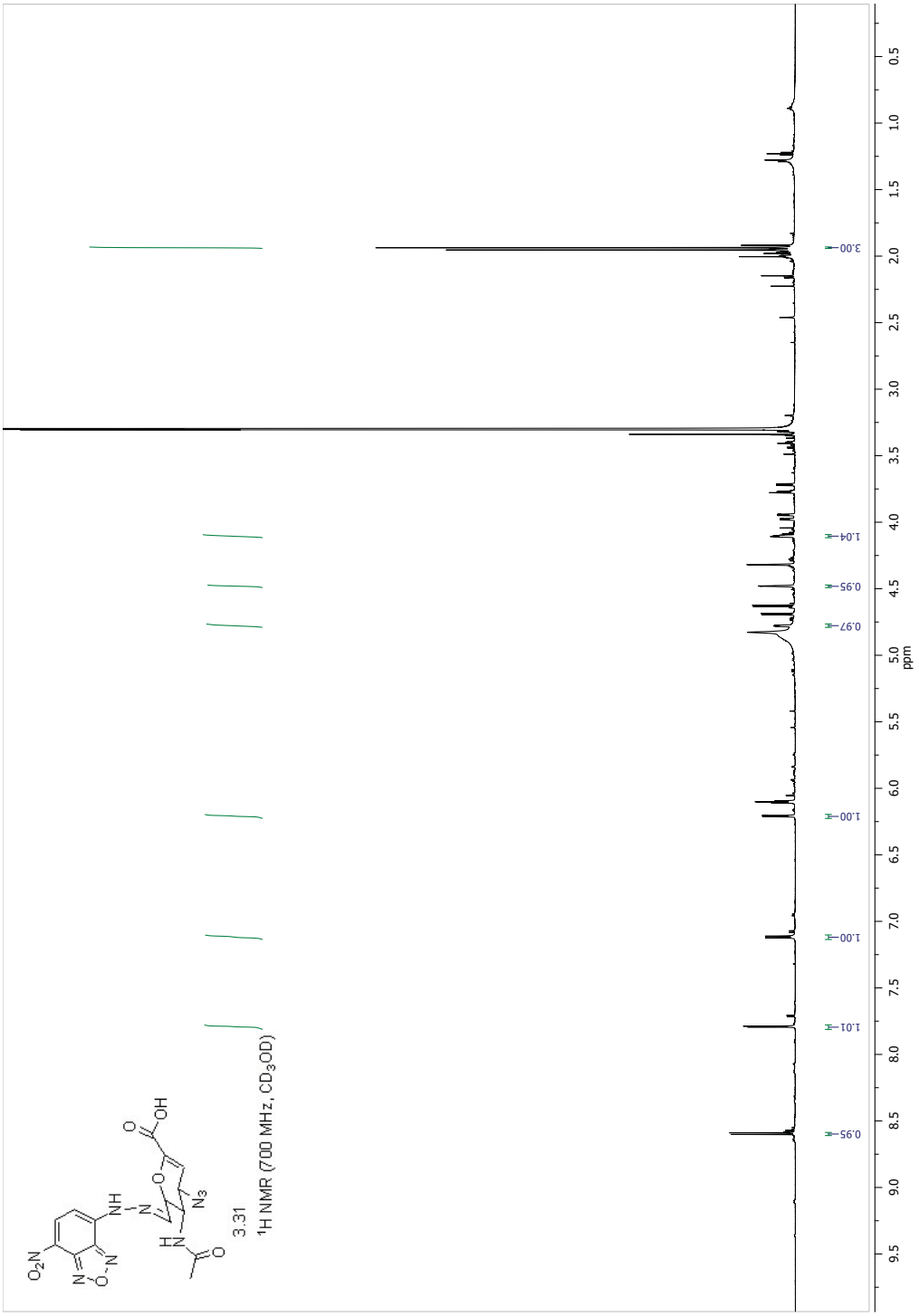
3.31
$^1$H NMR (700 MHz, $CD_3OD$)
3.00
1.04
0.95
0.97
1.00
1.00
1.01
0.95
ppm

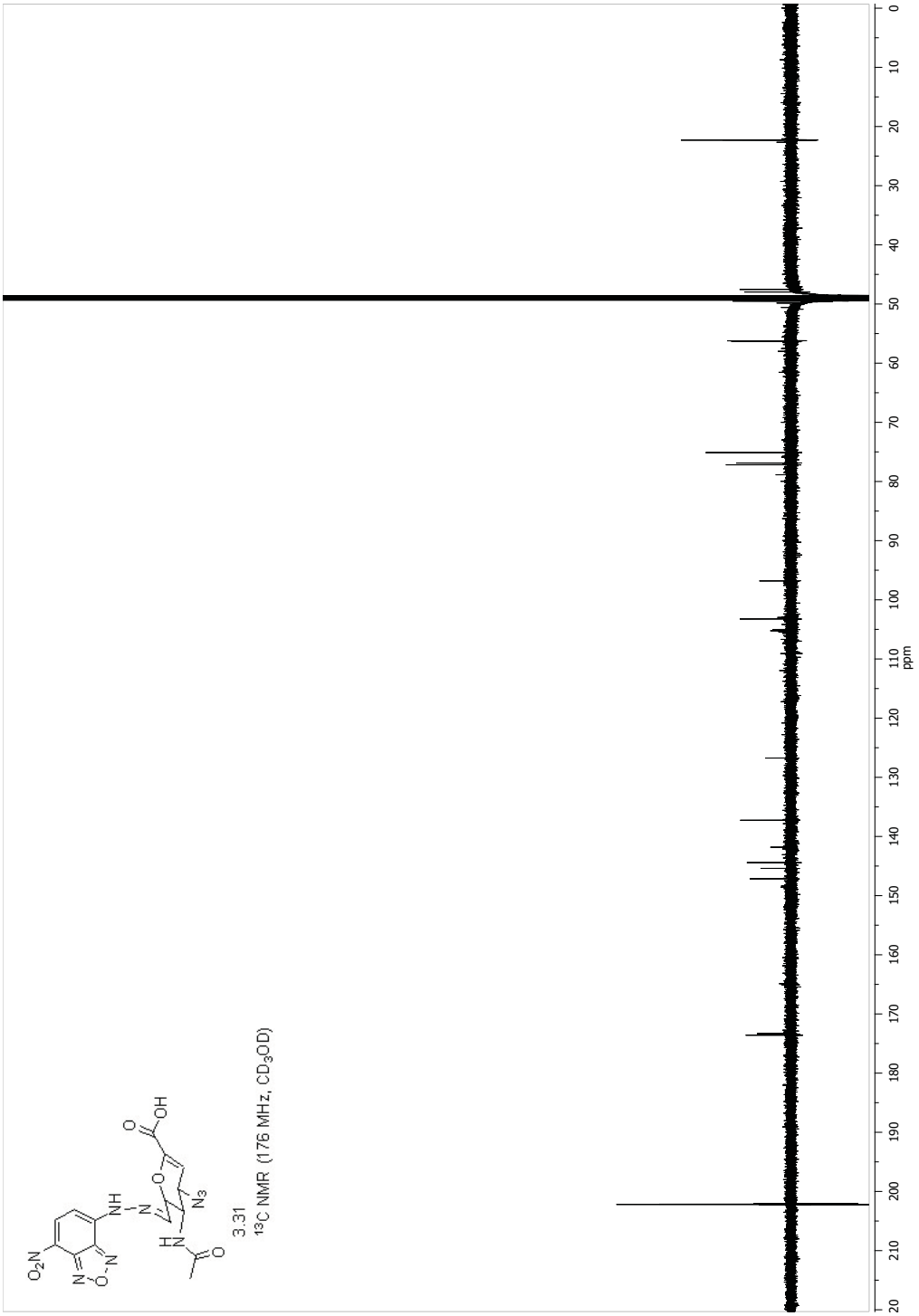
3.31
$^{13}$C NMR (176 MHz, $CD_3OD$)
ppm